(1)

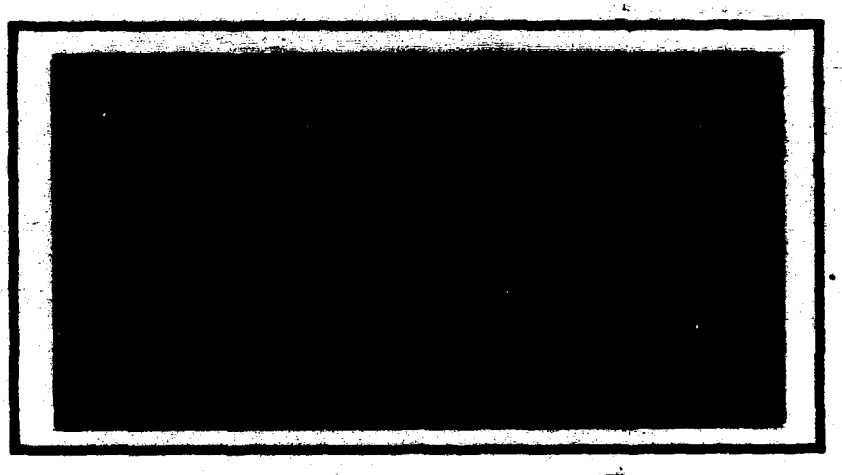

DEPARTMENT OF THE AIR FORCE

AIR UNIVERSITY

AIR FORCE INSTITUTE OF TECHNOLOGY

Wright-Patterson Air Force Base, Ohio

AFIT/GA/AA/88M-1

A NUMERICAL INVESTIGATION OF THIN-FILM HEAT TRANSFER GAGES

THESIS

Joseph Anthony Bonafede
First Lieutenant, USAF

AFIT/GA/AA/88M-1

AFIT/GA/AA/88M-1

A NUMERICAL INVESTIGATION OF THIN-FILM HEAT TRANSFER GAGES

THESIS

Presented to the Faculty of the School of Engineering
of the Air Force Institute of Technology
Air University
In Partial Fulfillment of the
Requirements for the Degree of
Master of Science in Astronautical Engineering and Space Facilities

Joseph Anthony Bonafede, B.S.
First Lieutenant, USAF

March, 1988

Acknowledgments

When faced with the undertaking and completion of this thesis, I was not alone, so I would like to thank those who stood by me in this task. First and formost is my advisor, Dr. Jim Hitchcock, who made the hard things seem easy and never gave up on me. Special thanks go to my sister, Jean, who helped tremendously with the figures and graphs. Special thanks also go to my brother, Greg, who proofread the document twice and has helped me in many other ways. Additionally, I thank Jeff Tustin for proofreading the document and being earnestly ready to help in any way possible.

I would also like to thank Chris Reid and Tom Passin for setting me up on PC TEX and Werner Willmann for supporting me at Lincoln Laboratory with printouts. Thanks to Laine Sellers and Paula Hagan for giving their time to help me with the printouts. Thanks also to Javier Gonzalez, Chris Mayer, Roger Claypoole and the brothers at M.I.T.'s ZBT for helping with LaTeX.

Often times, the most important help is moral support. I would like to thank the many friends and family who prayed often on my behalf and helped me in this way. Thanks to my family; Mom, Dad, John, Debbie, Jean, Greg, Mike and Blake. Knowing you are behind me has made all the difference. Special thanks to Jim and Mary Mayhew, who always had time to help, and to Maura Marler and Mike Ward. Thanks also to Jeff Grimshaw, who first helped with LaTeX. I would also like to thank the many friends from Patterson Park Church and the Officer's Christian Fellowship, especially Chris Hess, Dave Reske, Ryan Dunn, Janet Kinser, Robin Hunt and Peggy Nystrom, and thanks to Kim Franzoni, who has helped me since my move to Boston. Above all, I want to thank the Lord, who has taught me many more things beyond heat transfer through this time.

Joseph Anthony Bonafede

Table of Contents

List of Figures

List of Tables

List of Symbols

A	[Area]
Bi	non-dimensional Biot number, $\frac{hL}{k}$
C	constant used in the plane wall solution
c_p	specific heat at constant pressure, [Energy]/[Mass][Degree]
$\dot{E}$	heat energy, [Energy]/[Time]
h	coefficient of convective heat transfer, [Energy]/[Area][Time][Degree]
J	refers to a specific time index value
j	index variable for time
k	thermal conductivity, [Energy][Length]/[Area][Time][Degree]
L	axial dimension of the cylinder, [Length]
l	length, [Length]
M	refers to a specific axial index value
m	index variable for the axial direction
N	refers to a specific radial index value
n	index variable for the radial direction
q	heat flux, [Energy]/[Area][Time]
R	refers to a specific radial dimension, e.g. R_{CYL}, [Length]
R_t	thermal resistance, [Degree][Time]/[Energy]
r	radial dimension, [Length]
T	temperature, [Degree]
t	time, [Time]
V	[Volume]
x	variable used for distance in equations for a semi-infinite solid, [Length]
z	axial dimension, [Length]
α	thermal diffusivity, [Length]^2/[Time]
β	non-dimensional parameter, $\frac{{}_dBi_{FRONT}}{{}_pBi_{FRONT}}$

γ	non-dimensional surface heat generation, $\frac{q_g/d^h_{FRONT}}{d^T_{f_{FRONT}}-T_i}$
Δr	radial step, [Length]
Δt	time step, [Time]
Δz	axial step, [Length]
ζ	eigenvalue in the plane wall solution
θ	temperature difference, $(T - T_i)$, [Degree]
λ	variable of integration
ρ	density, [Mass]/[Volume]
τ	non-dimensional parameter, $\frac{T_{f_{BACK}}-T_i}{T_{fFRONT}-T_i}$

Subscripts

$_{AVE}$	average
$_{BACK}$	back surface of the cylinder
$_b$	back surface
$_{CYL}$	outer radius of the cylinder
$_{cond}$	conduction (used in $R_{t,cond}$)
$_{conv}$	convection (used in $R_{t,conv}$)
$_{DISK}$	outer radius of the heated disk
$_{F.D.}$	finite-difference solution
$_{FRONT}$	front surface of the cylinder
$_f$	fluid
$_g$	heat generation
$_{gen}$	refers to a specific value of heat generation
$_i$	initial
$_l$	index variable used in the plane wall solution
$_{la}$	lane (used in A_{la})
$_M$	refers to a specific axial index value
$_{MAX}$	maximum outer radius as in R_{MAX} or maximum value as in $\Delta\theta^+_{MAX}$

m	index variable for the axial direction
N	refers to a specific radial index value
n	index variable for the radial direction
SER	series solution
s	front surface
ss	steady-state

Superscripts

J	refers to a specific time index value
j	index variable for time
$+$	indicates a non-dimensional value
$'$	indicates properties of the surrounding material

Prescripts

d	disturbance problem
p	preheating problem

Units

K	degrees Kelvin
m	meters
W	watts

Overbar

$\overline{\quad}$	"overbar", denotes averaged properties between the cylinder and the surrounding material

Abstract

When using a thin-film gage to measure surface heat flux, one typically reduces the data for surface temperature to surface heat flux using a series solution for one-dimensional heat transfer in an initially isothermal, semi-infinite solid. However, the gage may not behave as an initially isothermal, semi-infinite solid due to multidimensional heat transfer and electrical preheating of the gage when the instrumentation is turned on.

To evaluate the accuracy of the series solution for use with thin-film gages, the heat transfer in a gage was numerically simulated using a two-dimensional, finite-difference model. The actual geometry of the probe was simplified to reduce the heat transfer to two dimensions. The simulation produced surface temperatures which were used in the series solution to find estimates of surface heat flux. The heat fluxes from the simulation and the series solution were then compared to evaluate the accuracy of the series solution.

The analysis provides good insight into the causes of inaccuracies when using the series solution. It also provides some quantitative results which may be helpful for estimating errors in actual laboratory use.

A NUMERICAL INVESTIGATION OF THIN-FILM HEAT TRANSFER GAGES

I. Introduction

1.1 Background and Motivation

A common experimental technique for measuring surface heat flux in the laboratory employs a thin-film gage. A thin-film gage is essentially a small quartz cylinder which has a thin, narrow strip of platinum—the thin-film sensor—plated on its front face. Two small wires connected to opposite ends of the thin-film sensor run along the side of the quartz cylinder to connect the sensor to recording instrumentation. Figure 1 is a diagram of a thin-film gage.

The thin-film gage does not directly measure surface heat flux. Instead, it measures the change in temperature of the surface of the quartz cylinder at the location of the thin-film sensor as a fuction of time. Because the platinum film is thin and has a relatively high thermal conductivity, the temperature of the thin-film sensor should be the same as the temperature of the quartz cylinder directly beneath it. The resistance of the thin-film sensor is a known function of temperature. Each gage is calibrated to determine the change in resistance as a function of change in temperature above some reference temperature [5:p.9]. As the surface temperature of the cylinder changes in response to a disturbance, the electrical resistance of the thin-film sensor will change. Then, if the gage is connected in one leg of a properly balanced Wheatstone bridge, the output voltage of the Wheatstone bridge will be proportional to the change in resistance of the thin-film sensor. Thus, the output voltage of the Wheatstone bridge circuit

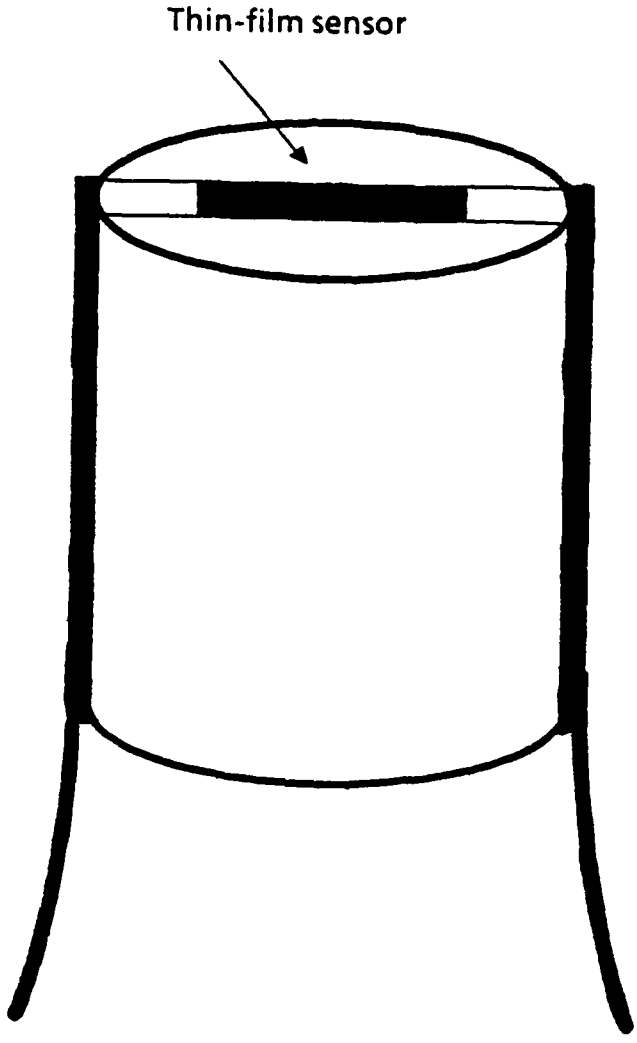

Figure 1. Diagram of a Thin-Film Gage

indirectly measures the change in surface temperature of the area of the quartz cylinder directly beneath the thin-film sensor.

Balancing the Wheatstone bridge requires consideration of the electrical heating in the thin-film sensor. When the input voltage is applied to the bridge, a small current will flow through each leg of the bridge circuit including the thin-film sensor. This small current will cause some electrical heating in the thin-film sensor changing the resistance of the sensor and unbalancing the bridge. Therefore, the circuit must be turned on and allowed to warm up until the transients settle down before the bridge can be balanced.

To measure the surface heat flux at the front surface of a test specimen, a thin-film gage is embedded in the specimen. The gage is held in place with a filler material which provides a sealed fit. The front surface of the gage must be flush with the front surface of the test specimen.

To get results for surface heat flux using the thin-film gage, one must convert the data for change in surface temperature as a function of time into values for surface heat flux as a function of time. In practice, the data is reduced using a series solution which assumes heat transfer in an initially isothermal, semi-infinite solid. In many ways, however, the gage does not behave as an initially isothermal, semi-infinite solid during the time when surface temperature data is being collected. First of all, the electrical heating in the thin-film sensor that occurs while the bridge is being balanced produces a non-uniform, initial temperature distribution in the quartz cylinder. Secondly, the electrical heating at any time generates non-uniform heat flow into the quartz cylinder which induces a three-dimensional temperature profile and heat flow pattern. Thirdly, heat flows radially in the presence of the disturbance because the gage is not thermally isolated from its surroundings and the thermal properties of the surrounding materials are not necessarily identical to those of the quartz cylinder. For the results for external surface heat flux to be accurate, the effect of the multidimensional heat transfer on the series solution

must be small.

Ideally, one hopes to measure the external surface heat flux that would be present in the test specimen if the gage were not there. The external surface heat flux is the heat flux from the disturbance not including the additional heat flux from the electrical heating in the thin-film sensor. However, it is readily apparent that at best the apparatus measures an average heat flux into the front surface of the gage itself in the region of the thin film. Nevertheless, if the average surface temperature measured at the gage approximates the surface temperature that would exist at the test specimen alone and the electrical heating and its effect on the thermal boundary layer is small, then the surface heat flux values obtained using the instrumented test specimen approximate the external surface heat flux that would exist at an uninstrumented test specimen. From this point on, this analysis will not investigate how well the surface heat flux measured at the gage approximates the external surface heat flux that would be present at the test specimen without the gage. Instead, the analysis investigates how well the series solution, which assumes heat transfer in an initially isothermal, semi-infinite solid, approximates the actual external surface heat flux at the gage.

1.2 Purpose

The purpose of this investigation is to numerically simulate the heat transfer in a thin-film gage with a finite-difference model. The simulation will produce surface temperatures which will then be used in the series solution to find estimates of the external surface heat flux. The heat fluxes from the simulation and the series solution will then be compared to evaluate the accuracy of the series solution.

1.3 Approach

Although the actual heat transfer in a thin-film gage is fully three-dimensional, the analysis uses a simplified model which limits the heat transfer to two

dimensions. The heat transfer is limited to two dimensions by modeling the region of electrical heat generation as a disk centered on the front surface of the quartz cylinder rather than the actual thin strip. The two dimensions in the heat transfer problem are now the radial dimension and the axial dimension into the quartz cylinder from the front surface. Figure 2 illustrates the simplified, two-dimensional geometry.

The series solution used to reduce the changes in surface temperature to values for surface heat flux is based on the assumption that the quartz cylinder behaves as an initially isothermal, semi-infinite solid when the temperature data is being collected. A number of variables influence the extent to which the cylinder departs from a semi-infinite solid. These variables include the following:

- Geometry parameters such as
  - the rati of the length of the quartz cylinder to its radius.
  - the area covered by the thin-film sensor compared to the total surface area of the front surface of the quartz cylinder. (In the two-dimensional model, the ratio of the radius of the heated disk to the radius of the cylinder describes this variable.)
- The magnitude of the thermal disturbance.
- The magnitude of the electrical heating in the thin-film sensor.
- The actual or effective thermal properties of the surrounding materials.

For the cylinder to behave as an initially isothermal, semi-infinte solid, the temperature distribution in the cylinder must be uniform at the start of test time, the heat transfer in the cylinder must be one-dimensional, and the cylinder must be longer than the distance into the cylinder to which the effects of the thermal disturbance at the front surface propagate. None of these assumptions may be correct in an actual laboratory experiment.

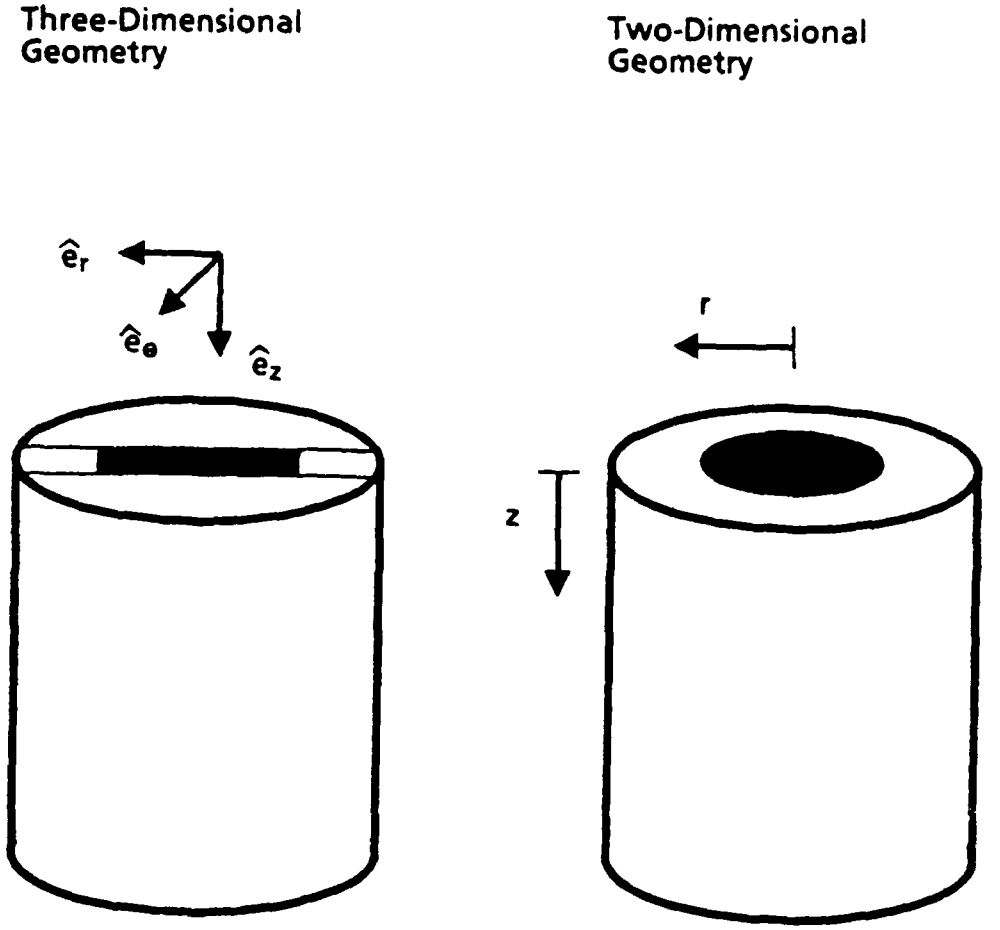

Figure 2. Simplified, Two-Dimensional Geometry

The first assumption, that the initial temperature distribution is uniform, is never exactly correct because the electrical heat generation in the thin-film during the time when the bridge is being balanced establishes a non-uniform temperature distribution. The magnitude of the non-uniform, initial temperature distribution depends upon the magnitude of the electrical heat generation, the external conditions and the amount of time allowed for the heat generation before the start of test time.

The second assumption, that heat transfer is one-dimensional, is also never correct. First of all, the initial temperature distribution established by the heat generation before the start of the test is multidimensional. Therefore, the heat transfer in the cylinder departs from one-dimensional from the very start. In the simplified model, the initial temperature distribution will be two-dimensional. Secondly, even in the absence of preheating, the localized surface heat generation and the fact that the cylinder is not ideally isolated from the surrounding materials will cause the one-dimensional assumption to fail eventually. The localized surface heat generation will produce three-dimensional heat transfer in general, but the heat transfer is limited to two dimensions by the simplified geometry of the model.

The third assumption, that the cylinder is long compared to the distance that the leading edge of the disturbance travels, is only valid for times less than the time it takes the leading edge of the thermal disturbance to travel the length of the quartz cylinder. A rule of thumb for the distance traveled by the leading edge of a thermal disturbance into a solid is [1:pp.60–61]

$$l \approx 4\sqrt{\alpha t} \tag{1}$$

where l is the distance to which the leading edge of the disturbance has traveled, α is the thermal diffusivity of the solid and t is the time after exposure to the disturbance. Using this rule of thumb, one would expect the assumption that the

cylinder is long to be valid only for test times less than

$$t \approx \frac{L^2}{16\alpha} \tag{2}$$

where L is the axial length of the cylinder.

The extent to which the cylinder departs from a semi-infite solid is hard to estimate. It is even more difficult to estimate the error in the values for external surface heat flux found using the series solution with the surface temperature changes from the cylinder. Because it is difficult to analytically estimate the multidimensional heat transfer in the cylinder and its effect on the results for external surface heat flux, this analysis estimates the effects through simulation. The simplified, two-dimensional heat transfer problem is simulated using a finite-difference model on a digital computer. The surface temperatures from the simulation are used to find the series solution estimate for surface heat flux which is then compared to the external surface heat flux of the simulation. The finite-difference model allows the variables to be changed arbitrarily so that one can investigate the effect of each variable individually.

In investigating the effect of heat transfer across the outer-radial boundary of the quartz cylinder, one can first bracket the results by looking at three limiting cases. In the first limiting case, one can model the cylinder as fully insulated at the outer-radial boundary so that no heat flows across the boundary. This limiting case is equivalent to surrounding the quartz cylinder by a material whose thermal conductivity is zero. In the second limiting case, one can surround the cylinder with a material whose thermal conductivity is infinite. The second material is assumed to be in thermal contact with a heat sink maintained at the initial temperature of the gage. In this case, the heat flux radially out of the cylinder is a theoretical maximum. In the third limiting case, one can again surround the cylinder with a material whose thermal conductivity is infinite. However, for this case, the temperature of the surrounding material is assumed to be that of the external disturbance. In this case, the heat flux radially into the cylinder is a theoretical

maximum. The first two cases bracket all possible effects due to heat flux radially out of the cylinder. The first and third cases bracket all possible effects due to heat flux radially into the cylinder.

In addition to bracketing the results, the analysis will consider a couple of intermediate cases for heat flux across the outer-radial boundary of the cylinder. In order for heat to flow across the outer-radial boundary of the cylinder, the surrounding material must have a non-zero thermal conductivity, and there also must be a temperature gradient at the boundary. The value of the thermal diffusivity in the surrounding material for the most part determines the direction of the heat flux established across the outer-radial boundary of the cylinder. Equation 1 shows that a thermal disturbance will propagate faster in a material with a larger thermal diffusivity. In other words, a material with a larger thermal diffusivity will heat up faster. Thus, if the thermal diffusivity of the surrounding material is smaller than the thermal diffusivity of the quartz cylinder, heat will flow radially out of the cylinder. On the other hand, if the thermal *diffusivity* of the surrounding material is greater than the thermal diffusivity of the quartz cylinder, heat may flow into the cylinder. It is important to note, however, that the electrical heat generation will always tend to establish a temperature gradient for heat to flow radially outward. For heat to flow into the cylinder, this temperature gradient must first be overcome.

Another simplification in the two-dimensional model involves the way in which the intermediate cases for heat flux across the outer-radial boundary of the cylinder are modeled. As mentioned in the first section, the gage is embedded in the test specimen using a filler material. Thus, the true heat transfer problem involves three materials: the quartz cylinder, the filler material, and the test specimen. However, the surrounding materials affect the results for external surface heat flux only to the extent that they induce heat flux into or out of the cylinder. The model for the intermediate cases for heat flux across the outer-radial bound-

ary of the cylinder uses only two materials: the quartz cylinder and a surrounding material. Using two materials is equivalent to modeling the effective tendency of the surrounding materials to induce heat flux across the outer-radial boundary of the cylinder.

II. The Finite-Difference Model

Before discussing the finite-difference model, it is instructive to first look at the differential equations for the two-dimensional model. A good understanding of the differential equations will help in developing the finite-difference model and in understanding the approximations caused by the discretization. Also, non-dimensionalizing the differential equations will yield the important non-dimensional parameters in the two-dimensional model.

2.1 The Differential Equations

Incropera and Dewitt derive the governing equations for heat transfer in a solid using an energy balance on the appropriate differential control volume [4:pp.43–53]. For a homogeneous, isotropic solid—one in which properties are constant with position and uniform in all directions—the governing equation for temperature in two-dimensional, cylindrical coordinates is

$$\frac{1}{r}\frac{\partial}{\partial r}\left(r\frac{\partial T}{\partial r}\right)+\frac{\partial^2 T}{\partial z^2}=\frac{1}{\alpha}\frac{\partial T}{\partial t} \tag{3}$$

where r is the radial dimension, z is the axial dimension and thermal diffusivity, α, is the ratio of thermal conductivity to thermal capacitance, $\alpha = k/\rho c_p$. A general solution of Equation 3 will give the temperature distribution in the solid as a function of the two spacial coordinates, z and r, and time t. The solution of Equation 3 is governed by the initial condition on time and the boundary conditions for each of the two spacial coordinates.

The initial condition for the two-dimensional model before preheating is simply

$$T(r,z)=T_i \qquad \text{for } t\leq 0 \tag{4}$$

The boundary conditions for the two-dimensional model require further explanation.

2.1.1 Front Surface Boundary Condition The front surface boundary condition must include consideration of the electrical heat generation in the thin-film sensor. As previously mentioned, the two-dimensional model models the sensor as a disk centered on the front surface of the cylinder. Using three assumptions, the thin-film sensor can be modeled simply as a region of surface heat generation. First, because the sensor is an extremely thin film of platinum, the total thermal capacity of the sensor is small. Secondly, the thermal contact between the platinum film and the quartz cylinder is assumed to be good so that the temperature of the lower side of the platinum film is the same as the surface temperature of the quartz below it. Lastly, the thermal conductivity of platinum is large. Because the sensor is very thin and has a large thermal conductivity, the temperature through the sensor essentially will be constant and equal to the temperature of the quartz below it. Because the thermal capacity of the sensor is small, its energy storage is negligible. Figure 3 illustrates an energy balance across the sensor using the above assumptions. Performing the energy balance yields

$$q_s = h_{FRONT}(T_{f_{FRONT}} - T_s) + q_g \tag{5}$$

where q_s is the heat flux into the cylinder, $h_{FRONT}(T_{f_{FRONT}} - T_s)$ is the heat flux into the disk from the fluid and q_g is the electrical heat generation per surface area of the disk. Then, the boundary condition for the front surface of the cylinder is

$$q_s = -k \left.\frac{\partial T}{\partial z}\right)_{z=0} = \begin{cases} h_{FRONT}(T_{f_{FRONT}} - T_s) + q_g & \text{for } 0 \le r \le R_{MAX} \\ h_{FRONT}(T_{f_{FRONT}} - T_s) & \text{for } R_{DISK} < r \le R_{MAX} \end{cases} \tag{6}$$

2.1.2 Back Surface Boundary Condition The boundary condition at the back surface is similar to the boundary condition at the front surface without the complication of the thin-film sensor. Using the sign convention that positive heat flux points in the positive z direction, positive heat flux at the back surface is heat flux out of the cylinder instead of into the cylinder:

$$q_b = -k \left.\frac{\partial T}{\partial z}\right)_{z=L} = -h_{BACK}(T_{f_{BACK}} - T_b) \tag{7}$$

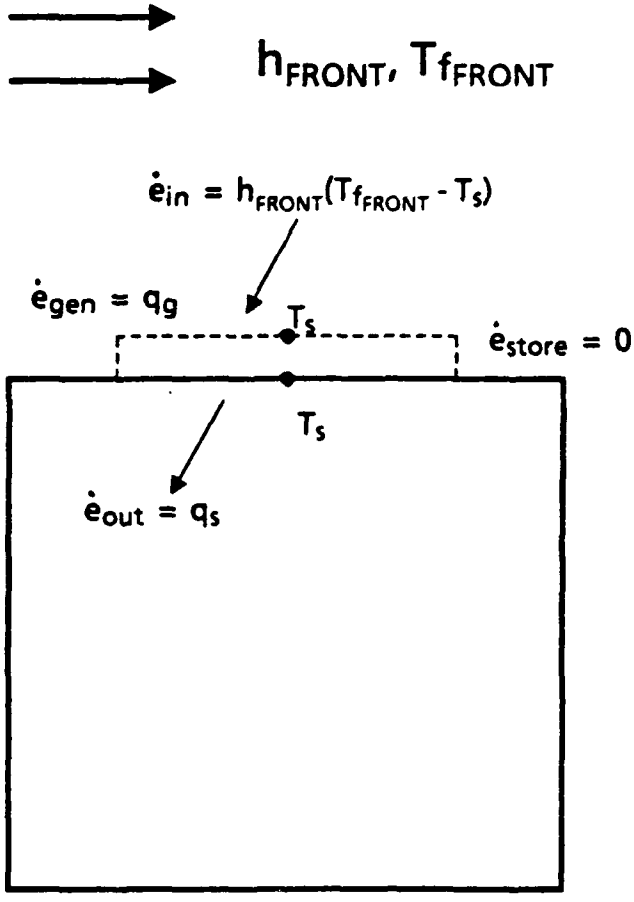

Figure 3. Energy Balance Across the Thin-Film Sensor

where T_b is the temperature on the back surface of the cylinder.

2.1.3 Inner-Radial Boundary Condition For the two-dimensional model, heat flux in the radial direction anywhere in the cylinder is the same regardless of the angular position in the cylinder. This radial symmetry can be satisfied only if the heat flux in the radial direction at the centerline is zero. Then, the inner-radial boundary condition for the two-dimensional model is

$$q_r = -k \left.\frac{\partial T}{\partial r}\right)_{r=0} = 0 \tag{8}$$

2.1.4 Outer-Radial Boundary Condition A general statement for the boundary condition at the outer radius of the cylinder is similar to the general statement for the boundary condition at the front and back surfaces. The heat flux crossing the outer-radial boundary must be equal to the heat flux in the radial direction on either side of the boundary. In this case, however, both sides of the boundary are solids, so the boundary condition uses Fourier's law for heat conduction on both sides:

$$q_r = -k \left.\frac{\partial T}{\partial r}\right)_{r=R_{CYL}^-} = -k' \left.\frac{\partial T}{\partial r}\right)_{r=R_{CYL}^+} \tag{9}$$

where k' is the thermal conductivity of the surrounding material. An important assumption in using this boundary condition is that the thermal contact between the quartz cylinder and the surrounding material is good.

As described in Section 1.3, it is worthwhile to investigate three limiting cases for the boundary condition at the outer radius of the cylinder. Each of the limiting cases can be modeled without actually including the surrounding material in the model.

The first limiting case is the case for no heat flux across the outer-radial boundary of the cylinder. The boundary condition for the *fully-insulated* or *adiabatic* case is

$$q_r = -k \left.\frac{\partial T}{\partial r}\right)_{r=R_{CYL}} = 0 \tag{10}$$

The second limiting case is the case for theoretically maximum heat flux out across the outer-radial boundary of the cylinder. This limiting case is equivalent to assuming that the thermal conductivity of the surrounding material is infinite and that the surrounding material is in thermal contact with a heat sink maintained at the initial temperature of the gage. Then, the temperature in the surrounding material is always the initial temperature. Thus, the outer-radial boundary condition on the cylinder for the limiting case of maximum heat flux out is simply a condition of constant temperature:

$$T(r = R_{CYL}, z) = T_i \tag{11}$$

The third limiting case is the limiting case for theoretically maximum heat flux in across the outer-radial boundary. This case is equivalent to assuming that the thermal conductivity of the surrounding material is infinite and that the surrounding material is maintained at the temperature of the external disturbance. The outer-radial boundary condition on the cylinder for the limiting case of maximum heat flux in is also a condition of constant temperature:

$$T(r = R_{CYL}, z) = T_f \tag{12}$$

When including the surrounding material in the model, the differential equations for heat transfer in the surrounding material are identical to those for heat transfer in the cylinder except that the properties for the surrounding material are used in place of the properties for quartz. The outer-radial boundary for the system is now the outer-radial boundary of the surrounding material, and one of the three limiting cases must be used for the outer-radial boundary condition on the system. Equation 9 then serves as a compatability equation at the discontinuity between the two materials.

2.2 *Non-Dimensional Parameters*

When non-dimensionalizing the differential equations, it is first necessary to specify the non-dimensional form for the variables. Then, the form of the equations will reveal the relevant non-dimensional parameters of the problem. In this problem, it is helpful to separate the total heat transfer problem into two separate problems which use different non-dimensional forms for the variables and have some different non-dimensional parameters.

The first of the two problems is the preheating problem. The preheating problem models the period of time during which the instrumentation circuitry is turned on and the bridge is being balanced. The test specimen is not exposed to the external disturbance during the preheating problem. Instead, the system is disturbed by the electrical heat generation. There are three basic assumptions for the preheating problem:

- The external fluid temperature on both the front and back surfaces remain at the initial temperature of the system.
- The values of the convection coefficients on both surfaces are typical free convection values.
- The surface heat generation is always some non-zero value.

For the preheating problem, the non-dimensional forms for the two dependent variables T and q are

$$ {}_p\theta^+ = \frac{T - T_i}{(q_g/{}_p h_{FRONT})} \tag{13} $$

$$ {}_pq^+ = \frac{q}{q_g} \tag{14} $$

The second problem is the disturbance problem. The disturbance problem models the heat transfer after the test specimen is exposed to the external disturbance. The initial temperature distribution for the disturbance problem is the

final temperature distribution from the preheating problem. There are three basic assumptions for the disturbance problem as well:

- The external fluid temperature at the front of the test specimen is different from the initial temperature of the system.
- The value of the convection coefficient on the front surface of the test specimen can be any typical forced convection value.
- Heat generation may or may not be present.

For the disturbance problem, the non-dimensional forms for the two dependent variables are

$$ {}_d\theta^+ = \frac{T - T_i}{{}_dT_{f_{FRONT}} - T_i} \tag{15} $$

$$ {}_dq^+ = \frac{q}{{}_dh_{FRONT}({}_dT_{f_{FRONT}} - T_i)} \tag{16} $$

It will be valuable to look at cases where the heat generation is zero. If the surface heat generation is zero, then the solution to the preheating problem is the trivial solution; the temperature remains at the initial temperature of the system until exposed to the external disturbance. Thus, the total heat transfer problem includes only the disturbance problem when the heat generation is zero.

The preheating problem and the disturbance problem are non-dimensionalized differently to account for the different conditions in the two problems. The preheating problem is non-dimensionalized with $q_g/{}_dh_{FRONT}$ in the denominator because the temperature difference ${}_dT_{f_{FRONT}} - T_i$ is zero in the preheaing problem but the heat generation is never zero. The disturbance problem is non-dimensionalized with the temperature difference ${}_dT_{f_{FRONT}} - T_i$ in the denominator instead to allow the surface heat generation to be zero for the disturbance problem.

The non-dimensional forms for the independent variables r, z and t are the same in both problems. They are

$$r^+ = \frac{r}{R_{CYL}} \tag{17}$$

$$z^+ = \frac{z}{L} \tag{18}$$

$$t^+ = \frac{\alpha t}{L^2} \tag{19}$$

With these definitions for the non-dimensional variables, the differential equations can be non-dimensionalized. The non-dimensional, governing equation for temperature within the solid for either problem is

$$\left[\frac{L}{R_{CYL}}\right]^2 \frac{1}{r^+}\frac{\partial}{\partial r^+}\left(r^+\frac{\partial\theta^+}{\partial r^+}\right) + \frac{\partial^2\theta^+}{\partial z^{+2}} = \frac{\partial\theta^+}{\partial t^+} \tag{20}$$

The initial condition for the preheating problem is

$$\theta^+(r^+, z^+) = 0 \qquad \text{for } t \leq 0 \tag{21}$$

Recall that the initial condition for the disturbance problem is the final temperature distribution from the preheating problem.

It is interesting to note that Equations (20) and (21) remain the same regardless of the non-dimensional form for temperature difference, $\theta = T - T_i$. One can multiply Equations (20) and (21) by any non-dimensional constant changing the form for the non-dimensional variable, θ, and the equations will remain the same.

The non-dimensional equations for the two seperate problems differ only in some of the boundary conditions. The non-dimensional boundary conditions for the preheating problem are as follows:

Top surface boundary condition;

$$-\left[\frac{{}^{p}h_{FRONT}L}{k}\right]^{-1}\frac{\partial\theta^+}{\partial z^+}\Bigg)_{z^+=0} = \begin{cases} -\theta_s^+ + 1 & \text{for } 0 \leq r^+ \leq \left[\frac{R_{DISK}}{R_{CYL}}\right] \\ -\theta_s^+ & \text{for } \left[\frac{R_{DISK}}{R_{CYL}}\right] < r^+ \leq \left[\frac{R_{MAX}}{R_{CYL}}\right] \end{cases} \tag{22}$$

Bottom surface boundary condition;

$$-\left[\frac{{}_{p}h_{BACK}L}{k}\right]^{-1}\left.\frac{\partial\theta^{+}}{\partial z^{+}}\right)_{z^{+}=1}=\theta_{b}^{+} \tag{23}$$

Inner-radial boundary condition;

$$\left.\frac{\partial\theta^{+}}{\partial r^{+}}\right)_{r^{+}=0}=0 \tag{24}$$

Outer-radial boundary conditions;

Boundary between materials —for use when including the surrounding material in the model,

$$\left.\frac{\partial\theta^{+}}{\partial r^{+}}\right)_{r^{+}=1^{-}}=\left[\frac{k'}{k}\right]\left.\frac{\partial\theta^{+}}{\partial r^{+}}\right)_{r^{+}=1^{+}} \tag{25}$$

or

Fully-insulated,

$$\left.\frac{\partial\theta^{+}}{\partial r^{+}}\right)_{r^{+}=1}=0 \tag{26}$$

Maximum heat flux out,

$$\theta^{+}(r^{+}=1,z^{+})=0 \tag{27}$$

Maximum heat flux in,

$$\theta^{+}(r^{+}=1,z^{+})=0 \tag{28}$$

for the limiting cases.

The non-dimensional boundary conditions for the disturbance problem are the following:

Top surface boundary condition;

$$-\left[\frac{{}_{d}h_{FRONT}L}{k}\right]^{-1}\left.\frac{\partial\theta^{+}}{\partial z^{+}}\right)_{z^{+}=0} \tag{29}$$

$$=\begin{cases}1-\theta_{s}^{+}+\left[\frac{(q_{g}/{}_{d}h_{FRONT})}{({}_{d}T_{f_{FRONT}}-T_{i})}\right] & \text{for } 0\leq r^{+}\leq\left[\frac{R_{DISK}}{R_{CYL}}\right]\\ 1-\theta_{s}^{+} & \text{for } \left[\frac{R_{DISK}}{R_{CYL}}\right]<r^{+}\leq\left[\frac{R_{MAX}}{R_{CYL}}\right]\end{cases} \tag{30}$$

Bottom surface boundary condition;

$$-\left[\frac{{}_{d}h_{BACK}L}{k}\right]^{-1}\left.\frac{\partial\theta^{+}}{\partial z^{+}}\right)_{z^{+}=1}=\theta_{b}^{+} \tag{31}$$

Inner-radial boundary condition;

$$\left.\frac{\partial\theta^{+}}{\partial r^{+}}\right)_{r^{+}=0}=0 \tag{32}$$

Outer-radial boundary conditions;

Boundary between materials —for use when including the surrounding material in the model,

$$\left.\frac{\partial\theta^{+}}{\partial r^{+}}\right)_{r^{+}=1^{-}}=\left[\frac{k'}{k}\right]\left.\frac{\partial\theta^{+}}{\partial r^{+}}\right)_{r^{+}=1^{+}} \tag{33}$$

or

Fully-insulated,

$$\left.\frac{\partial\theta^{+}}{\partial r^{+}}\right)_{r^{+}=1}=0 \tag{34}$$

Maximum heat flux out,

$$\theta^{+}(r^{+}=1,z^{+})=0 \tag{35}$$

Maximum heat flux in

$$\theta^{+}(r^{+}=1,z^{+})=1 \tag{36}$$

for the limiting cases.

The non-dimensional differential equations for the heat transfer in the cylinder during the preheating and disturbance problems include the following non-dimensional parameters which govern the solution:

External fluid conditions and electrical heat generation;

$${}_{p}Bi_{FRONT}=\frac{{}_{p}h_{FRONT}L}{k} \tag{37}$$

$$ {}_pBi_{BACK} = \frac{{}^ph_{BACK}L}{k} \tag{38} $$

$$ {}_dBi_{FRONT} = \frac{{}_dh_{FRONT}L}{k} \tag{39} $$

$$ {}_dBi_{BACK} = \frac{{}_dh_{BACK}L}{k} \tag{40} $$

$$ \gamma = \frac{(q_g/{}_dh_{FRONT})}{({}_dT_{f_{FRONT}} - T_i)} \tag{41} $$

$$ \tau = \frac{({}_dT_{f_{BACK}} - T_i)}{({}_dT_{f_{FRONT}} - T_i)} \tag{42} $$

Geometry ratios;

$$ \frac{L}{R_{CYL}} \tag{43} $$

$$ \frac{R_{DISK}}{R_{CYL}} \tag{44} $$

Property ratio

$$ \frac{k'}{k} \tag{45} $$

Two additional non-dimensional parameters arise when including the surrounding material in the analysis. The first is a geometry ratio specifying the extent of the surrounding material:

$$ \frac{R_{MAX}}{R_{CYL}} \tag{46} $$

The second is another property ratio—the ratio of thermal capacitances:

$$ \frac{(\rho c_p)}{(\rho c_p)'} \tag{47} $$

When incorporating the final temperature distribution from the preheating problem as the initial temperature distribution to the disturbance problem, another non-dimensional parameter can be defined for convenience. Non-dimensional temperature values from the preheating problem can be converted to the non-dimensional form used in the disturbance problem by multiplying by the generation ratio, γ, and a derived parameter, β, which is the ratio of the convection coefficient

at the front surface in the disturbance problem to the convection coefficient at the front surface in the preheating problem:

$$\beta = \frac{{}_{d}Bi_{FRONT}}{{}_{p}Bi_{FRONT}} \tag{48}$$

2.3 The Finite-Difference Equations

Without an analytical solution to the differential equations for the two-dimensional model, it is necessary to approximate the transient solution through simulation. The most common method for simulating heat transfer is to run a finite-difference model on a digital computer. Various finite-different schemes are available. This analysis uses an explicit finite-difference scheme derived using the control-volume approach. The explicit scheme uses second order, central differences for the spatial derivatives and first order, forward differences for the time derivatives. Incropera and Dewitt present the control-volume approach in developing finite-difference models for conduction heat transfer problems [4:pp.143–149,213–220]. The control-volume approach has the advantages of being easy to use and versatile in application to different and complicated boundary and geometry conditions. The control-volume approach is also a conservative approach which means that the finite-difference model developed using the control-volume approach will satisfy the statement of conservation of energy to within the truncation error for the model. The finite-difference models used for the single-material and the two-material problems with fully-insulated, outer-radial boundary conditions are given in Appendices D.1 and D.2, respectively.

2.3.1 Discretizing the Model The first step in developing the finite-difference model is to discretize the continuous model in both space and time. Figures 4 and 5 illustrate the discretized geometry of the single-material problem and the two-material problem, respectively. To discretize the geometry, the cylinder and the surrounding material are subdivided into nodal regions. Associated with each

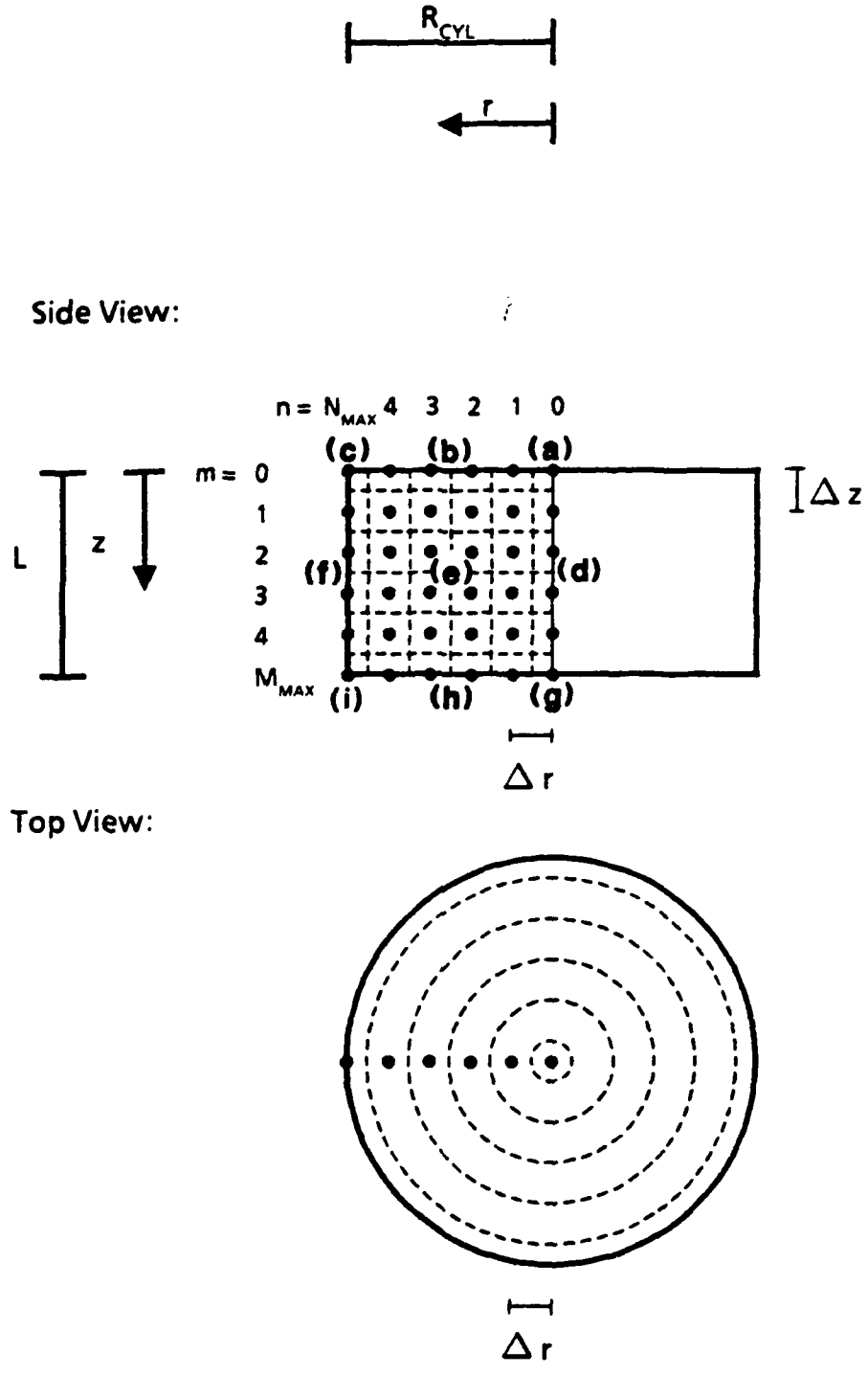

Figure 4. Discretized Geometry of the Single-Material Problem

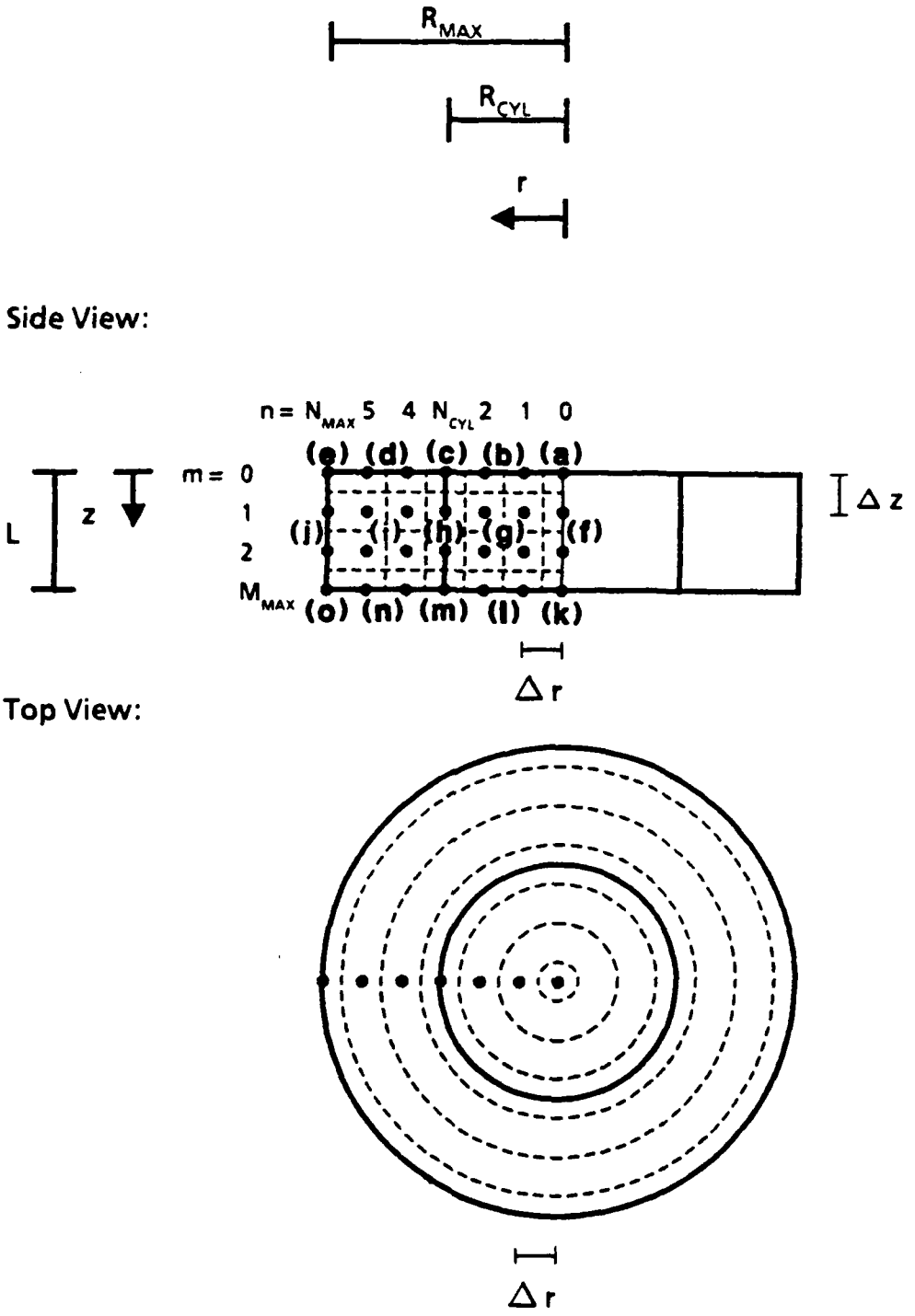

Figure 5. Discretized Geometry of the Two-Material Problem

nodal region is a reference point or reference level for the region called a node. All nodal regions are annular rings except for those on the centerline of the cylinder which are cylinders of radius $\Delta r/2$. Interior nodal regions—those not on an exterior system boundary—are annualar rings of width Δr and depth Δz. Nodal regions on exterior system boundaries are generally assigned half the step size of interior nodal regions. For nodal regions at any boundary, the node is placed on the boundary. Placing nodes directly on the boundary rather than one-half spacial step in from the boundary provides better resolution of the boundary conditions. Because the heat transfer in the two-dimensional model is axi-symmetric, the reference point for nodal regions other than those on the centerline of the cylinder can be any point on an annular ring at the reference radius and depth.

In general, discretizing the geometry means that the finite-difference model only solves for temperatures at the nodes. The temperature at a node represents an average temperature for the nodal region. For the purpose of deriving the finite-difference equations, conditions across the nodal region are often assumed constant and equal to the conditions associated with the node or the nodal region. Continuous time is discretized similarly, so the finite-difference model only solves for temperatures at discrete intervals in time as well.

To identify positions in the nodal geometry mesh, the index value n specifies the radial position of the node, and the index value m specifies the axial position of the node. When used as subscripts, the radial index is placed first such as in $\theta_{n,m}$. (The only exceptions are for values denoting surface conditions using the subscripts s and b to denote the axial positions on the front and back surfaces, respectively. Subscripts s and b are placed before the radial index value as in $\theta_{s,n}$.) The index value of zero for n denotes postions on the centerline of the cylinder where the radial dimension is zero. The index value of zero for m denotes positions on the front surface where the axial dimension is zero. Then, the radial position of a node with radial index n is $r = n\Delta r$. Similarly, the axial position of a node with axial

index m is $z = m\Delta z$. The index value j specifies the time level in discretized time. The time index j is usually placed as a superscript. The index value of zero for j denotes time $t = 0$, so the time denoted by index j is $t = j\Delta t$.

2.3.2 Nodal Equations In the explicit scheme, a finite-difference equation for each node estimates the temperature of the node at the new, unknown time level in terms of the temperatures of the node itself and surrounding nodes at the old, known time level. The finite-difference equations are developed using an energy balance on the individual nodal volumes.

For the purpose of deriving the finite-difference equations, one assumes that the heat flux at each surface of the nodal volume is directed into the nodal volume. Of course, the actual direction of the heat flux during the simulation depends on the temperature profile. This sign convention merely helps in developing the equations correctly. One also assumes that the heat flux at each surface of the nodal volume is constant and equal to the heat flux at the reference level. Then, the energy balance at each nodal volume is

$$q_1 A_1 + q_2 A_2 + q_3 A_3 + q_4 A_4 = (\rho c_p) V \frac{\partial T}{\partial t} \tag{49}$$

The subscripts $_{1\text{-}4}$ denote the inner-radial, outer-radial, front (smaller axial dimension) and back (larger axial dimenion) surfaces of the nodal volume, respectively.

The develoment of each nodal, finite-difference equation requires specific information about the node whose equation is being developed. Nevertheless, the procedure is basically the same for all nodes. To illustrate the process, the steps are outlined for an interior node in the cylinder. Figure 6 shows the nodal geometry for an interior node in the cylinder.

The first step is to specify the dimensions of the nodal region. For an interior node in the cylinder

$$A_1 \;=\; 2\pi(n - 1/2)\Delta r \Delta z \tag{50}$$

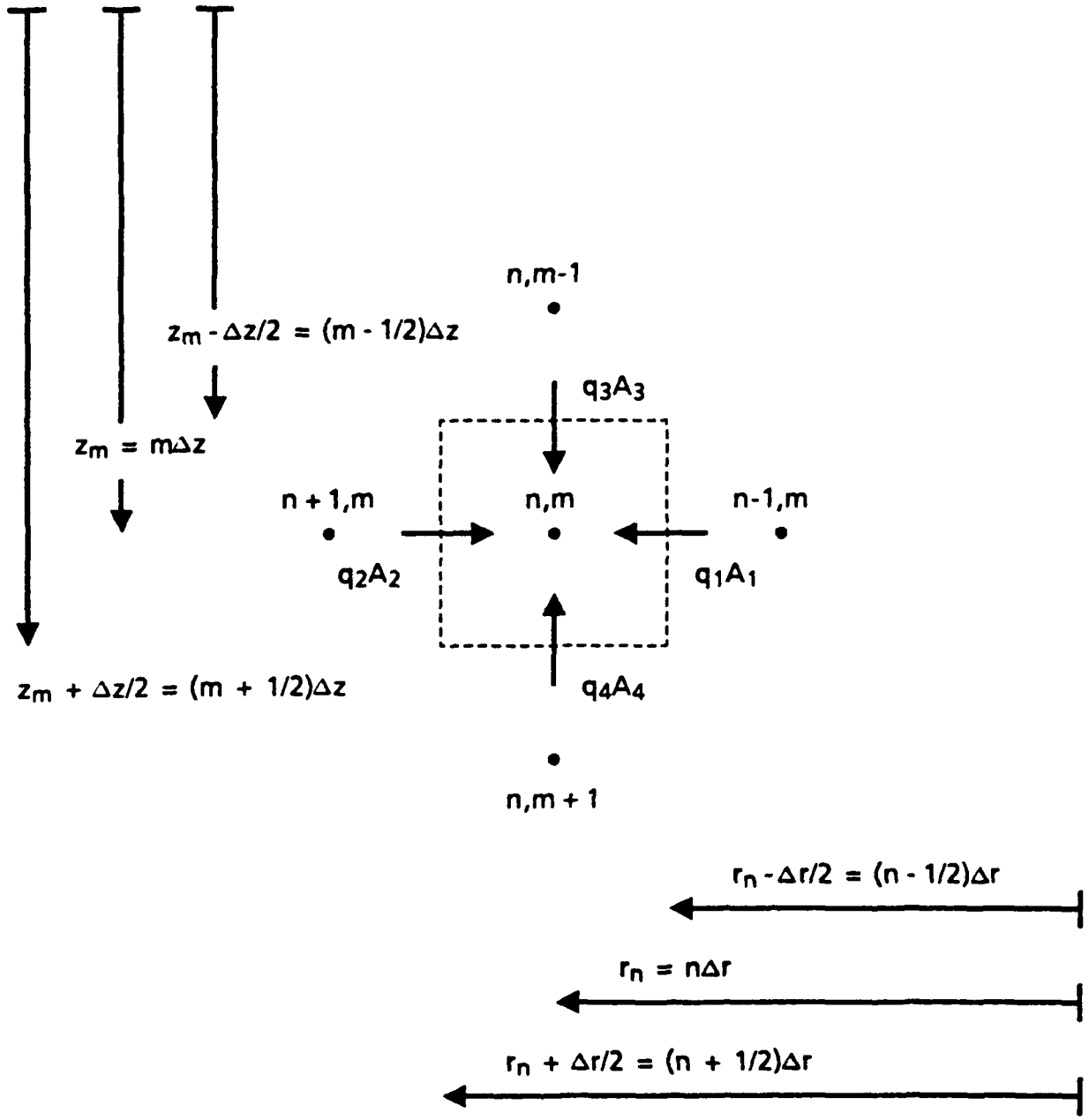

Figure 6. Nodal Geometry for an Interior Node in the Cylinder

$$A_2 = 2\pi(n+1/2)\Delta r\Delta z \tag{51}$$

$$A_3 = \pi\left[(n\Delta r+\Delta r/2)^2-(n\Delta r-\Delta r/2)^2\right]=\pi(2n)\Delta r^2 \tag{52}$$

$$A_4 = \pi(2n)\Delta r^2 \tag{53}$$

and

$$V=\pi(2n)\Delta r^2\Delta z \tag{54}$$

The next step is to determine a finite-difference expression for the heat flux at each of the surfaces of the nodal volume. For an interior node, a finite-difference expression for the heat flux at each surface is determined from Fourier's conduction law using a central difference to approximate the temperature gradient. Using the finite-difference expressions for heat flux and a forward difference to approximate the time derivative, a finite-difference expression for the energy balance at an interior node in the cylinder is

$$\begin{aligned}\rho c_p\left[\pi(2n)\Delta r^2\Delta z\right]\frac{(T^{j+1}_{n,m}-T^{j}_{n,m})}{\Delta t} &= \\ k\left[2\pi(n-1/2)\Delta r\Delta z\right]\frac{(T^{j}_{n-1,m}-T^{j}_{n,m})}{\Delta r} &\\ +\,k\left[2\pi(n+1/2)\Delta r\Delta z\right]\frac{(T^{j}_{n+1,m}-T^{j}_{n,m})}{\Delta r} &\\ +\,k\left[\pi(2n)\Delta r^2\right]\frac{(T^{j}_{n,m-1}-T^{j}_{n,m})}{\Delta z}+k\left[\pi(2n)\Delta r^2\right]\frac{(T^{j}_{n,m+1}-T^{j}_{n,m})}{\Delta z} &\end{aligned} \tag{55}$$

By calculating the spacial derivatives at the old time level, j, and not at the new time level, $j+1$, or some combination of the two, the finite-difference scheme will be an explicit scheme. The only unknown in each nodal equation is the temperature of the node at the new time level, $j+1$, used in the forward-difference approximation for the time derivative. Solving for the temperature of each node at the new time level is straightforward. Grouping temperature terms for the same node at the same time level toget' er and solving for the temperature at the new time level gives the dimensional form for the nodal finite-difference

equation for an interior node in the cylinder:

$$T_{n,m}^{j+1} = \alpha(1-1/2n)\frac{\Delta t}{(\Delta r)^2}T_{n-1,m}^{j} + \alpha(1+1/2n)\frac{\Delta t}{(\Delta r)^2}T_{n+1,m}^{j} + \alpha\frac{\Delta t}{(\Delta z)^2}T_{n,m-1}^{j} + \alpha\frac{\Delta t}{(\Delta z)^2}T_{n,m+1}^{j} \quad (56)$$

It is not necessary to derive the finite-difference equation at each node. Nodes that have similar geometry and the same boundary conditions will have identical finite-difference equations. The only difference in the equations will be the specific values of the indexing variables. Also, when including the surrounding material in the model, one must be careful to use the correct property values for each term in the energy balance. For the single-material problem, there are nine different forms for the nodal finite-difference equations corresponding to the nine different locations labeled (a)–(i) in Figure 4. For the two-material problem, in which both the cylinder and the surrounding material are included in the finite-difference nodal mesh, there are fifteen different forms for the nodal finite-difference equations corresponding to the locations labeled (a)–(o) in Figure 5.

2.3.3 Boundary Conditions An advantage of the control-volume approach in deriving the finite-difference equations is the ease with which the boundary conditions and material boundaries are incorporated in the finite-difference model. The continuous forms of the boundary conditions for the two-dimensional model were introduced in Sections 2.1.1–2.1.4. Recall that the single-material problem uses one of the three limiting cases for outer-radial boundary condition on the cylinder. The two-material problem must also use one of the three limiting cases for the outer-radial boundary condition on the surrounding material. The boundary between the materials in the two-material problem will require special consideration.

To incorporate the front surface boundary condition in the finite-difference model, the nodal energy balance for nodes at the front surface is modified. The

heat flux into the nodal region across the front surface, q_3, is determined from the front surface boundary condition, Equation (6):

$$q_3 = \begin{cases} h_{FRONT}(T_{f_{FRONT}} - T^j_{n,0}) + q_g & \text{for } 0 \leq n \leq N_{DISK} \\ h_{FRONT}(T_{f_{FRONT}} - T^j_{n,0}) & \text{for } N_{DISK} + 1 \leq n \leq N_{MAX} \end{cases} \tag{57}$$

The only approximation in applying the front surface boundary condition to the finite-difference model is the assumption that the heat flux is constant across the nodal region and equal to the heat flux evaluated at the node. Assuming that the heat flux is constant is equivalent to assuming that the temperature on the surface of the nodal region is constant and equal to the temperature at the node.

The back surface boundary conditon is incorporated similarly. The nodal energy balance for nodes on the back surface uses the back surface boundary condition of Equation (7) to determine the heat flux into the node across the back surface:

$$q_4 = h_{BACK}(T_{f_{BACK}} - T^j_{n,M_{MAX}}) \tag{58}$$

One of the three limiting cases for the outer-radial boundary condition must be used for the outer-radial boundary condition of the system. To use the fully-insulated case, the energy balance for nodes on the outer-radial boundary is modified by setting the heat flux into the node from a larger radial position equal to zero:

$$q_2 = 0 \tag{59}$$

The cases for maximum heat flux out across the boundary and maximum heat flux in across the boundary are realized by keeping the temperature of the node on the boundary equal to some constant. The nodes on the outer-radial boundary do not need a finite-difference equation since the temperature at the next time level does not change. In the case for maximum heat flux out, the temperature at each node on the outer-radial boundary remains at the initial temperature:

$$T_{N_{MAX},m} = T_i \tag{60}$$

In the case for maximum heat flux in across the outer-radial boundary, the temperature at each node on the outer-radial boundary remains at the fluid temperature:

$$T_{N_{MAX},m} = T_f \tag{61}$$

2.3.4 The Boundary Between Materials For the two-material problem, in which the thermal conductivities of the materials are different, the temperature gradient at the boundary between the materials is discontinuous. Nevertheless, energy is still conserved. Because the control-volume approach is based on the conservation of energy for each nodal volume, the development of the finite-difference equations for nodes on the boundary between the materials remains essentially the same. The same assumptions are used with special care to account for the change in properties. Figure 7 shows the nodal geometry for a node on the boundary between the materials.

The conductivities to use in the expression for heat fluxes q_1 and q_2 are readily apparent. Heat flux q_1 in the cylinder uses the thermal conductivity of the cylinder, while heat flux q_2 in the surrounding material uses the thermal conductivity of the surrounding material:

$$q_1 = k\frac{(T^j_{N_{CYL}-1,m} - T^j_{N_{CYL},m})}{\Delta r} \tag{62}$$

$$q_2 = k'\frac{(T^j_{N_{CYL}+1,m} - T^j_{N_{CYL},m})}{\Delta r} \tag{63}$$

The heat flux at the front and back surfaces, q_3 and q_4, is a function of both thermal conductivities. The axial temperature gradient at each surface is still assumed constant and equal to the axial temperature gradient evaluated at the boundary. However, the heat flux at the portion of the surface in the cylinder is determined using the thermal conductivity of the cylinder, while the heat flux at the portion of the surface in the surrounding material is determined using the thermal conductivity of the surrounding material. The heat flow through each portion of each surface is the product of the heat flux at each portion of each surface times

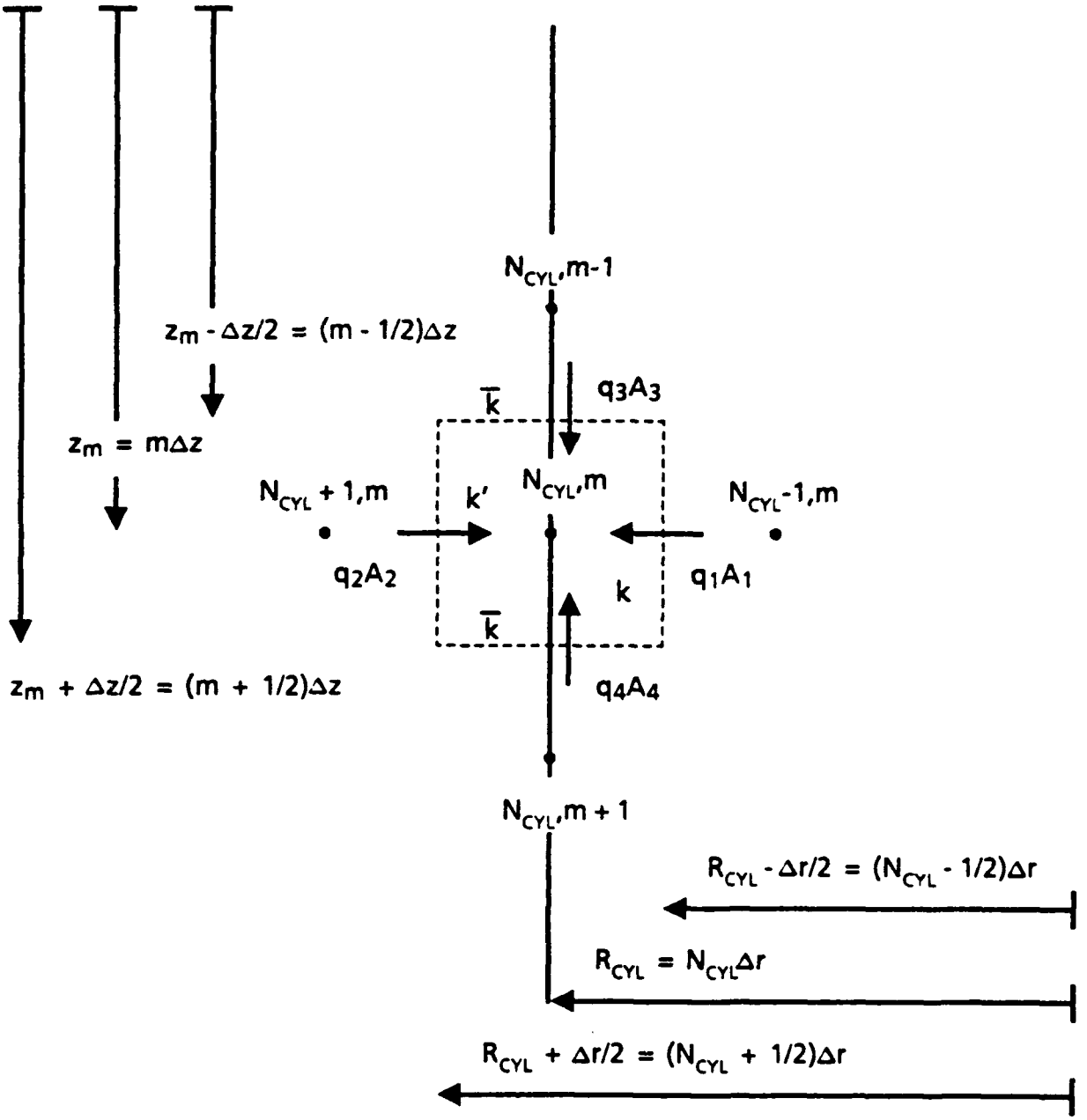

Figure 7. Nodal Geometry for a Node on the Boundary Between Materials

the area of the portion of the surface. Then, the total heat flow across each surface is equal to the sum of the heat flows across each portion. Finally, the average heat flux across each surface is the total heat flow divided by the total surface area.

An equivalent method of calculating the heat flux at each surface is to use an average value for thermal conductivity, $\overline{k}$, which is weighted according to the fraction of the surface area in each of the two materials:

$$\overline{k} = \frac{k(N_{CYL} - 1/4) + k'(N_{CYL} + 1/4)}{2N_{CYL}} \tag{64}$$

Then, the finite-difference expressions for q_3 and q_4 are

$$q_3 = \overline{k}\frac{(T^j_{N_{CYL},m-1} - T^j_{N_{CYL},m})}{\Delta z} \tag{65}$$

$$q_4 = \overline{k}\frac{(T^j_{N_{CYL},m+1} - T^j_{N_{CYL},m})}{\Delta z} \tag{66}$$

The total thermal capacity of the nodal volume is equal to the thermal capacity contributed by the surrounding material plus the thermal capacity contributed by the quartz material. The thermal capacity contributed by the surrounding material is the thermal capacitance of the surrounding material times the part of the nodal volume made up by the surrounding material. The thermal capacity contributed by the quartz material is determined similarly. Again, an equivalent method of calculating the total thermal capacity is to multiply the total nodal volume by an average thermal capacitance which this time is weighted by the fraction of volume in each material:

$$(\overline{\rho c_p}) = \frac{(\rho c_p)(N_{CYL} - 1/4) + (\rho c_p)'(N_{CYL} + 1/4)}{2N_{CYL}} \tag{67}$$

Then, the energy storage term for nodal volumes on the boundary between the materials is

$$\dot{E}_{store} = (\overline{\rho c_p})\Delta V\frac{(T^{j+1}_{N_{CYL},m} - T^j_{N_{CYL},m})}{\Delta t} \tag{68}$$

2.3.5 Non-Dimensional Nodal Equations The nodal equations are non-dimensionalized the same way that the differential equations are non-dimensionalized. First, the non-dimensional form of the variables is specified. Then, the non-dimensional form of the equations determines the relevant non-dimensional parameters in the problem. As explained in Section 2.2, the total heat transfer problem is divided into two seperate problems, the preheating problem and the disturbance problem. The two problems use different non-dimensional forms for the dependent variables T and q but the same non-dimensional forms for the independent variables r, z and t. The non-dimensional nodal equations are the same except for the nodes on both the front and back surfaces (see Section 2.2).

The non-dimensional forms for temperature and heat flux in the preheating and disturbance problems are given in Equations (13)–(16) in Section 2.2. As in the dimensional form of the nodal equations, the independent variables in the non-dimensional nodal equations are expressed as an index value multiplied by a non-dimensional step size:

$$r^+ = n\Delta r^+ \tag{69}$$

$$z^+ = m\Delta z^+ \tag{70}$$

$$t^+ = j\Delta t^+ \tag{71}$$

The non-dimensional step sizes are

$$\Delta r^+ = \frac{\Delta r}{R_{CYL}} = \frac{1}{N_{CYL}} \tag{72}$$

$$\Delta z^+ = \frac{\Delta z}{L} = \frac{1}{M_{MAX}} \tag{73}$$

$$\Delta t^+ = \frac{\alpha \Delta t}{L^2} \tag{74}$$

The outer-radial boundary of the cylinder is always at non-dimensional radius of 1.0. Then, for the two-material problem, non-dimensional radius values in the surrounding material are greater than 1.0. Similarly, the back surface of the cylinder is always at non-dimensional axial dimension of 1.0.

The non-dimensional, finite-difference model does include the very same non-dimensional parameters introduced in Section 2.2. Three additional non-dimensional parameters in the finite-difference model are the non-dimensional step sizes; Δr, Δz and Δt. One can think of the index variables n, m and j as being the independent variables in the finite-difference model, while the non-dimensional step sizes are additional parameters peculiar to the finite-difference model. The continuous model should be equivalent to the limiting case of the finite-difference model as the step sizes approach zero. Two other property ratios, $\overline{k}/k$ and $\rho c_p/\overline{\rho c_p}$, appear in the non-dimensional nodal equations for nodes on the boundary between the two materials. However, these two property ratios are functions of other independent, non-dimensional parameters:

$$\frac{\overline{k}}{k} = \frac{(1 - 1/4\Delta r^+) + \left[\frac{k'}{k}\right](1 + 1/4\Delta r^+)}{2} \tag{75}$$

$$\frac{(\rho c_p)}{(\overline{\rho c_p})} = \left(\frac{(1 - 1/4\Delta r^+) + \left[\frac{(\rho c_p)}{(\rho c_p)'}\right]^{-1}(1 + 1/4\Delta r^+)}{2}\right)^{-1} \tag{76}$$

The non-dimensional nodal equations for the single-material and two-material problems using the fully-insulated, outer-radial boundary condition are given in Appendices A.1 and A.2, respectively. To use the outer-radial boundary conditions for maximum heat flux out or maximum heat flux in, the nodal equations for nodes on the outer-radial boundary are omitted, and the temperatures for nodes on the outer-radial boundary are set to the appropriate constant values. For the limiting case of maximum heat flux out, the non-dimensional temperature at the outer-radial boundary is zero. For the limiting case of maximum heat flux in, the non-dimensional temperature at the outer-radial boundary is zero for the preheating problem and one for the disturbance problem (see Equations 27, 28, 35 and 36).

2.3.6 Stability Criterion When using an explicit method, the time step can not be chosen arbitrarily. The time step must be small enough to ensure that the system is stable. The instability in an explicit method results from evaluating the

finite-difference expression for net heat flux into the nodal volume at the old time step rather than at the new time step or a combination of the new and old [4:p.215]. The change in temperature during a time step tends to reduce the temperature gradients that caused the net heat flux, which then decreases the magnitude of the net heat flux into the control volume. For example, if heat is flowing into a control volume at some time level, the temperature in that control volume will increase. The increase in temperature of the control volume will tend to reduce the temperature gradients that caused the heat to flow into the control volume, which in turn decreases the rate at which heat continues to flow into the control volume.

The explicit method ignores this compensatory effect. Instead, the explicit method evaluates the net heat flux into the nodal volume at the old time level and assumes that this net rate of energy flow into the control volume is constant throughout the next time step. It then predicts the temperature at the node for the new time level using the net rate of energy flow evaluated from the old time level. As a result, if the time step is too large, the explicit method can predict a change in temperature which violates the second law of thermodynamics. The overprediction in each step of the explicit method can also cause the solution to oscillate without necessarily becoming unstable. Instabilities occur when these oscillations grow so that eventually the temperatures alternate between increasingly larger positive and negative values.

Incropera and Dewitt suggest a criterion to use in finding the maximum allowable time step [4:p.215]. The criterion they suggest is easy to use and not only assures that the system will be stable but also helps to assure that the solution will not oscillate. For heat transfer with constant boundary conditions, temperatures at each node should change smoothly in one direction. Temperatures should not increase in one time step, decrease in the next, and increase in the following. Incropera and Dewitt suggest limiting the time step so that the coefficients in front

of the temperature terms in all the nodal equations (see Appendix A) are positive. It is easy to see that this criterion assures stability; if this criterion is satified, there is no mechanism for non-dimensional temperatures to become negative. It is important to apply the criterion to all nodal equations and not just the interior nodal equations. If a solution diverges at any node, the whole solution will eventually diverge. In fact, the nodal equations for nodes on the boundaries in the two-dimensional model will have more severe stability requirements because their dimensions are smaller. Although the criterion suggested by Incropera and Dewitt is a sufficient but not necessary criterion for stability, the time steps determined using the criterion are often very close to time steps which cause instability in the two-dimensional model.

For the single-material problem, the nodal equation for the node at the centerline and on the surface with the larger Biot number, usually the front surface, has the most severe stability requirement (node (a) in Figure 4):

$$\Delta t^+ < \left(4 \left[\frac{L}{R_{CYL}} \right]^2 N_{CYL}^2 - 2M_{MAX}^2 - 2Bi_{MAX} M_{MAX} \right)^{-1} \tag{77}$$

For the two-material problem, the nodal equation with the most severe stability requirement depends on the values of the property ratios. In any case, the node with the most severe stability requirement is again a node on the surface with the larger Biot number, usually the front surface. The node with the governing requirement may be the node at the centerline, the node at the material boundary or any of the nodes between the material boundary and the outer-radial boundary (node (a), node (c) or nodes in region (d) in Figure 5). The stability requirement for these three nodal equations in their respective order are

$$\Delta t^+ < \left(4 \left[\frac{L}{R_{CYL}} \right]^2 N_{CYL}^2 - 2M_{MAX}^2 - 2Bi_{MAX} M_{MAX} \right)^{-1} \tag{78}$$

$$\Delta t^+ < \left\{ \left[\frac{(\rho c_p)}{(\overline{\rho c_p})} \right] \left[\frac{L}{R_{CYL}} \right]^2 N_{CYL} \left[(N_{CYL} - 1/2) + \left[\frac{k'}{k} \right] (N_{CYL} + 1/2) \right] \right.$$

$$+2\left[\frac{(\rho c_p)}{(\overline{\rho c_p})}\right]\left[\frac{\bar{k}}{k}\right]M_{MAX}^2+2\left[\frac{(\rho c_p)}{(\overline{\rho c_p})}\right]Bi_{MAX}M_{MAX}\Bigg\}^{-1} \tag{79}$$

and

$$\Delta t^+ < \left(2\left[\frac{(\rho c_p)}{(\rho c_p)'}\right]\left[\frac{k'}{k}\right]\left[\frac{L}{R_{CYL}}\right]^2 N_{CYL}^2+2\left[\frac{(\rho c_p)}{(\rho c_p)'}\right]\left[\frac{k'}{k}\right]M_{MAX}^2 +2\left[\frac{(\rho c_p)}{(\rho c_p)'}\right]Bi_{MAX}M_{MAX}\right)^{-1} \tag{80}$$

The second two stability requirements can become more severe than the first for cases in which $(\rho c_p)/(\rho c_p)' > 1$ or $k'/k > 1$ or both.

2.3.7 Convergence Criterion for the Preheating Problem The preheating problem models the time after the instrumentation is turned on during which the Wheatstone bridge is being balanced. The preheating of the quartz cylinder continues until the temperature of the thin-film sensor stabilizes enough that the bridge can be balanced. When simulating the preheating problem, some criterion must be used to determine when to end the preheating problem and begin the disturbance problem. The criterion used in the simulation models the decision to end the preheating problem by quitting when the rate of change in the solution is less than some tolerance value. Specifically, at each time level the criterion picks the largest change in non-dimensional temperature at any node, divides the absolute value of that largest change by the largest non-dimensional temperature in the system, and then divides this normalized maximum change by the time step to arrive at a maximum normalized rate of change. The maximum normalized rate of change is then compared with the tolerance value. Figure 8 illustrates the decision.

The maximum change is normalized with the largest non-dimensional temperature at that time step to better model the decision process. To an external observer the system seems to stabilize when the *noticeable* rate of change is small. The normalized rate of change measures the noticeable rate of change. For example, a non-dimensional temperature change of 0.002 in one time step can represent

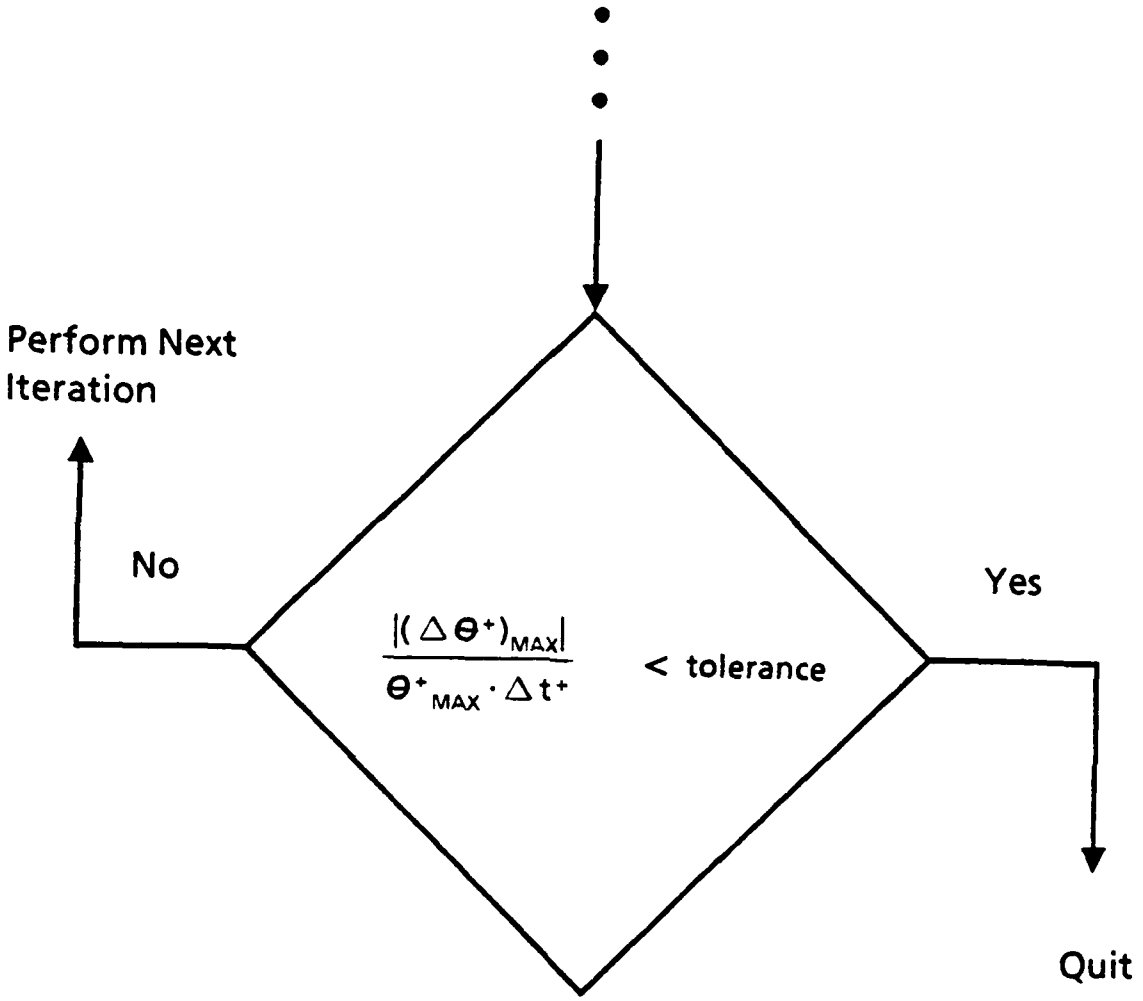

Figure 8. Convergence Criterion

a significant rate of change when the maximum non-dimensional temperature value at that time is 0.04. However, the same non-dimensional temperature change of 0.002 in another time step can represent an insignificant and unnoticeable rate of change if the maximum non-dimensional temperature value at that time is on the order of 1.

2.4 The One-Dimensional Series Solution

Thin-film heat transfer gages measure the temperature on the front surface of the gage at the location of the thin-film sensor. Surface heat flux is derived from this data using the one-dimensional series solution first proposed by Cook and Felderman [2:pp.561–562]. The underlying assumption for the series solution is that the quartz cylinder behaves as an initially isothermal, semi-infinite solid.

The governing equation for temperature in a semi-infinite solid is [4:p.202]

$$\frac{\partial \theta}{\partial t} = \alpha \frac{\partial^2 \theta}{\partial x^2} \tag{81}$$

where x is the distance into the solid. The initial condition and the boundary condition for large x in an initially isothermal, semi-infinite solid are

$$\theta(x, t \leq 0) = 0 \tag{82}$$

$$\theta(x \rightarrow \infty, t > 0) = 0 \tag{83}$$

The series solution is based on the solution for temperature in a semi-infinite solid with constant surface temperature. The front surface boundary condition on x for the problem with constant surface temperature is

$$\theta(x = 0, t > 0) = \theta_s \tag{84}$$

The solution for temperature in the semi-infinite solid with constant surface temperature is [4:p.203]

$$\theta(x, t) = \theta_s \text{erfc}\left(\frac{x}{2\sqrt{\alpha t}}\right) \tag{85}$$

Using the Duhammel superposition method and this temperature solution, one can derive a complete expression for the temperature distribution within an initially isothermal, semi-infinite solid when the surface temperature is some known function of time. This expression is in the form of an integration over time of the surface temperature. One can then solve for the surface heat flux at any time using Fourier's conduction law immediately below the surface, $q_s = -k\frac{d\theta}{dx}\Big)_{x=0}$. The expression for surface heat flux is also in the form of an integration over time of the surface temperature. The integral expression used by Cook and Felderman, modified slightly to be in terms of basic properties, is

$$q_s(t) = \frac{k}{\pi^{1/2}\alpha^{1/2}}\left[\frac{\theta_s(t)}{t^{1/2}} + \frac{1}{2}\int_{\lambda=0}^{\lambda=t}\frac{\theta_s(t)-\theta_s(\lambda)}{(t-\lambda)^{3/2}}d\lambda\right] \tag{86}$$

Cook and Felderman proposed to approximate the exact integral solution for surface heat flux by approximating the surface temperature function as a piecewise linear function of time. Then, the integral in Equation 86 can be performed exactly. The resulting equation for surface heat flux is in the form of a series summation of surface temperatures at discrete values of time. Rearranged slightly, Cook and Felderman's series solution for surface heat flux is [5:p.12]

$$q_s(t_J) = \frac{2k}{\pi^{1/2}\alpha^{1/2}}\left[\frac{\theta_s(t_0)}{2t_J^{1/2}} + \sum_{j=1}^{J}\frac{\theta_s(t_j)-\theta_s(t_{j-1})}{(t_J-t_j)^{1/2}+(t_J-t_{j-1})^{1/2}}\right] \tag{87}$$

For a solid that does behave like an initially isothermal, semi-infinite solid, the only approximation results from modeling the actual surface temperature function as a piecewise linear function of time. Cook and Felderman tested the series solution for some cases in which surface heat flux into a semi-infinite solid is known analytically. They show that when exact values for surface temperature are used in the series, the series solution is well behaved and fairly accurate. Surface heat flux values tend to be slightly high, but accuracy improves when smaller time intervals are used.

2.5 *Comparing the Series Solution Estimate with the Simulated Surface Heat Flux*

The temperatures from the two-dimensional simulation are used in the series solution to get the series solution estimate for external surface heat flux. The objective of this analysis is to evaluate the accuracy of the series solution by comparing these series solution estimates to the actual, external surface heat flux from the simulation.

To use the series solution with temperatures from the two-dimensional model, the series solution must also be non-dimensionalized. Using the non-dimensional form for the disturbance problem, the non-dimensional series solution is

$$q^{+J}_{s} = \frac{2}{{}_{d}Bi_{FRONT}(\pi\Delta t^{+})^{1/2}}\left[\frac{\theta^{+0}_{s}}{2J} + \sum_{j=1}^{J}\frac{\theta^{+j}_{s} - \theta^{+j-1}_{s}}{(J-j)^{1/2} + (J-j+1)^{1/2}}\right] \tag{88}$$

When using the gages in the laboratory, one calculates a single value for the surface temperature from the change in resistance of the thin-film sensor. When the temperature is not constant over the front surface of the gage, the temperature determined from the resistance change of the sensor is some average temperature of the surface of the gage at the thin film.

A good way to model the process of finding a single average temperature is to average the nodal temperatures in the region covered by the thin-film sensor. The average should be a weighted average in which the individual nodal temperatures are weighted by the fraction of the total surface area of the sensor covered by each of the nodal regions. For the two-dimensional model, a simplified form of the weighted average is

$$\theta^{+}_{s,AVE} = \frac{1/4\theta^{+}_{s,0} + 2\sum_{n=1}^{N_{DISK}} n\theta^{+}_{s,n}}{(N_{DISK} + 1/2)^{2}} \tag{89}$$

The average surface temperatures can then be used in the series solution to find the series solution estimate for external surface heat flux.

The surface heat flux value to which the series solution estimate is compared is the actual average, external surface heat flux from the finite-difference model

in the region of the heated disk. From Equation (30), the non-dimensional, external surface heat flux at each node in the region of the heated disk during the disturbance problem is

$$q^{+J}_{s,n} = 1 - \theta^{+J}_{s,n} \tag{90}$$

The average, external surface heat flux is found using Equation (89) and replacing the nodal temperatures with the nodal surface heat fluxes.

An alternate and equivalent method for finding the average, external surface heat flux from the finite-difference model is to use the average surface temperatures from Equation (89) directly in Equation (90). Similarly, an alternate and equivalent method for finding the series solution estimate is to use the temperatures at each node in the non-dimensional series approximation to find series solution estimates for heat flux at each node and then to take a weighted average of these series solution estimates.

The series solution and finite-difference estimates for external surface heat flux are compared by finding their difference. The difference in the two estimates is automatically normalized with respect to the maximum theoretical, external surface heat flux by the non-dimensional form used in the disturbance problem. The external surface heat flux is maximum if the surface temperature is the undisturbed initial temperature, T_i:

$$q_{s,MAX} = {}_d h_{f_{FRONT}}({}_d T_{f_{FRONT}} - T_i) \tag{91}$$

This maximum, external surface heat flux is 1.0 in non-dimensional terms. Then, the difference in the non-dimensional series solution and finite-difference estimates multiplied by 100.00 is also the percent difference of the two estimates relative the maximum theoretical, external surface heat flux:

$$\text{Percent Difference} = (q^{+}_{SER} - q^{+}_{F.D.}) \times 100.00 \tag{92}$$

The code used in the analysis to compare the series solution and the finite-difference estimates for external surface heat flux is given in Appendix D.3.

III. Check Cases

Check cases on the finite-difference model serve the same purpose that calibration serves in laboratory experiments. Check cases test the model for gross errors (i.e. typing errors and other debugging problems) and systematic errors that result from finite-differencing. The check cases will each be simplified problems for which an analytical solution exists. As a result, they will check individual aspects of the model separately. The check cases should ultimately show how accurate the model is for its intended use and in what ways or under what conditions the model may be inaccurate.

The check cases for the finite-difference model are divided into three categories. The first two are steady-state cases for one-dimensional heat transfer in the axial direction and then the radial direction. The third catagory includes transient cases for one-dimensional heat transfer in the axial direction only. The steady-state cases primarily check the accuracy of the spatial derivatives in each of the two directions. The accuracy to which the solutions converge on the correct steady-state values should indicate the accuracy of the derivatives. Another check on the accuracy of the derivatives would be to observe the transient temperature profiles during the steady-state cases to assure that the transient solutions progress logically toward the steady-state solution. Also, one can check for gross errors simply by assuring that the heat transfer is indeed one-dimensional at each time step.

The transient cases check the accuracy of the time derivatives in the model in conjunction with the axial derivatives only. However, if the time derivatives are accurate for axial heat transfer, then they should also be accurate for radial heat transfer. The transient cases also check the accuracy of the series solution for surface heat flux when the solid does behave as an initially isothermal, semi-infinite solid. Although the transient cases could be used to check the accuracy of transient temperature profiles in the solid, the transient cases were used to check the

accuracy of only transient surface temperatures since the model is primarily used to produce transient surface temperatures for the analysis. The series solution was checked using both the analytical values for surface temperature and the surface temperatures produced by the finite-difference model in order to distinguish between inaccuracies inherent to the series solution and those caused by the surface temperatures produced by the finite-difference model.

3.1 One-Dimensional, Steady-State Heat Transfer in the Axial Direction

The one-dimensional, steady-state check cases for heat transfer in the axial direction are separated into cases using the preheating problem and cases using the disturbance problem. To obtain one-dimensional heat transfer in the preheating problem, the heat generation must be uniform over the front surface. Uniform surface heat generation is obtained by making the heated disk as wide as the cylinder and by using the single-material problem only. The check cases for the preheating problem include cases in which the Biot number at the back surface is either zero or non-zero.

One-dimensional heat transfer can be obtained in the disturbance problem using either uniform surface heat generation or no surface heat generation. When surface heat generation is absent, heat transfer will be one-dimensional for both the single-material problem and the two-material problem with property ratios of unity. Because the results for the two problems are identical, only the results for the single-material problem are shown. The check cases for the disturbance problem include cases in which surface heat generation is either uniform over the surface of the cylinder or absent and in which the Biot number at the back surface is either zero or non-zero.

The analytical solutions for one-dimensional, steady-state heat transfer in the axial direction were determined using thermal networks developed from the electrical analogy [4:pp.64–65]. For one-dimensional, steady-state heat transfer in

the axial direction, Equation (3) reduces to

$$\frac{\partial}{\partial z}\left(\frac{\partial T}{\partial z}\right) = 0 \tag{93}$$

Heat flux is constant because the temperature gradient is constant. When the temperature gradient is constant, both the temperature gradient and the temperature profile through the solid are completely specified by the temperatures at the front and back surfaces. Then, for one-dimensional, steady-state heat transfer in the axial direction, the following system of simultaneous equations completely specifies the analytical solution:

$$q_z = k\frac{(T_s - T_b)}{L} \tag{94}$$

$$q_s = h_{FRONT}(T_{f_{FRONT}} - T_s) + q_{gen} \tag{95}$$

$$q_b = h_{BACK}(T_b - T_{f_{BACK}}) \tag{96}$$

$$q_z = q_s = q_b \tag{97}$$

The simultaneous equations governing one-dimensional, steady-state heat transfer in the axial direction are similar to equations governing current flow in electrical networks. Therefore, one can apply the mathematics used with electric circuits to analyze the heat transfer. In the electical analogy, heat flux is analogous to current density, and temperature difference is analogous to voltage difference. Nodes in the thermal network represent positions whose temperatures appear in the simultaneous equations. The four nodes in the thermal networks for the check cases represent the external fluid at the front and back surfaces and the front and back surfaces of the solid itself. Equation (97) is a statement of energy balance for the front and back surfaces of the solid. It is analogous to a statement of Kirchhoff's current law at the nodes corresponding to the front and back surfaces of the solid. Equations (94)–(96) are thermal analogies to Ohm's law from which thermal resistances for convection at the front and back surfaces and conduction through

the solid can be defined as follows:

$$(R_{t,conv})_{FRONT} = \frac{1}{h_{FRONT}} \quad (98)$$

$$(R_{t,conv})_{BACK} = \frac{1}{h_{BACK}} \quad (99)$$

$$R_{t,cond} = \frac{L}{k} \quad (100)$$

The heat generation on the front surface is modeled as a constant current into the network at the front surface.

To use the electrical analogy with the finite-difference model, non-dimensional thermal resistances and surface heat generation are determined by non-dimensionalizing the terms in Equations (94)–(97). Non-dimensional thermal resistances, surface heat generation and fluid temperatures for use in the preheating and disturbance problems are summarized by Table 1. To help visualize the thermal networks, the initial temperature, T_i, can be defined as a ground potential from which all other potentials are referenced.

Results for two cases, one a preheating problem and the other a disturbance problem are shown in Figures 9 and 10. The figures include a diagram of the corresponding thermal network for the conditions of the check case. The preheating problem shown in Figure 9 uses Biot numbers of 1.0 for the front surface and 0.5 for the back surface. The disturbance problem shown in Figure 10 uses Biot numbers of 0.5 for the front surface and zero for the back surface and a non-dimensional surface heat generation of 0.2. The analytical solution for this case is independent of the Biot number on the front surface. All cases used a non-dimensional time step of 0.004 and a non-dimensional step size of 0.1 in the axial direction. Results for the other preheating problems and disturbance problems are given in Appendices B.1.1 and B.1.2, respectively.

The finite-difference model requires a tolerance for use in the convergence criterion for all the steady-state problems. Section 2.3.7 explains the convergence

Table 1. Summary of Non-Dimensional Terms in the Electrical Analogy

	Preheating Problem	**Disturbance Problem**
θ^+	$\frac{T - T_i}{(q_g / {}_p h_{FRONT})}$	$\frac{T - T_i}{({}_d T_{f_{FRONT}} - T_i)}$
q^+	$\frac{q}{q_g}$	$\frac{q}{{}_d h_{FRONT}({}_d T_{f_{FRONT}} - T_i)}$
$R^+_{t,cond}$	$\frac{{}_p h_{FRONT} L}{k} = {}_p Bi_{FRONT}$	$\frac{{}_d h_{FRONT} L}{k} = {}_d Bi_{FRONT}$
$(R^+_{t,conv})_{FRONT}$	1	1
$(R^+_{t,conv})_{BACK}$	$\frac{{}_p Bi_{FRONT}}{{}_p Bi_{BACK}}$	$\frac{{}_d Bi_{FRONT}}{{}_d Bi_{BACK}}$
q^+_{gen}	1	$\frac{q_g / {}_d h_{FRONT}}{({}_d T_{f_{FRONT}} - T_i)} = \gamma$
$\theta^+_{f_{FRONT}}$	0	1
$\theta^+_{f_{BACK}}$	0	0

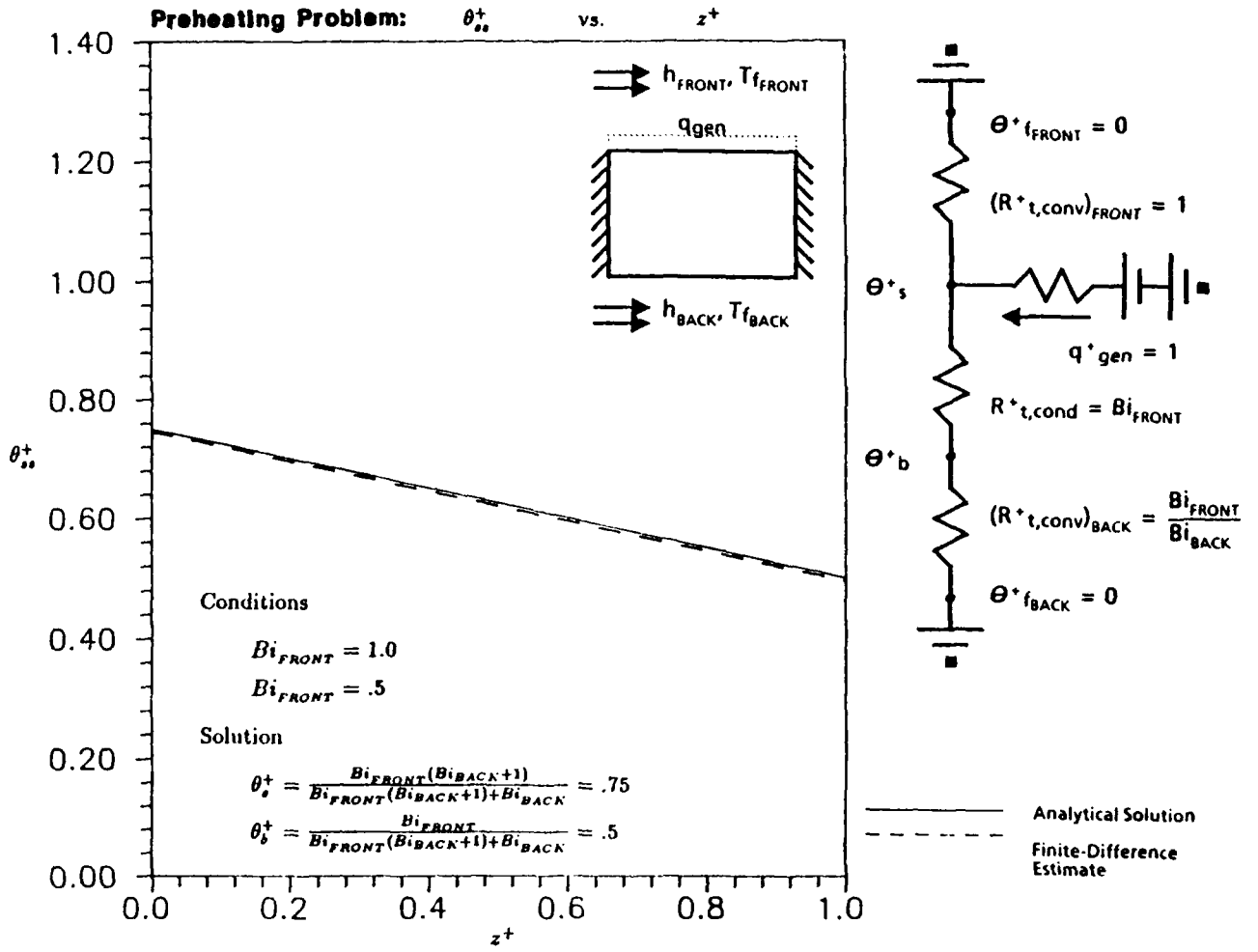

Figure 9. Sample Result for Steady State Heat Transfer in the Axial Direction Using the Preheating Problem

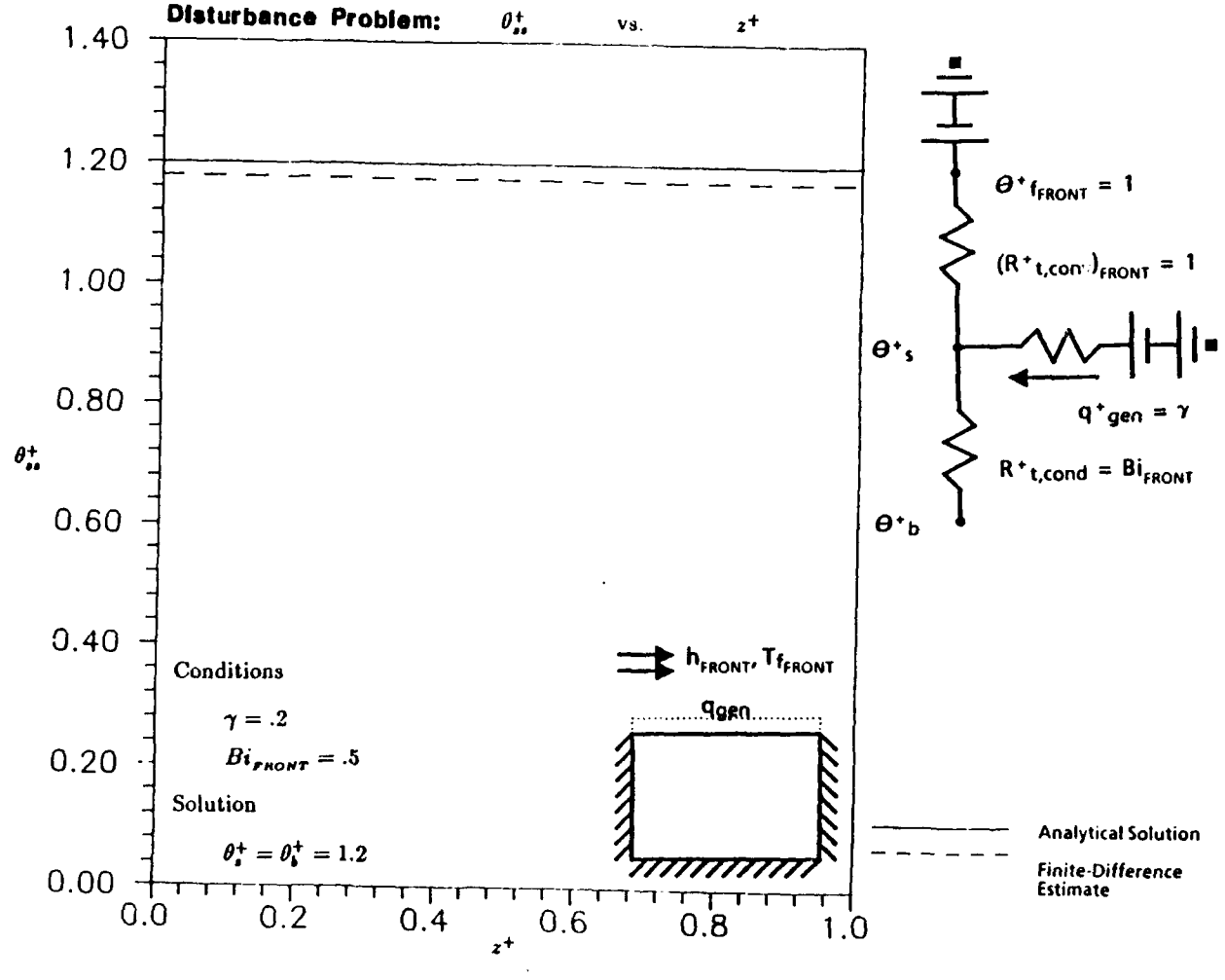

Figure 10. Sample Result for Steady State Heat Transfer in the Axial Direction Using the Disturbance Problem

criterion used in the model. The finite-difference model converges when the rate of change becomes small rather than when the error in the steady-state solution becomes small. As a result, the proximity of the transient solution to the true, analytical, steady-state solution when the model converges varies with the conditions as well as with the tolerance used in the convergence criterion. The steady-state check cases used a tolerance of 0.01 in the convergence criterion (see Section 2.3.7). For all check cases in the axial direction, a tolerance of 0.01 in the convergence criterion caused the transient solution to converge within 2 percent of the steady-state solution.

The two cases shown in Figures 9 and 10 were run with different values for the tolerance in the convergence criterion to demonstrate that the transient solutions do progress logically towards the steady-state solution. Figures 11 and 12 show the results. Also, the heat transfer in all cases was indeed one-dimensional indicating that there probably are no gross errors in the derivatives for the axial direction.

3.2 One-Dimensional, Steady-State Heat Transfer in the Radial Direction

There are four cases for one-dimensional, steady-state heat transfer in the radial direction. To obtain one-dimensional heat transfer in the radial direction, the heat flux across the front and back surfaces must be set to zero by setting the Biot numbers and the surface heat generation equal to zero. Because surface heat flux is zero, the resulting nodal equations in both the preheating and the disturbance problems are the same.

Both the single-material and the two-material problems produce one-dimensional heat transfer in the radial direction. For simplicity, property ratios of unity were used in the cases run on the two-material problem. Because of the way in which the radial dimension is non-dimensionalized, the results for the single-material problem and the two-material problem are different. Therefore, results for both problems are given.

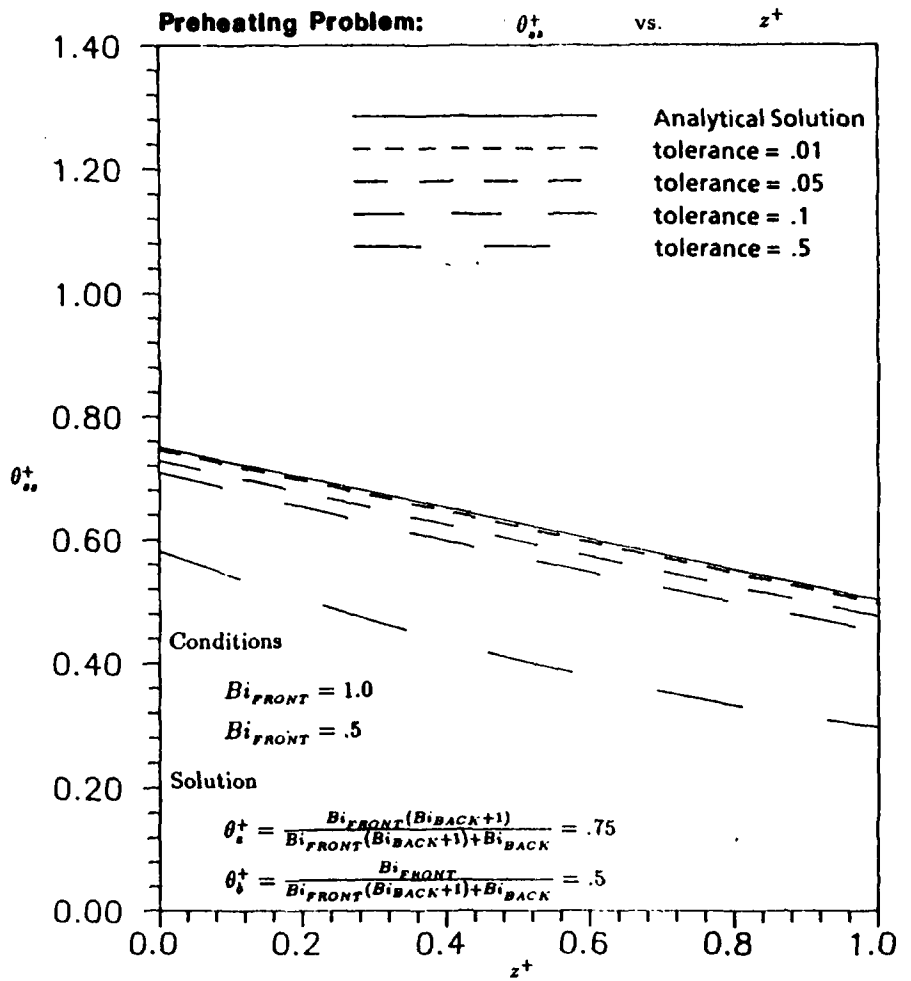

Figure 11. Sample Result for Steady State Heat Transfer in the Axial Direction Using the Preheating Problem with Different Values for the Tolerance

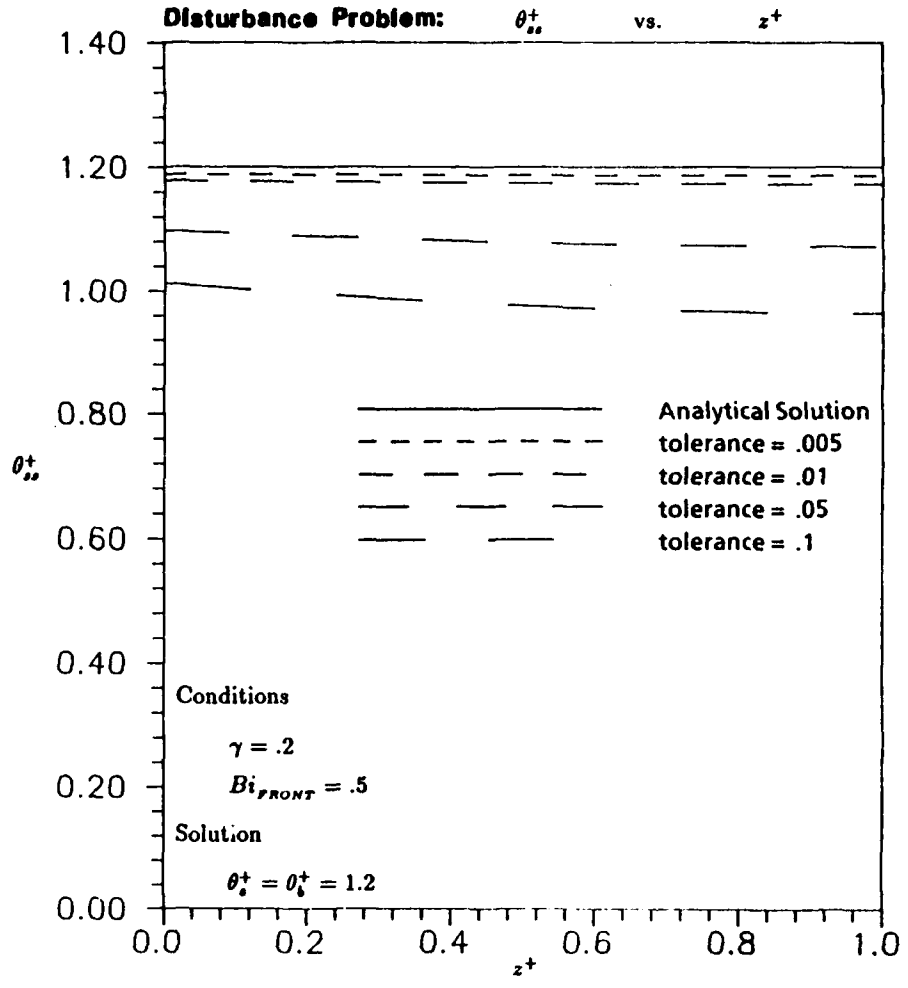

Figure 12. Sample Result for Steady State Heat Transfer in the Axial Direction Using the Disturbance Problem with Different Values for the Tolerance

The analytical solutions for one-dimensional, steady-state heat transfer in the radial direction were determined by solving the differential equation. For one-dimensional, steady-state heat transfer in the radial direction, Equation (3) in non-dimensional form reduces to

$$\frac{1}{r^+}\frac{\partial}{\partial r^+}\left(r^+\frac{\partial \theta^+}{\partial r^+}\right) = 0 \tag{101}$$

Integrating the equation twice yields

$$\frac{\partial \theta^+}{\partial r^+} = \frac{C_1}{r^+} \tag{102}$$

$$\theta^+ = C_1 \ln(r^+) + C_2 \tag{103}$$

where C_1 and C_2 are constants whose value depends on the boundary conditions.

When the inner-radial boundary condition is the symmetry condition of Equation (8), C_1 is equal to zero. When the inner-radial boundary condition is a specified temperature, it is necessary in general to specify the temperature at an inner radius other than zero, so one or more of the inner-radial nodes must be maintained at a constant temperature. The analytical solution for the rest of the model is then equivalent to the solution for heat transfer in a hollow cylinder with a specified temperature at the inner radius. Heat transfer in a hollow cylinder with inner radius

$$R^+_{INNER} = 1.5\Delta r^+$$

is simulated by equating the temperature of the first two radial nodes to a constant value. Because their temperatures are held constant, the nodal equations for these first two radial nodes are not used. Therefore, the check cases which specify a temperature for the inner-radial boundary condition do not check the radial derivatives for the nodal equations on the centerline.

The first radial check case checks the radial derivatives for nodes on the centerline by using the symmetry condition for the inner-radial boundary condition. The next three radial check cases check the three limiting cases for the outer-radial

boundary condition. Table 2 summarizes the boundary conditions and analytical solutions for the four one-dimensional, steady-state check cases for radial heat transfer.

For each check case using the single-material problem, the non-dimensional radial step size was 0.1. For each check case using the two-material problem, the non-dimensional radial step size was 0.2 and the non-dimensional geometry parameter, R_{MAX}/R_{CYL}, was 2.0. All cases used a total of eleven nodes in the radial direction, a non-dimensional time step of 0.003 and a tolerance of 0.01. Table 3 summarizes the analytical solutions for each of the radial check cases for both the single-material and two-material problems.

Figure 13 shows the results for the second check case using the single-material problem. The tolerance used in the convergence criterion was again varied to demonstrate that the transient solution does progress logically toward the steady-state solution, and this result is shown in Figure 14. The results for the other check cases using the single-material and two-material problems are given in Appendices B.2.1 and B.2.2, respectively. In the steady-state cases for heat transfer in the radial direction, some of the solutions converged farther from the true steady state solution than others. In general, cases in which heat flows radially outward seem to have a much slower rate of change so that the transient solution converges farther from the true steady-state solution. Cases using the two-material problem also generally converged farther from the true steady-state solution. Nevertheless, the transient profiles do progress logically and eventually converge on the steady state solution. The heat transfer was indeed one-dimensional in each case showing that there probably are no gross errors in the radial derivatives.

3.3 One-Dimensional, Transient Heat Transfer in the Axial Direction

Three cases for one-dimensional, transient heat transfer were used to check the finite-difference model and the series solution. The transient check cases only

	Boundary Conditions	Analytical Solution
Case 1	$\left.\frac{d\theta^+}{dr^+}\right)_{r^+=0} = 0$ $\theta^+(r^+ = R^+_{MAX}) = 1$	$\theta^+_{ss}(r^+) = 1 \quad \text{for } 0 \le r^+ \le R^+_{MAX}$
Case 2	$\theta^+(r^+ = R^+_{INNER}) = 1$ $\left.\frac{d\theta^+}{dr^+}\right)_{r^+=R^+_{MAX}} = 0$	$\theta^+_{ss}(r^+) = 1 \quad \text{for } 0 \le r^+ \le R^+_{MAX}$
Case 3	$\theta^+(r^+ = R^+_{INNER}) = 1$ $\theta^+(r^+ = R^+_{MAX}) = 0$	$\theta^+_{ss} = \begin{cases} 1 & \text{for } 0 \le r^+ \le R^+_{INNER} \\ \frac{-\ln(r^+/R^+_{MAX})}{\ln(R^+_{MAX}/R^+_{INNER})} & \text{for } R^+_{INNER} \le r^+ \le R^+_{MAX} \end{cases}$
Case 4	$\theta^+(r^+ = R^+_{INNER}) = 0$ $\theta^+(r^+ = R^+_{MAX}) = 1$	$\theta^+_{ss} = \begin{cases} 0 & \text{for } 0 \le r^+ \le R^+_{INNER} \\ \frac{\ln(r^+/R^+_{INNER})}{\ln(R^+_{MAX}/R^+_{INNER})} & \text{for } R^+_{INNER} \le r^+ \le R^+_{MAX} \end{cases}$

Table 2. Boundary Conditions and Analytical Solutions for Steady-State Heat Transfer in the Radial Direction

	Single-Material Problem	Two-Material Problem
Δr^+	.10	.20
R^+_{INNER}	.15	.30
R^+_{MAX}	1.00	2.00
Case 1	$\theta^+_{ss}(r^+) = 1 \quad \text{for } 0 \le r^+ \le 1.0$	$\theta^+_{ss}(r^+) = 1 \quad \text{for } 0 \le r^+ \le 2.0$
Case 2	$\theta^+_{ss}(r^+) = 1 \quad \text{for } 0 \le r^+ \le 1.0$	$\theta^+_{ss}(r^+) = 1 \quad \text{for } 0 \le r^+ \le 2.0$
Case 3	$\theta^+_{ss} = \begin{cases} 1 & \text{for } 0 \le r^+ \le .15 \\ \frac{\ln(r^+)}{\ln(.15)} & \text{for } .15 \le r^+ \le 1.0 \end{cases}$	$\theta^+_{ss} = \begin{cases} 1 & \text{for } 0 \le r^+ \le .30 \\ \frac{\ln(r^+)-\ln(2.0)}{\ln(.30)} & \text{for } .30 \le r^+ \le 2.0 \end{cases}$
Case 4	$\theta^+_{ss} = \begin{cases} 0 & \text{for } 0 \le r^+ \le .15 \\ \frac{\ln(r^+)-\ln(.15)}{-\ln(.15)} & \text{for } .15 \le r^+ \le 1.0 \end{cases}$	$\theta^+_{ss} = \begin{cases} 0 & \text{for } 0 \le r^+ \le .30 \\ \frac{\ln(r^+)-\ln(.30)}{\ln(2.0-\ln(.30)} & \text{for } .30 \le r^+ \le 2.0 \end{cases}$

Table 3. Analytical Solutions used in the Steady-State Check Cases for Heat Transfer in the Radial Direction

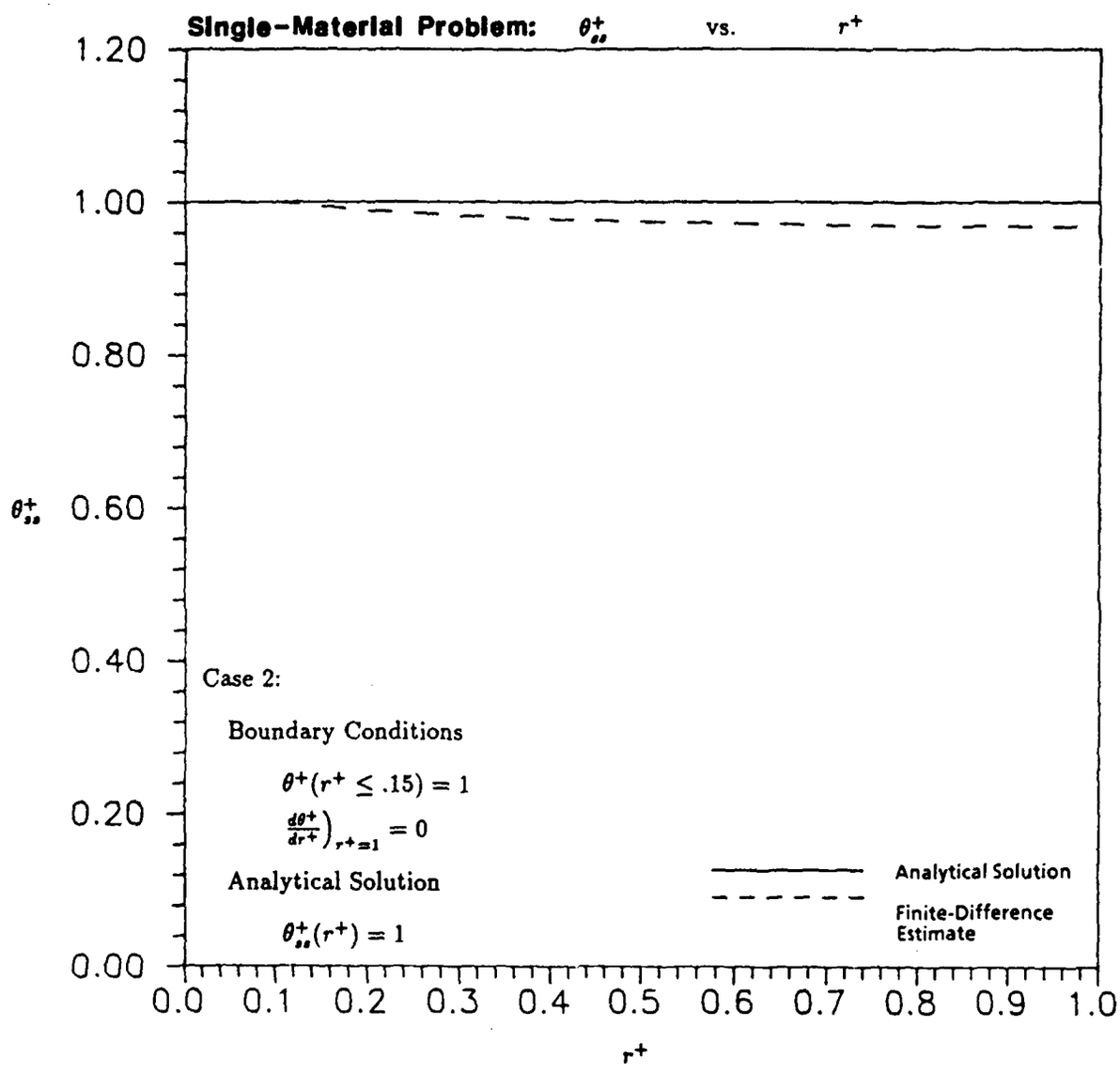

Figure 13. Sample Result for Steady State Heat Transfer in the Radial Direction

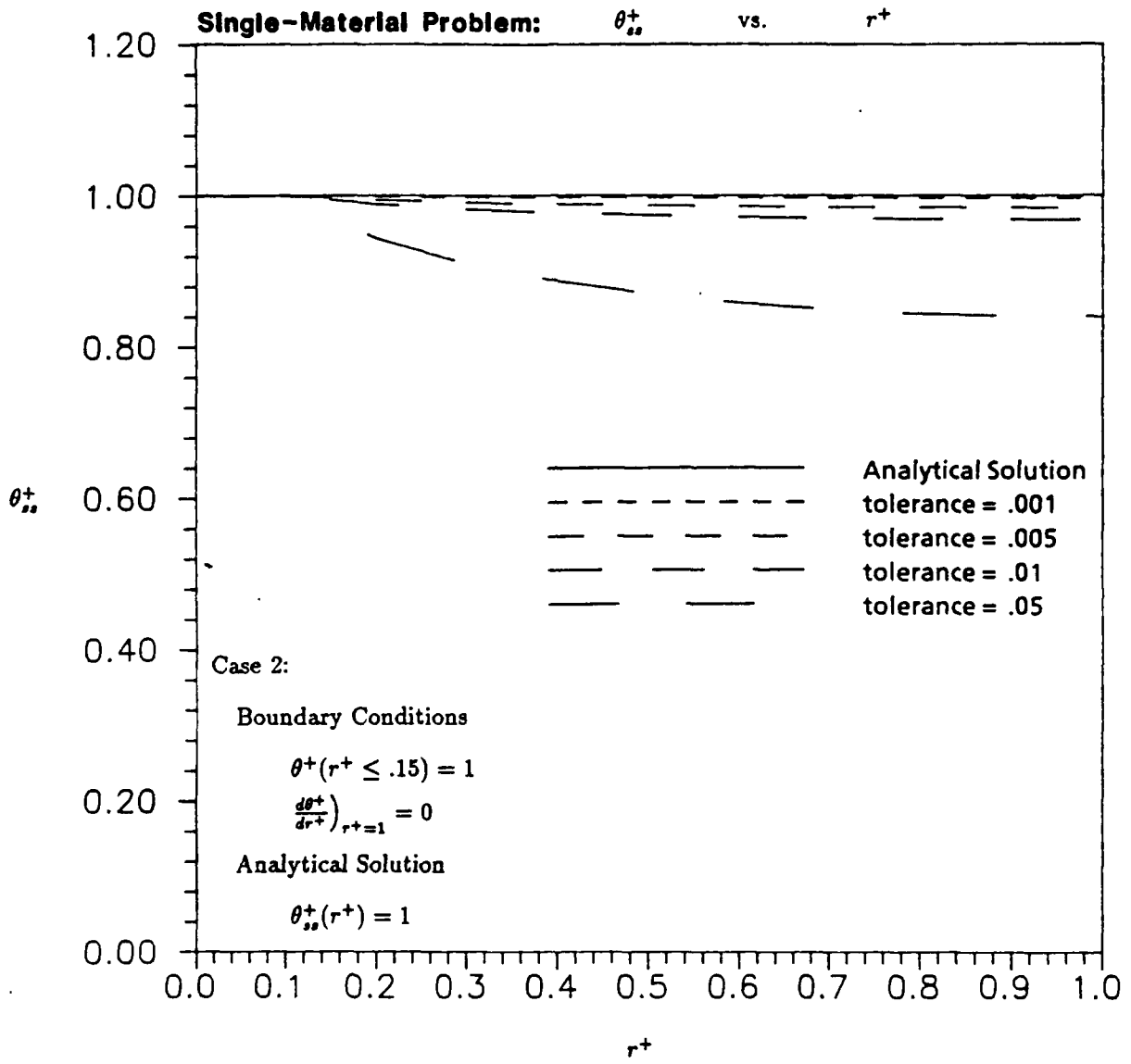

Figure 14. Sample Result for Steady State Heat Transfer in the Radial Direction with Different Values for the Tolerance

include problems with axial heat transfer. This should be sufficient since both the axial and radial derivatives proved accurate for steady-state heat transfer.

The transient cases were used in the following ways:

- To check the accuracy of the finite-difference model in producing non-dimensional surface temperatures and surface heat flux values.
- To check the accuracy of the non-dimensional series solution for cases in which the solid does behave as an initially isothermal, semi-infinite solid.
- To investigate the problems encountered when using the non-dimensional surface temperatures produced by the finite-difference model in the series solution.
- To determine suitable spatial and time steps to get sufficient accuracy from the model in the analysis and to estimate this accuracy.

Since heat transfer is one-dimensional in these check cases, it is not necessary to average surface temperatures or surface heat fluxes. Nevertheless, each case averaged the temperatures and heat fluxes of the first three radial nodes on the front surface in order to check the equations for finding average surface temperature and heat flux. The simulation of each case on the finite-difference model used non-dimensional spatial step sizes of 0.1 and three different non-dimensional time steps of 0.004, 0.001 and 0.0005.

The sections that follow describe each of the transient check cases giving the analytical solution for each and showing how each was implemented on the finite-difference model. The final section summarizes the results from the transient cases. Graphs from the first transient check case—the semi-infinite solid with convection—are used to illustrate points in the discussion. Graphs for the other two transient check cases are given in Appendices B.3.1 and B.3.2.

3.3.1 The Semi-Infinite Solid with Convection One-dimensional heat transfer in a semi-infinite solid with constant external fluid temperature and convection coefficient is readily simulated using the finite-difference model for the disturbance problem with a fully-insulated, outer-radial boundary. Figure 15 illustrates the conditions used in the two-dimensional model to simulate this transient solution. The parameters γ, τ and ${}_dBi_{BACK}$ are set to zero. Both the single-material problem and the two-material problem work. However, since both produce identical results, the results from only one are shown.

The cylinder will behave as a semi-infinite solid only for times less than the time it takes the leading edge of the thermal disturbance to travel the length of the cylinder. Using the approximation given by Equation (2), the simulation for this transient check case should only be valid for non-dimensional times less than

$$t^+ \approx \frac{1}{16} = 0.0625 \tag{104}$$

The check case was run slightly longer to non-dimensional time of 0.075.

The analytical solutions for non-dimensional surface temperature and surface heat flux for this transient check case are [4:pp.202–206]

$$\theta^+_s = 1 - \exp\left((Bi)^2 t^+\right) \operatorname{erfc}\left((Bi)t^{+1/2}\right) \tag{105}$$

$$q^+_s = 1 - \theta^+_s = \exp\left((Bi)^2 t^+\right) \operatorname{erfc}\left((Bi)t^{+1/2}\right) \tag{106}$$

where Bi is the Biot number at the front surface in the simulation, which was chosen to be 2.0.

3.3.2 The Semi-Infinite Solid with Constant Surface Heat Flux One-dimensional heat transfer in a semi-infinite solid with constant surface heat flux is simulated by a modified version of the finite-difference model for the preheating problem with a fully-insulated, outer radial boundary. By setting ${}_pBi_{FRONT}$ equal to zero and the ratio R_{DISK}/R_{CYL} equal to one, the heat flux over the front surface of the

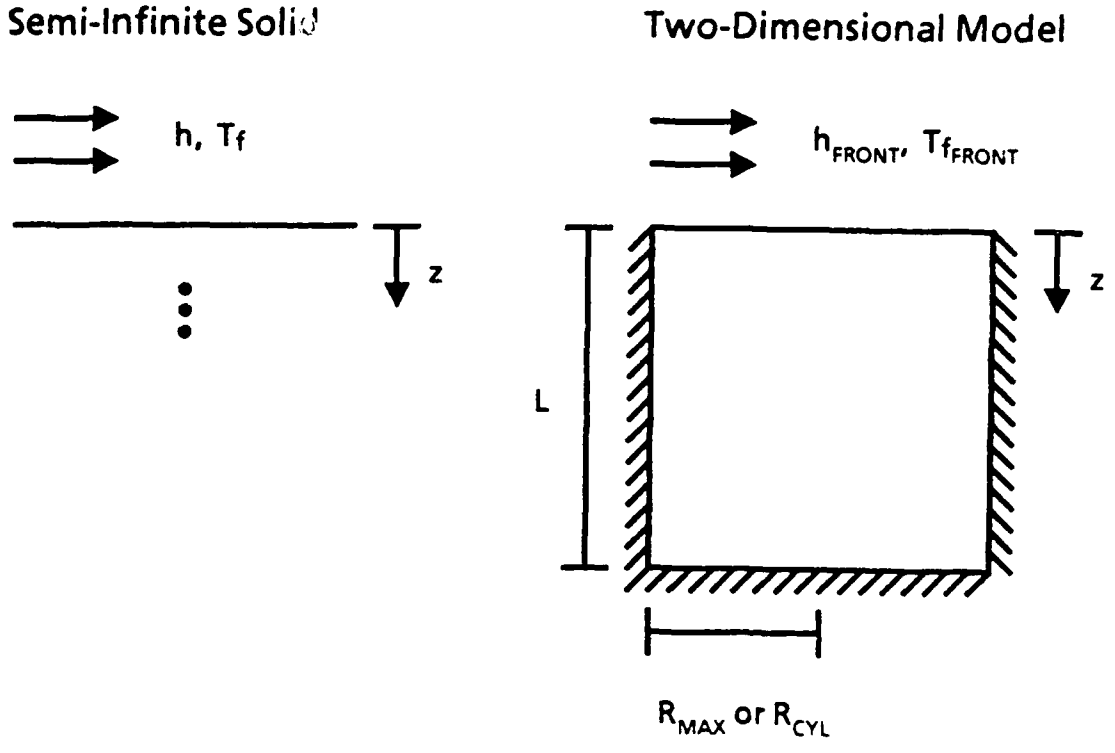

Figure 15. Simulating a Semi-Infinite Solid with Constant External Fluid Temperature and Convection Coefficient

cylinder is constant and equal to the surface heat generation:

$$q_s = q_g \tag{107}$$

Because both the fluid temperature and the convection coefficient are not defined in the analytical solution for this case, the non-dimensional form of the dependent variables must be changed to

$$_p\theta^{++} = \frac{T - T_i}{(q_g L/k)} \tag{108}$$

$$_pq^{++} = \frac{q}{q_g} \tag{109}$$

The non-dimensional equations using this non-dimensional form for the dependent variables are again identical to the previous equations except in the boundary conditions for the front and back surfaces. The nodal equations for nodes on the front and back surfaces can be easily modified to use this non-dimensional form in the finite-difference model.

Figure 16 illustrates the conditions used in the two-dimensional model to simulate this transient solution. The Biot number for the back surface is set to zero. Because the simulation uses surface heat generation, only the single-material problem will produce one-dimensional heat transfer. The simulation is again only valid for times less than the time it takes the leading edge of the disturbance to travel the length of the cylinder. This transient check case was also run to non-dimensional time of 0.075.

The analytical solutions for non-dimensional surface temperature and surface heat flux using the modified, non-dimensional form for the preheating problem are [4:pp.202-206]

$$\theta_s^{++} = \frac{2t^{+1/2}}{\pi^{1/2}} \tag{110}$$

$$q_s^{++} = 1 \tag{111}$$

Because the surface heat flux is inherent in the finite-difference model, it is not necessary to check the finite-difference model's estimate for surface heat flux. This

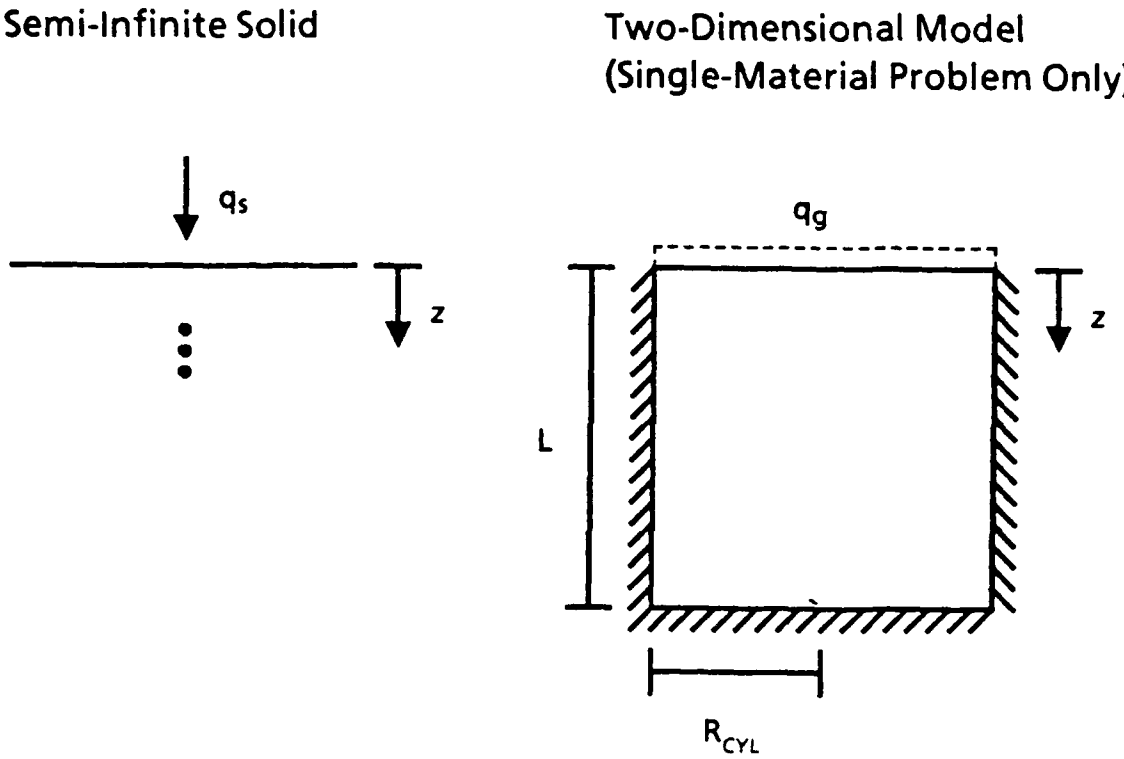

Figure 16. Simulating a Semi-Infinite Solid with Constant Surface Heat Flux

transient check case is still useful, however, for checking the accuracy of the finite-difference model's estimate for surface temperature and the accuracy of the series solution's estimates for surface heat flux using both the analytical surface temperatures and the surface temperatures produced by the model.

3.3.3 The Plane Wall with Convection One-dimensional heat transfer in a plane wall with constant external fluid temperature and convection coefficient on both sides is also easily simulated using the disturbance problem with a fully-insulated, outer-radial boundary condition. The parameter γ is set to zero, while the parameter τ is set to one. The Biot numbers for the front and back surfaces must be equal. Because surface heat generation is not used, both the single-material and two-material problems work for this transient check. However, the results are again identical, so the results from only one are shown. Figure 17 illustrates the conditions used in the model to simulate one-dimensional heat transfer in a plane wall with convection.

Although the simulation for the heat transfer in a plane wall is valid for all time, the cylinder ceases to behave as a semi-infinite solid for times greater than the time it takes the leading edge of the disturbance to reach the midplane of the wall:

$$t^+ \approx 1/64 \approx 0.016 \tag{112}$$

For times greater than this, then, one can not use this transient check case to check the accuracy of the series solution. However, this transient check case is still useful for checking the accuracy of values for surface temperature and heat flux produced by the finite-difference model. The transient check case using the plane wall solution was also run to non-dimensional time of 0.075.

The analytical solutions for the plane wall are infinite-series solutions. The

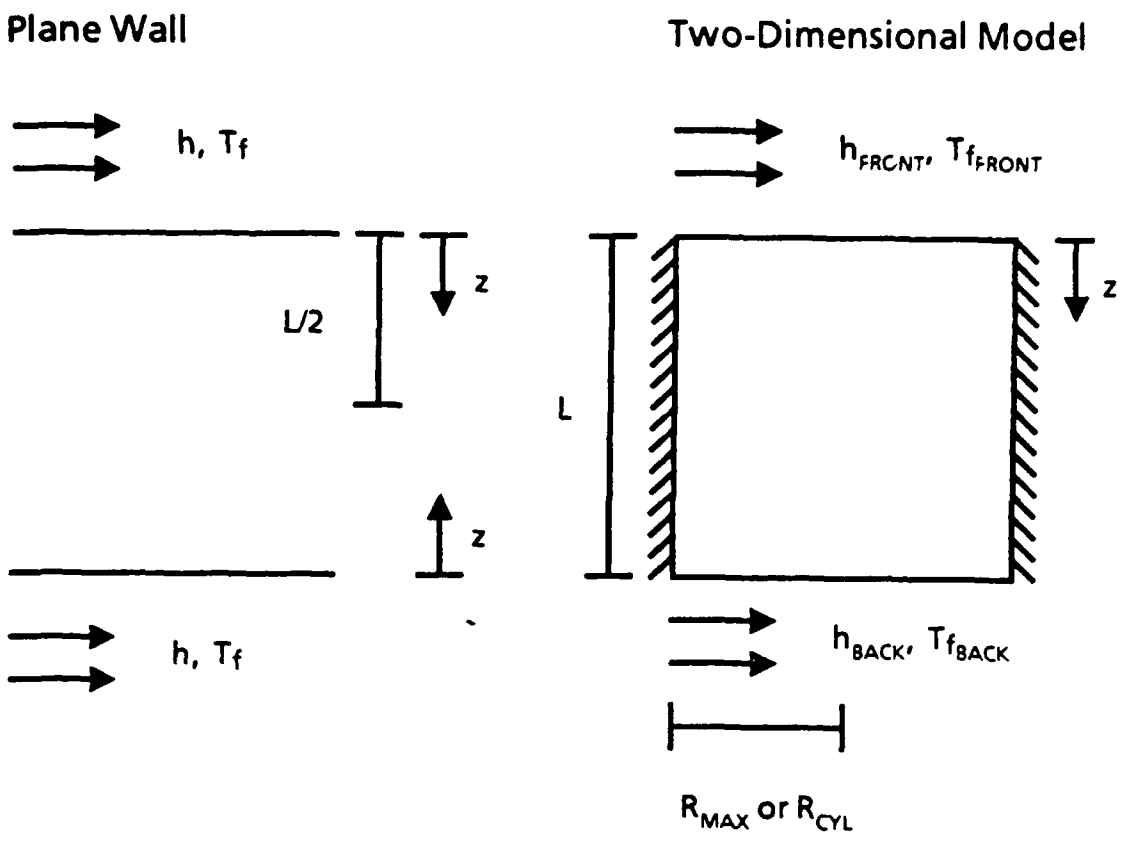

Figure 17. Simulating the Plane Wall with Constant External Fluid Temperature and Convection Coefficient on Both Sides

solutions can be approximated by the the first four terms to give [4:pp.183–187]

$$\theta_s^+ = 1 - \sum_{l=1}^{4} C_l \exp\left(-4\zeta_l^2 t^+\right) \cos\left(\zeta_l\right) \tag{113}$$

$$q_s^+ = 1 - \theta_s^+ = \sum_{l=1}^{4} C_l \exp\left(-4\zeta_l^2 t^+\right) \cos\left(\zeta_l\right) \tag{114}$$

where the coefficient C_l is given by

$$C_l = \frac{4 \sin\left(\zeta_l\right)}{2\zeta_l + \sin\left(2\zeta_l\right)} \tag{115}$$

and the constants ζ_l are the l^{th} eigenvalues of the characteristic equation

$$2\zeta_l \tan\left(\zeta_l\right) = Bi \tag{116}$$

Bi is the Biot number for both front and back surfaces. For the Biot number of 2.0 used in the simulation, the first four eigenvalues are

$$\zeta_1 = 0.8603 \quad \text{rad} \tag{117}$$

$$\zeta_2 = 3.4256 \quad \text{rad} \tag{118}$$

$$\zeta_3 = 6.4376 \quad \text{rad} \tag{119}$$

$$\zeta_4 = 9.5293 \quad \text{rad} \tag{120}$$

For non-dimensional time of 0.002, the magnitude of the fourth term in the series is 0.0104. Since this is an alternating series, the error in the solution using the truncated series is less than 0.0104 in magnitude for all non-dimensional times greater than 0.002.

3.3.4 Results from the Transient Check Cases Because the first check case is similar to the disturbance problem of the analysis, the model should behave similarly in the analysis as in this first check case. For this reason, the accuracy of the model in the first check case should give a good indication of the accuracy of the model in the analysis. The one major shortcoming is the fact that this first check case does not exercise the radial derivatives. Nevertheless, the results from

the first transient check case are given in this section, and from these results an estimate of the expected accuracy of the model in the analysis is determined. The graphs of the results for the second and third transient check cases are given in Appendices B.3.1 and B.3.2, respectively. For the most part, the trends in the accuracy seen in the first check case are also seen in the other two transient check cases.

Figure 18 shows the surface temperatures produced by the finite-difference model in the first check case using values of 0.004, 0.001, and 0.005 for the non-dimensional time step. There are some problems with the surface temperatures produced by the finite-difference model. First of all, as the non-dimensional time step is reduced, the surface temperatures converge on values lower than the analytical values. This error in the surface temperatures produced by the finite-difference model is most likely related to the magnitude of the temperature gradients near the surface. The error is greatest for small times when the temperature gradients are largest. Nevertheless, the surface temperatures produced by the model are quite accurate if sufficiently small non-dimensional spatial and time steps are used. Using spatial steps of 0.1 and a time step of 0.001 or less, the finite-difference estimates for surface temperature are within 2.7 percent of the analytical value at non-dimensional time of 0.01 and within 0.03 percent of the analytical value at non-dimensional time of 0.05.

The rate of change of surface temperature with respect to time as seen by the slope of the curves in Figure 18 is severely affected by these seemingly small errors in the surface temperatures produced by the model. For small time, the slope of the curves for the surface temperatures produced by the model is significantly lower than in the analytical solution. For larger times, the slope is slightly higher. This error in the rate of change of surface temperature is important because the series solution uses the rate of change of surface temperature rather than the surface temperatures themselves to determine the surface heat flux.

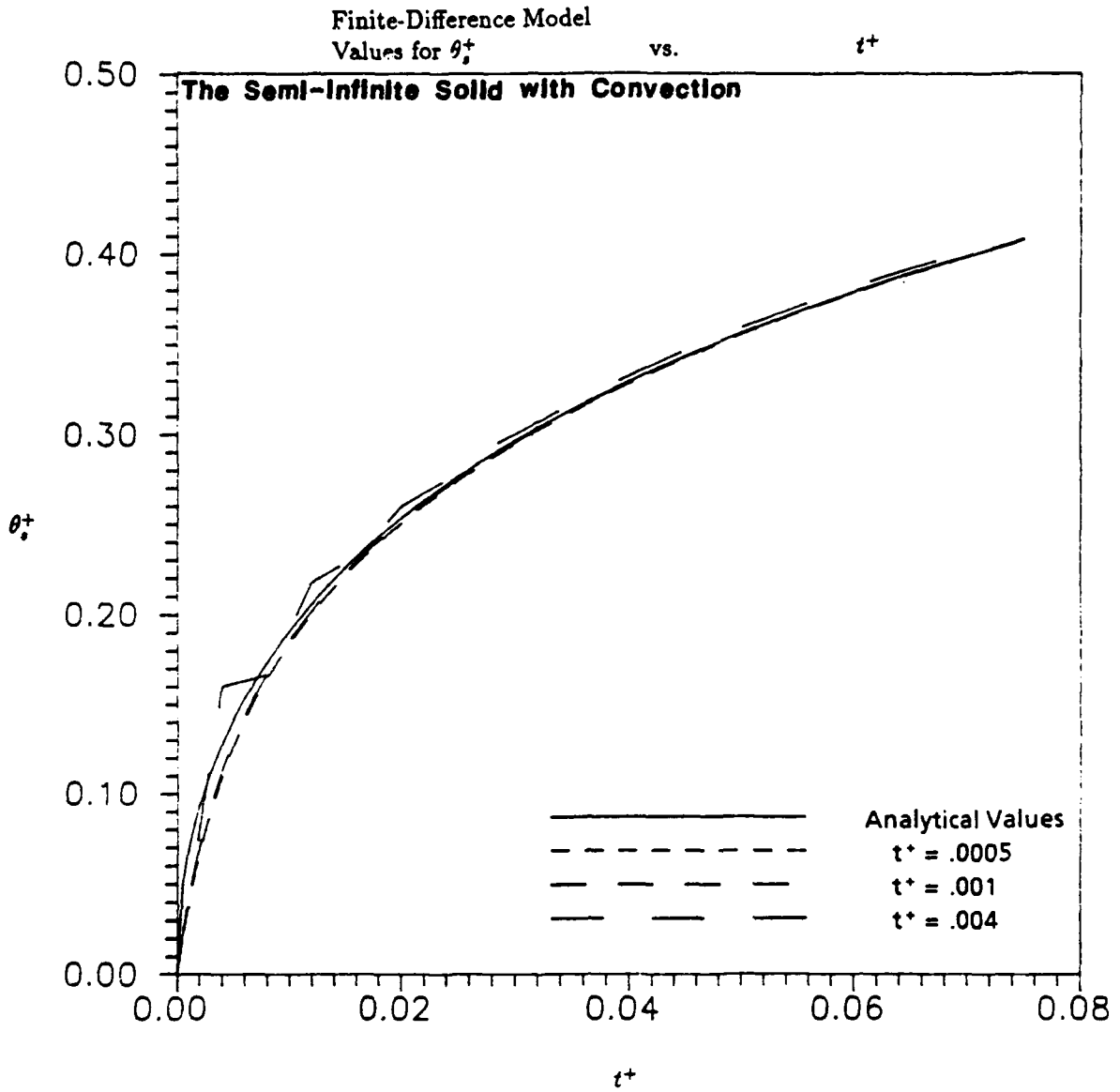

Figure 18. Finite-Difference Model Values for θ_s^+ vs. t^+ for the Semi-Infinite Solid with Convection

Stability and oscillation are also a concern with the explicit finite-difference model. Oscillations can have a significant effect on the results for surface heat flux using the series solution because the oscillations cause large errors in the calculated rate of change of surface temperature. Figure 18 shows oscillations in the finite-difference estimates for surface temperature using a non-dimensional time step of 0.004.

Oscillations are a more likely problem for small time when the curvature of the surface temperature function of time is greatest. The oscillations are caused by the over prediction in the explicit scheme as described in Section 2.3.6. The non-dimensional surface temperature at the end of the first time step is grossly over predicted because the non-dimensional time step is too big to accurately follow the solution when the rate of change in slope is high. The over predicted surface temperature at the end of the first time step causes the rate of change for the next time step to be low, which in turn causes the surface temperature at the end of the following time step to be under predicted. The process repeats itself a few times until the oscillations die out when the curvature of the surface temperature function becomes small enough for the finite-difference model to follow the solution with the given time step. As is readily seen in Figure 18, the oscillations cause much greater error in the slope of the curve for surface temperature than in the actual values for surface temperature. The time step needed to prevent oscillations depends on the conditions in the simulation and the spatial step sizes being used.

Because of the way in which the disturbance problem is non-dimensionalized, the accuracy of the finite-difference estimates for surface heat flux depends solely on the accuracy of the surface temperatures produced by the model (see Equation (90) and the discussion in Section 2.5). Figure 19 shows the finite-difference estimates for surface heat flux from the first transient check case using non-dimensional time steps of 0.004, 0.001, and 0.0005. The finite-difference estimates tend to be high since the surface temperatures tend to be low. Also, if the non-dimensional

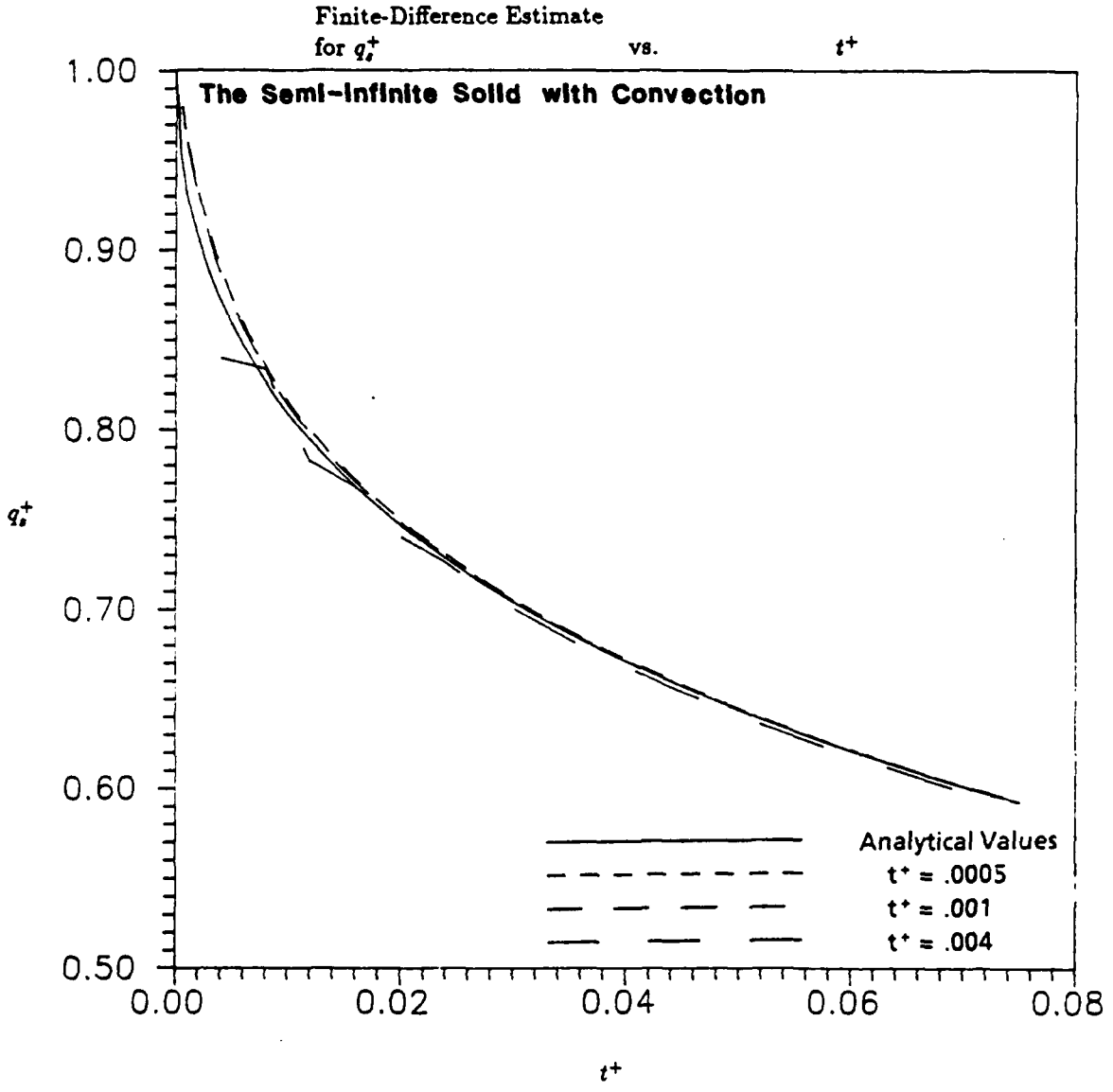

Figure 19. Finite-Difference Estimates for q_s^+ vs. t^+ for the Semi-Infinite Solid with Convection

time step is too big, the finite-difference estimates for surface heat flux oscillate about the analytical values. Nevertheless, the accuracy is quite good when using small enough step sizes. Using non-dimensional spatial step sizes of 0.1 and a non-dimensional time step of 0.001 or less, the finite-difference estimate for surface heat flux is within 0.7 percent of the analytical value at non-dimensional time of 0.01 and within 0.02 percent of the analytical value at non-dimensional time of 0.05.

Errors in the series solution for surface heat flux when using surface temperatures produced by the finite-difference model may be due either to the inaccuracies in the surface temperatures produced by the model or to the inherent inaccuracy of the series solution. To distinguish between the two causes, the series solution for surface heat flux was run using both the analytical values for surface temperatures and the surface temperatures produced by the finite-difference model. It is important to ensure that large errors in the series solution during the analysis are not caused by inaccuracies in the surface temperatures produced by the finite-difference model. If this is the case, then the finite-difference model does not model the laboratory experiment with sufficient accuracy, and the results are meaningless. Running the series solution with the analytical values for surface temperature is also helpful for evaluating any inherent inaccuracy in the series solution. The series solution is not an exact solution, and its accuracy depends on the time step used in the series.

Figure 20 shows the series solution estimates for surface heat flux in the first transient check case when using analytical values for surface temperature. Because the approximation in the series solution comes from assuming a piecewise linear function of time for the surface temperature, the series solution is more prone to error at small time when the curvature in the surface temperature function of time is larger. Since more recent terms in the series solution are weighted more heavily, the series estimate becomes increasingly more accurate for larger time as the curvature in the surface temperature function of time in this transient check

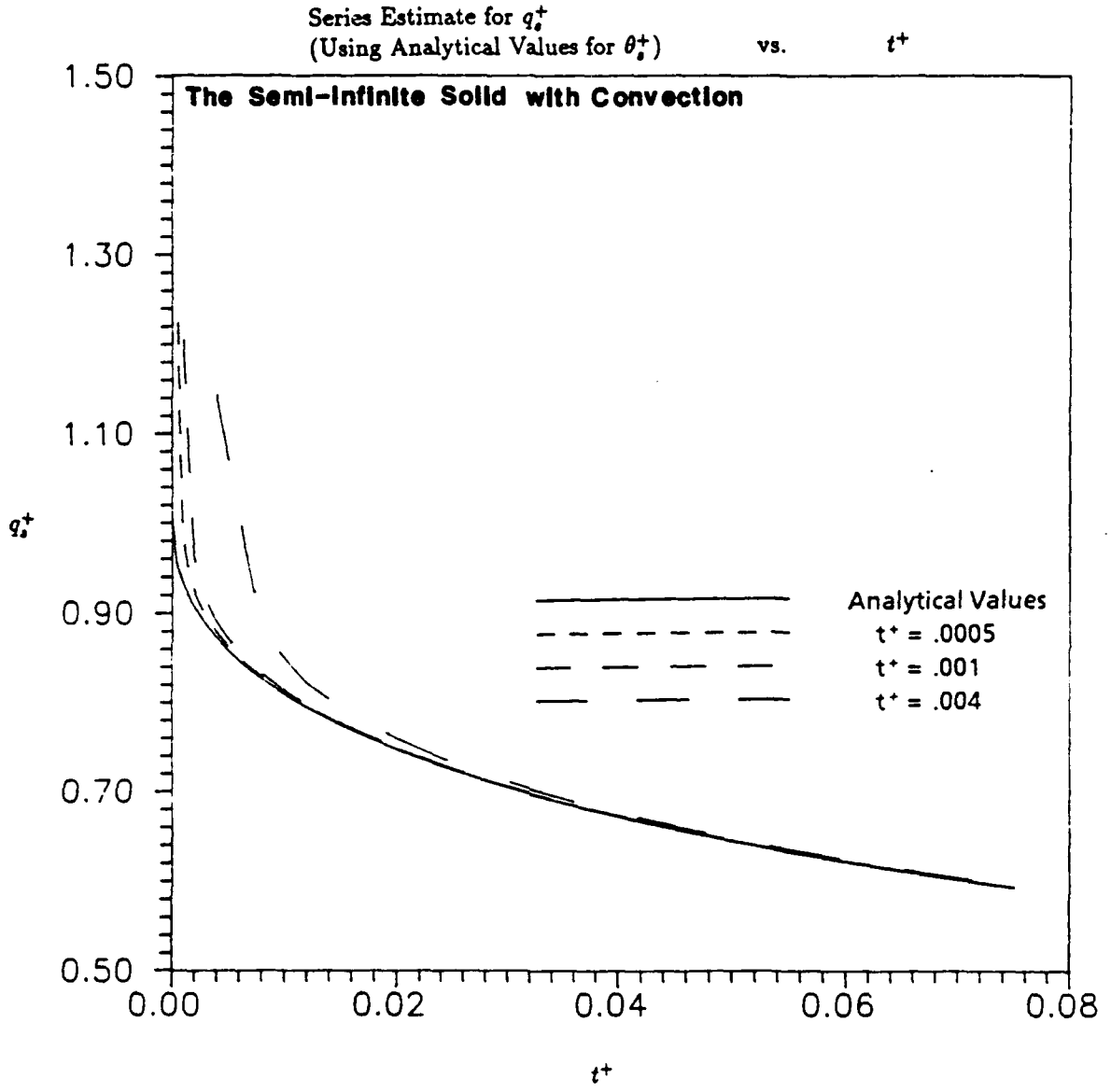

Figure 20. Series Solution Estimates for q_s^+ (Using Analytical Values for θ_s^+) vs. t^+ for the Semi-Infinite Solid with Convection

case decreases. For cases in which the surface temperature rises monotonically such as this, the series solution will tend to overestimate surface heat flux. Overall, the series solution is quite accurate if a small enough time step is used in the solution. Using a non-dimensional time step of 0.001 or less in the series solution gave series solution estimates for surface heat flux within 0.6 percent of the analytical value at non-dimensional time of 0.01 and within 0.05 percent of the analytical value at non-dimensional time of 0.05.

There are, however, significant problems with the series solution when using surface temperatures produced by the finite-difference model. These errors are caused by inaccuracies in the surface temperatures and not by the series solution. The error in the series solution estimate is significant even though the error in the value of the surface temperatures is small because the series solution uses the rate of change of surface temperature to evaluate surface heat flux. In comparison, the finite-difference estimates for surface heat flux do not have the same problems because the finite-difference estimates use the actual value of the surface temperature rather than the rate of change of surface temperature. First of all, the rate of change of surface temperatures produced by the finite-difference model is low for small time, so the series estimates are also initially low. For larger times, the rate of change is slightly high which may cause the series solution to be higher than it would be otherwise. However, any over prediction in the series solution for larger times may be offset by the initial under prediction as is the case in the second transient check case (see Figure 57 in Appendix B.3.1). Secondly, if the non-dimensional time step used in the model is too big so that oscillations are present in the surface temperatures, the series solution estimates can oscillate severely due to the extreme oscillation in the rate of change of surface temperature.

Figure 21 shows the series solution estimates for surface heat flux when using the surface temperatures produced by the finite-difference model in the first transient check case with non-dimensional time steps of 0.004, 0.001 and 0.0005 in

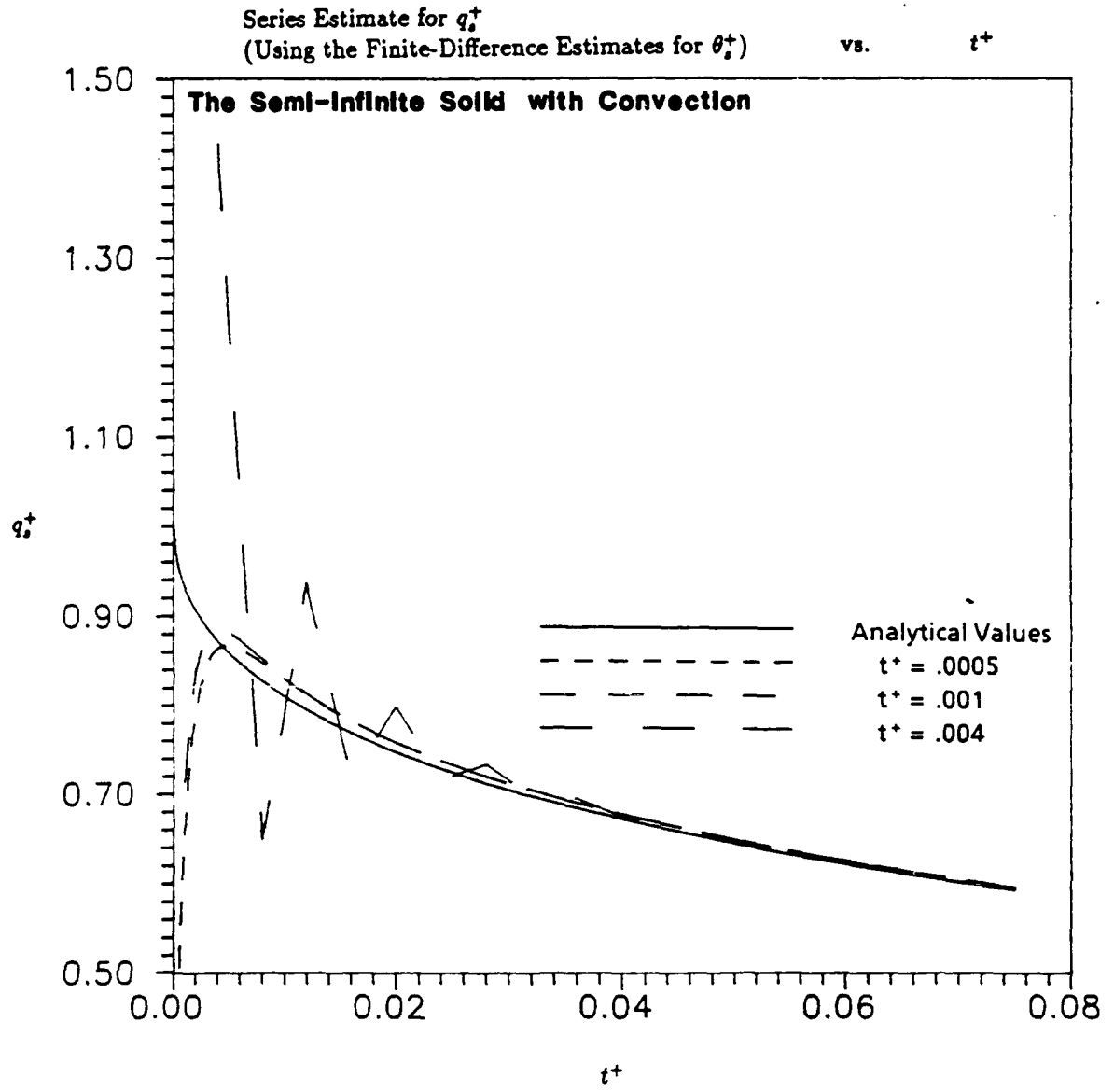

Figure 21. Series Solution Estimates for q_s^+ (Using the Finite-Difference Model Values for θ_s^+) vs. t^+ for the Semi-Infinite Solid with Convection

both the finite-differnce model and the series. Even with a non-dimensional time step of 0.0005, the initial under prediction in the series solution is severe. A severe initial under prediction occurs in all three transient check cases (see Figures 57 and 61 in Appendices B.3.1 and B.3.2, respectively). However, by non-dimensional time of 0.01, the series solution regains its accuracy. Using non-dimensional spatial step sizes of 0.1 in the finite-difference model and a non-dimensional time step of 0.001 or less in both the finite-difference model and the series solution gave series solution estimates for surface heat flux within 2.7 percent of the analytical value at non-dimensional time of 0.01 and within 0.7 percent of the analytical value at non-dimensional time of 0.05.

In summary, the finite-difference model produces surface temperatures with good accuracy using non-dimensional, spatial step sizes less than or equal to 0.1 and a non-dimensional time step less than or equal to 0.001. The series solution is also quite accurate given exact data when the non-dimensional time step in the series is less than or equal to 0.001. However, the series solution for surface heat flux using the surface temperatures produced by the finite-difference model does have some problems. For small times, the series solution under predicts the surface heat flux due to the large error in the initial rate of change of the surface temperatures produced by the finite-difference model. The series solution can also have significant errors if oscillations are present in the surface temperatures produced by the finite-difference model. Nevertheless, the series solution for surface heat flux using surface temperatures produced by the model is accurate for non-dimensional times greater than 0.01 if non-dimensional spatial step sizes less than or equal to 0.01 are used in the model and non-dimensional time steps less than or equal to 0.001 are used in both the model and the series.

Accurate results in the analysis require accurate results for both the finite-difference estimates for surface heat flux and the series solution estimates for surface heat flux using the surface temperatures produced by the finite-difference model.

For non-dimensional times greater than 0.01 in the first transient check case, the finite-difference estimates are within 0.7 percent of the analytical values for surface heat flux and the series solution estimates are within 2.7 percent of the analytical values when using non-dimensional spatial step sizes of 0.1 in the finite-difference model and non-dimensional time steps less than or equal to 0.001 in both the model and the series. To be conservative, one can assume that these percentages apply to the maximum non-dimensional, external surface heat flux of 1.0. Then, the non-dimensional error in the finite-difference estimate for surface heat flux is always less than 0.007 and the non-dimensional error in the series solution estimate is always less than 0.027. This error estimate is more conservative for longer times since the error decreases with time. It is important to note that the transient check cases did not employ the radial derivatives. One would expect the radial derivatives to add some additional error to the results in the analysis. Then, a reasonable and conservative estimate of the expected error in the percent difference used in the analysis, $(q^+_{SER} - q^+_{F.D.}) \times 100.00$, for non-dimensional times greater than 0.01 would be 4.0. Figure 22 shows the finite-difference and the series solution estimates for surface heat flux using the surface temperatures produced by the finite-difference model in the first transient check case with a non-dimensional time step of 0.0005 in both the model and the series.

The transient check cases also point out the need to collect temperature data carefully when using the series solution on experimental data. The series solution is extremely sensitive to errors in the data for surface temperatures because the series solution uses the rate of change of temperature to evaluate surface heat flux.

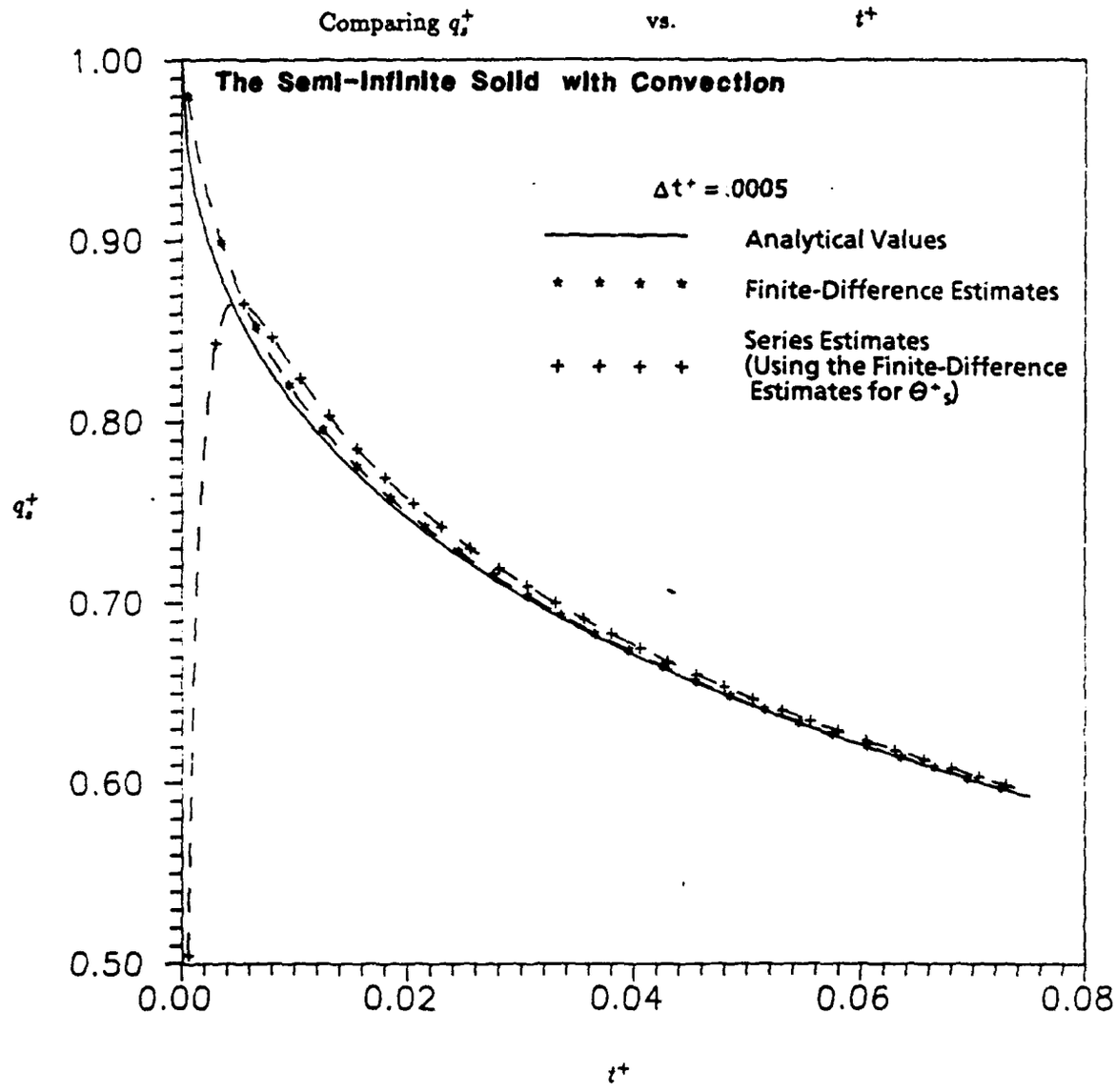

Figure 22. Comparing the Finite-Difference Estimates, Series Solution Estimates (Using the Finite-Difference Model Values for θ_s^+) and Analytical Values for q_s^+ vs. t^+ for the Semi-Infinite Solid with Convection

IV. Analysis and Results

This analysis investigates the effect of various parameters in the two-dimensional model on the accuracy of the series solution for the average surface heat flux in the region of the heated disk. Because the total number of parameters in the model is large, the analysis is limited by allowing only some of the parameters to vary and setting the others constant. A limited range or number of values is investigated for each of the parameters which is allowed to vary.

Section 2.2 lists the non-dimensional parameters in the two-dimensional model. Four additional non-dimensional parameters occur in the finite-difference model. They are the tolerance used in the convergence criterion for the preheating problem and the three non-dimensional step sizes; Δz^+, Δr^+ and Δt^+.

Some of the parameters are set constant for all runs. The Biot numbers at the front and back surfaces during the preheating problem are set to 0.01. This value is chosen using a typical convection coefficient for free convection of 4.0 $\mathbf{W/m^2 \cdot K}$ and typical values for L and k from References [3] and [7:p.672], respectively. The parameter τ in the disturbance problem is set to zero, and the Biot number at the back surface during the disturbance problem is kept at 0.01. Setting τ to zero and keeping ${}_dBi_{BACK}$ equal to 0.01 implies that the conditions at the back of the test specimen remain the same for both the preheating and the disturbance problems and are typical conditions for free convection. Only two values, 0.1 and 1.0, are used to investigate a reasonable range for the Biot number at the front surface during the disturbance problem. Because ${}_pBi_{FRONT}$ is held constant, the parameter β equivalently describes the Biot number at the front surface during the disturbance problem when preheating is used.

The transient check cases show that the percent difference, $(q^+_{SER} - q^+_{F.D.}) \times 100.00$, should be accurate to within 4.0 in the analysis for non-dimensional

times greater than 0.01 when using non-dimensional spatial step sizes of 0.1 or less and a non-dimensional time step of 0.001 or less. The spatial step sizes actually used depend on the value of the geometry parameter R_{DISK}/R_{CYL}. The geometry parameter R_{DISK}/R_{CYL} is set to 1/6, 1/8 and 1/12 using non-dimensional spatial step sizes of 0.111 (1/9), 0.083 (1/12) and 0.056 (1/18), respectively. The largest non-dimensional time step used in any of the runs is 0.001.

The time step required to maintain stability in the finite-difference model varies between runs. In some cases, a time step much smaller than 0.001 is used. The accuracy of the series solution improves when smaller time steps are used in the series. However, each run uses the temperature values at non-dimensional time steps of 0.001 in the series solution regardless of the time step used in the finite-difference model to avoid disturbing the results by varying the time step used in the series solution. All runs are ended at non-dimensional time of 0.07 since thin-film gages are generally not used for times longer than the estimated time it takes the leading edge of a thermal disturbance to reach the back surface of the cylinder, which is approximately 0.0625 in non-dimensional time (see Equation (2)).

In another attempt to clarify and simplify the analysis, the runs are separated into groups which isolate the causes of two-dimensional heat transfer. One group of runs, the *adiabatic cases*, investigates the effect of localized heat generation and preheating with no heat flux across the outer-radial boundary of the cylinder. Another group of runs, the *non-adiabatic cases with no heat generation or preheating*, investigates the effect of allowing heat flux across the outer-radial boundary of the cylinder in the absence of heat generation or preheating. A third group of runs, the *combined cases* or *non-adiabatic cases with heat generation and preheating*, investigates the effect of adding preheating and subsequent heat generation to a few of the runs from the non-adiabatic cases.

4.1 Adiabatic Cases

The adiabatic cases investigate the effect on the series solution of the two-dimensional heat transfer caused by heat generation and preheating in the absence of heat flux across the outer-radial boundary of the cylinder. All runs in the adiabatic cases use the single material problem with the ***fully-insulated***, outer-radial boundary condition of Equations (26) and (34). All runs also use the preheating problem except the few which investigate the effect of heat generation during the disturbance with no prior preheating.

A number of parameters are allowed to vary for the adiabatic cases. Values between 0.0 and 0.5 are investigated for the parameter γ. The geometry parameter L/R_{CYL} is varied between 0.2 and 5.0, while the geometry parameter R_{DISK}/R_{CYL} is varied between the three values 1/6, 1/8 and 1/12. The tolerance used in the convergence criterion for the preheating problem is varied between the three values of 0.5, 0.1 and 0.05; and a few runs do not use any preheating. Finally, all runs are duplicated using values of 10.0 and 100.0 for the parameter β.

The results from the adiabatic cases show that preheating and subsequent surface heat generation should have no effect on the results as long as the transients from the preheating problem are allowed to settle down before beginning the test. Figure 23 shows the results with the parameter γ varying and using a value of 10.0 for β, 1/8 for R_{DISK}/R_{CYL}, 1.0 for L/R_{CYL} and 0.1 for the tolerance. The results seem to show a trend in the series solution to overestimate slightly with increasing value of γ. However, the percent differences are less than the expected error in the model. Using a value of 0.5 for γ, the percent difference is between 0.5 and 0.7 between non-dimensional time of 0.01 and 0.07, and the percent difference is less using smaller values for γ. When a larger value for β is used, the percent difference is larger but still less than the expected error in the model. Figure 63 in Appendix C.1 shows the results with γ varying using a value of 100.0 for β. The percent difference using a value of 0.5 for γ increases to between 2.0 and 3.0 when

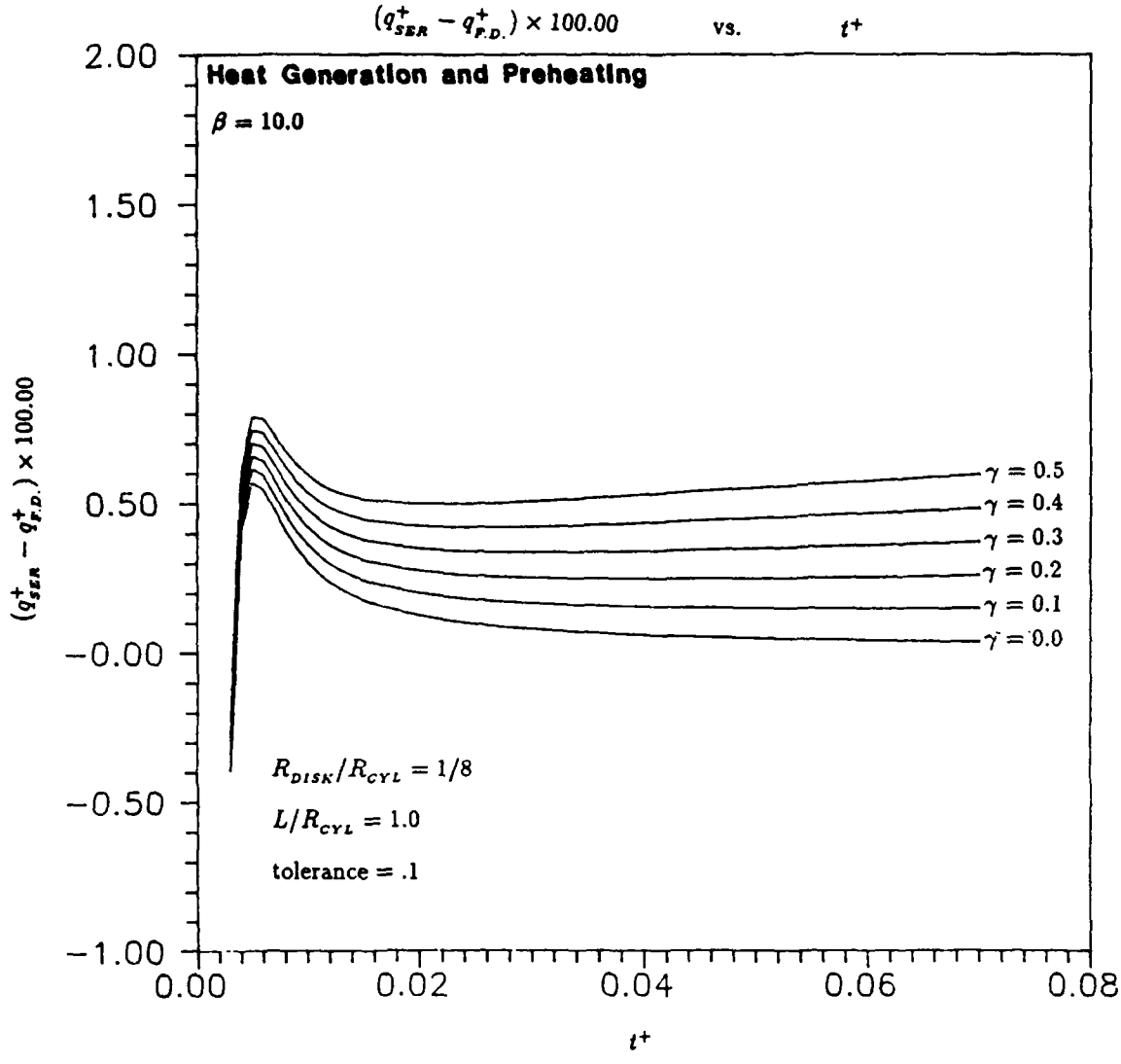

Figure 23. Results with Heat Generation and Preheating as γ Varies Using $\beta = 10.0$

β is 100.0.

Although heat generation does not affect the results when the transients from the preheating problem are allowed to settle down, the effect of heat generation is large if the preheating problem is not run. Figure 24 shows the results with the tolerance for the convergence criterion of the preheating problem varying and using a value of 10.0 for β, 1/8 for R_{DISK}/R_{CYL}, 1.0 for L/R_{CYL} and values of 0.05 and 0.2 for γ. Tolerances of 0.5, 0.1 and 0.005 cause the preheating problem to converge at non-dimensional times of 0.118, 2.600 and 10.326, respectively. Changing the tolerance between these three values cause only slight changes in the percent differences which remained below the expected error of the model. However, there is significant overestimation when heat generation is used with no preheating. The percent difference when using a value of 0.2 for γ and without preheating is between 6.0 and 10.0. Figure 64 in Appendix C.1 shows even greater overestimation when using a value of 100.0 for β.

The overestimation in the series solution caused by not allowing the transients to settle down during the preheating problem stands to reason. The overestimation results from greater increases in surface temperature than would be present from the external disturbance alone since the disturbance from the heat generation has not established itself yet. The series solution attributes the greater increase in surface temperature to a greater external surface heat flux than is actually present. It is likely, however, that if one used a thin-film gage for very short times, i.e. only as long as the assumption of one-dimensional heat transfer was valid, and were able to expose the system to the disturbance at the same time as turning on the instrumentation, one could correct the series solution for the overestimation caused by the heat generation. For one-dimensional heat transfer, the disturbance in the region of the heated disk would be composed of two separate disturbances, the surface heat generation and the external disturbance. Superposition holds because the equations are linear. Therefore, the resulting surface temperature changes are

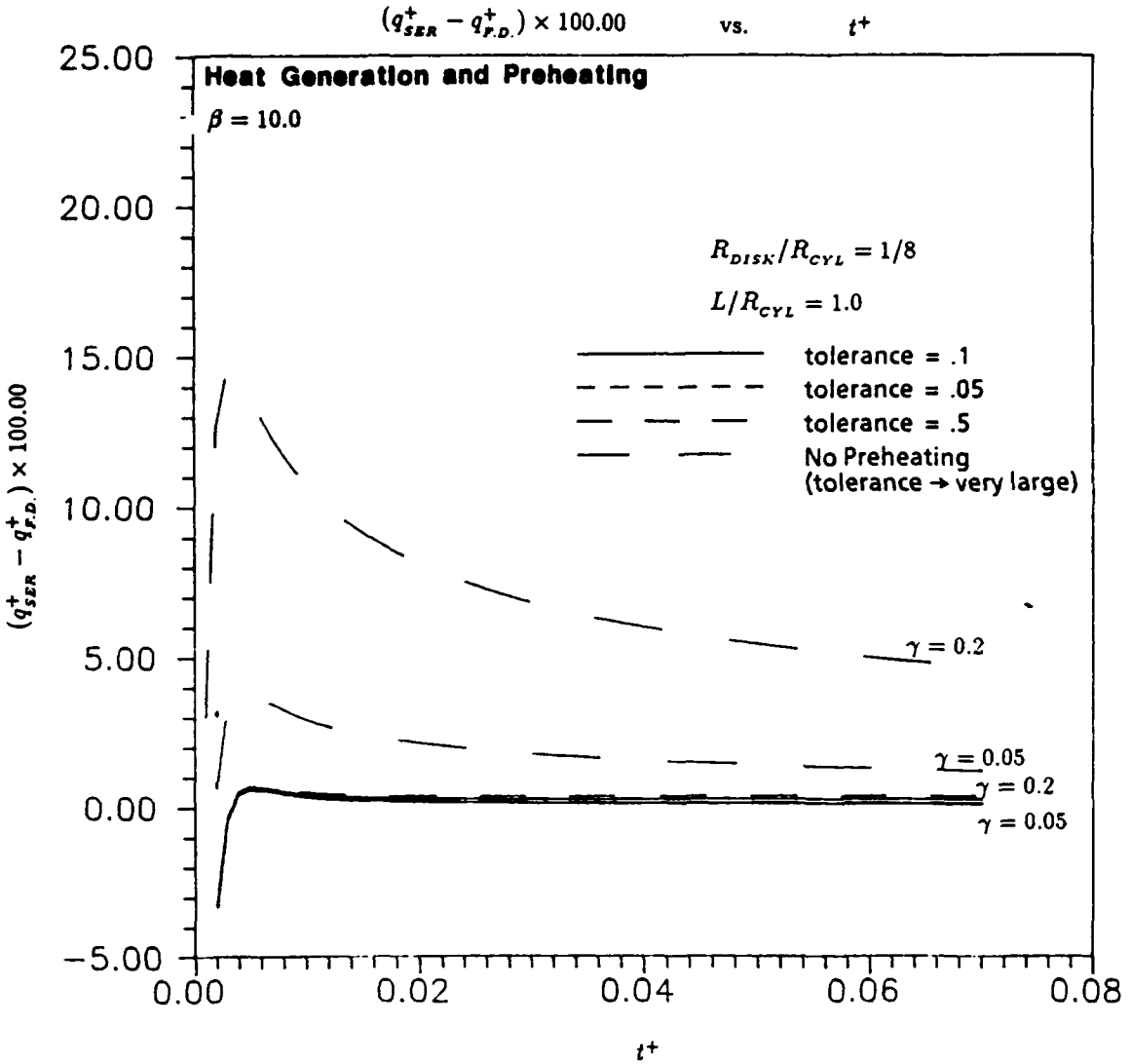

Figure 24. Results with Heat Generation and Preheating as the Tolerance Varies Using $\beta = 10.0$

the sum of the changes due to the two separate disturbances. Given the total surface temperature changes, the series solution should accurately estimate the total surface heat flux and could be corrected to yield the heat flux due to the external disturbance alone by subtracting the value of the surface heat generation. For longer times, one can not make this correction because the heat transfer from the localized surface heat generation becomes two-dimensional. Even though superposition still holds, the correction needed for the series solution will be something less than the value of the surface heat generation.

Varying the parameter L/R_{CYL} does not affect the results. Figure 25 shows results with the parameter L/R_{CYL} varying using a value of 10.0 for β, 1/8 for R_{DISK}/R_{CYL}, 0.1 for the tolerance and values of 0.05 and 0.2 for γ. The percent difference is small and less than the expected accuracy of the model. Figure 65 in Appendix C.1 shows similar results using a value of 100.0 for β.

Varying the parameter R_{DISK}/R_{CYL} also does not affect the results. Figure 26 shows the results with the parameter R_{DISK}/R_{CYL} varying using a value of 10.0 for β, 1/8 for R_{DISK}/R_{CYL}, 0.1 for the tolerance and values of 0.05 and 0.2 for γ. The percent difference is again very small and less than the expected error in the model. Figure 66 in Appendix C.1 shows similar results using a value of 100.0 for β. The percent differences are larger but still less than the expected accuracy of the model.

4.2 Non-Adiabatic Cases with No Heat Generation or Preheating

The non-adiabatic cases with no heat generation or preheating investigate the effect on the series solution of the two-dimensional heat transfer which results from allowing heat flux across the outer radial boundary of the cylinder in the absence of heat generation or preheating. The preheating problem is not used for these cases, and the parameter γ is set to zero.

The effects of allowing heat flux across the outer-radial boundary of the

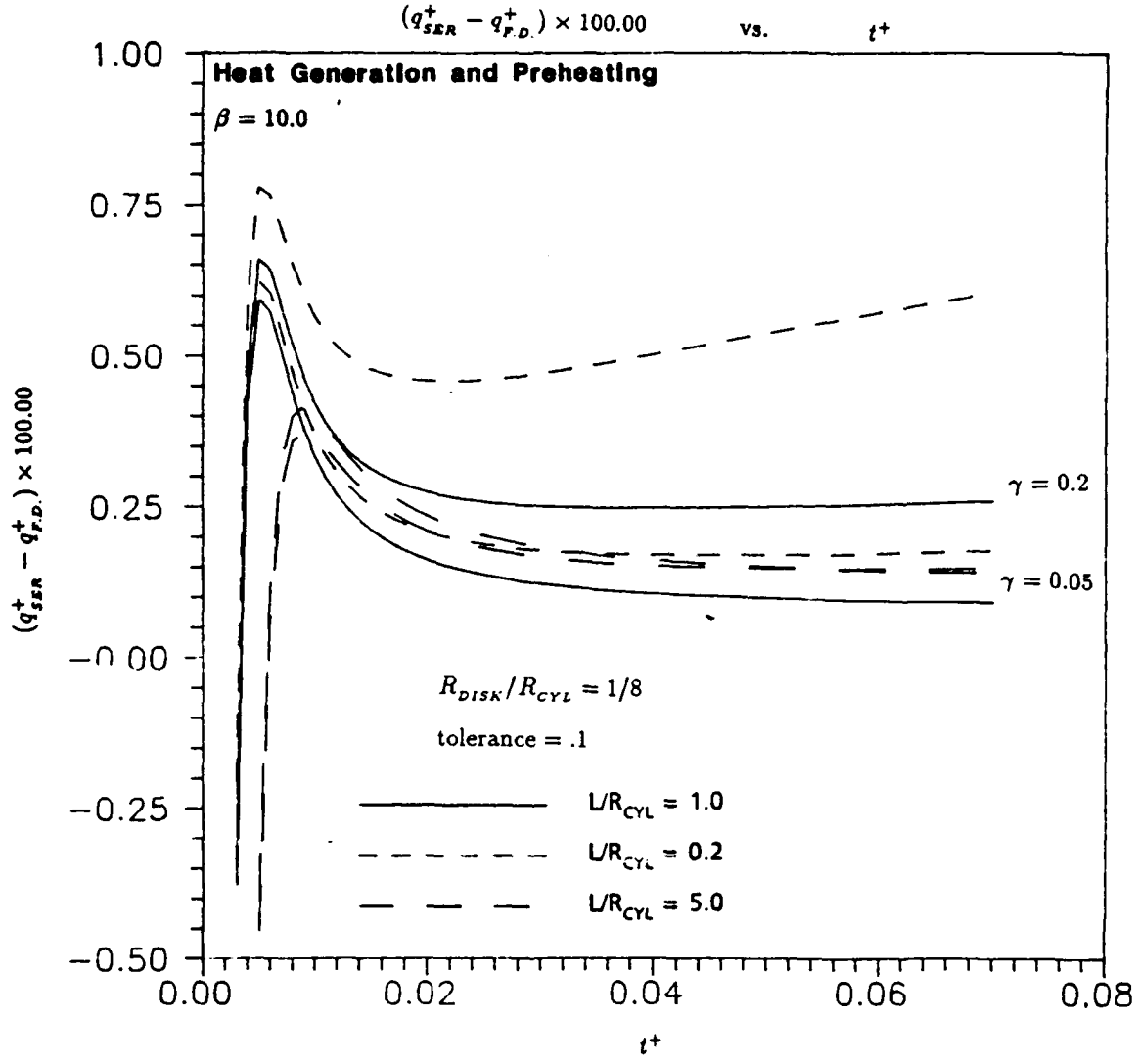

Figure 25. Results with Heat Generation and Preheating as L/R_{CYL} Varies Using $\beta = 10.0$

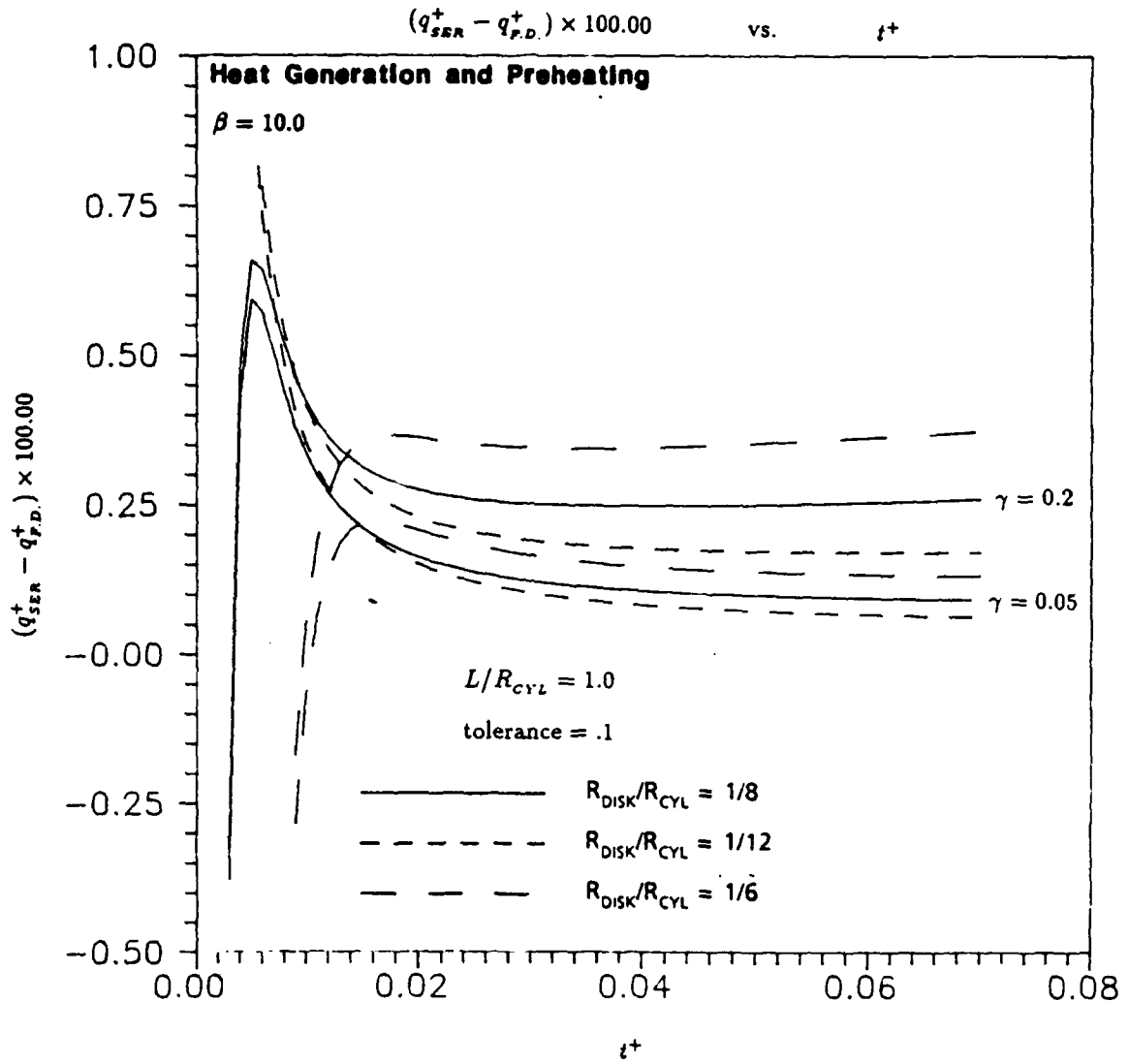

Figure 26. Results with Heat Generation and Preheating as R_{DISK}/R_{CYL} Varies Using $\beta = 10.0$

cylinder are bounded by the effects seen in the limiting cases. Each of the three limiting cases for heat flux across the outer-radial boundary of the cylinder is implemented using the single-material problem. The limiting case for heat flux out across the outer-radial boundary of the cylinder uses Equation (35) for the outer-radial boundary condition on the cylinder. The limiting case for heat flux in across the outer-radial boundary of the cylinder uses Equation (36) for the outer-radial boundary condition on the cylinder. The case for no heat flux across the outer-radial boundary of the cylinder is the adiabatic case.

In the absence of heat generation and preheating, the heat transfer in the adiabatic case will be one-dimensional, so the series solution should be the true solution for times up to the time when the leading edge of the external disturbance reaches the back of the cylinder. The only approximation in the series solution for the adiabatic case with no heat generation or preheating is caused by assuming the surface temperature to be a piece-wise linear function of time (see Section 2.4). Figures 23 and 63 show that using a value of 0.0 for γ in the adiabatic case does indeed yield a percent difference very near 0.0. Thus, the percent difference due to any intermediate condition causing heat flux out across the outer-radial boundary of the cylinder will be bounded by zero and the percent difference found in the limiting case for heat flux out. Likewise, the percent difference due to any intermediate condition causing heat flux in across the outer-radial boundary of the cylinder will be bounded by zero and the percent difference found in the limiting case for heat flux in.

Two intermediate cases for heat flux across the outer-radial boundary of the cylinder are also investigated. Both use the two-material problem with a geometry parameter R_{MAX}/R_{CYL} equal to 2.0. The intermediate case for heat flux out models teflon as the insulating material in a test specimen. The property ratios k'/k and $(\rho c_p)/(\rho c_p)'$ are .33 and .49, respectively, [7], [4:p.688] and [6:p.608]. The boundary

condition on the outer-radius of the surrounding material for this case is

$$\theta^+(r^+ = 2.0) = 0 \tag{121}$$

The intermediate case for heat flux in across the boundary uses property ratios of 1.0 and 6.0 for k'/k and $(\rho c_p)/(\rho c_p)'$, respectively. The boundary condition on the outer-radius of the surrounding material for this case is

$$\left.\frac{\partial \theta^+}{\partial r^+}\right)_{r^+=2.0} = 0 \tag{122}$$

Because the non-adiabatic cases with no heat generation or preheating do not use the preheating problem, the parameter β does not really apply. Instead, values of 0.1 and 1.0 are used for the parameter ${}_dBi_{FRONT}$, the Biot number at the front surface. The geometry parameter L/R_{CYL} is varied between 0.2 and 5.0, and the geometry parameter R_{DISK}/R_{CYL} is varied between the three values of 1/6, 1/8 and 1/12.

Figures 27, 28, 29 and 30 show the results for the limiting case for heat flux out, the intermediate case for heat flux out, the limiting case for heat flux in and the intermediate case for heat flux in, respectively, as the geometry parameter L/R_{CYL} varies using a value of 10.0 for the parameter β and 1/8 for the geometry parameter R_{DISK}/R_{CYL}. As seen in the results, the series solution underestimates the external surface heat flux for the cases with outward radial heat flux and overestimates the external surface heat flux for cases with inward radial heat flux. For all cases, there is a bounding value for the geometry parameter L/R_{CYL} such that any lower value for L/R_{CYL} gives a minimal percent difference. For the limiting case for heat flux out, limiting L/R_{CYL} to 1.0 keeps the percent difference less than 2.0. For the intermediate case for heat flux out, limiting L/R_{CYL} to 2.0 keeps the percent difference less than 6.0. For the limiting case for heat flux in, limiting L/R_{CYL} to 0.6 keeps the percent difference less than 5.0. Finally, for the intermediate case for heat flux in, limiting L/R_{CYL} to 1.0 keeps the percent differnce less than 2.0.

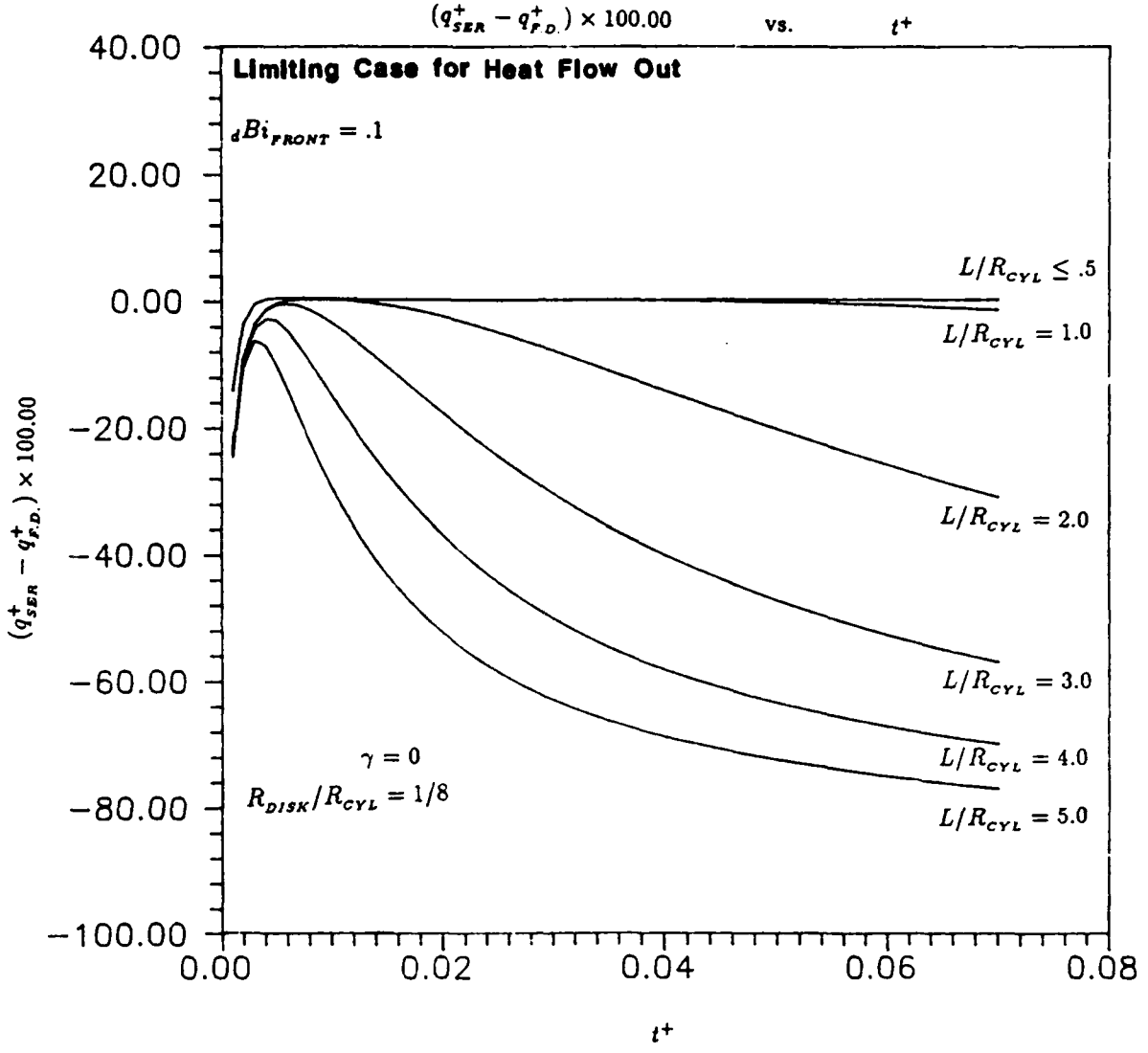

Figure 27. Results for the Limiting Case for Heat Flux Out Across the Outer-Radial Boundary with No Heat Generation as L/R_{CYL} Varies Using ${}_dBi_{FRONT} = .1$

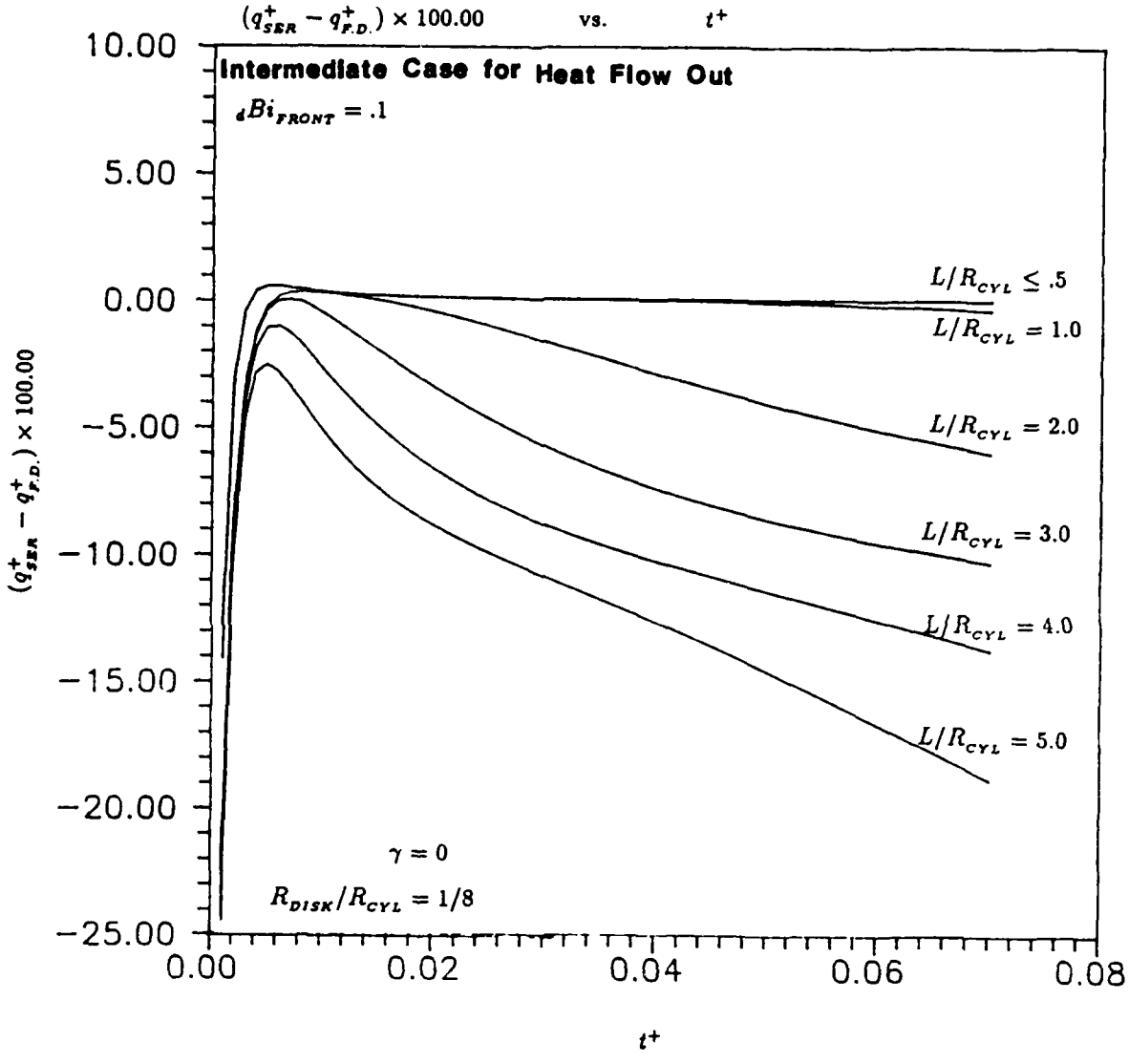

Figure 28. Results for the Intermediate Case for Heat Flux Out Across the Outer-Radial Boundary with No Heat Generation as L/R_{CYL} Varies Using ${}_dBi_{FRONT} = .1$

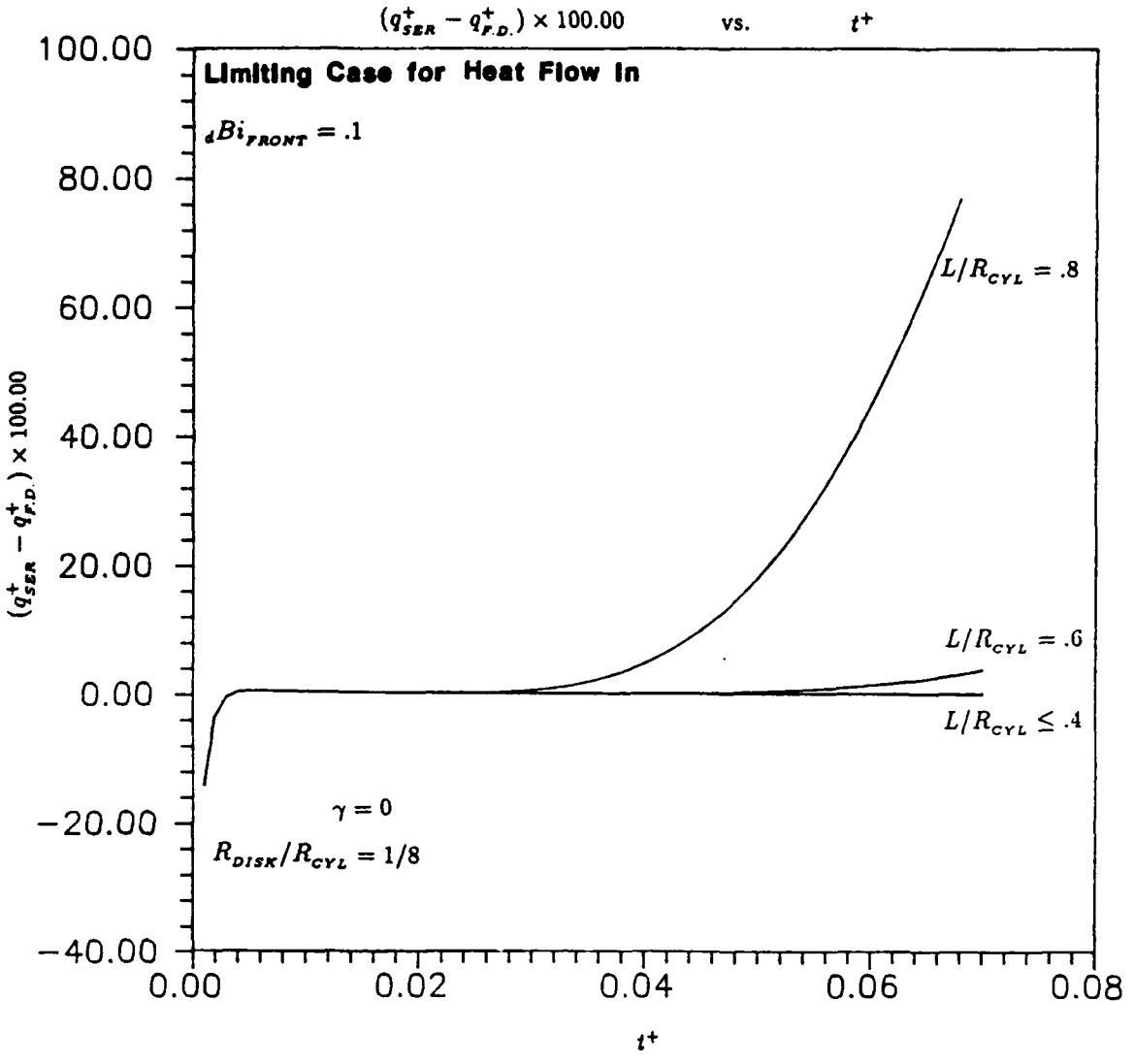

Figure 29. Results for the Limiting Case for Heat Flux In Across the Outer-Radial Boundary with No Heat Generation as L/R_{CYL} Varies Using ${}_dBi_{FRONT} = .1$

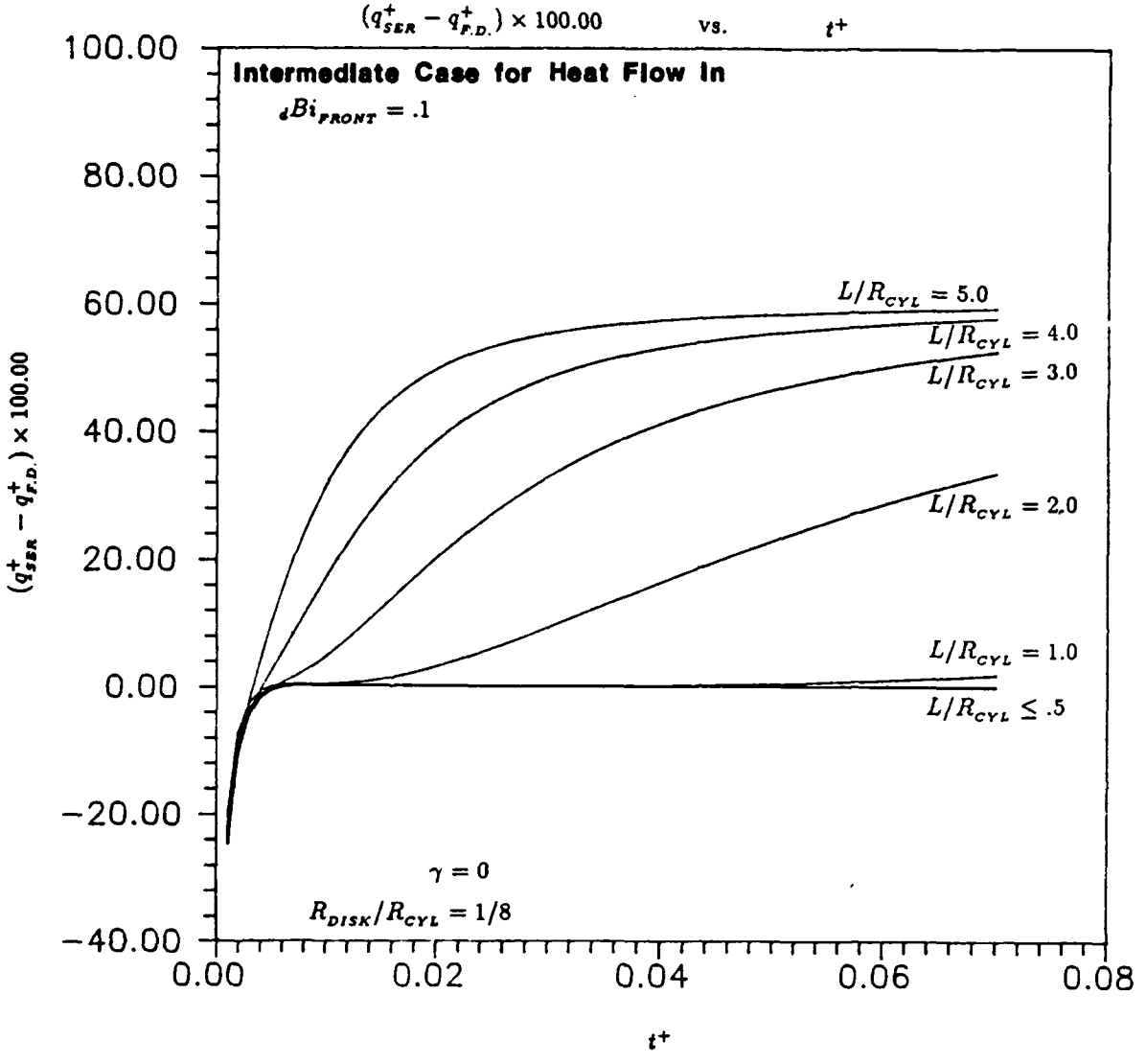

Figure 30. Results for the Intermediate Case for Heat Flux In Across the Outer-Radial Boundary with No Heat Generation as L/R_{CYL} Varies Using ${}_dBi_{FRONT} = .1$

For values of L/R_{CYL} larger than these bounding values, the percent differences become large. For the limiting case for heat heat flux out, using a value of 2.0 for L/R_{CYL} and 0.1 for ${}_dBi_{FRONT}$ gives a steadily increasing percent difference which reaches 30 by non-dimensional time of 0.07. For the intermediate case for heat flux out, using a value of 4.0 for L/R_{CYL} and 0.1 for ${}_dBi_{FRONT}$ gives a steadily increasing percent difference which reaches 13 by non-dimensional time of 0.07. For the limiting case for heat flux in, using a value of 0.8 for L/R_{CYL} and 0.1 for ${}_dBi_{FRONT}$ gives a rapidly increasing percent difference which reaches 85 by non-dimensional time of 0.07. Finally, for the intermediate case for heat flux in, using a value of 2.0 for L/R_{CYL} and 0.1 for ${}_dBi_{FRONT}$ gives a steadily increasing percent difference which reaches 34 by non-dimensional time of 0.07. In all cases, the error in the series solution increases with time, so one may obtain better accuracy with larger values for the parameter L/R_{CYL} if one is only interested in results for shorter times. Although the results from the limiting case for heat flux in are severe, one should note that the conditions which this limiting case model are quite severe and unlikely to approximate any actual conditions in the laboratory.

For a short time after the disturbance, the heat transfer in the region of the disk should be approximately one-dimensional. Therefore, the series solution should theoretically be accurate for short times. Some of the results clearly show this delay in the onset of error in the series solution. As would be expected, the delay in terms of non-dimensional time is greater with smaller values of L/R_{CYL} since the tendency to produce radial gradients is less. As the value of L/R_{CYL} decreases, the resistance to heat transfer in the radial direction increases relative to the resistance to heat transfer in the axial direction, so the radial gradients should be smaller when using smaller values for L/R_{CYL}.

The trend for the series solution to overestimate or underestimate depending on the direction of the establishing radial gradients makes sense and can be explained by examining typical flux plots for the transient heat transfer in the

cylinder [4:pp.135–137]. A flux plot is a network of isotherms and heat flow lines. The heat flow lines are drawn with arrows to indicate the direction of the heat flow and temperature gradient. Heat flow lines must always be perpendicular to isotherms. The area between adjacent heat flow lines is termed a *lane*. Heat can be visualized as flowing in these lanes. In a well drawn flux plot, the heat flux between two adjacent isotherms in a lane can be estimated by

$$qA_{la} \approx k\frac{\Delta T}{\Delta d} \tag{123}$$

where q is the heat flux, k is the thermal conductivity, A_l is the approximate area of the lane perpendicular to the heat flow line, ΔT is the temperature difference between the isotherms and Δd is the approximate distance between the isotherms. Heat energy must be conserved, so any heat which does not continue to flow in the lane will cause the temperature to rise. Figure 31 shows a typical flux plot for heat transfer in an initially isothermal, semi-infinite solid. In contrast, Figure 32 shows typical flux plots for heat transfer in the intermediate cases for heat flux out and heat flux in across the outer-radial boundary.

The series solution uses the time history of changes in the surface temperature to estimate the surface heat flux. The series solution is accurate only if the changes in surface temperature that do occur are equal to those that would occur in an initially isothermal, semi-infinite solid with the same time history of surface heat flux. For the cases that establish outward radial heat flux, the changes in surface temperature for any given time history of surface heat flux are less than the changes in surface temperature that would occur in an initally isothermal, semi-infinite solid with the same time history of surface heat flux. Given the smaller changes in surface temperature, the series solution underestimates the surface heat flux.

The trend for surface temperature changes to be less in runs that establish outward radial gradients can be visualized by examining the typical flux plots. Figures 31 and 32 show flux plots for heat transfer in a semi-infinite solid and in the cylinder with outward radial gradients, respectively. As can be seen by

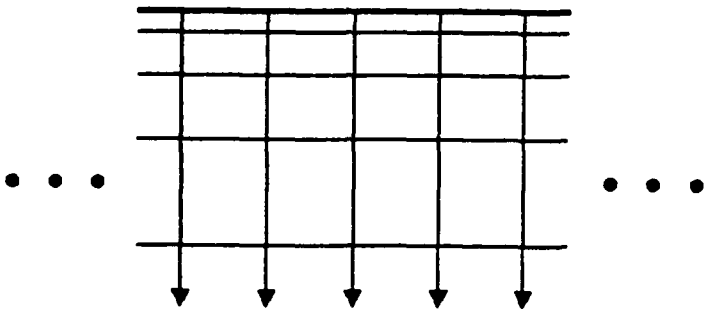

Figure 31. Typical Flux Plot for Heat Transfer in an Initially Isothermal, Semi-Infinite Solid

a. Heat Flux Out Across the Outer-Radial Boundary

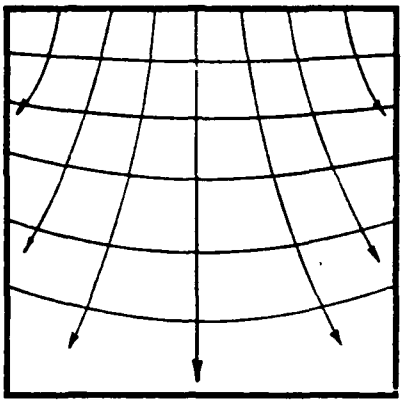

b. Heat Flux In Across the Outer-Radial Boundary

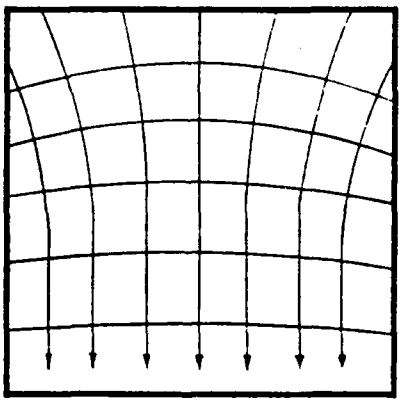

Figure 32. Typical Flux Plots for Heat Transfer in the Intermediate Cases for Heat Flux Out and In Across the Outer-Radial Boundary of the Cylinder

the increasing area of the lanes in its flux plot, the heat flux within the solid with outward radial gradients will be less than the heat flux within the semi-infinite solid when the same surface heat flux is present in both in accordance with Equation (123). Then, the temperature changes which result from the same time history of surface heat flux will be less since smaller temperature changes are required to establish the heat flux through the cylinder. With inward radial gradients, the area of the lanes decreases, so the temperature changes will be greater, and the series solution overestimates.

Figures 67, 68, 69 and 70 in Appendix C.2 show the results for the limiting case for heat flux out, the intermediate case for heat flux out, the limiting case for heat flux in and the intermediate case for heat flux in as the parameter L/R_{CYL} varies using a value of 1.0 for ${}_dBi_{FRONT}$ instead. The results using a larger value for ${}_dBi_{FRONT}$ show the very same trends but with slightly less percent differences. It must be noted, however, that the dimensional error in the series solution is still greater for the larger value of ${}_dBi_{FRONT}$ since the percent difference is normalized with the value of ${}_dBi_{FRONT}$ in the denominator. The smaller percent difference when using the larger value for ${}_dBi_{FRONT}$ may be misleading also because of the way the results are displayed. It is likely that the fractional amount of the true surface heat flux by which the series solution overestimates or underestimates stays fairly constant when the value for ${}_dBi_{FRONT}$ varies. The way to show this would be to evaluate a new percent difference using the finite-difference estimate for surface heat flux as the normalizing factor. The non-dimensional temperatures at the front surface in the disturbance problem will tend to increase when using larger values for ${}_dBi_{FRONT}$, so non-dimensional surface heat flux values decrease. If, in fact, the series solution errs by a constant fractional amount of the finite-difference estimate when the value for ${}_dBi_{FRONT}$ changes, then the percent difference is less for larger values of ${}_dBi_{FRONT}$ only because the finite-difference estimates for surface heat fluxes are smaller.

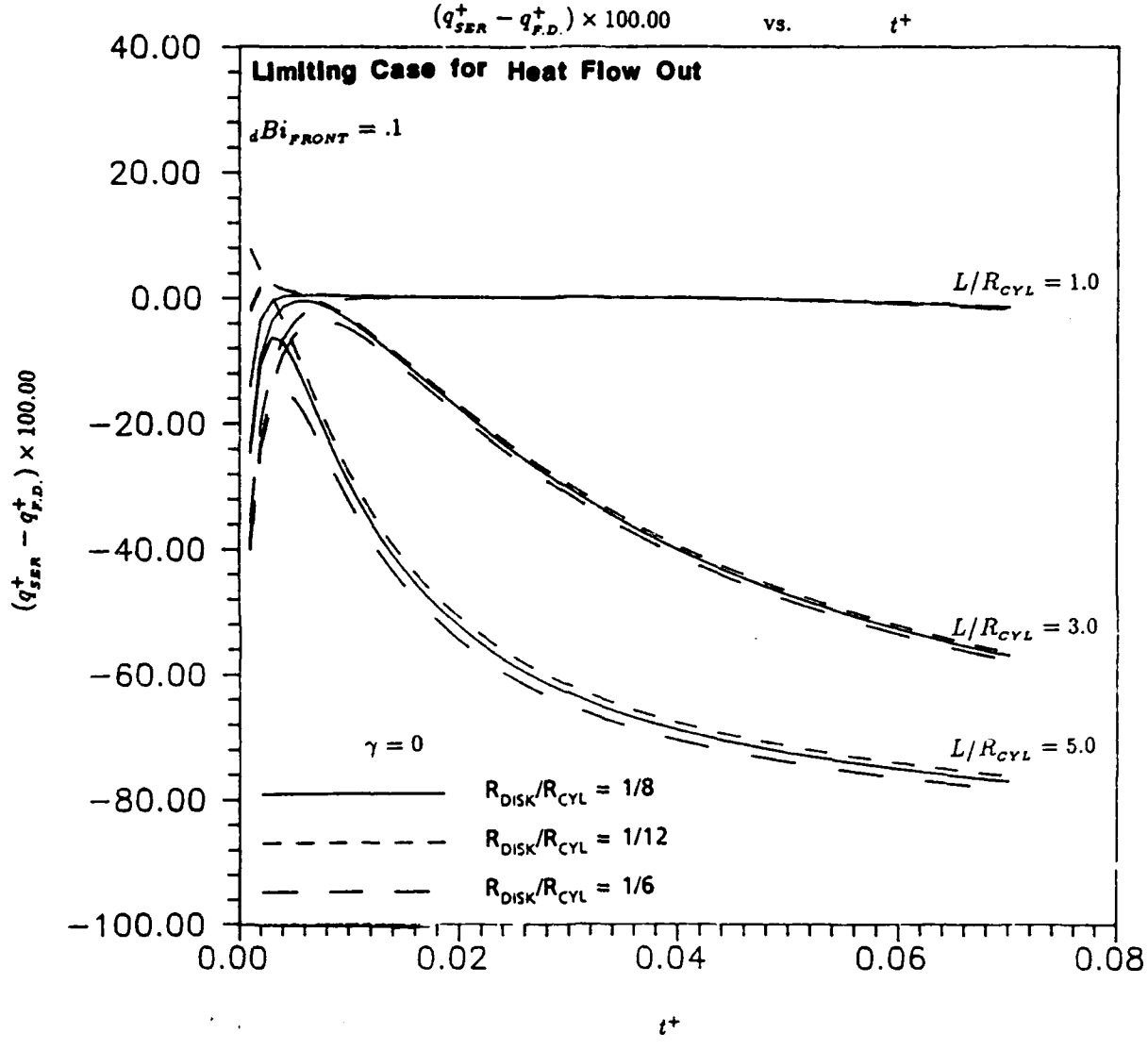

Figure 33. Results for the Limiting Case for Heat Flux Out Across the Outer-Radial Boundary with No Heat Generation as R_{DISK}/R_{CYL} Varies Using ${}_dBi_{FRONT} = .1$

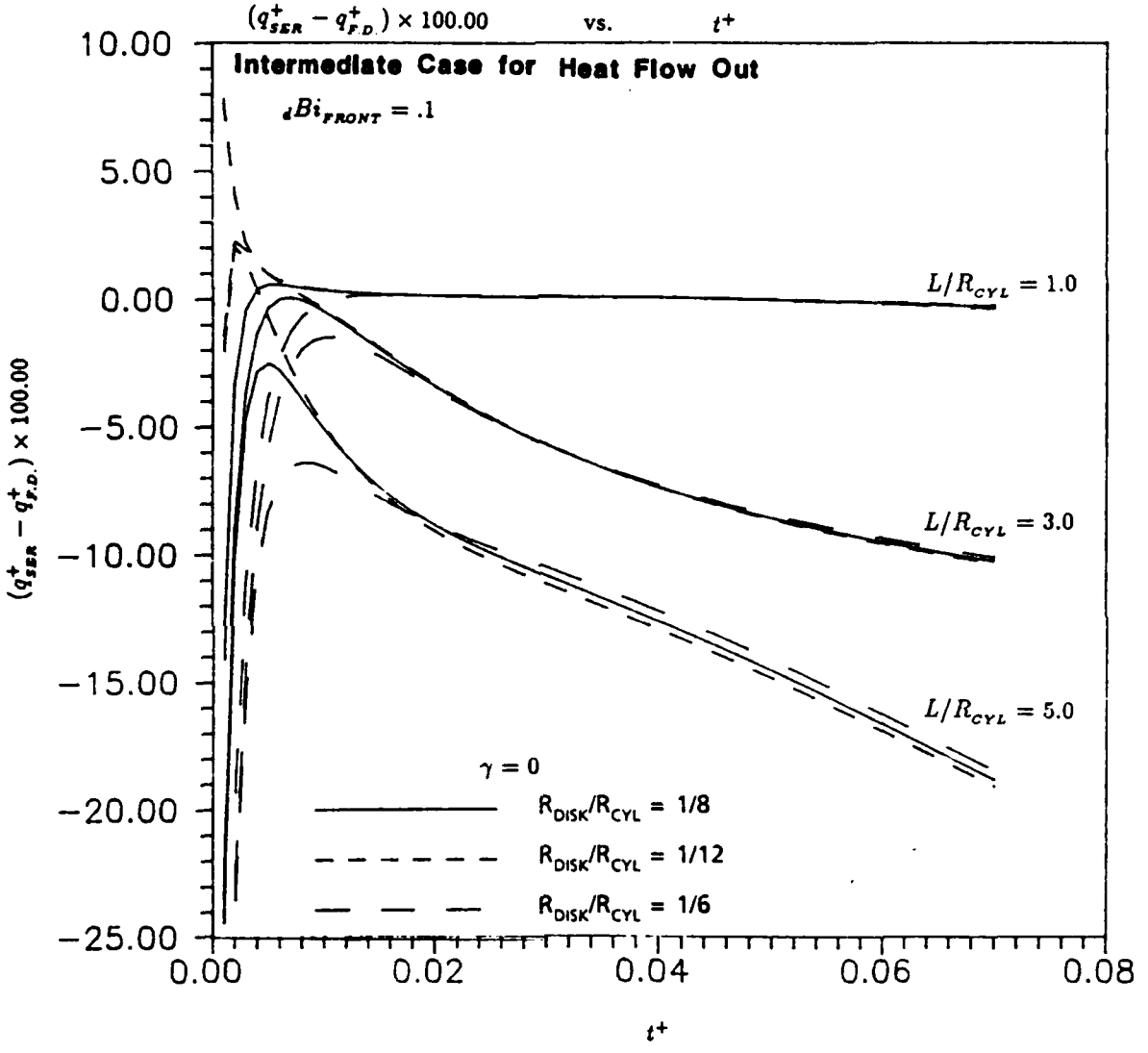

Figure 34. Results for the Intermediate Case for Heat Flux Out Across the Outer-Radial Boundary with No Heat Generation as R_{DISK}/R_{CYL} Varies Using $_dBi_{FRONT} = .1$

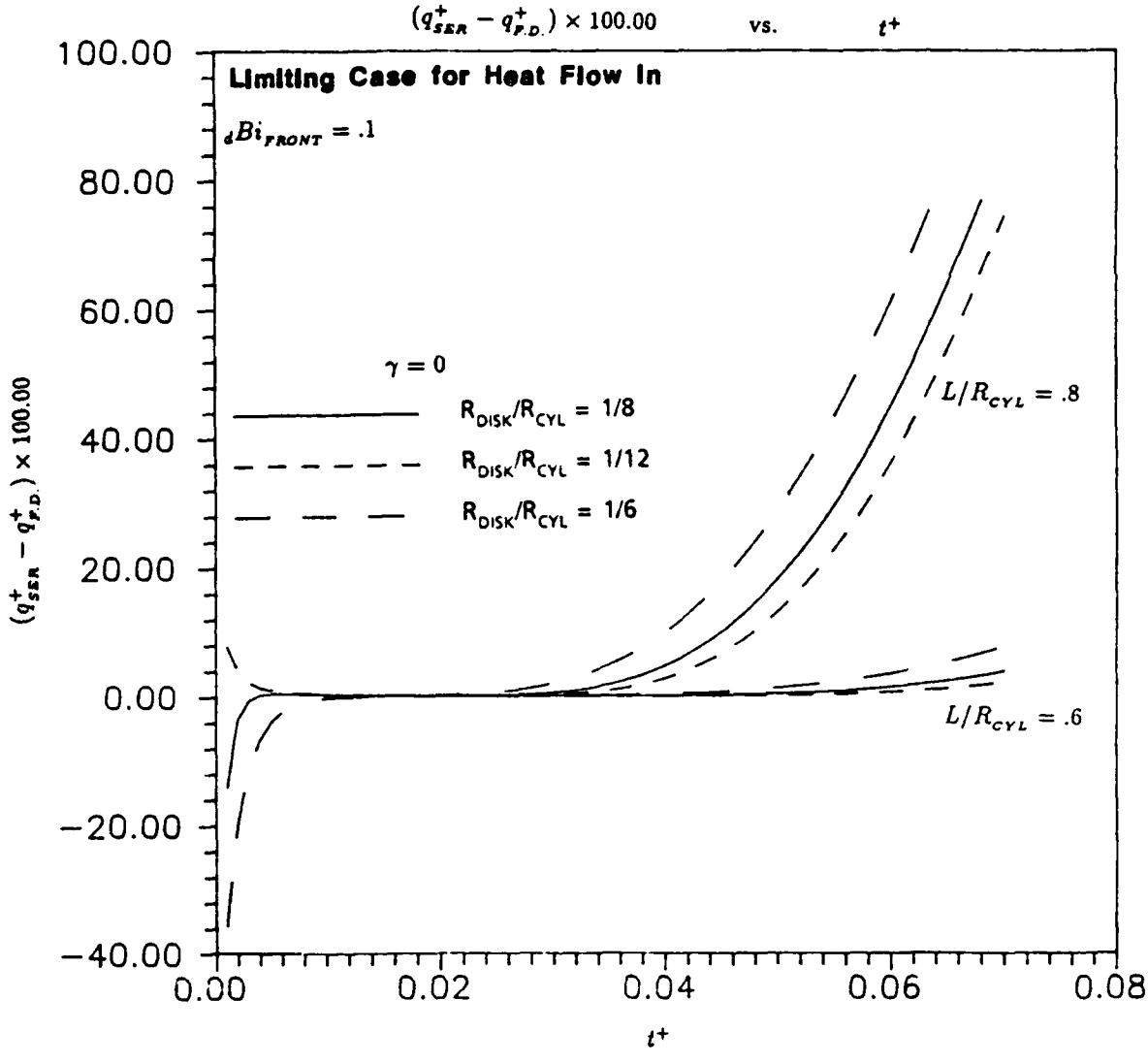

Figure 35. Results for the Limiting Case for Heat Flux In Across the Outer-Radial Boundary with No Heat Generation as R_{DISK}/R_{CYL} Varies Using ${}_dBi_{FRONT} = .1$

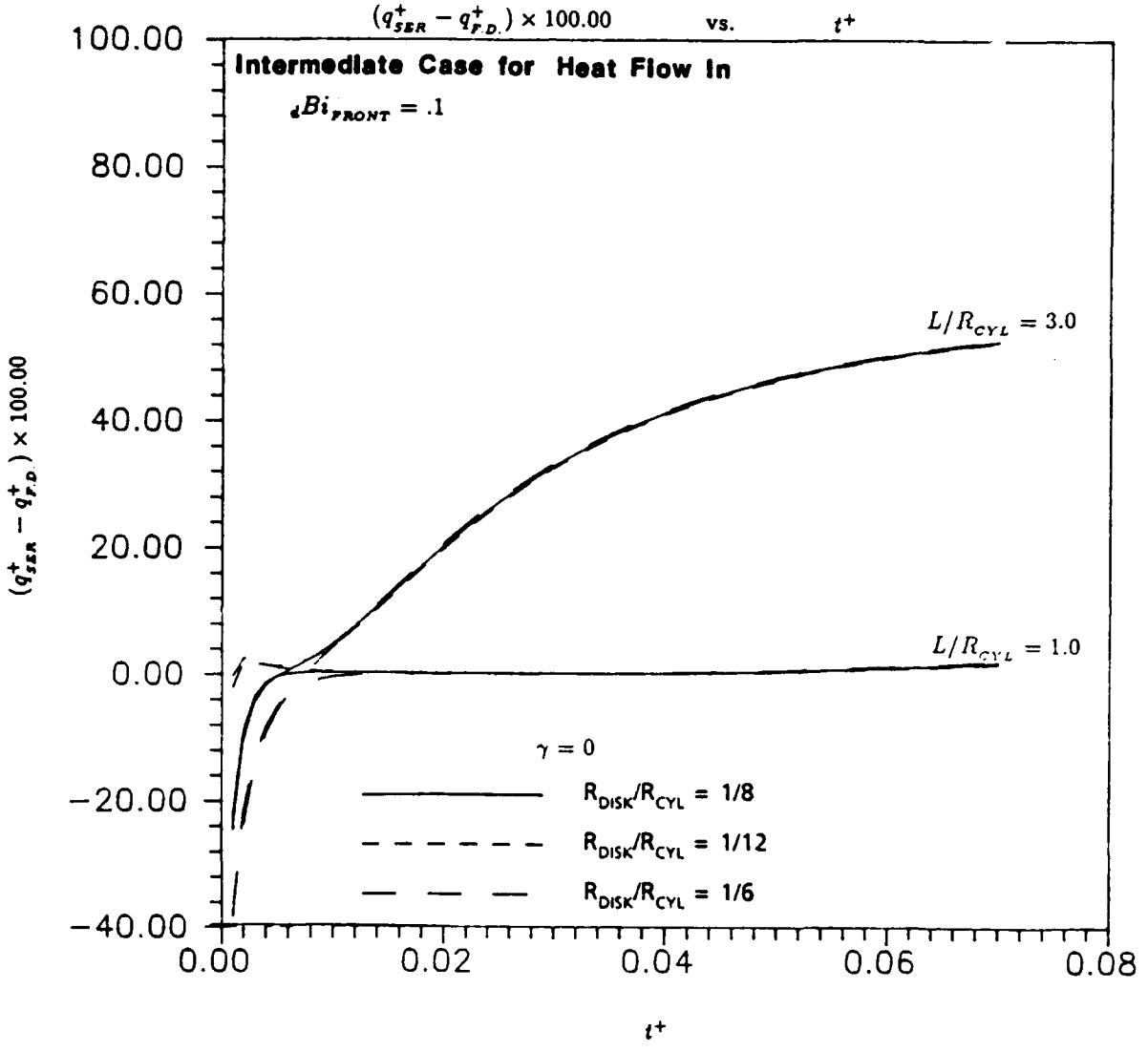

Figure 36. Results for the Intermediate Case for Heat Flux In Across the Outer-Radial Boundary with No Heat Generation as R_{DISK}/R_{CYL} Varies Using $_dBi_{FRONT} = .1$

The geometry parameter R_{DISK}/R_{CYL} has little impact on the results. Figures 33, 34, 35 and 36 show the results as the parameter R_{DISK}/R_{CYL} varies using a value of 0.1 for ${}_dBi_{FRONT}$. Varying R_{DISK}/R_{CYL} in the absence of heat generation merely changes the area over which the surface temperature is averaged for use in the series solution. In all cases except the intermediate case for heat flux out, a larger value for R_{DISK}/R_{CYL} produces slightly more error in the series solution. This trend makes sense since the heat transfer should be more one-dimensional closer to the centerline of the cylinder and since the radial derivative is zero directly at the centerline. The impact of varying the geometry parameter R_{DISK}/R_{CYL} increases for larger values of L/R_{CYL} which also makes sense since the radial derivatives are greater with larger values of L/R_{CYL}. However, it should be noted that the change in the percent difference as the parameter L/R_{CYL} varies in most cases is less than the expected accuracy in the model, so the results are inconclusive. The trends could be trends in the error equation of the finite-difference model rather than actual trends in the results. Figures 71, 72, 73 and 74 in Appendix C.2 show the results as R_{DISK}/R_{CYL} varies using a value of 1.0 for ${}_dBi_{FRONT}$. These results are very similar.

4.3 Non-Adiabatic Cases with Heat Generation and Preheating

The non-adiabatic cases with heat generation and preheating investigate the effect on the series solution when both causes of two-dimensional heat transfer are present. These runs are a subset of the runs in the previous section to which preheating and subsequent heat generation are added.

Both the preheating and the disturbance problems are used for all runs. It should be noted that the limiting cases for heat flux out and in are identical in the preheating problem since the outer-radial boundary condition is the same in both as is seen by Equations 27 and 28 in Section 2.2. The limiting case for heat flux in models the condition where the thermal conductivity in the surrounding material

is infinite and the temperature of the surrounding material is the temperature of the fluid at the front surface. In the preheating problem, the temperature of the fluid at the front surface is the initial temperature.

The tolerance used in the convergence criterion for the preheating problem is 0.1 for all runs. All runs use a value of 1/8 for the geometry parameter R_{DISK}/R_{CYL}. Each of the four cases is run with a few values for the geometry parameter L/R_{CYL}. Values of 0.0, 0.05 and 0.2 for the parameter γ are run with each of the values for L/R_{CYL}. All runs are duplicated using values of 10.0 and 100.0 for the parameter β.

Figures 37, 38, 39 and 40 show the results for the limiting case for heat flux out, the intermediate case for heat flux out, the limiting case for heat flux in and the intermediate case for heat flux in, respectively, using a value of 10.0 for β. Figures 75, 76, 77 and 78 in Appendix C.3 show the results for the limiting case for heat flux out, the intermediate case for heat flux out, the limiting case for heat flux in and the intermediate case for heat flux in, respectively, using a value of 100.0 for β. As in the adiabatic cases, the preheating and subsequent heat generation has no impact on the results.

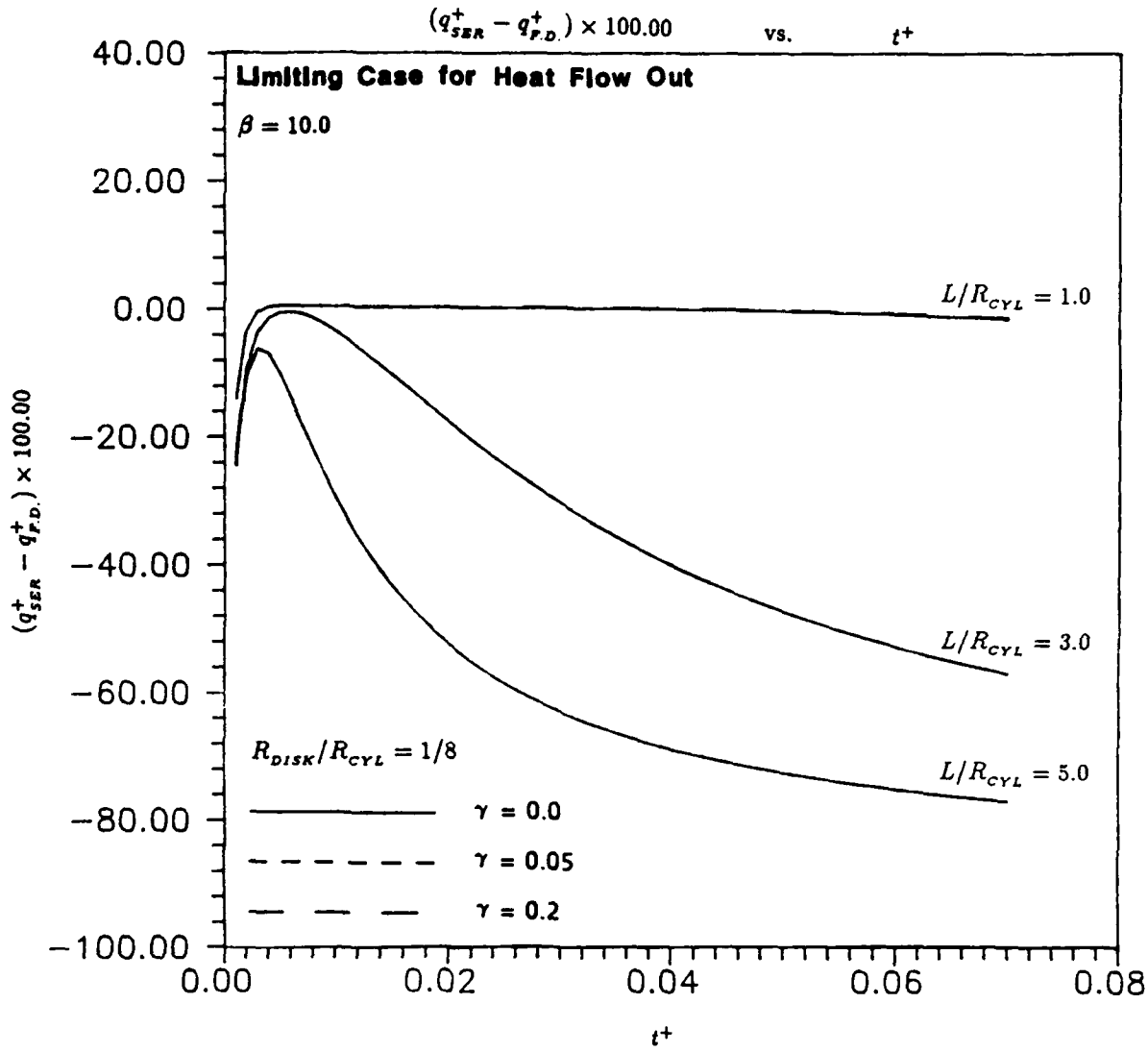

Figure 37. Results for the Limiting Case for Heat Flux Out Across the Outer-Radial Boundary with Heat Generation and Preheating Using β = 10.0

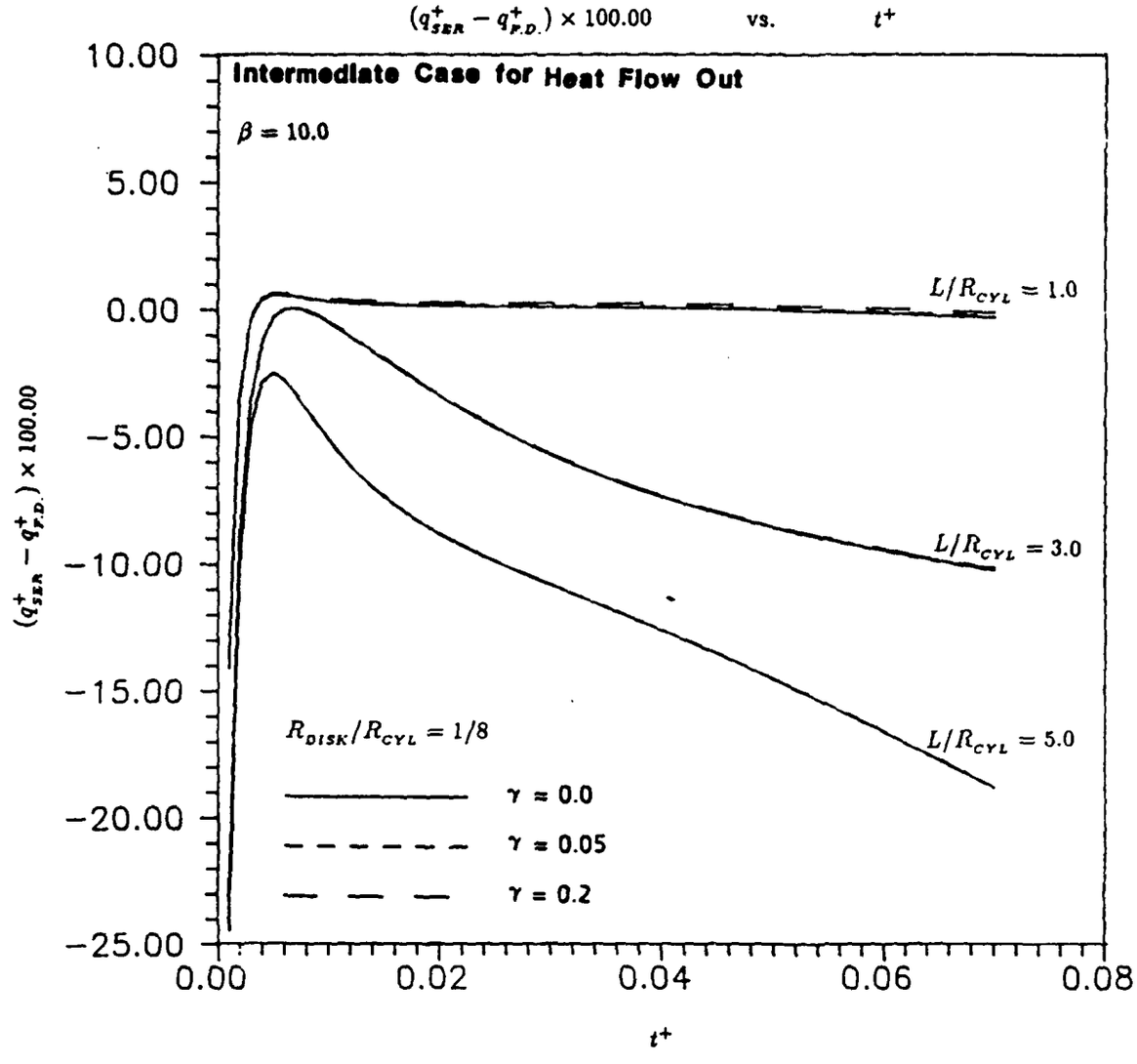

Figure 38. Results for the Intermediate Case for Heat Flux Out Across the Outer-Radial Boundary with Heat Generation and Preheating Using $\beta = 10.0$

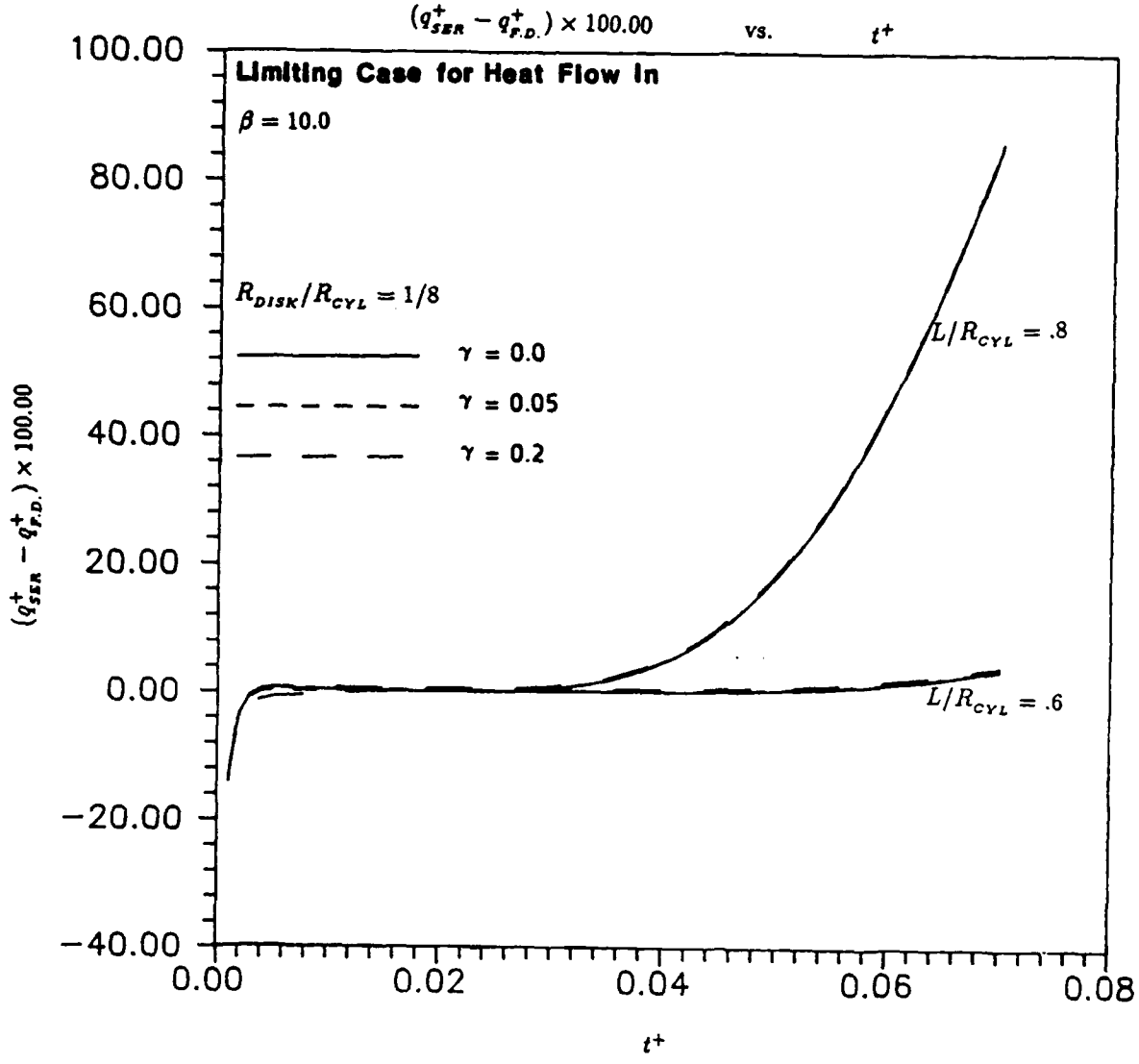

Figure 39. Results for the Limiting Case for Heat Flux In Across the Outer-Radial Boundary with Heat Generation and Preheating Using $\beta = 10.0$

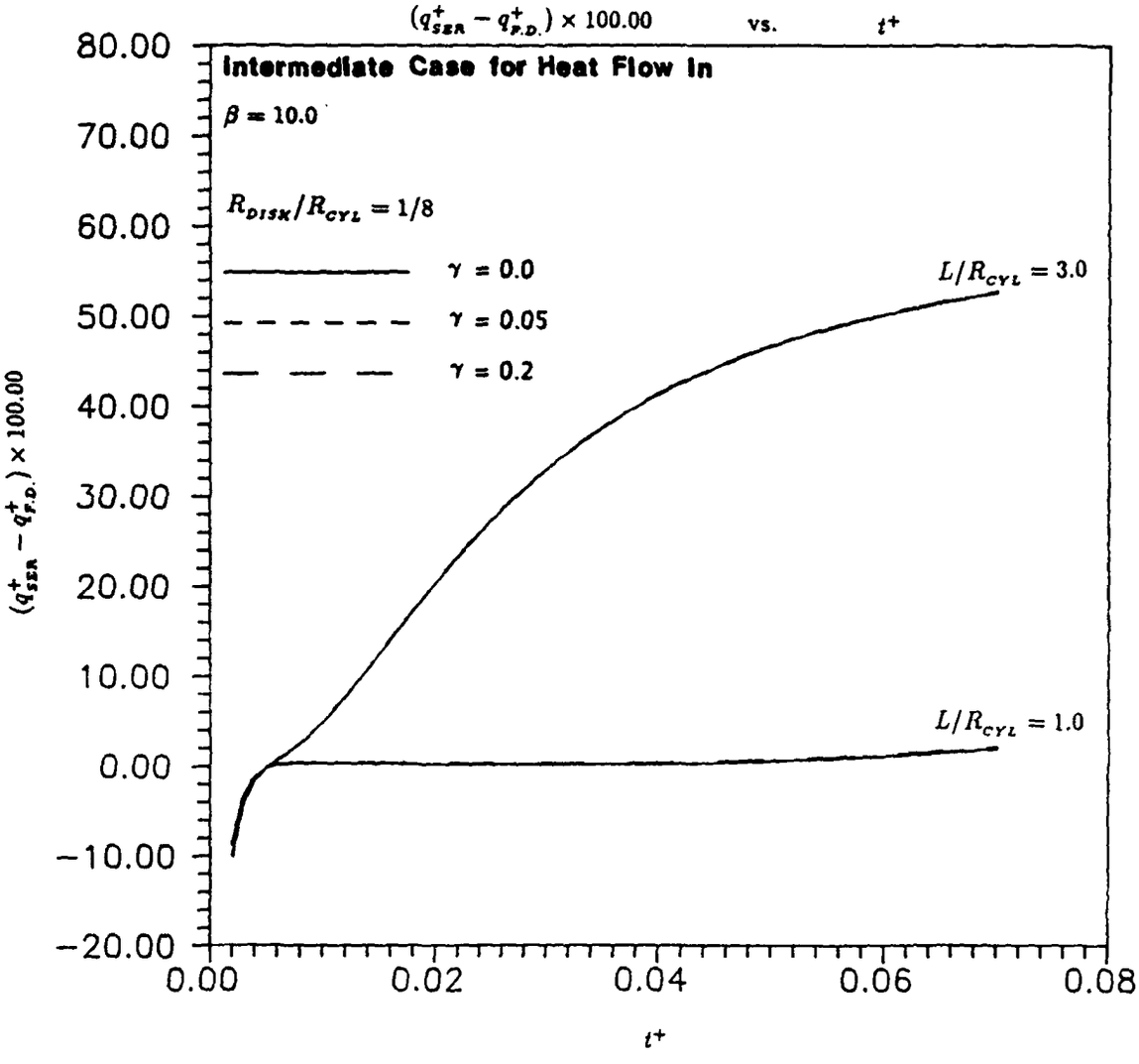

Figure 40. Results for the Intermediate Case for Heat Flux In Across the Outer-Radial Boundary with Heat Generation and Preheating Using $\beta = 10.0$

V. Conclusions and Recommendations

This thesis numerically investigates the accuracy of the one-dimensional series solution in determining the external surface heat flux actually present at the film in thin-film heat transfer gages. The heat transfer problem is simplified to two dimensions. From an overall point of view, the two possible causes for error in the series solution are the electrical heat generation in the thin-film sensor and the radial heat transfer induced by non-adiabatic conditions at the boundary of the gage.

The results show that the electrical heat generation should not cause errors as long as the instrumentation is turned on and the transients from the electrical heat generation are allowed to settle down prior to the test. It should not take long for the transients to settle down sufficiently to keep the error small. In tests using an adiabatic condition at the boundary of the gage, a non-dimensional time of 0.118, which is approximately twice as long as the time it takes the leading edge of a thermal disturbance to travel through the gage, was sufficient. The transients should settle down even quicker with non-adiabatic conditions since the temperature changes will be less.

The radial heat transfer induced from non-adiabatic conditions at the boundary of the gage can cause very significant errors in the results for long times. Because of limitations on the model, this investigation only looks at non-dimensional times greater than 0.01. The two most significant non-dimensional parameters which influence the error caused by the non-adiabatic conditions are the ratio of the thermal diffusivities in the insulating and cylinder materials and the geometry parameter L/R_{CYL}. Outward radial gradients caused by using an insulating material with a smaller thermal diffusivity than that of the cylinder material will cause the measured heat flux to be less than the actual, external surface heat flux. Inward radial gradients caused by using an insulating material with a greater ther-

mal diffusivity will cause the measured heat flux to be greater than the actual. In either case, a larger value of the geometry parameter L/R_{CYL} increases the error.

Limiting cases which bound the effects caused by non-adiabatic conditions were investigated. In the limiting case for outward radial heat flux, keeping the geometry parameter L/R_{CYL} less than 1.0 limited the error in the measurement for heat flux to less than 2 percent of the theoretically maximum, external surface heat flux for non-dimensional times up to 0.07. In the limiting case for inward radial heat flux, keeping the geometry parameter L/R_{CYL} less than 0.6 limited the error to 5 percent. In an intermediate case for outward radial heat flux, which used a value of 1/6 for the ratio of the thermal diffusivities of the surrounding material and the cylinder material, keeping the geometry parameter L/R_{CYL} less than 2.0 limited the error to 6 percent. Finally, in an intermediate case for inward radial heat flux, which used a ratio of 6.0 for the thermal diffusivities, keeping the geometry parameter L/R_{CYL} less than 1.0 limited the error to 2 percent.

Using values of L/R_{CYL} larger than these can produce large errors in the results. In the limiting case for outward radial heat flux, using a value of 2.0 for the geometry parameter L/R_{CYL} and 0.1 for the Biot number at the front surface produced a steadily increasing error which reached 30 percent by non-dimensional time of 0.07. In the limiting case for inward radial heat flux, using a value of 0.8 for the geometry parameter L/R_{CYL} and 0.1 for the Biot number at the front surface produced an error which reached 85 percent. In the intermediate case for outward radial heat flux, using a value of 4.0 for L/R_{CYL} and 0.1 for the Biot number produced an error which reached 13 percent. Finally, in the intermediate case for inward radial heat flux, using a value of 2.0 for L/R_{CYL} and 0.1 for the Biot number produced an error which reached 34 percent. Since the error increases with time, one can attain better accuracy with larger values of the geometry parameter L/R_{CYL} and greater differences in the thermal diffusivities if one uses shorter test times.

The error caused by a non-adiabatic condition at the boundary of the gage can be significant. One can try to limit this error in three ways. First, one can use as good an insulating material as possible in mounting the gage. Although this technique promises to improve the accuracy in the series solution, it may cause the heat flux at the gage to be very different from the heat flux that would occur in the absence of the gage because the temperature changes due to the electrical heating will be greater. Secondly, one could try to match properties between the cylinder material and the insulating material to limit the temperature difference across the boundary of the cylinder. This technique should improve the accuracy of the series solution while minimizing the deleterious effect of the electrical heating in the thin film. Thirdly, one can use a gage with a smaller geometry ratio L/R_{CYL}.

The results from this investigation must be weighed in view of the accuracy of the model as estimated from the transient check cases for one-dimensional heat transfer in the axial direction. As a conservative estimate, the model should be accurate to within a percent difference of 4.0 for non-dimensional times greater than 0.01 where the percent difference is the percent of the theoretically maximum, external surface heat flux by which the series solution estimate differs from the actual heat flux in the finite-difference model, i.e. $(q^+_{SER} - q^+_{F.D.}) \times 100.00$.

Appendices

Appendix A. *Nodal Equations*

A.1 Single-Material Problem with Fully-Insulated, Outer-Radial Boundary Condition

Preheating Problem:

Note 1: Nodal Equations (a)–(i) apply to the corresponding positions in Figure 4.

Note 2: For nodes on the front surface of the cylinder, Equations (a)–(c), the last term in the nodal finite-difference equation is included only if the node lies within the heated disk.

(a)

$$\begin{aligned}\theta^{+j+1}_{0,0} &= 4\left[\frac{L}{R_{CYL}}\right]^2 \frac{\Delta t^+}{(\Delta r^+)^2}\theta^{+j}_{1,0} + 2\frac{\Delta t^+}{(\Delta z^+)^2}\theta^{+j}_{0,1} \\ &+ \left(1 - 4\left[\frac{L}{R_{CYL}}\right]^2 \frac{\Delta t^+}{(\Delta r^+)^2} - 2\frac{\Delta t^+}{(\Delta z^+)^2} - 2_p Bi_{FRONT}\frac{\Delta t^+}{\Delta z^+}\right)\theta^{+j}_{0,0} \\ &+ 2_p Bi_{FRONT}\frac{\Delta t^+}{\Delta z^+}\end{aligned}$$

(b)

$$\begin{aligned}\theta^{+j+1}_{n,0} &= \left[\frac{L}{R_{CYL}}\right]^2 (1 - 1/(2n))\frac{\Delta t^+}{(\Delta r^+)^2}\theta^{+j}_{n-1,0} \\ &+ \left[\frac{L}{R_{CYL}}\right]^2 (1 + 1/(2n))\frac{\Delta t^+}{(\Delta r^+)^2}\theta^{+j}_{n+1,0} + 2\frac{\Delta t^+}{(\Delta z^+)^2}\theta^{+j}_{n,1} \\ &+ \left(1 - 2\left[\frac{L}{R_{CYL}}\right]^2 \frac{\Delta t^+}{(\Delta r^+)^2} - 2\frac{\Delta t^+}{(\Delta z^+)^2} - 2_p Bi_{FRONT}\frac{\Delta t^+}{\Delta z^+}\right)\theta^{+j}_{n,0} \\ &+ 2_p Bi_{FRONT}\frac{\Delta t^+}{\Delta z^+}\end{aligned}$$

(c)

$$\theta^{+j+1}_{N_{CYL},0} = 2\left[\frac{L}{R_{CYL}}\right]^2\left(\frac{N_{CYL}-1/2}{N_{CYL}-1/4}\right)\frac{\Delta t^+}{(\Delta r^+)^2}\theta^{+j}_{N_{CYL}-1,0} + 2\frac{\Delta t^+}{(\Delta z^+)^2}\theta^{+j}_{N_{CYL},1} + \left(1-2\left[\frac{L}{R_{CYL}}\right]^2\left(\frac{N_{CYL}-1/2}{N_{CYL}-1/4}\right)\frac{\Delta t^+}{(\Delta r^+)^2} - 2\frac{\Delta t^+}{(\Delta z^+)^2} - 2_pBi_{FRONT}\frac{\Delta t^+}{\Delta z^+}\right)\theta^{+j}_{N_{CYL},0} + 2_pBi_{FRONT}\frac{\Delta t^+}{\Delta z^+}$$

(d)

$$\theta^{+j+1}_{0,m} = 4\left[\frac{L}{R_{CYL}}\right]^2\frac{\Delta t^+}{(\Delta r^+)^2}\theta^{+j}_{1,m} + \frac{\Delta t^+}{(\Delta z^+)^2}\theta^{+j}_{0,m-1} + \frac{\Delta t^+}{(\Delta z^+)^2}\theta^{+j}_{0,m+1} + \left(1-4\left[\frac{L}{R_{CYL}}\right]^2\frac{\Delta t^+}{(\Delta r^+)^2} - 2\frac{\Delta t^+}{(\Delta z^+)^2}\right)\theta^{+j}_{0,m}$$

(e)

$$\theta^{+j+1}_{n,m} = \left[\frac{L}{R_{CYL}}\right]^2(1-1/(2n))\frac{\Delta t^+}{(\Delta r^+)^2}\theta^{+j}_{n-1,m} + \left[\frac{L}{R_{CYL}}\right]^2(1+1/(2n))\frac{\Delta t^+}{(\Delta r^+)^2}\theta^{+j}_{n+1,m} + \frac{\Delta t^+}{(\Delta z^+)^2}\theta^{+j}_{n,m-1} + \frac{\Delta t^+}{(\Delta z^+)^2}\theta^{+j}_{n,m+1} + \left(1-2\left[\frac{L}{R_{CYL}}\right]^2\frac{\Delta t^+}{(\Delta r^+)^2} - 2\frac{\Delta t^+}{(\Delta z^+)^2}\right)\theta^{+j}_{n,m}$$

(f)

$$\theta^{+j+1}_{N_{CYL},m} = 2\left[\frac{L}{R_{CYL}}\right]^2\left(\frac{N_{CYL}-1/2}{N_{CYL}-1/4}\right)\frac{\Delta t^+}{(\Delta r^+)^2}\theta^{+j}_{N_{CYL}-1,m} + \frac{\Delta t^+}{(\Delta z^+)^2}\theta^{+j}_{N_{CYL},m-1} + \frac{\Delta t^+}{(\Delta z^+)^2}\theta^{+j}_{N_{CYL},m+1} + \left(1-2\left[\frac{L}{R_{CYL}}\right]^2\left(\frac{N_{CYL}-1/2}{N_{CYL}-1/4}\right)\frac{\Delta t^+}{(\Delta r^+)^2}\right.$$

$$- 2\frac{\Delta t^+}{(\Delta z^+)^2}\frac{\Delta t^+}{\Delta z^+}\Bigg)\theta^{+j}_{N_{CYL},m}$$

(g)

$$\begin{aligned}\theta^{+j+1}_{0,M_{MAX}} &= 4\left[\frac{L}{R_{CYL}}\right]^2\frac{\Delta t^+}{(\Delta r^+)^2}\theta^{+j}_{1,M_{MAX}} + 2\frac{\Delta t^+}{(\Delta z^+)^2}\theta^{+j}_{0,M_{MAX}-1}\\ &+\left(1-4\left[\frac{L}{R_{CYL}}\right]^2\frac{\Delta t^+}{(\Delta r^+)^2} - 2\frac{\Delta t^+}{(\Delta z^+)^2}\right.\\ &\left.- 2_pBi_{BACK}\frac{\Delta t^+}{\Delta z^+}\right)\theta^{+j}_{0,M_{MAX}}\end{aligned}$$

(h)

$$\begin{aligned}\theta^{+j+1}_{n,0} &= \left[\frac{L}{R_{CYL}}\right]^2(1-1/(2n))\frac{\Delta t^+}{(\Delta r^+)^2}\theta^{+j}_{n-1,M_{MAX}}\\ &+\left[\frac{L}{R_{CYL}}\right]^2(1+1/(2n))\frac{\Delta t^+}{(\Delta r^+)^2}\theta^{+j}_{n+1,M_{MAX}}\\ &+2\frac{\Delta t^+}{(\Delta z^+)^2}\theta^{+j}_{n,M_{MAX}-1}\\ &+\left(1-2\left[\frac{L}{R_{CYL}}\right]^2\frac{\Delta t^+}{(\Delta r^+)^2} - 2\frac{\Delta t^+}{(\Delta z^+)^2}\right.\\ &\left.- 2_pBi_{BACK}\frac{\Delta t^+}{\Delta z^+}\right)\theta^{+j}_{n,M_{MAX}}\end{aligned}$$

(i)

$$\begin{aligned}\theta^{+j+1}_{N_{CYL},M_{MAX}} &= 2\left[\frac{L}{R_{CYL}}\right]^2\left(\frac{N_{CYL}-1/2}{N_{CYL}-1/4}\right)\frac{\Delta t^+}{(\Delta r^+)^2}\theta^{+j}_{N_{CYL}-1,M_{MAX}}\\ &+2\frac{\Delta t^+}{(\Delta z^+)^2}\theta^{+j}_{N_{CYL},M_{MAX}-1}\\ &+\left(1-2\left[\frac{L}{R_{CYL}}\right]^2\left(\frac{N_{CYL}-1/2}{N_{CYL}-1/4}\right)\frac{\Delta t^+}{(\Delta r^+)^2} - 2\frac{\Delta t^+}{(\Delta z^+)^2}\right.\\ &\left.- 2_pBi_{BACK}\frac{\Delta t^+}{\Delta z^+}\right)\theta^{+j}_{N_{CYL},M_{MAX}}\end{aligned}$$

Disturbance Problem:

Note 1: Nodal Equations (a)–(i) apply to the corresponding positions in Figure 4.

Note 2: For nodes on the front surface of the cylinder, Equations (a)–(c), the last term in the nodal finite-difference equation, i.e. the term including the parameter γ, is included only if the node lies within the heated disk.

(a)

$$\begin{aligned}\theta^{+j+1}_{0,0} &= 4\left[\frac{L}{R_{CYL}}\right]^2 \frac{\Delta t^+}{(\Delta r^+)^2}\theta^{+j}_{1,0} + 2\frac{\Delta t^+}{(\Delta z^+)^2}\theta^{+j}_{0,1} \\ &+ \left(1 - 4\left[\frac{L}{R_{CYL}}\right]^2 \frac{\Delta t^+}{(\Delta r^+)^2} - 2\frac{\Delta t^+}{(\Delta z^+)^2} - 2_d Bi_{FRONT}\frac{\Delta t^+}{\Delta z^+}\right)\theta^{+j}_{0,0} \\ &+ 2_d Bi_{FRONT}\frac{\Delta t^+}{\Delta z^+} + 2_d Bi_{FRONT}\frac{\Delta t^+}{\Delta z^+}(\gamma)\end{aligned}$$

(b)

$$\begin{aligned}\theta^{+j+1}_{n,0} &= \left[\frac{L}{R_{CYL}}\right]^2 (1 - 1/(2n))\frac{\Delta t^+}{(\Delta r^+)^2}\theta^{+j}_{n-1,0} \\ &+ \left[\frac{L}{R_{CYL}}\right]^2 (1 + 1/(2n))\frac{\Delta t^+}{(\Delta r^+)^2}\theta^{+j}_{n+1,0} + 2\frac{\Delta t^+}{(\Delta z^+)^2}\theta^{+j}_{n,1} \\ &+ \left(1 - 2\left[\frac{L}{R_{CYL}}\right]^2 \frac{\Delta t^+}{(\Delta r^+)^2} - 2\frac{\Delta t^+}{(\Delta z^+)^2} - 2_d Bi_{FRONT}\frac{\Delta t^+}{\Delta z^+}\right)\theta^{+j}_{n,0} \\ &+ 2_d Bi_{FRONT}\frac{\Delta t^+}{\Delta z^+} + 2_d Bi_{FRONT}\frac{\Delta t^+}{\Delta z^+}(\gamma)\end{aligned}$$

(c)

$$\begin{aligned}\theta^{+j+1}_{N_{CYL},0} &= 2\left[\frac{L}{R_{CYL}}\right]^2 \left(\frac{N_{CYL} - 1/2}{N_{CYL} - 1/4}\right)\frac{\Delta t^+}{(\Delta r^+)^2}\theta^{+j}_{N_{CYL}-1,0} \\ &+ 2\frac{\Delta t^+}{(\Delta z^+)^2}\theta^{+j}_{N_{CYL},1} \\ &+ \left(1 - 2\left[\frac{L}{R_{CYL}}\right]^2 \left(\frac{N_{CYL} - 1/2}{N_{CYL} - 1/4}\right)\frac{\Delta t^+}{(\Delta r^+)^2}\right.\end{aligned}$$

$$- 2\frac{\Delta t^+}{(\Delta z^+)^2} - 2_d Bi_{FRONT}\frac{\Delta t^+}{\Delta z^+}\Bigg)\theta^{+j}_{N_{CYL},0}$$
$$+ 2_d Bi_{FRONT}\frac{\Delta t^+}{\Delta z^+} + 2_d Bi_{FRONT}\frac{\Delta t^+}{\Delta z^+}(\gamma)$$

(d)

$$\theta^{+j+1}_{0,m} = 4\left[\frac{L}{R_{CYL}}\right]^2\frac{\Delta t^+}{(\Delta r^+)^2}\theta^{+j}_{1,m} + \frac{\Delta t^+}{(\Delta z^+)^2}\theta^{+j}_{0,m-1}$$
$$+ \frac{\Delta t^+}{(\Delta z^+)^2}\theta^{+j}_{0,m+1}$$
$$+ \left(1 - 4\left[\frac{L}{R_{CYL}}\right]^2\frac{\Delta t^+}{(\Delta r^+)^2} - 2\frac{\Delta t^+}{(\Delta z^+)^2}\right)\theta^{+j}_{0,m}$$

(e)

$$\theta^{+j+1}_{n,m} = \left[\frac{L}{R_{CYL}}\right]^2(1 - 1/(2n))\frac{\Delta t^+}{(\Delta r^+)^2}\theta^{+j}_{n-1,m}$$
$$+ \left[\frac{L}{R_{CYL}}\right]^2(1 + 1/(2n))\frac{\Delta t^+}{(\Delta r^+)^2}\theta^{+j}_{n+1,m}$$
$$+ \frac{\Delta t^+}{(\Delta z^+)^2}\theta^{+j}_{n,m-1} + \frac{\Delta t^+}{(\Delta z^+)^2}\theta^{+j}_{n,m+1}$$
$$+ \left(1 - 2\left[\frac{L}{R_{CYL}}\right]^2\frac{\Delta t^+}{(\Delta r^+)^2} - 2\frac{\Delta t^+}{(\Delta z^+)^2}\right)\theta^{+j}_{n,m}$$

(f)

$$\theta^{+j+1}_{N_{CYL},m} = 2\left[\frac{L}{R_{CYL}}\right]^2\left(\frac{N_{CYL} - 1/2}{N_{CYL} - 1/4}\right)\frac{\Delta t^+}{(\Delta r^+)^2}\theta^{+j}_{N_{CYL}-1,m}$$
$$+ \frac{\Delta t^+}{(\Delta z^+)^2}\theta^{+j}_{N_{CYL},m-1} + \frac{\Delta t^+}{(\Delta z^+)^2}\theta^{+j}_{N_{CYL},m+1}$$
$$+ \Bigg(1 - 2\left[\frac{L}{R_{CYL}}\right]^2\left(\frac{N_{CYL} - 1/2}{N_{CYL} - 1/4}\right)\frac{\Delta t^+}{(\Delta r^+)^2}$$
$$- 2\frac{\Delta t^+}{(\Delta z^+)^2}\frac{\Delta t^+}{\Delta z^+}\Bigg)\theta^{+j}_{N_{CYL},m}$$

(g)

$$\theta^{+j+1}_{0,M_{MAX}} = 4\left[\frac{L}{R_{CYL}}\right]^2\frac{\Delta t^+}{(\Delta r^+)^2}\theta^{+j}_{1,M_{MAX}} + 2\frac{\Delta t^+}{(\Delta z^+)^2}\theta^{+j}_{0,M_{MAX}-1}$$

$$+\left(1-4\left[\frac{L}{R_{CYL}}\right]^2\frac{\Delta t^+}{(\Delta r^+)^2}-2\frac{\Delta t^+}{(\Delta z^+)^2}\right.$$
$$\left.-2_dBi_{BACK}\frac{\Delta t^+}{\Delta z^+}\right)\theta^{+j}_{0,M_{MAX}}$$
$$+2_dBi_{BACK}\frac{\Delta t^+}{\Delta z^+}(\tau)$$

(h)

$$\theta^{+j+1}_{n,0} = \left[\frac{L}{R_{CYL}}\right]^2(1-1/(2n))\frac{\Delta t^+}{(\Delta r^+)^2}\theta^{+j}_{n-1,M_{MAX}}$$
$$+\left[\frac{L}{R_{CYL}}\right]^2(1+1/(2n))\frac{\Delta t^+}{(\Delta r^+)^2}\theta^{+j}_{n+1,M_{MAX}}$$
$$+2\frac{\Delta t^+}{(\Delta z^+)^2}\theta^{+j}_{n,M_{MAX}-1}$$
$$+\left(1-2\left[\frac{L}{R_{CYL}}\right]^2\frac{\Delta t^+}{(\Delta r^+)^2}-2\frac{\Delta t^+}{(\Delta z^+)^2}\right.$$
$$\left.-2_dBi_{BACK}\frac{\Delta t^+}{\Delta z^+}\right)\theta^{+j}_{n,M_{MAX}}$$
$$+2_dBi_{BACK}\frac{\Delta t^+}{\Delta z^+}(\tau)$$

(i)

$$\theta^{+j+1}_{N_{CYL},M_{MAX}} = 2\left[\frac{L}{R_{CYL}}\right]^2\left(\frac{N_{CYL}-1/2}{N_{CYL}-1/4}\right)\frac{\Delta t^+}{(\Delta r^+)^2}\theta^{+j}_{N_{CYL}-1,M_{MAX}}$$
$$+2\frac{\Delta t^+}{(\Delta z^+)^2}\theta^{+j}_{N_{CYL},M_{MAX}-1}$$
$$+\left(1-2\left[\frac{L}{R_{CYL}}\right]^2\left(\frac{N_{CYL}-1/2}{N_{CYL}-1/4}\right)\frac{\Delta t^+}{(\Delta r^+)^2}\right.$$
$$\left.-2\frac{\Delta t^+}{(\Delta z^+)^2}-2_dBi_{BACK}\frac{\Delta t^+}{\Delta z^+}\right)\theta^{+j}_{N_{CYL},M_{MAX}}$$
$$+2_dBi_{BACK}\frac{\Delta t^+}{\Delta z^+}(\tau)$$

A.2 Two-Material Problem with Fully-Insulated, Outer-Radial Boundary Condition

Preheating Problem:

Note 1: Nodal Equations (a)–(o) apply to the corresponding positions in Figure 5.

Note 2: For nodes on the front surface of the cylinder, Equations (a)–(c), the last term in the nodal finite-difference equation is included only if the node lies within the heated disk.

(a)

$$\theta^{+j+1}_{0,0} = 4\left[\frac{L}{R_{CYL}}\right]^2 \frac{\Delta t^+}{(\Delta r^+)^2}\theta^{+j}_{1,0} + 2\frac{\Delta t^+}{(\Delta z^+)^2}\theta^{+j}_{0,1} + \left(1 - 4\left[\frac{L}{R_{CYL}}\right]^2 \frac{\Delta t^+}{(\Delta r^+)^2} - 2\frac{\Delta t^+}{(\Delta z^+)^2} - 2_p Bi_{FRONT}\frac{\Delta t^+}{\Delta z^+}\right)\theta^{+j}_{0,0} + 2_p Bi_{FRONT}\frac{\Delta t^+}{\Delta z^+}$$

(b)

$$\theta^{+j+1}_{n,0} = \left[\frac{L}{R_{CYL}}\right]^2 (1 - 1/(2n))\frac{\Delta t^+}{(\Delta r^+)^2}\theta^{+j}_{n-1,0} + \left[\frac{L}{R_{CYL}}\right]^2 (1 + 1/(2n))\frac{\Delta t^+}{(\Delta r^+)^2}\theta^{+j}_{n+1,0} + 2\frac{\Delta t^+}{(\Delta z^+)^2}\theta^{+j}_{n,1} + \left(1 - 2\left[\frac{L}{R_{CYL}}\right]^2 \frac{\Delta t^+}{(\Delta r^+)^2} - 2\frac{\Delta t^+}{(\Delta z^+)^2} - 2_p Bi_{FRONT}\frac{\Delta t^+}{\Delta z^+}\right)\theta^{+j}_{n,0} + 2_p Bi_{FRONT}\frac{\Delta t^+}{\Delta z^+}$$

(c)

$$\theta^{+j+1}_{N_{CYL},0} = \left[\frac{\rho c_p}{(\rho c_p)'}\right]\left[\frac{L}{R_{CYL}}\right]^2 (1 - 1/(2N_{CYL}))\frac{\Delta t^+}{(\Delta r^+)^2}\theta^{+j}_{N_{CYL}-1,0}$$

$$
\begin{aligned}
&+\left[\frac{\rho c_p}{(\rho c_p)'}\right]\left[\frac{k'}{k}\right]\left[\frac{L}{R_{CYL}}\right]^2(1+1/(2N_{CYL}))\frac{\Delta t^+}{(\Delta r^+)^2}\theta^{+j}_{N_{CYL}+1,0}\\
&+2\left[\frac{\rho c_p}{(\rho c_p)'}\right]\left[\frac{k'}{k}\right]\frac{\Delta t^+}{(\Delta z^+)^2}\theta^{+j}_{N_{CYL},1}\\
&+\left(1-\left[\frac{\rho c_p}{(\rho c_p)'}\right]\left[\frac{k'}{k}\right]\left[\frac{L}{R_{CYL}}\right]^2(1-1/(2N_{CYL}))\frac{\Delta t^+}{(\Delta r^+)^2}\right.\\
&\quad-\left[\frac{\rho c_p}{(\rho c_p)'}\right]\left[\frac{k'}{k}\right]\left[\frac{L}{R_{CYL}}\right]^2(1+1/(2N_{CYL}))\frac{\Delta t^+}{(\Delta r^+)^2}\\
&\quad-2\left[\frac{\rho c_p}{(\rho c_p)'}\right]\left[\frac{k'}{k}\right]\frac{\Delta t^+}{(\Delta z^+)^2}\\
&\quad\left.-2\left[\frac{\rho c_p}{(\rho c_p)'}\right]{}_pBi_{FRONT}\frac{\Delta t^+}{\Delta z^+}\right)\theta^{+j}_{N_{CYL},0}\\
&+2\left[\frac{\rho c_p}{(\rho c_p)'}\right]{}_pBi_{FRONT}\frac{\Delta t^+}{\Delta z^+}
\end{aligned}
$$

(d)

$$
\begin{aligned}
\theta^{+j+1}_{n,0} &= \left[\frac{\rho c_p}{(\rho c_p)'}\right]\left[\frac{k'}{k}\right]\left[\frac{L}{R_{CYL}}\right]^2(1-1/(2n))\frac{\Delta t^+}{(\Delta r^+)^2}\theta^{+j}_{n-1,0}\\
&+\left[\frac{\rho c_p}{(\rho c_p)'}\right]\left[\frac{k'}{k}\right]\left[\frac{L}{R_{CYL}}\right]^2(1+1/(2n))\frac{\Delta t^+}{(\Delta r^+)^2}\theta^{+j}_{n+1,0}\\
&+2\left[\frac{\rho c_p}{(\rho c_p)'}\right]\left[\frac{k'}{k}\right]\frac{\Delta t^+}{(\Delta z^+)^2}\theta^{+j}_{n,1}\\
&+\left(1-2\left[\frac{\rho c_p}{(\rho c_p)'}\right]\left[\frac{k'}{k}\right]\left[\frac{L}{R_{CYL}}\right]^2\frac{\Delta t^+}{(\Delta r^+)^2}-2\left[\frac{\rho c_p}{(\rho c_p)'}\right]\left[\frac{k'}{k}\right]\frac{\Delta t^+}{(\Delta z^+)^2}\right.\\
&\quad\left.-2\left[\frac{\rho c_p}{(\rho c_p)'}\right]{}_pBi_{FRONT}\frac{\Delta t^+}{\Delta z^+}\right)\theta^{+j}_{n,0}
\end{aligned}
$$

(e)

$$
\begin{aligned}
\theta^{+j+1}_{N_{MAX},0} &= 2\left[\frac{\rho c_p}{(\rho c_p)'}\right]\left[\frac{k'}{k}\right]\left[\frac{L}{R_{CYL}}\right]^2\left(\frac{N_{MAX}-1/2}{N_{MAX}-1/4}\right)\frac{\Delta t^+}{(\Delta r^+)^2}\theta^{+j}_{N_{MAX}-1,0}\\
&+2\left[\frac{\rho c_p}{(\rho c_p)'}\right]\left[\frac{k'}{k}\right]\frac{\Delta t^+}{(\Delta z^+)^2}\theta^{+j}_{N_{MAX},1}\\
&+\left(1-2\left[\frac{\rho c_p}{(\rho c_p)'}\right]\left[\frac{k'}{k}\right]\left[\frac{L}{R_{CYL}}\right]^2\left(\frac{N_{MAX}-1/2}{N_{MAX}-1/4}\right)\frac{\Delta t^+}{(\Delta r^+)^2}\right.
\end{aligned}
$$

$$
\begin{aligned}
&- 2\left[\frac{\rho c_p}{(\rho c_p)'}\right]\left[\frac{k'}{k}\right]\frac{\Delta t^+}{(\Delta z^+)^2} \\
&- 2\left[\frac{\rho c_p}{(\rho c_p)'}\right]{}_pBi_{FRONT}\frac{\Delta t^+}{\Delta z^+}\Bigg)\theta^{+j}_{N_{MAX},0}
\end{aligned}
$$

(f)

$$
\begin{aligned}
\theta^{+j+1}_{0,m} &= 4\left[\frac{L}{R_{CYL}}\right]^2\frac{\Delta t^+}{(\Delta r^+)^2}\theta^{+j}_{1,m} + \frac{\Delta t^+}{(\Delta z^+)^2}\theta^{+j}_{0,m-1} + \frac{\Delta t^+}{(\Delta z^+)^2}\theta^{+j}_{0,m+1} \\
&+ \left(1 - 4\left[\frac{L}{R_{CYL}}\right]^2\frac{\Delta t^+}{(\Delta r^+)^2} - 2\frac{\Delta t^+}{(\Delta z^+)^2}\right)\theta^{+j}_{0,m}
\end{aligned}
$$

(g)

$$
\begin{aligned}
\theta^{+j+1}_{n,m} &= \left[\frac{L}{R_{CYL}}\right]^2(1 - 1/(2n))\frac{\Delta t^+}{(\Delta r^+)^2}\theta^{+j}_{n-1,m} \\
&+ \left[\frac{L}{R_{CYL}}\right]^2(1 + 1/(2n))\frac{\Delta t^+}{(\Delta r^+)^2}\theta^{+j}_{n+1,m} \\
&+ \frac{\Delta t^+}{(\Delta z^+)^2}\theta^{+j}_{n,m-1} + \frac{\Delta t^+}{(\Delta z^+)^2}\theta^{+j}_{n,m+1} \\
&+ \left(1 - 2\left[\frac{L}{R_{CYL}}\right]^2\frac{\Delta t^+}{(\Delta r^+)^2} - 2\frac{\Delta t^+}{(\Delta z^+)^2}\right)\theta^{+j}_{n,m}
\end{aligned}
$$

(h)

$$
\begin{aligned}
\theta^{+j+1}_{N_{CYL},m} &= \left[\frac{\rho c_p}{(\rho c_p)'}\right]\left[\frac{L}{R_{CYL}}\right]^2(1 - 1/(2N_{CYL}))\frac{\Delta t^+}{(\Delta r^+)^2}\theta^{+j}_{N_{CYL}-1,m} \\
&+ \left[\frac{\rho c_p}{(\rho c_p)'}\right]\left[\frac{k'}{k}\right]\left[\frac{L}{R_{CYL}}\right]^2(1 + 1/(2N_{CYL}))\frac{\Delta t^+}{(\Delta r^+)^2}\theta^{+j}_{N_{CYL}+1,m} \\
&+ \left[\frac{\rho c_p}{(\rho c_p)'}\right]\left[\frac{k'}{k}\right]\frac{\Delta t^+}{(\Delta z^+)^2}\theta^{+j}_{N_{CYL},m-1} \\
&+ \left[\frac{\rho c_p}{(\rho c_p)'}\right]\left[\frac{k'}{k}\right]\frac{\Delta t^+}{(\Delta z^+)^2}\theta^{+j}_{N_{CYL},m+1} \\
&+ \Bigg(1 - \left[\frac{\rho c_p}{(\rho c_p)'}\right]\left[\frac{L}{R_{CYL}}\right]^2(1 - 1/(2N_{CYL}))\frac{\Delta t^+}{(\Delta r^+)^2} \\
&\quad - \left[\frac{\rho c_p}{(\rho c_p)'}\right]\left[\frac{k'}{k}\right]\left[\frac{L}{R_{CYL}}\right]^2(1 + 1/(2N_{CYL}))\frac{\Delta t^+}{(\Delta r^+)^2} \\
&\quad - 2\left[\frac{\rho c_p}{(\rho c_p)'}\right]\left[\frac{k'}{k}\right]\frac{\Delta t^+}{(\Delta z^+)^2}\Bigg)\theta^{+j}_{N_{CYL},m}
\end{aligned}
$$

(i)

$$\theta^{+j+1}_{n,m} = \left[\frac{\rho c_p}{(\rho c_p)'}\right]\left[\frac{k'}{k}\right]\left[\frac{L}{R_{CYL}}\right]^2 (1-1/(2n))\frac{\Delta t^+}{(\Delta r^+)^2}\theta^{+j}_{n-1,m}$$
$$+\left[\frac{\rho c_p}{(\rho c_p)'}\right]\left[\frac{k'}{k}\right]\left[\frac{L}{R_{CYL}}\right]^2 (1+1/(2n))\frac{\Delta t^+}{(\Delta r^+)^2}\theta^{+j}_{n+1,m}$$
$$+\left[\frac{\rho c_p}{(\rho c_p)'}\right]\left[\frac{k'}{k}\right]\frac{\Delta t^+}{(\Delta z^+)^2}\theta^{+j}_{n,m-1}+\left[\frac{\rho c_p}{(\rho c_p)'}\right]\left[\frac{k'}{k}\right]\frac{\Delta t^+}{(\Delta z^+)^2}\theta^{+j}_{n,m+1}$$
$$+\left(1-2\left[\frac{\rho c_p}{(\rho c_p)'}\right]\left[\frac{k'}{k}\right]\left[\frac{L}{R_{CYL}}\right]^2\frac{\Delta t^+}{(\Delta r^+)^2}\right.$$
$$\left.-2\left[\frac{\rho c_p}{(\rho c_p)'}\right]\left[\frac{k'}{k}\right]\frac{\Delta t^+}{(\Delta z^+)^2}\right)\theta^{+j}_{n,m}$$

(j)

$$\theta^{+j+1}_{N_{MAX},m} = 2\left[\frac{\rho c_p}{(\rho c_p)'}\right]\left[\frac{k'}{k}\right]\left[\frac{L}{R_{CYL}}\right]^2\left(\frac{N_{MAX}-1/2}{N_{MAX}-1/4}\right)\frac{\Delta t^+}{(\Delta r^+)^2}\theta^{+j}_{N_{MAX}-1,m}$$
$$+\left[\frac{\rho c_p}{(\rho c_p)'}\right]\left[\frac{k'}{k}\right]\frac{\Delta t^+}{(\Delta z^+)^2}\theta^{+j}_{N_{MAX},m-1}$$
$$+\left[\frac{\rho c_p}{(\rho c_p)'}\right]\left[\frac{k'}{k}\right]\frac{\Delta t^+}{(\Delta z^+)^2}\theta^{+j}_{N_{MAX},m+1}$$
$$+\left(1-2\left[\frac{\rho c_p}{(\rho c_p)'}\right]\left[\frac{k'}{k}\right]\left[\frac{L}{R_{CYL}}\right]^2\left(\frac{N_{MAX}-1/2}{N_{MAX}-1/4}\right)\frac{\Delta t^+}{(\Delta r^+)^2}\right.$$
$$\left.-2\left[\frac{\rho c_p}{(\rho c_p)'}\right]\left[\frac{k'}{k}\right]\frac{\Delta t^+}{(\Delta z^+)^2}\right)\theta^{+j}_{N_{MAX},m}$$

(k)

$$\theta^{+j+1}_{0,M_{MAX}} = 4\left[\frac{L}{R_{CYL}}\right]^2\frac{\Delta t^+}{(\Delta r^+)^2}\theta^{+j}_{1,M_{MAX}}+2\frac{\Delta t^+}{(\Delta z^+)^2}\theta^{+j}_{0,M_{MAX}-1}$$
$$+\left(1-4\left[\frac{L}{R_{CYL}}\right]^2\frac{\Delta t^+}{(\Delta r^+)^2}-2\frac{\Delta t^+}{(\Delta z^+)^2}\right.$$
$$\left.-2_pBi_{BACK}\frac{\Delta t^+}{\Delta z^+}\right)\theta^{+j}_{0,M_{MAX}}$$

(l)

$$\theta^{+j+1}_{n,0} = \left[\frac{L}{R_{CYL}}\right]^2(1-1/(2n))\frac{\Delta t^+}{(\Delta r^+)^2}\theta^{+j}_{n-1,M_{MAX}}$$

$$+\left[\frac{L}{R_{CYL}}\right]^2(1+1/(2n))\frac{\Delta t^+}{(\Delta r^+)^2}\theta^{+j}_{n+1,M_{MAX}}$$
$$+2\frac{\Delta t^+}{(\Delta z^+)^2}\theta^{+j}_{n,M_{MAX}-1}$$
$$+\left(1-2\left[\frac{L}{R_{CYL}}\right]^2\frac{\Delta t^+}{(\Delta r^+)^2}-2\frac{\Delta t^+}{(\Delta z^+)^2}-2_pBi_{BACK}\frac{\Delta t^+}{\Delta z^+}\right)\theta^{+j}_{n,M_{MAX}}$$

(m)

$$\theta^{+j+1}_{N_{CYL},M_{MAX}} = \left[\frac{\rho c_p}{(\rho c_p)'}\right]\left[\frac{L}{R_{CYL}}\right]^2(1-1/(2N_{CYL}))\frac{\Delta t^+}{(\Delta r^+)^2}\theta^{+j}_{N_{CYL}-1,M_{MAX}}$$
$$+\left[\frac{\rho c_p}{(\rho c_p)'}\right]\left[\frac{k'}{k}\right]\left[\frac{L}{R_{CYL}}\right]^2(1+1/(2N_{CYL}))\frac{\Delta t^+}{(\Delta r^+)^2}\theta^{+j}_{N_{CYL}+1,M_{MAX}}$$
$$+2\left[\frac{\rho c_p}{(\rho c_p)'}\right]\left[\frac{k'}{k}\right]\frac{\Delta t^+}{(\Delta z^+)^2}\theta^{+j}_{N_{CYL},M_{MAX}-1}$$
$$+\left(1-\left[\frac{\rho c_p}{(\rho c_p)'}\right]\left[\frac{L}{R_{CYL}}\right]^2(1-1/(2N_{CYL}))\frac{\Delta t^+}{(\Delta r^+)^2}\right.$$
$$-\left[\frac{\rho c_p}{(\rho c_p)'}\right]\left[\frac{k'}{k}\right]\left[\frac{L}{R_{CYL}}\right]^2(1+1/(2N_{CYL}))\frac{\Delta t^+}{(\Delta r^+)^2}$$
$$-2\left[\frac{\rho c_p}{(\rho c_p)'}\right]\left[\frac{k'}{k}\right]\frac{\Delta t^+}{(\Delta z^+)^2}$$
$$\left.-2\left[\frac{\rho c_p}{(\rho c_p)'}\right]{}_pBi_{BACK}\frac{\Delta t^+}{\Delta z^+}\right)\theta^{+j}_{N_{CYL},M_{MAX}}$$

(n)

$$\theta^{+j+1}_{n,M_{MAX}} = \left[\frac{\rho c_p}{(\rho c_p)'}\right]\left[\frac{k'}{k}\right]\left[\frac{L}{R_{CYL}}\right]^2(1-1/(2n))\frac{\Delta t^+}{(\Delta r^+)^2}\theta^{+j}_{n-1,M_{MAX}}$$
$$+\left[\frac{\rho c_p}{(\rho c_p)'}\right]\left[\frac{k'}{k}\right]\left[\frac{L}{R_{CYL}}\right]^2(1+1/(2n))\frac{\Delta t^+}{(\Delta r^+)^2}\theta^{+j}_{n+1,M_{MAX}}$$
$$+2\left[\frac{\rho c_p}{(\rho c_p)'}\right]\left[\frac{k'}{k}\right]\frac{\Delta t^+}{(\Delta z^+)^2}\theta^{+j}_{n,M_{MAX}-1}$$
$$+\left(1-2\left[\frac{\rho c_p}{(\rho c_p)'}\right]\left[\frac{k'}{k}\right]\left[\frac{L}{R_{CYL}}\right]^2\frac{\Delta t^+}{(\Delta r^+)^2}\right.$$
$$-2\left[\frac{\rho c_p}{(\rho c_p)'}\right]\left[\frac{k'}{k}\right]\frac{\Delta t^+}{(\Delta z^+)^2}$$
$$\left.-2\left[\frac{\rho c_p}{(\rho c_p)'}\right]{}_pBi_{BACK}\frac{\Delta t^+}{\Delta z^+}\right)\theta^{+j}_{n,M_{MAX}}$$

(o)

$$
\begin{aligned}
\theta^{+j+1}_{N_{MAX},M_{MAX}} = {} & 2\left[\frac{\rho c_p}{(\rho c_p)'}\right]\left[\frac{k'}{k}\right]\left[\frac{L}{R_{CYL}}\right]^2\left(\frac{N_{MAX}-1/2}{N_{MAX}-1/4}\right)\frac{\Delta t^+}{(\Delta r^+)^2}\theta^{+j}_{N_{MAX}-1,M_{MAX}} \\
& + 2\left[\frac{\rho c_p}{(\rho c_p)'}\right]\left[\frac{k'}{k}\right]\frac{\Delta t^+}{(\Delta z^+)^2}\theta^{+j}_{N_{MAX},M_{MAX}-1} \\
& + \left(1 - 2\left[\frac{\rho c_p}{(\rho c_p)'}\right]\left[\frac{k'}{k}\right]\left[\frac{L}{R_{CYL}}\right]^2\left(\frac{N_{MAX}-1/2}{N_{MAX}-1/4}\right)\frac{\Delta t^+}{(\Delta r^+)^2}\right. \\
& \quad - 2\left[\frac{\rho c_p}{(\rho c_p)'}\right]\left[\frac{k'}{k}\right]\frac{\Delta t^+}{(\Delta z^+)^2} \\
& \quad \left. - 2\left[\frac{\rho c_p}{(\rho c_p)'}\right]{}_pBi_{BACK}\frac{\Delta t^+}{\Delta z^+}\right)\theta^{+j}_{N_{MAX},M_{MAX}}
\end{aligned}
$$

Disturbance Problem:

Note 1: Nodal Equations (a)-(o) apply to the corresponding positions in Figure 5.

Note 2: For nodes on the front surface of the cylinder, Equations (a)-(c), the last term in the nodal finite-difference equation, i.e. the term including the parameter γ, is included only if the node lies within the heated disk.

(a)

$$\begin{aligned}\theta^{+j+1}_{0,0} &= 4\left[\frac{L}{R_{CYL}}\right]^2 \frac{\Delta t^+}{(\Delta r^+)^2}\theta^{+j}_{1,0} + 2\frac{\Delta t^+}{(\Delta z^+)^2}\theta^{+j}_{0,1} \\ &+ \left(1 - 4\left[\frac{L}{R_{CYL}}\right]^2 \frac{\Delta t^+}{(\Delta r^+)^2} - 2\frac{\Delta t^+}{(\Delta z^+)^2} - 2_d Bi_{FRONT}\frac{\Delta t^+}{\Delta z^+}\right)\theta^{+j}_{0,0} \\ &+ 2_d Bi_{FRONT}\frac{\Delta t^+}{\Delta z^+} + 2_d Bi_{FRONT}\frac{\Delta t^+}{\Delta z^+}(\gamma)\end{aligned}$$

(b)

$$\begin{aligned}\theta^{+j+1}_{n,0} &= \left[\frac{L}{R_{CYL}}\right]^2 (1 - 1/(2n))\frac{\Delta t^+}{(\Delta r^+)^2}\theta^{+j}_{n-1,0} \\ &+ \left[\frac{L}{R_{CYL}}\right]^2 (1 + 1/(2n))\frac{\Delta t^+}{(\Delta r^+)^2}\theta^{+j}_{n+1,0} + 2\frac{\Delta t^+}{(\Delta z^+)^2}\theta^{+j}_{n,1} \\ &+ \left(1 - 2\left[\frac{L}{R_{CYL}}\right]^2 \frac{\Delta t^+}{(\Delta r^+)^2} - 2\frac{\Delta t^+}{(\Delta z^+)^2} - 2_d Bi_{FRONT}\frac{\Delta t^+}{\Delta z^+}\right)\theta^{+j}_{n,0} \\ &+ 2_d Bi_{FRONT}\frac{\Delta t^+}{\Delta z^+} + 2_d Bi_{FRONT}\frac{\Delta t^+}{\Delta z^+}(\gamma)\end{aligned}$$

(c)

$$\begin{aligned}\theta^{+j+1}_{N_{CYL},0} &= \left[\frac{\rho c_p}{(\rho c_p)'}\right]\left[\frac{L}{R_{CYL}}\right]^2 (1 - 1/(2N_{CYL}))\frac{\Delta t^+}{(\Delta r^+)^2}\theta^{+j}_{N_{CYL}-1,0} \\ &+ \left[\frac{\rho c_p}{(\rho c_p)'}\right]\left[\frac{k'}{k}\right]\left[\frac{L}{R_{CYL}}\right]^2 (1 + 1/(2N_{CYL}))\frac{\Delta t^+}{(\Delta r^+)^2}\theta^{+j}_{N_{CYL}+1,0} \\ &+ 2\left[\frac{\rho c_p}{(\rho c_p)'}\right]\left[\frac{k'}{k}\right]\frac{\Delta t^+}{(\Delta z^+)^2}\theta^{+j}_{N_{CYL},1}\end{aligned}$$

$$
\begin{aligned}
&+\left(1-\left[\frac{\rho c_p}{(\rho c_p)'}\right]\left[\frac{L}{R_{CYL}}\right]^2(1-1/(2N_{CYL}))\frac{\Delta t^+}{(\Delta r^+)^2}\right.\\
&\quad-\left[\frac{\rho c_p}{(\rho c_p)'}\right]\left[\frac{k'}{k}\right]\left[\frac{L}{R_{CYL}}\right]^2(1+1/(2N_{CYL}))\frac{\Delta t^+}{(\Delta r^+)^2}\\
&\quad-2\left[\frac{\rho c_p}{(\rho c_p)'}\right]\left[\frac{k'}{k}\right]\frac{\Delta t^+}{(\Delta z^+)^2}\\
&\quad\left.-2\left[\frac{\rho c_p}{(\rho c_p)'}\right]{}_dBi_{FRONT}\frac{\Delta t^+}{\Delta z^+}\right)\theta^{+j}{}_{N_{CYL},0}\\
&+2\left[\frac{\rho c_p}{(\rho c_p)'}\right]{}_dBi_{FRONT}\frac{\Delta t^+}{\Delta z^+}+2\left[\frac{\rho c_p}{(\rho c_p)'}\right]{}_dBi_{FRONT}\frac{\Delta t^+}{\Delta z^+}(\gamma)
\end{aligned}
$$

(d)

$$
\begin{aligned}
\theta^{+j+1}{}_{n,0} &= \left[\frac{\rho c_p}{(\rho c_p)'}\right]\left[\frac{k'}{k}\right]\left[\frac{L}{R_{CYL}}\right]^2(1-1/(2n))\frac{\Delta t^+}{(\Delta r^+)^2}\theta^{+j}{}_{n-1,0}\\
&+\left[\frac{\rho c_p}{(\rho c_p)'}\right]\left[\frac{k'}{k}\right]\left[\frac{L}{R_{CYL}}\right]^2(1+1/(2n))\frac{\Delta t^+}{(\Delta r^+)^2}\theta^{+j}{}_{n+1,0}\\
&+2\left[\frac{\rho c_p}{(\rho c_p)'}\right]\left[\frac{k'}{k}\right]\frac{\Delta t^+}{(\Delta z^+)^2}\theta^{+j}{}_{n,1}\\
&+\left(1-2\left[\frac{\rho c_p}{(\rho c_p)'}\right]\left[\frac{k'}{k}\right]\left[\frac{L}{R_{CYL}}\right]^2\frac{\Delta t^+}{(\Delta r^+)^2}-2\left[\frac{\rho c_p}{(\rho c_p)'}\right]\left[\frac{k'}{k}\right]\frac{\Delta t^+}{(\Delta z^+)^2}\right.\\
&\quad\left.-2\left[\frac{\rho c_p}{(\rho c_p)'}\right]{}_dBi_{FRONT}\frac{\Delta t^+}{\Delta z^+}\right)\theta^{+j}{}_{n,0}\\
&+2\left[\frac{\rho c_p}{(\rho c_p)'}\right]{}_dBi_{FRONT}\frac{\Delta t^+}{\Delta z^+}
\end{aligned}
$$

(e)

$$
\begin{aligned}
\theta^{+j+1}{}_{N_{MAX},0} &= 2\left[\frac{\rho c_p}{(\rho c_p)'}\right]\left[\frac{k'}{k}\right]\left[\frac{L}{R_{CYL}}\right]^2\left(\frac{N_{MAX}-1/2}{N_{MAX}-1/4}\right)\frac{\Delta t^+}{(\Delta r^+)^2}\theta^{+j}{}_{N_{MAX}-1,0}\\
&+2\left[\frac{\rho c_p}{(\rho c_p)'}\right]\left[\frac{k'}{k}\right]\frac{\Delta t^+}{(\Delta z^+)^2}\theta^{+j}{}_{N_{MAX},1}\\
&+\left(1-2\left[\frac{\rho c_p}{(\rho c_p)'}\right]\left[\frac{k'}{k}\right]\left[\frac{L}{R_{CYL}}\right]^2\left(\frac{N_{MAX}-1/2}{N_{MAX}-1/4}\right)\frac{\Delta t^+}{(\Delta r^+)^2}\right.\\
&\quad-2\left[\frac{\rho c_p}{(\rho c_p)'}\right]\left[\frac{k'}{k}\right]\frac{\Delta t^+}{(\Delta z^+)^2}\\
&\quad\left.-2\left[\frac{\rho c_p}{(\rho c_p)'}\right]{}_dBi_{FRONT}\frac{\Delta t^+}{\Delta z^+}\right)\theta^{+j}{}_{N_{MAX},0}
\end{aligned}
$$

$$+ 2\left[\frac{\rho c_p}{(\rho c_p)'}\right] {}_d Bi_{FRONT} \frac{\Delta t^+}{\Delta z^+}$$

(f)

$$\begin{aligned}
\theta^{+j+1}_{0,m} &= 4\left[\frac{L}{R_{CYL}}\right]^2 \frac{\Delta t^+}{(\Delta r^+)^2}\theta^{+j}_{1,m} + \frac{\Delta t^+}{(\Delta z^+)^2}\theta^{+j}_{0,m-1} \\
&\quad + \frac{\Delta t^+}{(\Delta z^+)^2}\theta^{+j}_{0,m+1} \\
&\quad + \left(1 - 4\left[\frac{L}{R_{CYL}}\right]^2 \frac{\Delta t^+}{(\Delta r^+)^2} - 2\frac{\Delta t^+}{(\Delta z^+)^2}\right)\theta^{+j}_{0,m}
\end{aligned}$$

(g)

$$\begin{aligned}
\theta^{+j+1}_{n,m} &= \left[\frac{L}{R_{CYL}}\right]^2 (1 - 1/(2n)) \frac{\Delta t^+}{(\Delta r^+)^2}\theta^{+j}_{n-1,m} \\
&\quad + \left[\frac{L}{R_{CYL}}\right]^2 (1 + 1/(2n)) \frac{\Delta t^+}{(\Delta r^+)^2}\theta^{+j}_{n+1,m} \\
&\quad + \frac{\Delta t^+}{(\Delta z^+)^2}\theta^{+j}_{n,m-1} + \frac{\Delta t^+}{(\Delta z^+)^2}\theta^{+j}_{n,m+1} \\
&\quad + \left(1 - 2\left[\frac{L}{R_{CYL}}\right]^2 \frac{\Delta t^+}{(\Delta r^+)^2} - 2\frac{\Delta t^+}{(\Delta z^+)^2}\right)\theta^{+j}_{n,m}
\end{aligned}$$

(h)

$$\begin{aligned}
\theta^{+j+1}_{N_{CYL},m} &= \left[\frac{\rho c_p}{(\rho c_p)'}\right]\left[\frac{L}{R_{CYL}}\right]^2 (1 - 1/(2N_{CYL})) \frac{\Delta t^+}{(\Delta r^+)^2}\theta^{+j}_{N_{CYL}-1,m} \\
&\quad + \left[\frac{\rho c_p}{(\rho c_p)'}\right]\left[\frac{k'}{k}\right]\left[\frac{L}{R_{CYL}}\right]^2 (1 + 1/(2N_{CYL})) \frac{\Delta t^+}{(\Delta r^+)^2}\theta^{+j}_{N_{CYL}+1,m} \\
&\quad + \left[\frac{\rho c_p}{(\rho c_p)'}\right]\left[\frac{k'}{k}\right] \frac{\Delta t^+}{(\Delta z^+)^2}\theta^{+j}_{N_{CYL},m-1} \\
&\quad + \left[\frac{\rho c_p}{(\rho c_p)'}\right]\left[\frac{k'}{k}\right] \frac{\Delta t^+}{(\Delta z^+)^2}\theta^{+j}_{N_{CYL},m+1} \\
&\quad + \left(1 - \left[\frac{\rho c_p}{(\rho c_p)'}\right]\left[\frac{L}{R_{CYL}}\right]^2 (1 - 1/(2N_{CYL})) \frac{\Delta t^+}{(\Delta r^+)^2}\right. \\
&\qquad - \left[\frac{\rho c_p}{(\rho c_p)'}\right]\left[\frac{k'}{k}\right]\left[\frac{L}{R_{CYL}}\right]^2 (1 + 1/(2N_{CYL})) \frac{\Delta t^+}{(\Delta r^+)^2} \\
&\qquad \left. - 2\left[\frac{\rho c_p}{(\rho c_p)'}\right]\left[\frac{k'}{k}\right] \frac{\Delta t^+}{(\Delta z^+)^2}\right)\theta^{+j}_{N_{CYL},m}
\end{aligned}$$

(i)

$$\theta^{+j+1}_{n,m} = \left[\frac{\rho c_p}{(\rho c_p)'}\right]\left[\frac{k'}{k}\right]\left[\frac{L}{R_{CYL}}\right]^2 (1-1/(2n))\frac{\Delta t^+}{(\Delta r^+)^2}\theta^{+j}_{n-1,m}$$
$$+\left[\frac{\rho c_p}{(\rho c_p)'}\right]\left[\frac{k'}{k}\right]\left[\frac{L}{R_{CYL}}\right]^2 (1+1/(2n))\frac{\Delta t^+}{(\Delta r^+)^2}\theta^{+j}_{n+1,m}$$
$$+\left[\frac{\rho c_p}{(\rho c_p)'}\right]\left[\frac{k'}{k}\right]\frac{\Delta t^+}{(\Delta z^+)^2}\theta^{+j}_{n,m-1}+\left[\frac{\rho c_p}{(\rho c_p)'}\right]\left[\frac{k'}{k}\right]\frac{\Delta t^+}{(\Delta z^+)^2}\theta^{+j}_{n,m+1}$$
$$+\left(1-2\left[\frac{\rho c_p}{(\rho c_p)'}\right]\left[\frac{k'}{k}\right]\left[\frac{L}{R_{CYL}}\right]^2\frac{\Delta t^+}{(\Delta r^+)^2}\right.$$
$$\left.-2\left[\frac{\rho c_p}{(\rho c_p)'}\right]\left[\frac{k'}{k}\right]\frac{\Delta t^+}{(\Delta z^+)^2}\right)\theta^{+j}_{n,m}$$

(j)

$$\theta^{+j+1}_{N_{MAX},m} = 2\left[\frac{\rho c_p}{(\rho c_p)'}\right]\left[\frac{k'}{k}\right]\left[\frac{L}{R_{CYL}}\right]^2\left(\frac{N_{MAX}-1/2}{N_{MAX}-1/4}\right)\frac{\Delta t^+}{(\Delta r^+)^2}\theta^{+j}_{N_{MAX}-1,m}$$
$$+\left[\frac{\rho c_p}{(\rho c_p)'}\right]\left[\frac{k'}{k}\right]\frac{\Delta t^+}{(\Delta z^+)^2}\theta^{+j}_{N_{MAX},m-1}$$
$$+\left[\frac{\rho c_p}{(\rho c_p)'}\right]\left[\frac{k'}{k}\right]\frac{\Delta t^+}{(\Delta z^+)^2}\theta^{+j}_{N_{MAX},m+1}$$
$$+\left(1-2\left[\frac{\rho c_p}{(\rho c_p)'}\right]\left[\frac{k'}{k}\right]\left[\frac{L}{R_{CYL}}\right]^2\left(\frac{N_{MAX}-1/2}{N_{MAX}-1/4}\right)\frac{\Delta t^+}{(\Delta r^+)^2}\right.$$
$$\left.-2\left[\frac{\rho c_p}{(\rho c_p)'}\right]\left[\frac{k'}{k}\right]\frac{\Delta t^+}{(\Delta z^+)^2}\right)\theta^{+j}_{N_{MAX},m}$$

(k)

$$\theta^{+j+1}_{0,M_{MAX}} = 4\left[\frac{L}{R_{CYL}}\right]^2\frac{\Delta t^+}{(\Delta r^+)^2}\theta^{+j}_{1,M_{MAX}}+2\frac{\Delta t^+}{(\Delta z^+)^2}\theta^{+j}_{0,M_{MAX}-1}$$
$$+\left(1-4\left[\frac{L}{R_{CYL}}\right]^2\frac{\Delta t^+}{(\Delta r^+)^2}-2\frac{\Delta t^+}{(\Delta z^+)^2}\right.$$
$$\left.-2_d Bi_{BACK}\frac{\Delta t^+}{\Delta z^+}\right)\theta^{+j}_{0,M_{MAX}}+2_d Bi_{BACK}\frac{\Delta t^+}{\Delta z^+}(\tau)$$

(l)

$$\theta^{+j+1}_{n,0} = \left[\frac{L}{R_{CYL}}\right]^2(1-1/(2n))\frac{\Delta t^+}{(\Delta r^+)^2}\theta^{+j}_{n-1,M_{MAX}}$$

$$+\left[\frac{L}{R_{CYL}}\right]^2(1+1/(2n))\frac{\Delta t^+}{(\Delta r^+)^2}\theta^{+j}_{n+1,M_{MAX}}$$
$$+2\frac{\Delta t^+}{(\Delta z^+)^2}\theta^{+j}_{n,M_{MAX}-1}$$
$$+\left(1-2\left[\frac{L}{R_{CYL}}\right]^2\frac{\Delta t^+}{(\Delta r^+)^2}-2\frac{\Delta t^+}{(\Delta z^+)^2}\right.$$
$$\left.-2_dBi_{BACK}\frac{\Delta t^+}{\Delta z^+}\right)\theta^{+j}_{n,M_{MAX}}+2_dBi_{BACK}\frac{\Delta t^+}{\Delta z^+}(\tau)$$

(m)

$$\theta^{+j+1}_{N_{CYL},M_{MAX}} = \left[\frac{\rho c_p}{(\rho c_p)'}\right]\left[\frac{L}{R_{CYL}}\right]^2(1-1/(2N_{CYL}))\frac{\Delta t^+}{(\Delta r^+)^2}\theta^{+j}_{N_{CYL}-1,M_{MAX}}$$
$$+\left[\frac{\rho c_p}{(\rho c_p)'}\right]\left[\frac{k'}{k}\right]\left[\frac{L}{R_{CYL}}\right]^2(1+1/(2N_{CYL}))\frac{\Delta t^+}{(\Delta r^+)^2}\theta^{+j}_{N_{CYL}+1,M_{MAX}}$$
$$+2\left[\frac{\rho c_p}{(\rho c_p)'}\right]\left[\frac{k'}{k}\right]\frac{\Delta t^+}{(\Delta z^+)^2}\theta^{+j}_{N_{CYL},M_{MAX}-1}$$
$$+\left(1-\left[\frac{\rho c_p}{(\rho c_p)'}\right]\left[\frac{L}{R_{CYL}}\right]^2(1-1/(2N_{CYL}))\frac{\Delta t^+}{(\Delta r^+)^2}\right.$$
$$-\left[\frac{\rho c_p}{(\rho c_p)'}\right]\left[\frac{k'}{k}\right]\left[\frac{L}{R_{CYL}}\right]^2(1+1/(2N_{CYL}))\frac{\Delta t^+}{(\Delta r^+)^2}$$
$$-2\left[\frac{\rho c_p}{(\rho c_p)'}\right]\left[\frac{k'}{k}\right]\frac{\Delta t^+}{(\Delta z^+)^2}$$
$$\left.-2\left[\frac{\rho c_p}{(\rho c_p)'}\right]{}_dBi_{BACK}\frac{\Delta t^+}{\Delta z^+}\right)\theta^{+j}_{N_{CYL},M_{MAX}}$$
$$+2\left[\frac{\rho c_p}{(\rho c_p)'}\right]{}_dBi_{BACK}\frac{\Delta t^+}{\Delta z^+}(\tau)$$

(n)

$$\theta^{+j+1}_{n,M_{MAX}} = \left[\frac{\rho c_p}{(\rho c_p)'}\right]\left[\frac{k'}{k}\right]\left[\frac{L}{R_{CYL}}\right]^2(1-1/(2n))\frac{\Delta t^+}{(\Delta r^+)^2}\theta^{+j}_{n-1,M_{MAX}}$$
$$+\left[\frac{\rho c_p}{(\rho c_p)'}\right]\left[\frac{k'}{k}\right]\left[\frac{L}{R_{CYL}}\right]^2(1+1/(2n))\frac{\Delta t^+}{(\Delta r^+)^2}\theta^{+j}_{n+1,M_{MAX}}$$
$$+2\left[\frac{\rho c_p}{(\rho c_p)'}\right]\left[\frac{k'}{k}\right]\frac{\Delta t^+}{(\Delta z^+)^2}\theta^{+j}_{n,M_{MAX}-1}$$
$$+\left(1-2\left[\frac{\rho c_p}{(\rho c_p)'}\right]\left[\frac{k'}{k}\right]\left[\frac{L}{R_{CYL}}\right]^2\frac{\Delta t^+}{(\Delta r^+)^2}\right.$$

$$
\begin{aligned}
&- 2\left[\frac{\rho c_p}{(\rho c_p)'}\right]\left[\frac{k'}{k}\right]\frac{\Delta t^+}{(\Delta z^+)^2} \\
&- 2\left[\frac{\rho c_p}{(\rho c_p)'}\right]{}_dBi_{BACK}\frac{\Delta t^+}{\Delta z^+}\Bigg)\theta^{+j}_{n,M_{MAX}} \\
&+ 2\left[\frac{\rho c_p}{(\rho c_p)'}\right]{}_dBi_{BACK}\frac{\Delta t^+}{\Delta z^+}(\tau)
\end{aligned}
$$

(o)

$$
\begin{aligned}
\theta^{+j+1}_{N_{MAX},M_{MAX}} = \; & 2\left[\frac{\rho c_p}{(\rho c_p)'}\right]\left[\frac{k'}{k}\right]\left[\frac{L}{R_{CYL}}\right]^2\left(\frac{N_{MAX}-1/2}{N_{MAX}-1/4}\right)\frac{\Delta t^+}{(\Delta r^+)^2}\theta^{+j}_{N_{MAX}-1,M_{MAX}} \\
& + 2\left[\frac{\rho c_p}{(\rho c_p)'}\right]\left[\frac{k'}{k}\right]\frac{\Delta t^+}{(\Delta z^+)^2}\theta^{+j}_{N_{MAX},M_{MAX}-1} \\
& + \Bigg(1 - 2\left[\frac{\rho c_p}{(\rho c_p)'}\right]\left[\frac{k'}{k}\right]\left[\frac{L}{R_{CYL}}\right]^2\left(\frac{N_{MAX}-1/2}{N_{MAX}-1/4}\right)\frac{\Delta t^+}{(\Delta r^+)^2} \\
& \quad - 2\left[\frac{\rho c_p}{(\rho c_p)'}\right]\left[\frac{k'}{k}\right]\frac{\Delta t^+}{(\Delta z^+)^2} \\
& \quad - 2\left[\frac{\rho c_p}{(\rho c_p)'}\right]{}_dBi_{BACK}\frac{\Delta t^+}{\Delta z^+}\Bigg)\theta^{+j}_{N_{MAX},M_{MAX}} \\
& + 2\left[\frac{\rho c_p}{(\rho c_p)'}\right]{}_dBi_{BACK}\frac{\Delta t^+}{\Delta z^+}(\tau)
\end{aligned}
$$

Appendix B. *Graphs of Results from the Check Cases*

B.1 Steady-State Check Cases for Heat Transfer in the Axial Direction

B.1.1 Preheating Problems

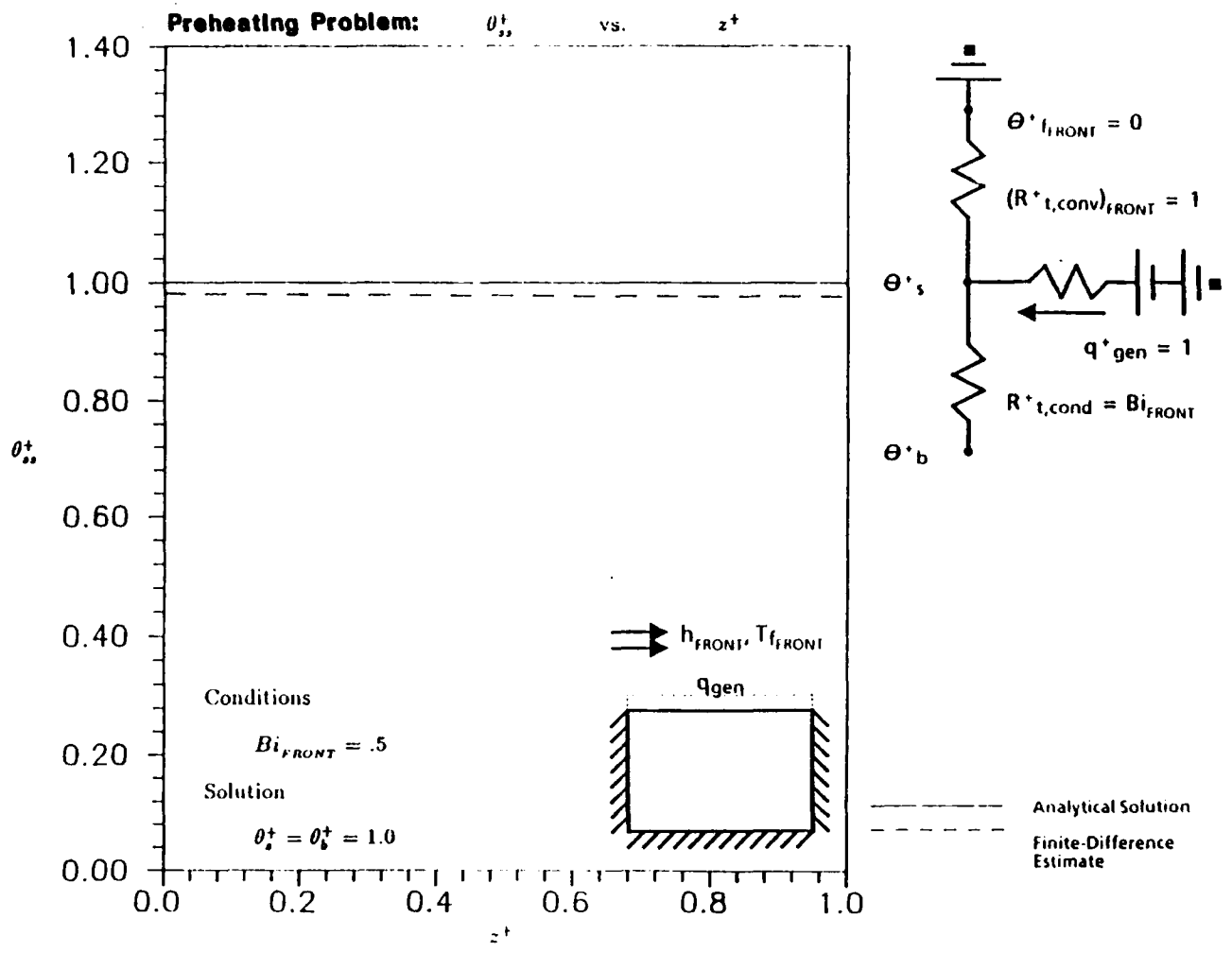

Figure 41. Other Results for Steady State Heat Transfer in the Axial Direction Using the Preheating Problem, Figure (a)

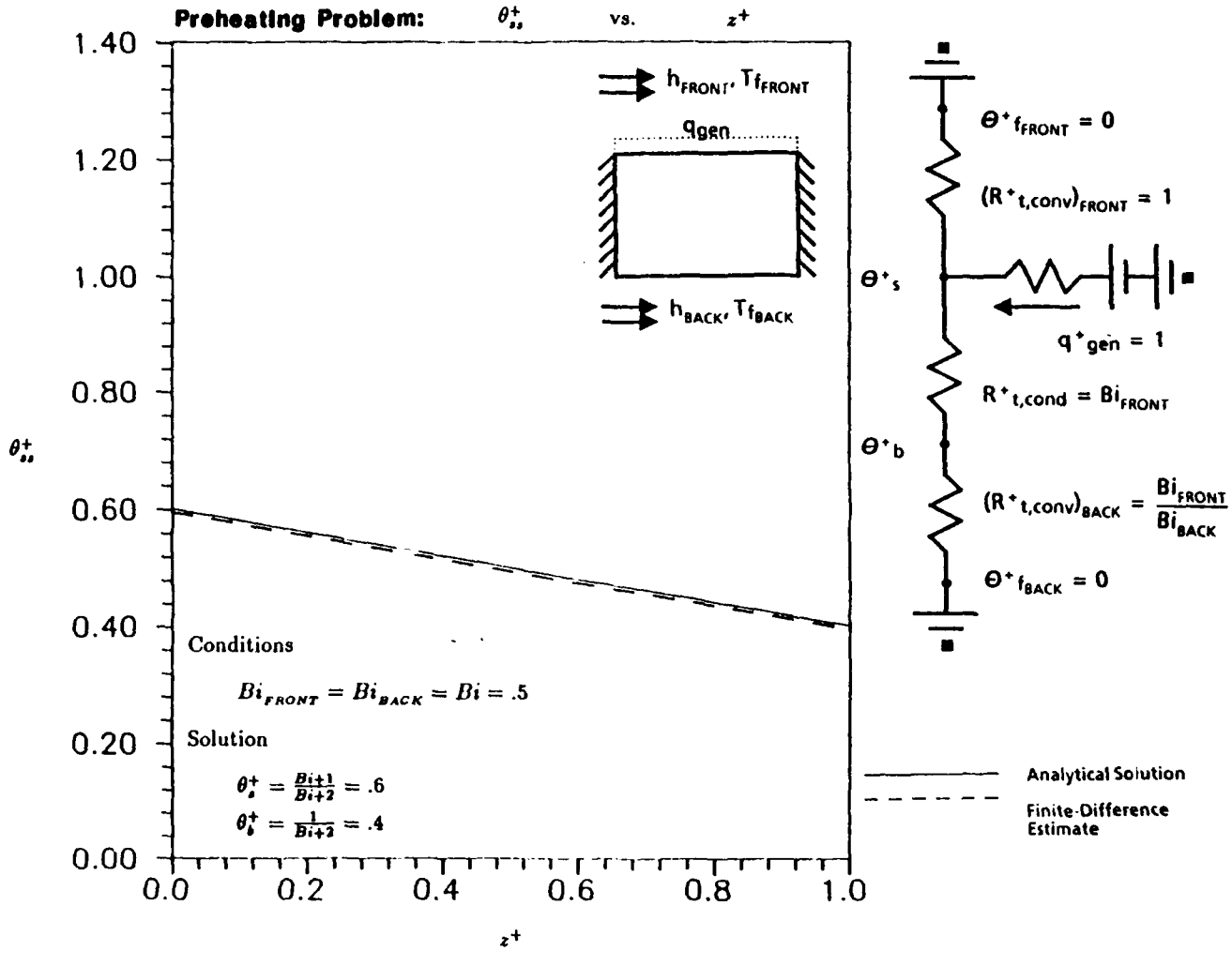

Figure 42. Other Results for Steady State Heat Transfer in the Axial Direction Using the Preheating Problem, Figure (b)

B.1.2 Disturbance Problems

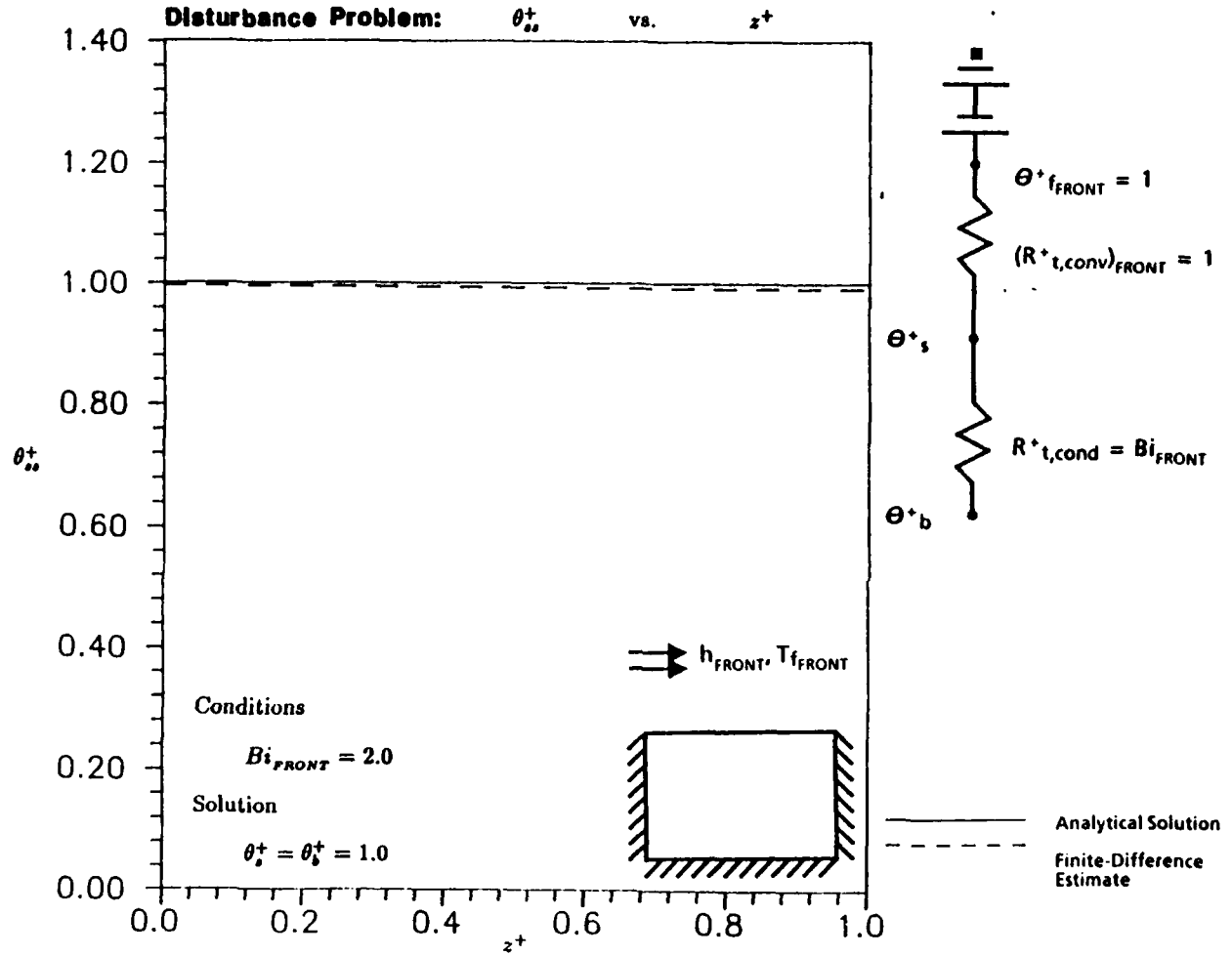

Figure 43. Other Results for Steady State Heat Transfer in the Axial Direction Using the Disturbance Problem, Figure (a)

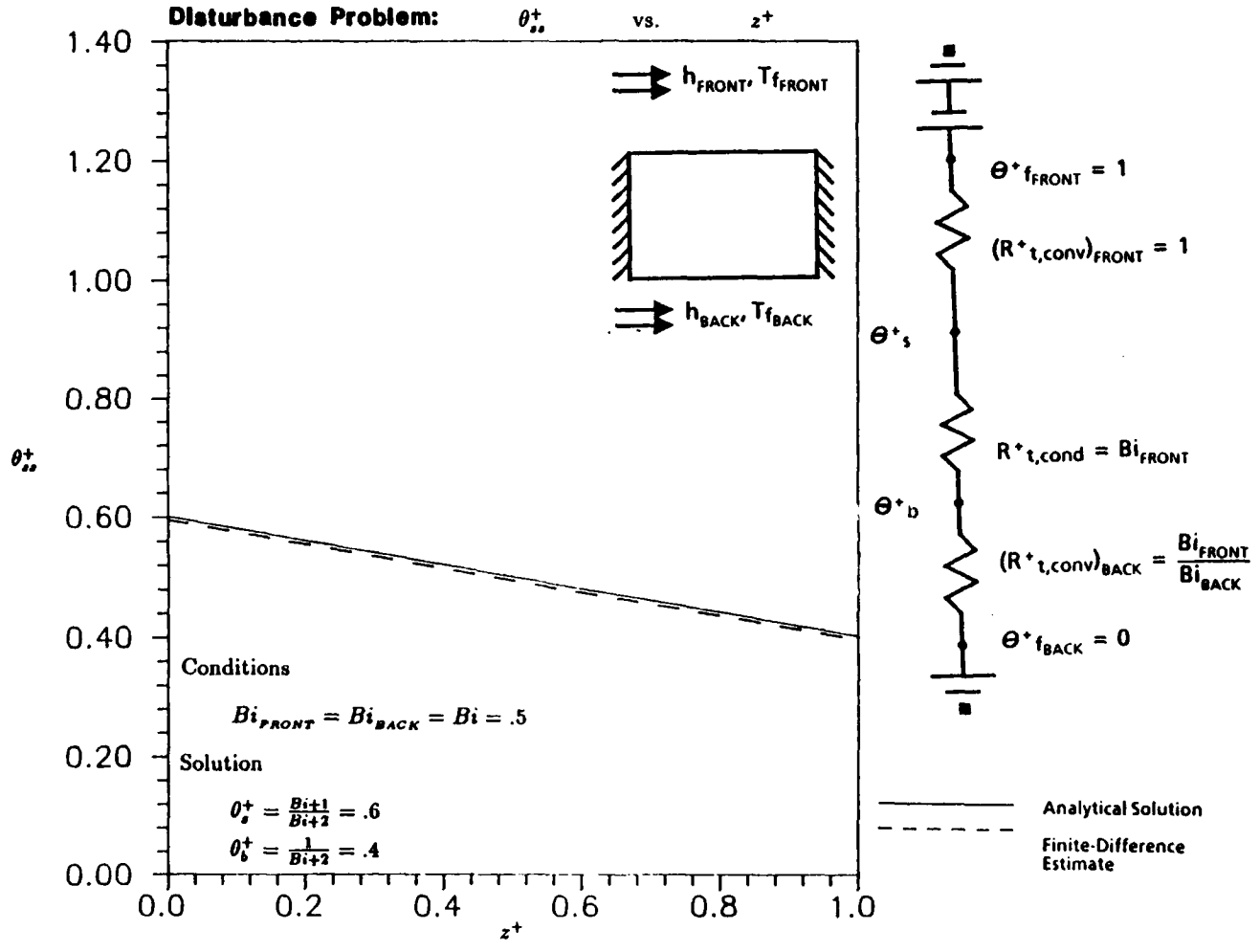

Figure 44. Other Results for Steady State Heat Transfer in the Axial Direction Using the Disturbance Problem, Figure (b)

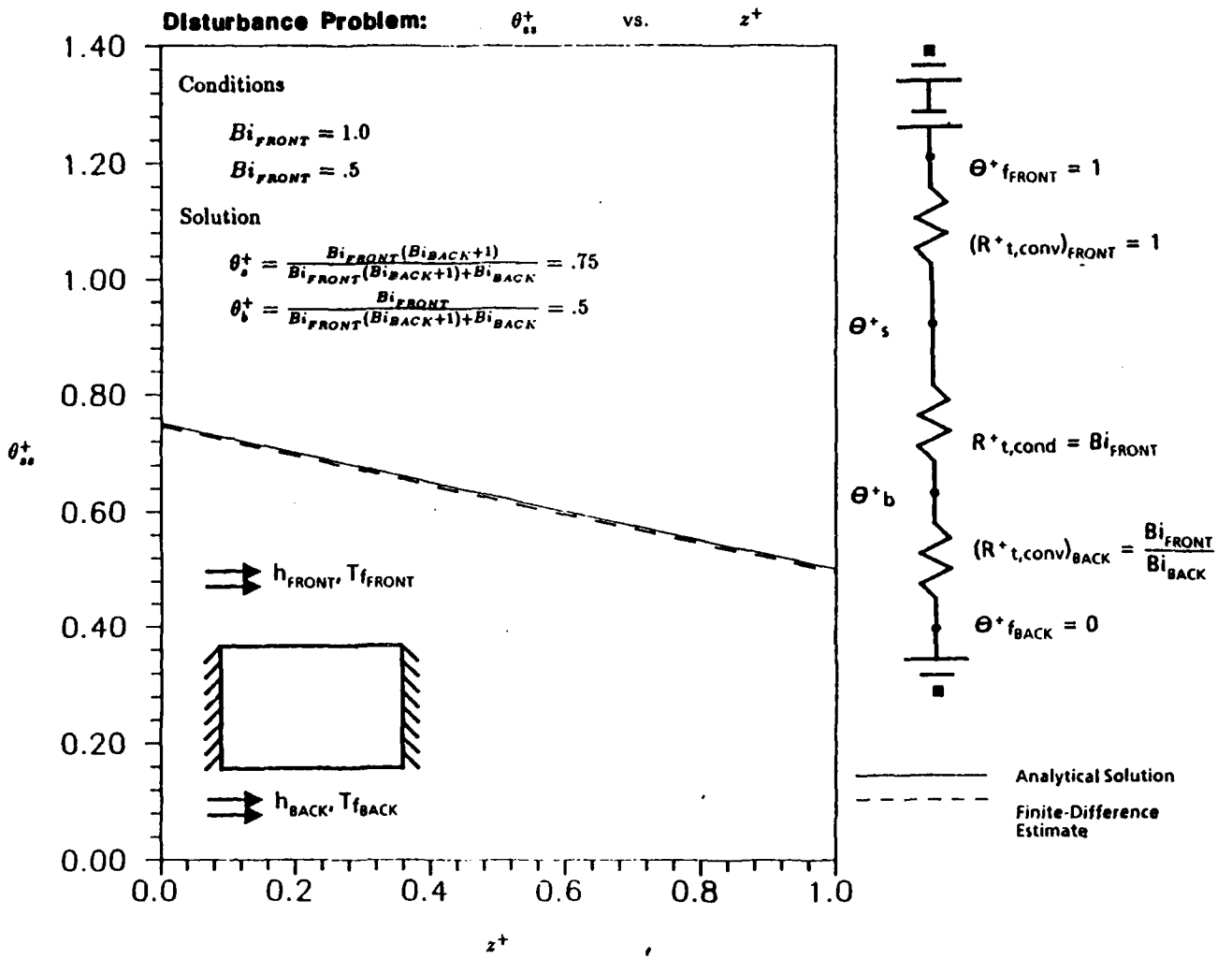

Figure 45. Other Results for Steady State Heat Transfer in the Axial Direction Using the Disturbance Problem, Figure (c)

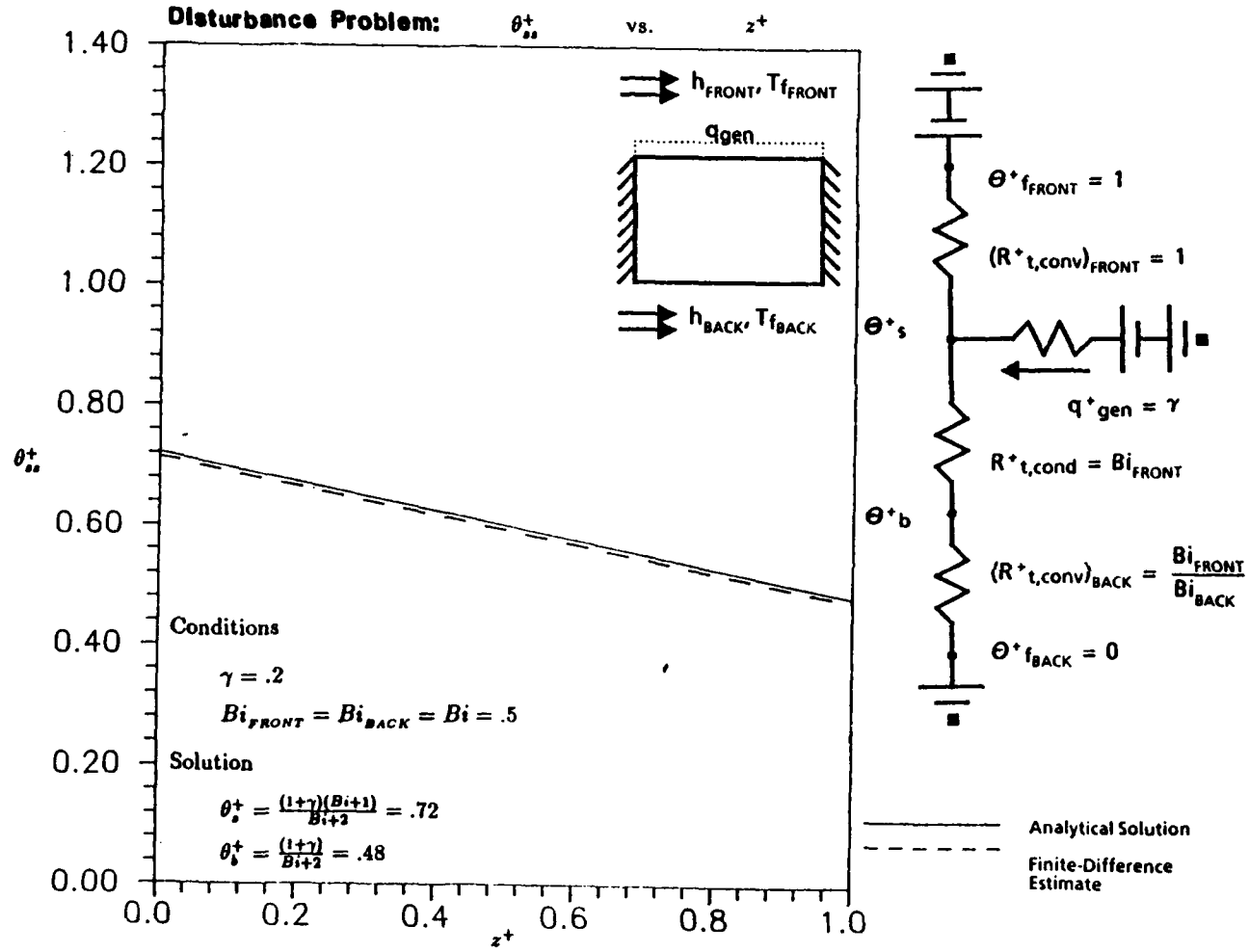

Figure 46. Other Results for Steady State Heat Transfer in the Axial Direction Using the Disturbance Problem, Figure (d)

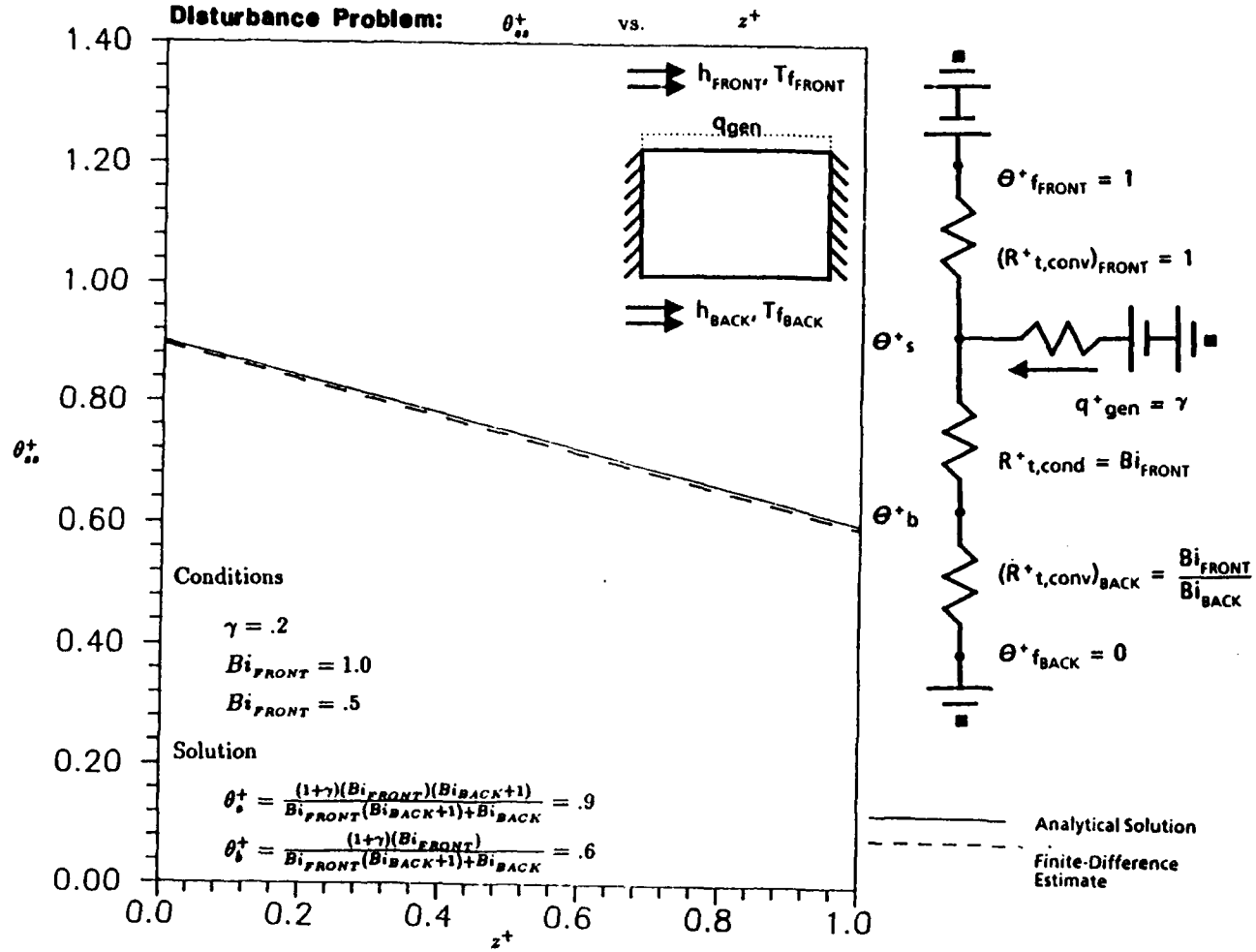

Figure 47. Other Results for Steady State Heat Transfer in the Axial Direction Using the Disturbance Problem, Figure (e)

B.2 Steady-State Check Cases for Heat Transfer in the Radial Direction

Case numbers refer to the cases given in Tables 2 and 3. See Figure 13 in Section 3.2 for the results from Case 2 using the single-material problem.

B.2.1 Single-Material Problems

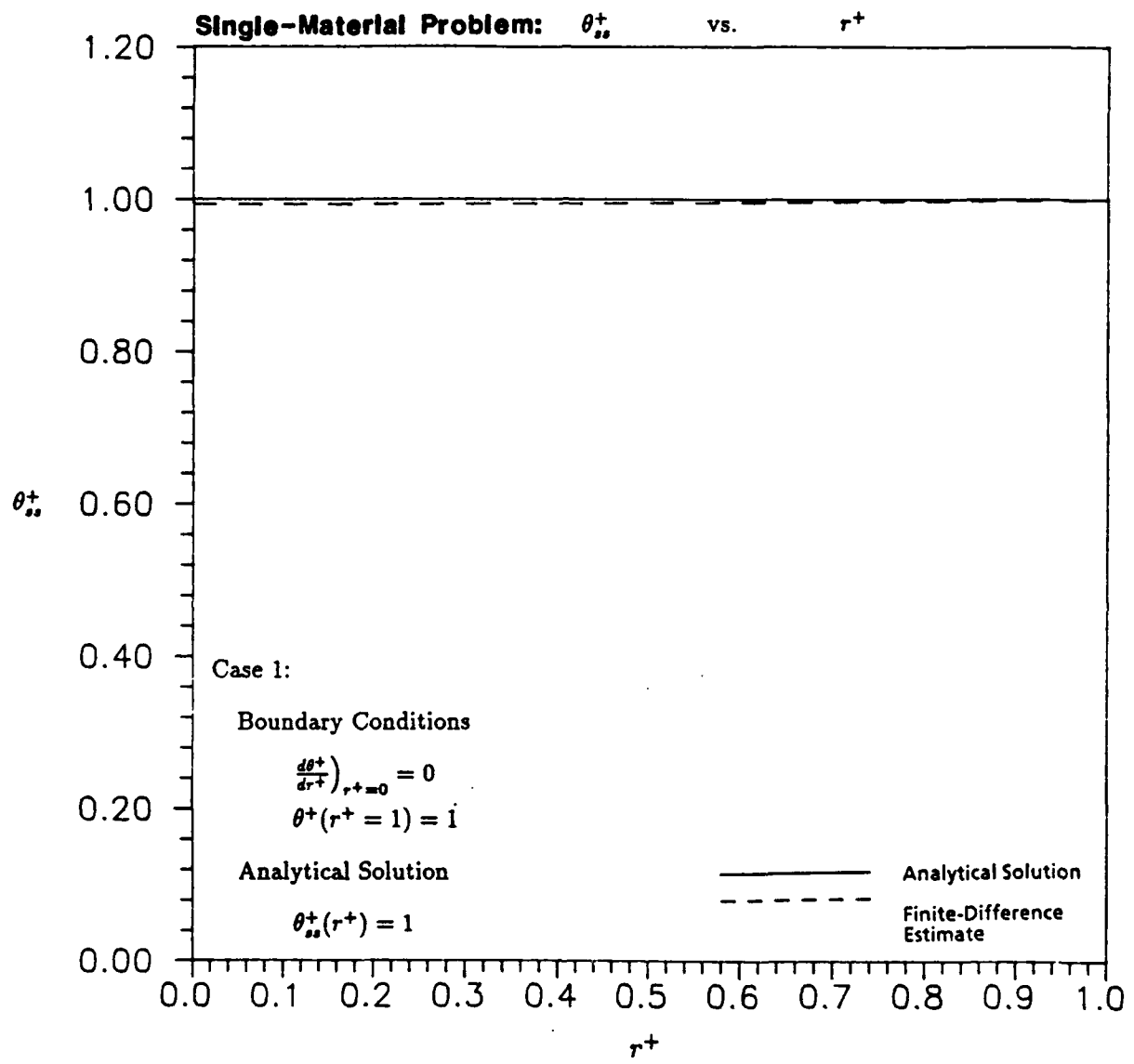

Figure 48. Case 1 for Steady State Heat Transfer in the Radial Direction Using the Single-Material Problem

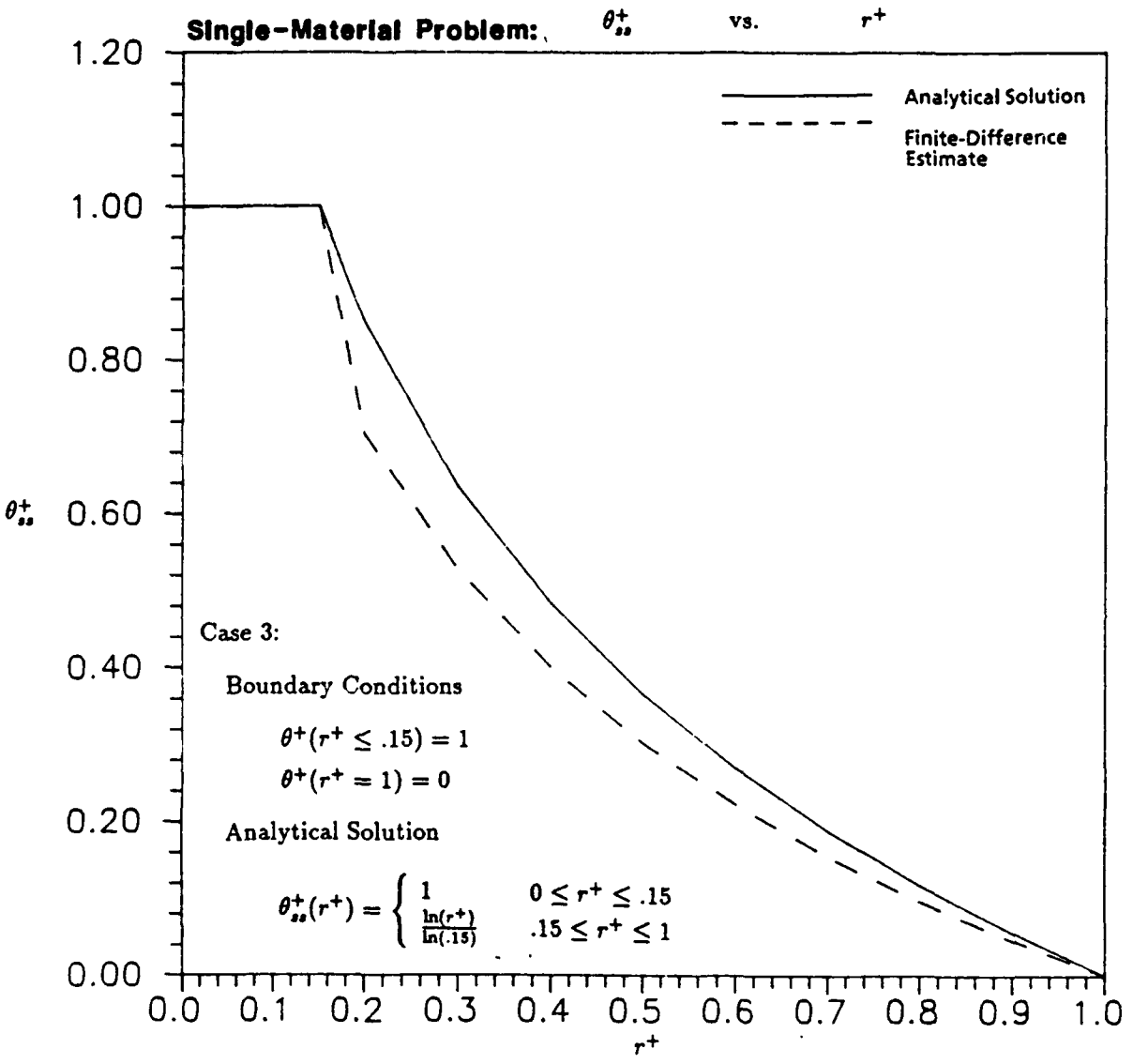

Figure 49. Case 3 for Steady State Heat Transfer in the Radial Direction Using the Single-Material Problem

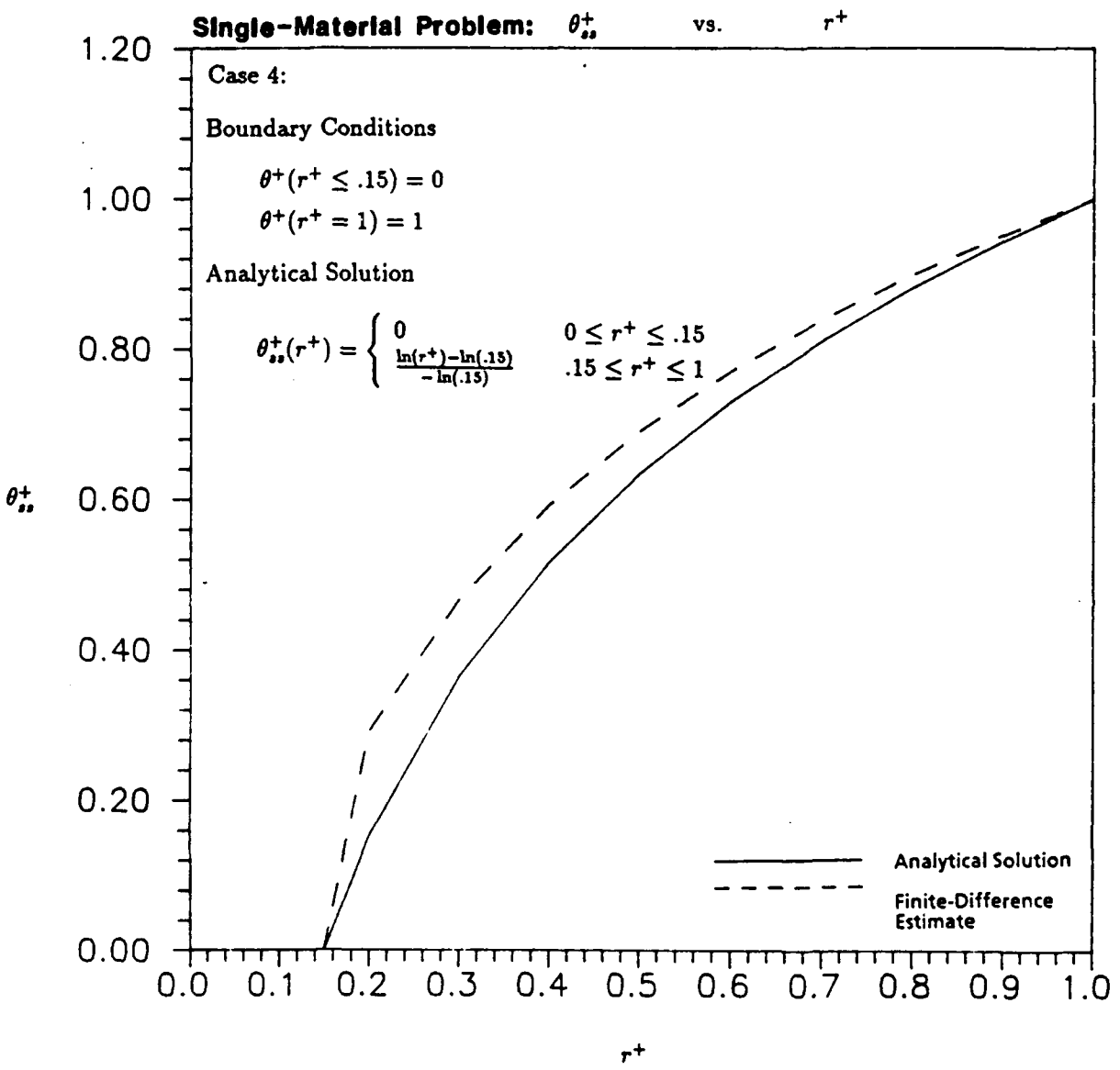

Figure 50. Case 4 for Steady State Heat Transfer in the Radial Direction Using the Single-Material Problem

B.2.2 Two-Material Problems

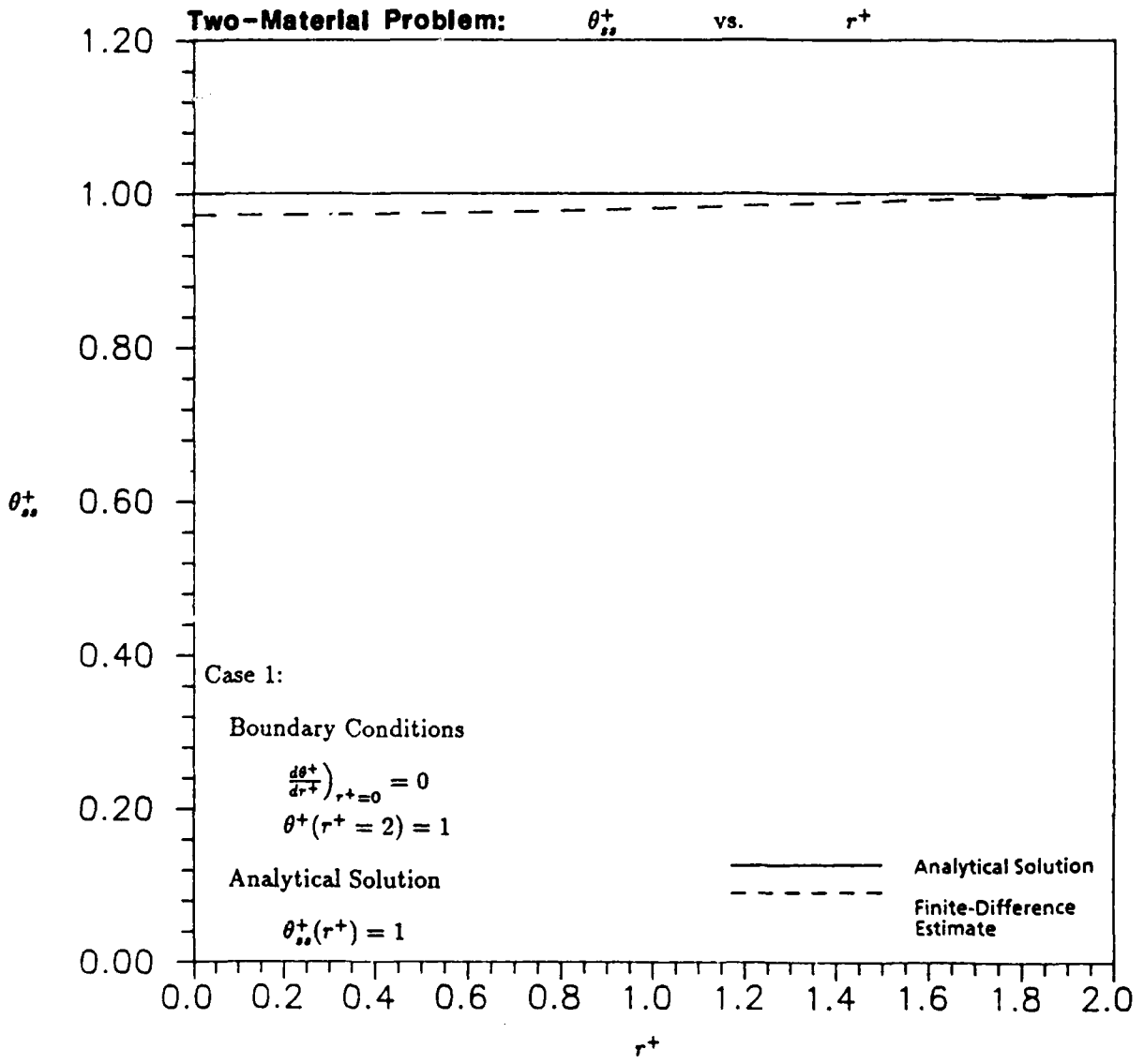

Figure 51. Case 1 for Steady State Heat Transfer in the Radial Direction Using the Two-Material Problem

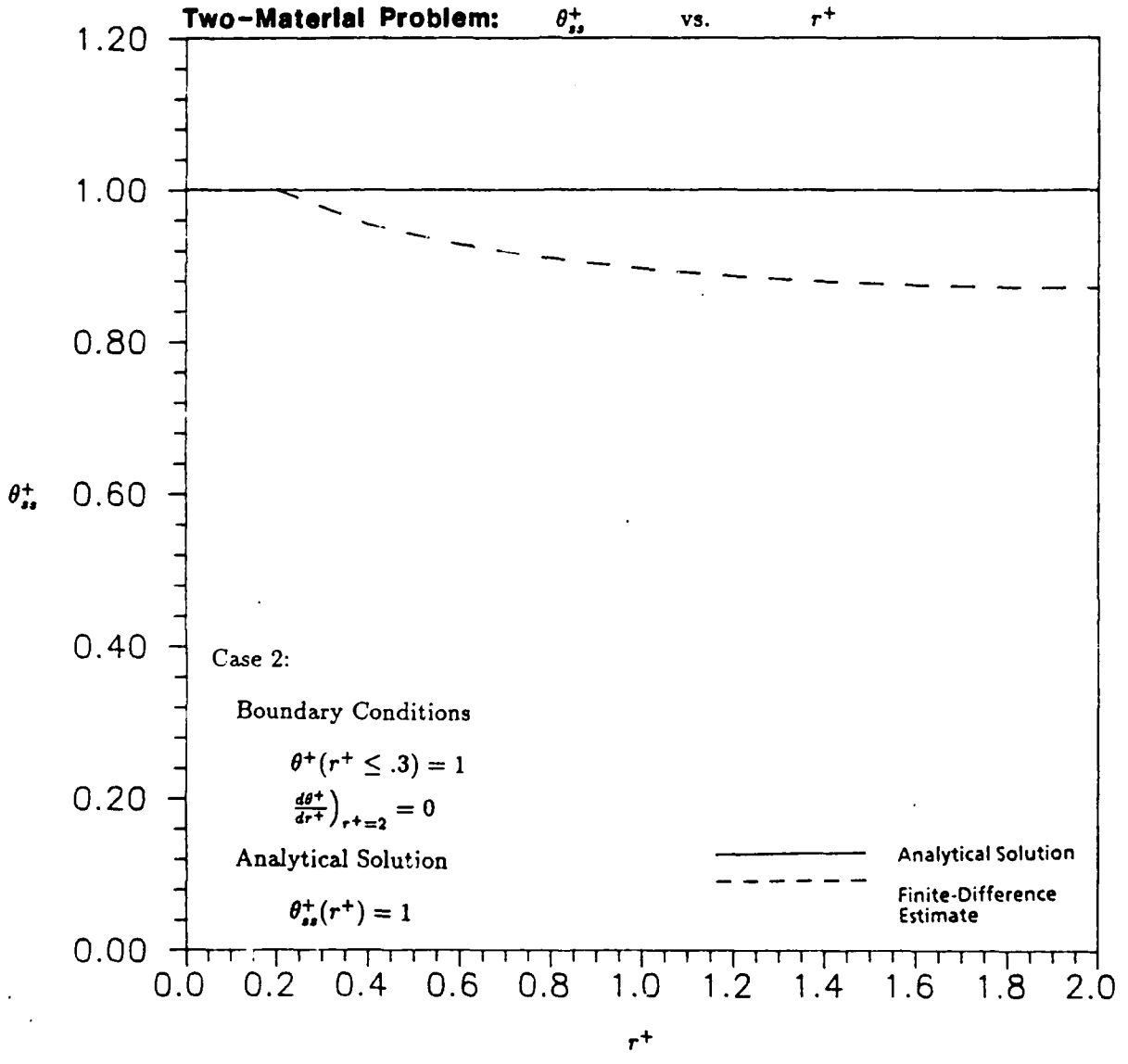

Figure 52. Case 2 for Steady State Heat Transfer in the Radial Direction Using the Two-Material Problem

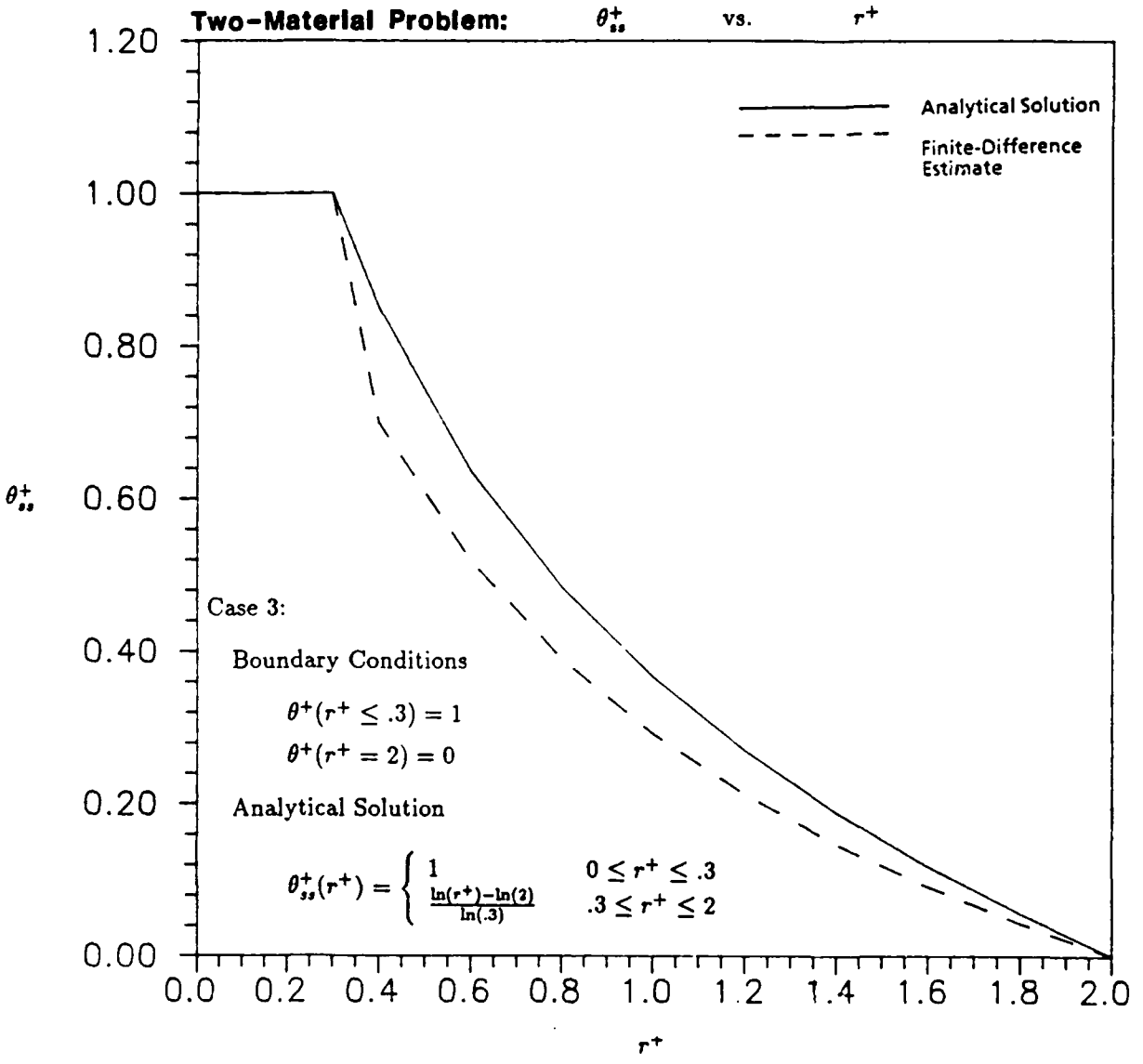

Figure 53. Case 3 for Steady State Heat Transfer in the Radial Direction Using the Two-Material Problem

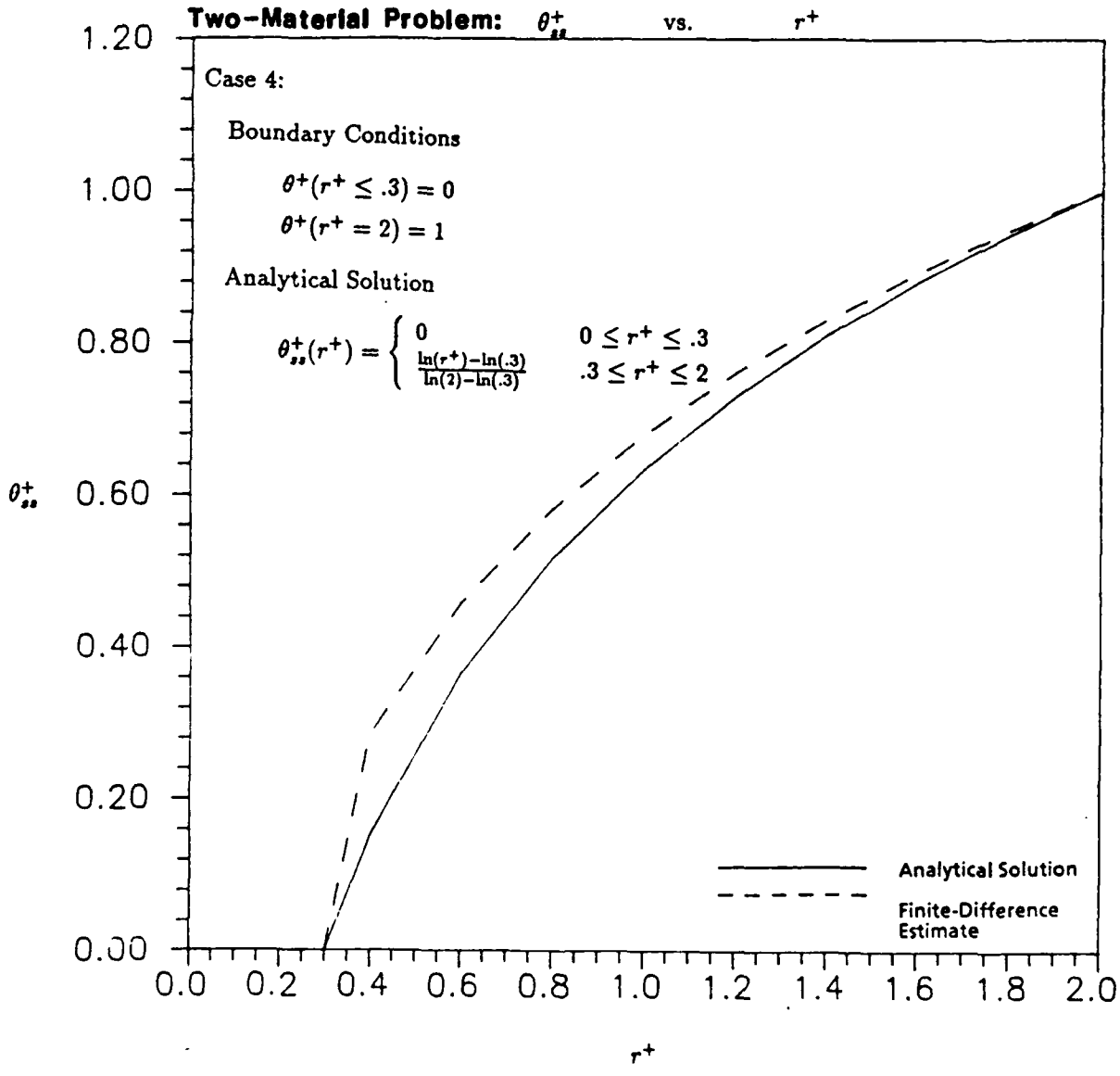

Figure 54. Case 4 for Steady State Heat Transfer in the Radial Direction Using the Two-Material Problem

B.3 Transient Check Cases

B.3.1 The Semi-Infinite Solid with Constant Surface Heat Flux

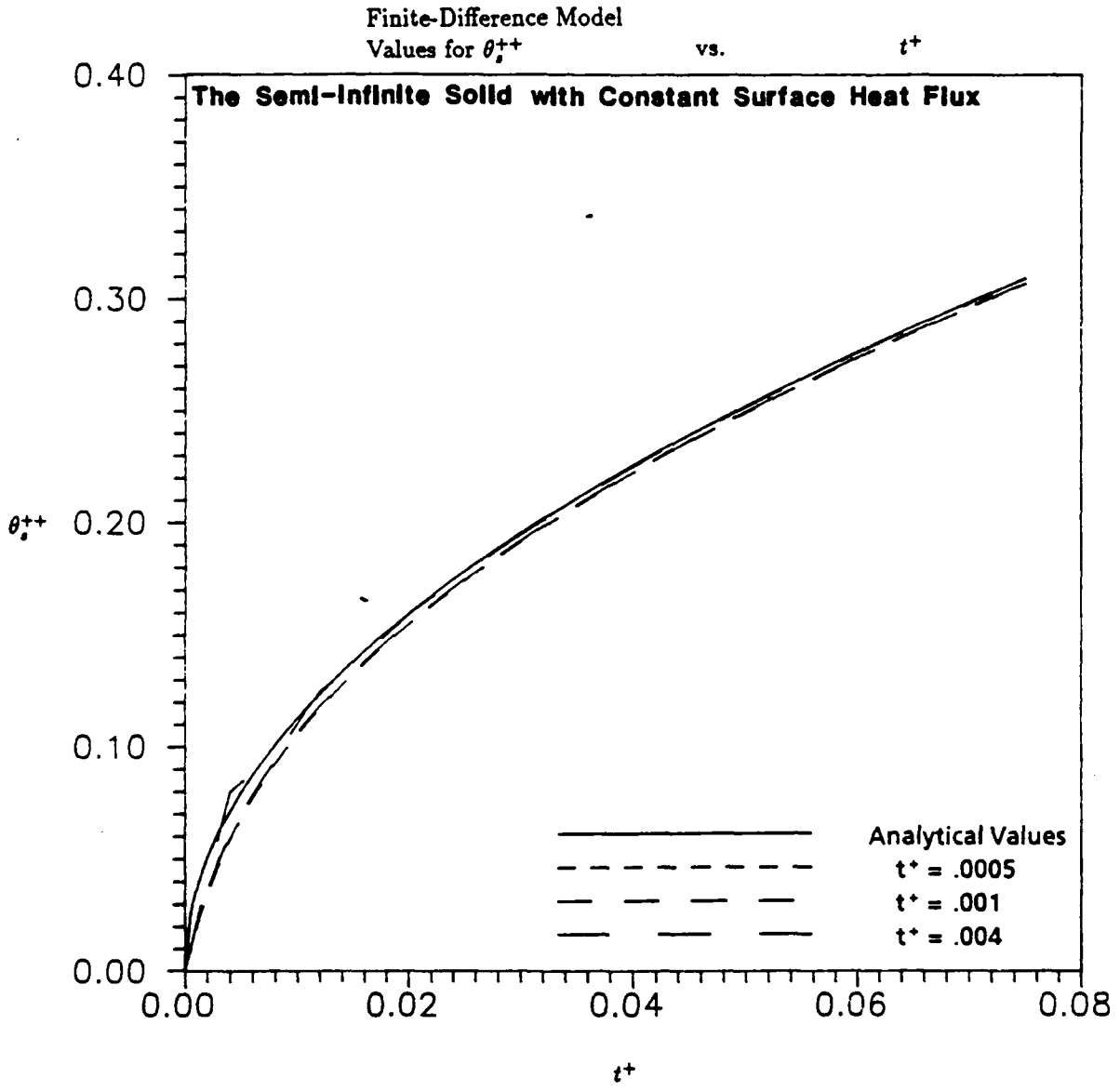

Figure 55. Finite-Difference Model Values for θ_s^+ vs. t^+ for the Semi-Infinite Solid with Constant Surface Heat Flux

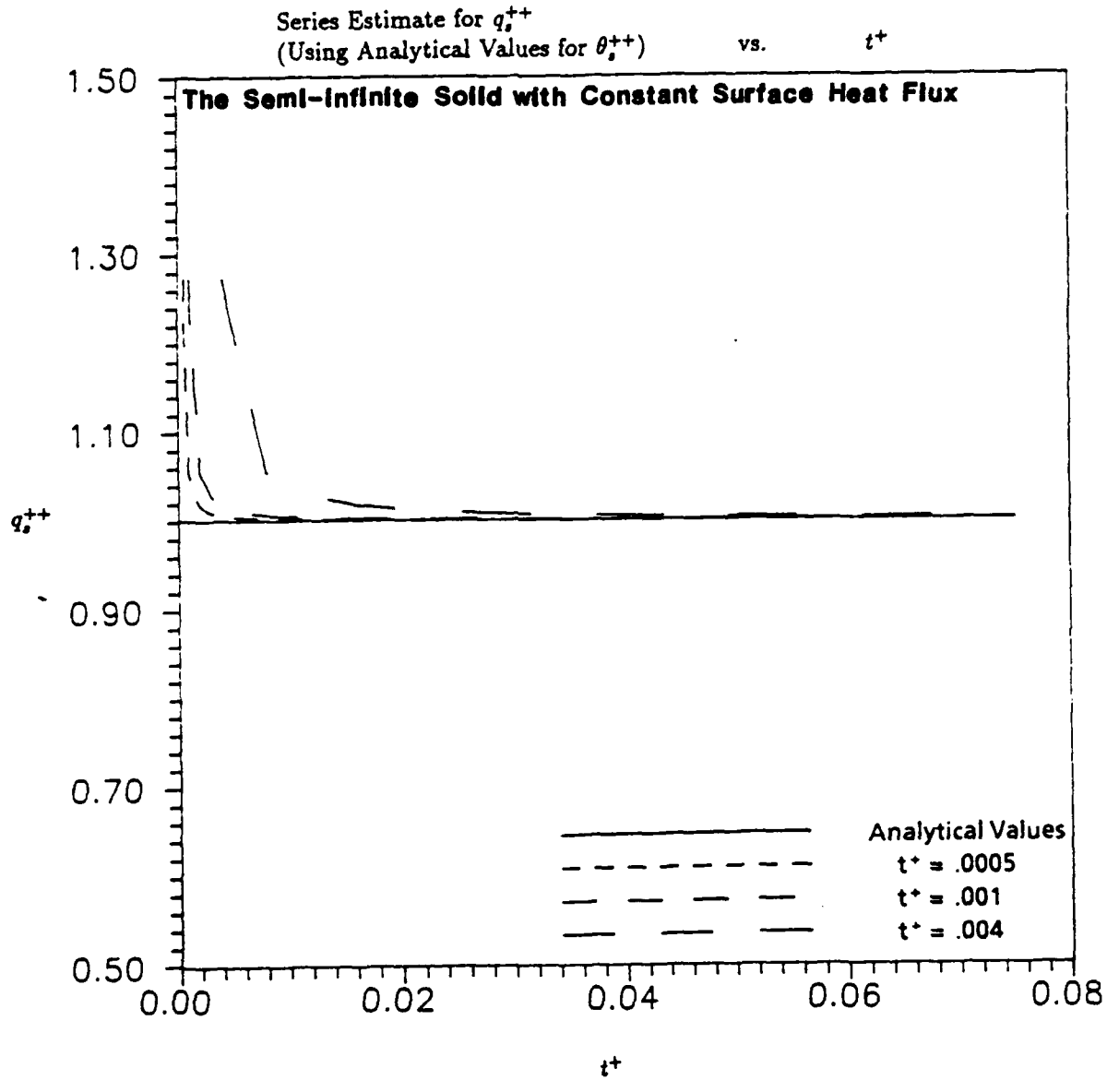

Figure 56. Series Solution Estimates for q_s^+ (Using Analytical Values for θ_s^+) vs. t^+ for the Semi-Infinite Solid with Constant Surface Heat Flux

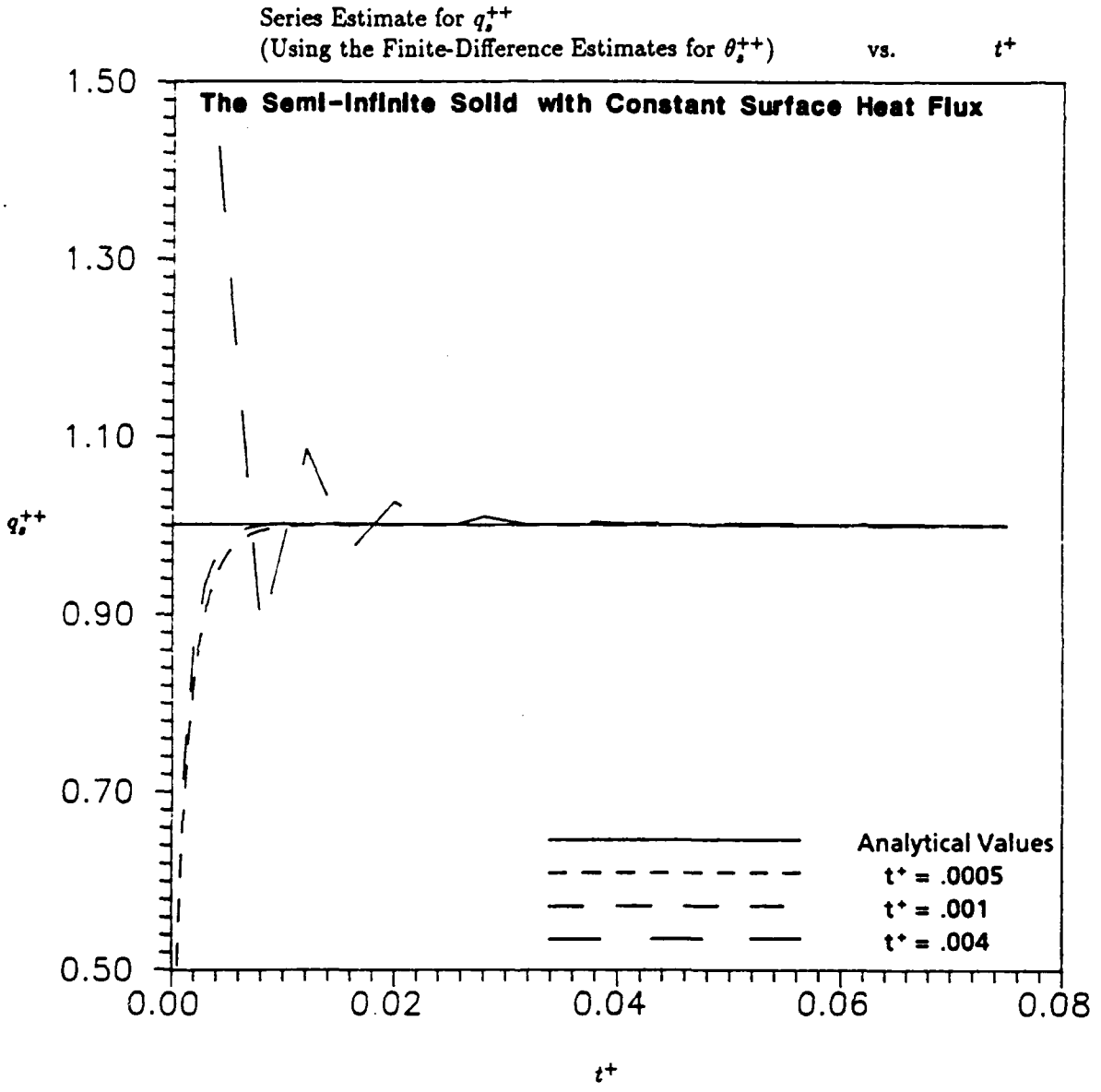

Figure 57. Series Solution Estimates for q_s^+ (Using the Finite-Difference Model Values for θ_s^+) vs. t^+ for the Semi-Infinite Solid with Constant Surface Heat Flux

B.3.2 The Plane Wall with Convection

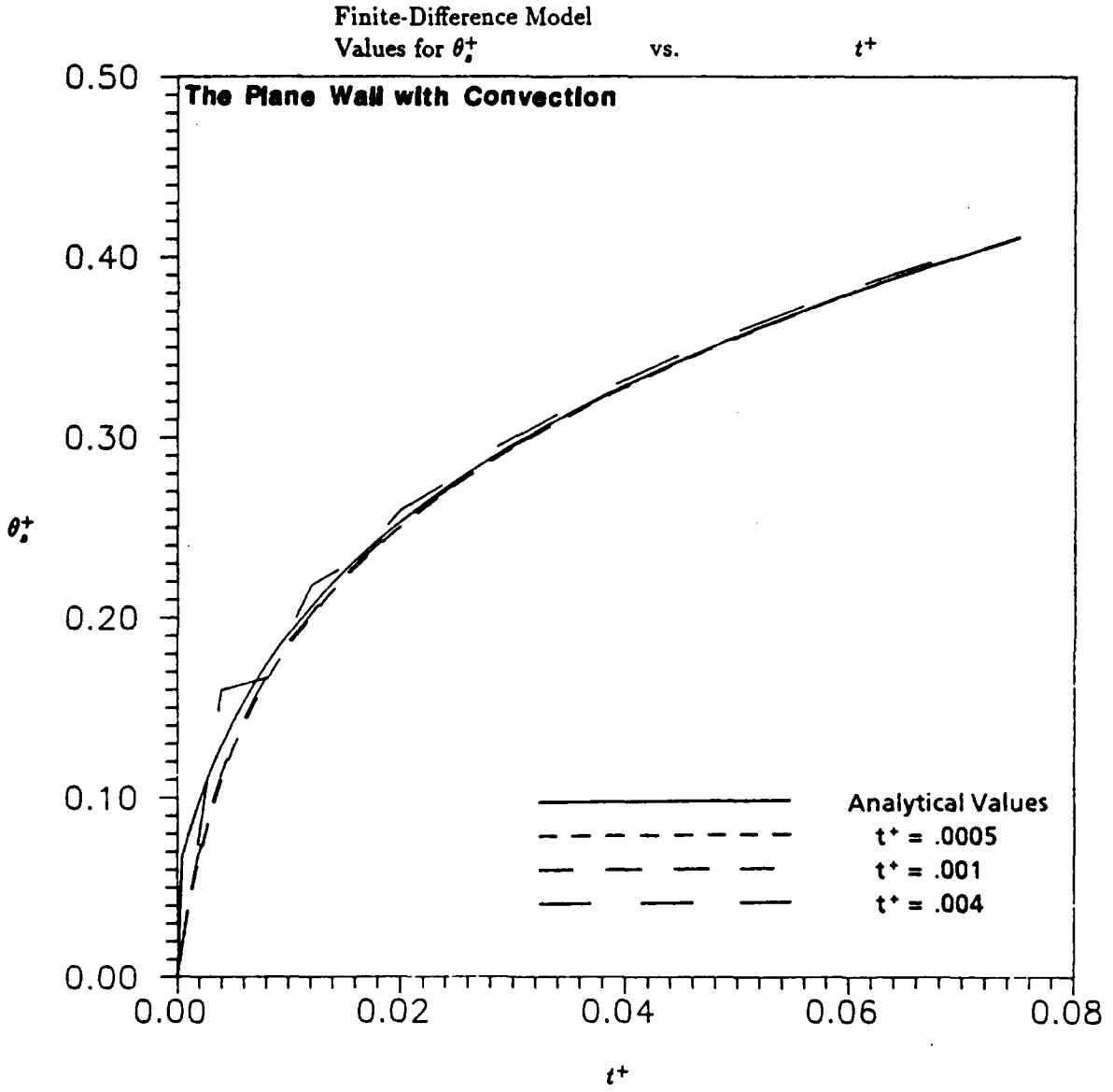

Figure 58. Finite-Difference Model Values for θ_s^+ vs. t^+ for the Plane Wall with Convection

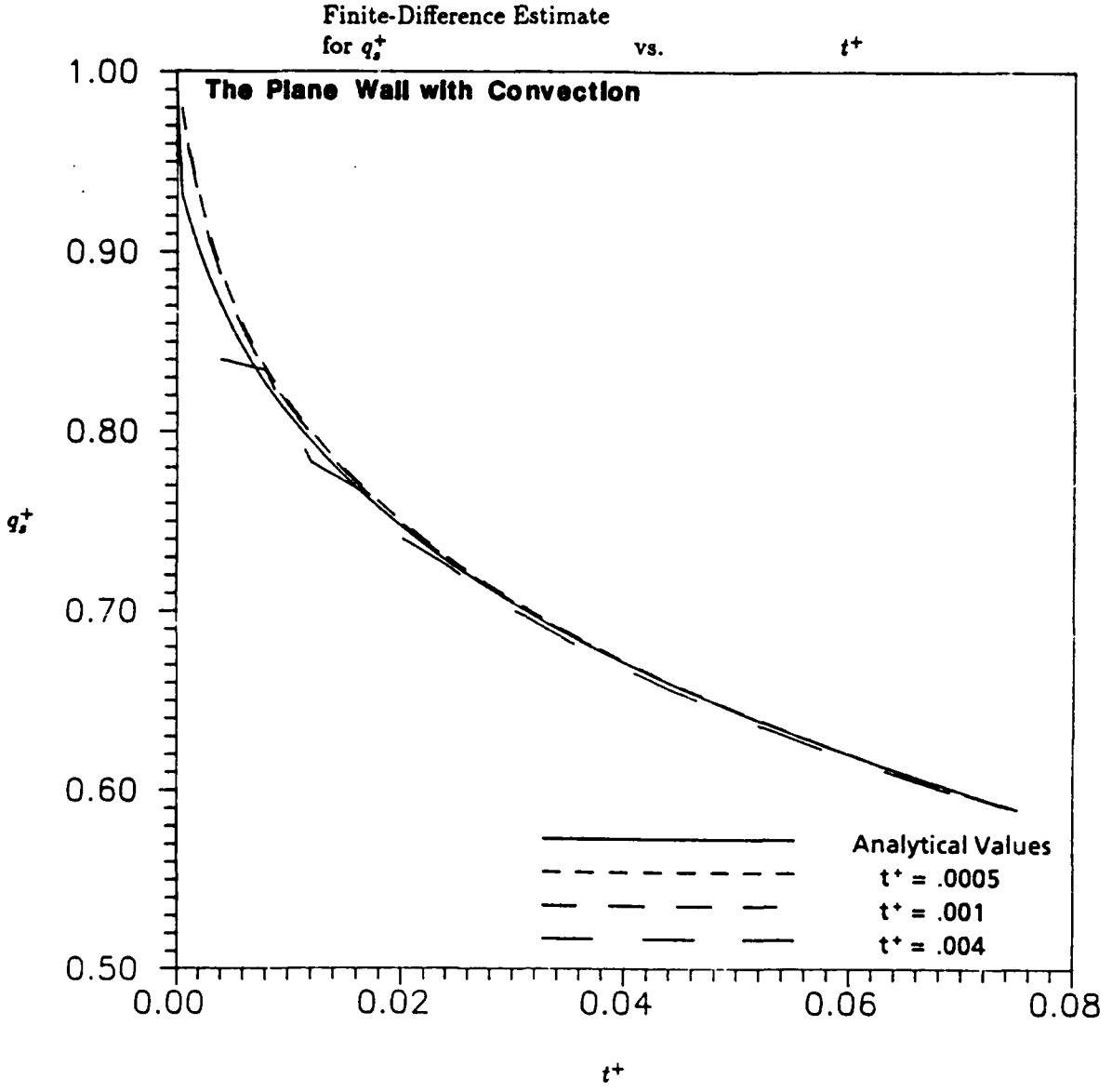

Figure 59. Finite-Difference Estimates for q_s^+ vs. t^+ for the Plane Wall with Convection

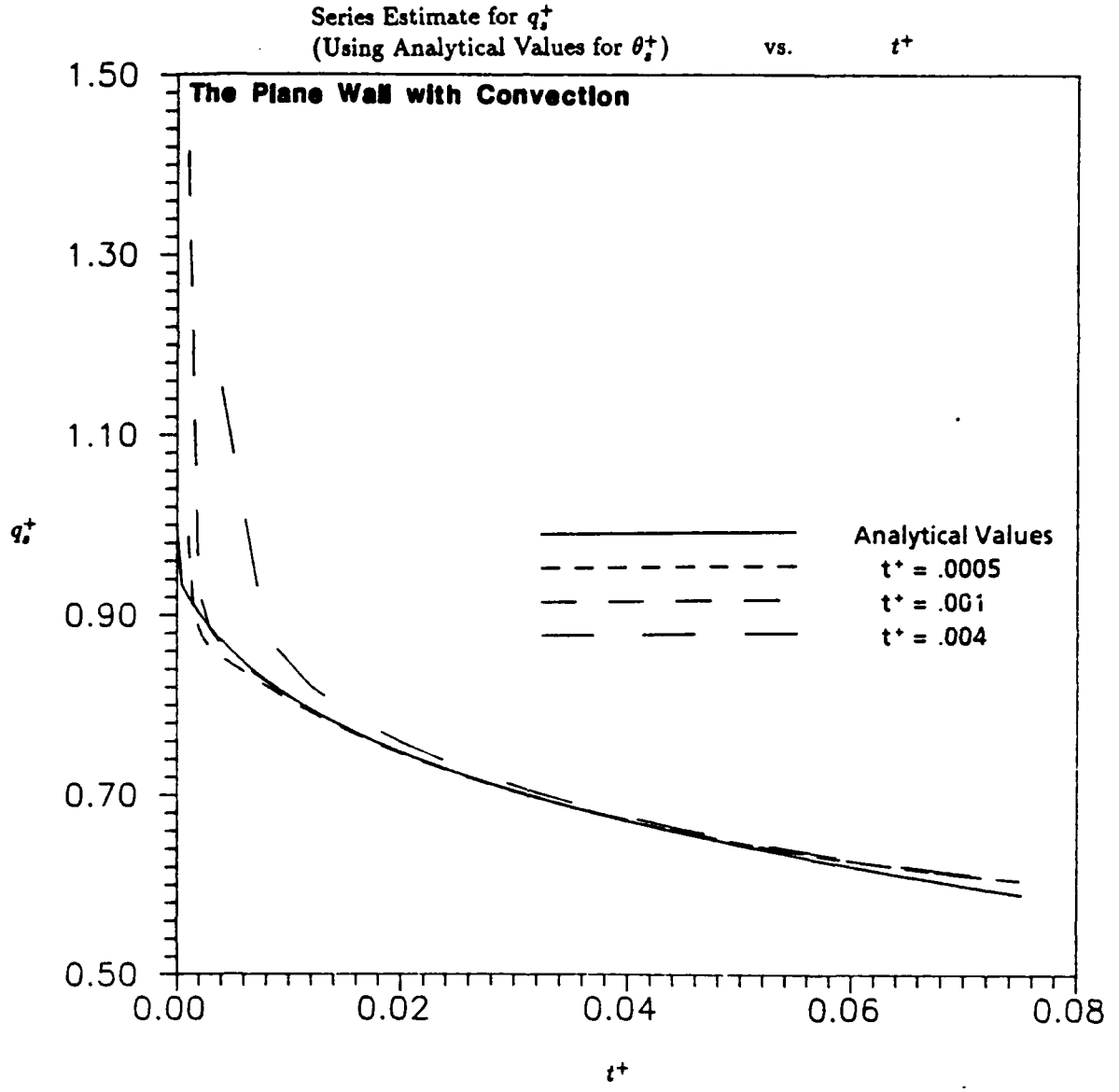

Figure 60. Series Solution Estimates for q_s^+ (Using Analytical Values for θ_s^+) vs. t^+ for the Plane Wall with Convection

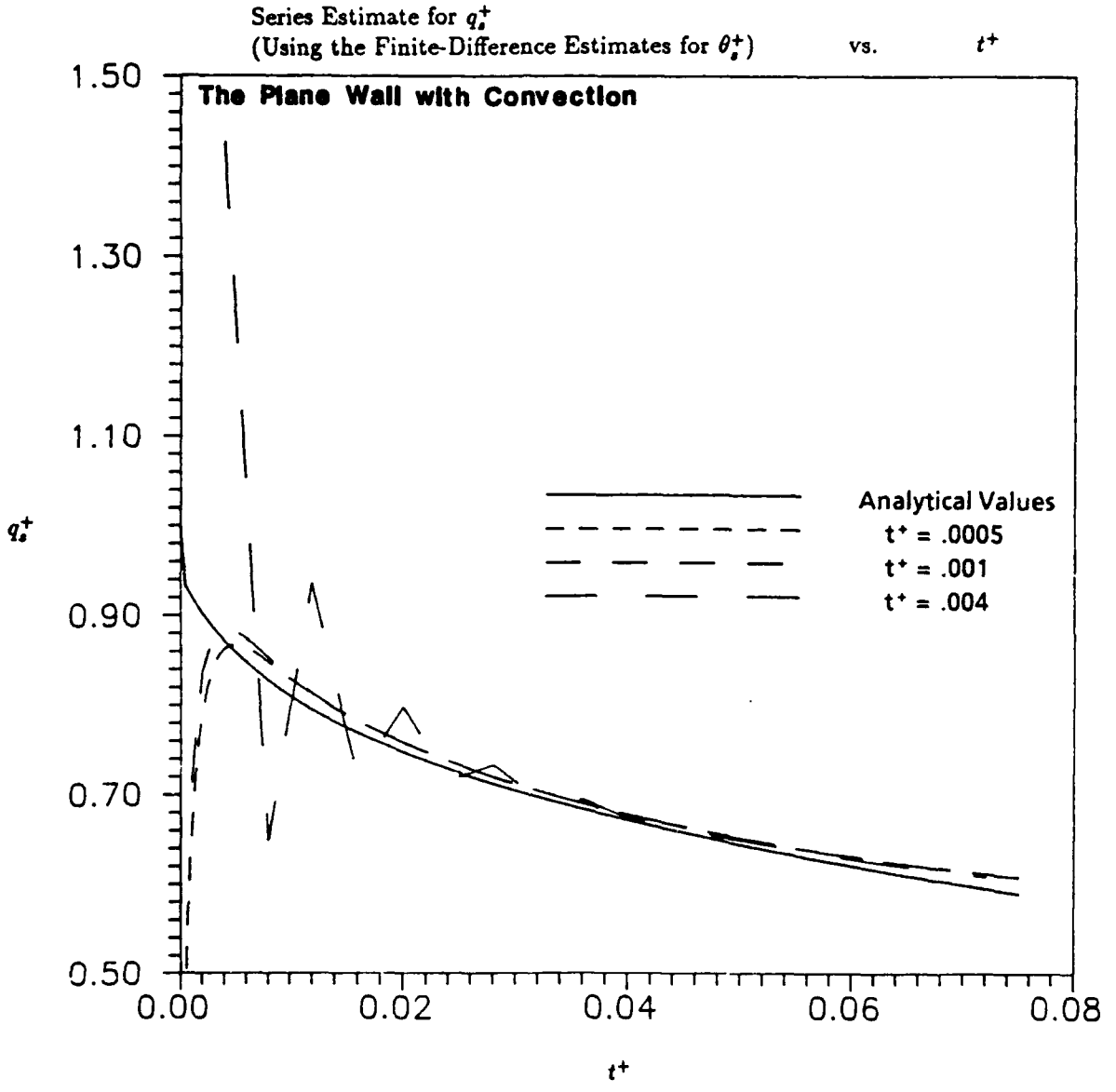

Figure 61. Series Solution Estimates for q_s^+ (Using the Finite-Difference Model Values for θ_s^+) vs. t^+ for the Plane Wall with Convection

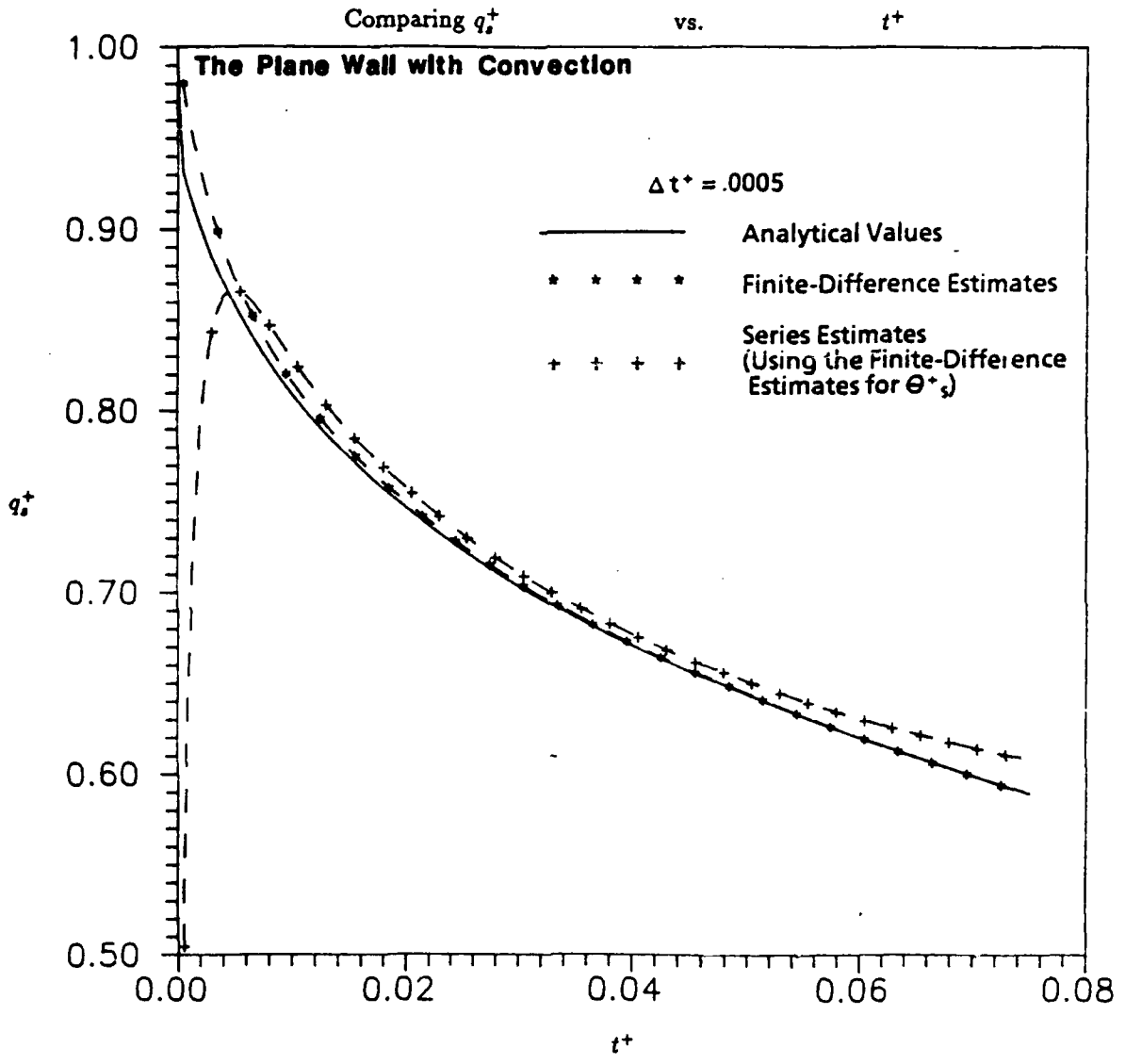

Figure 62. Comparing the Finite-Difference Estimates, Series Solution Estimates (Using the Finite-Difference Model Values for θ_s^+) and Analytical Values for q_s^+ vs. t^+ for the Plane Wall with Convection

Appendix C. *Other Graphs of Results*

C.1 Results for the Adiabatic Cases Using $\beta = 100.0$

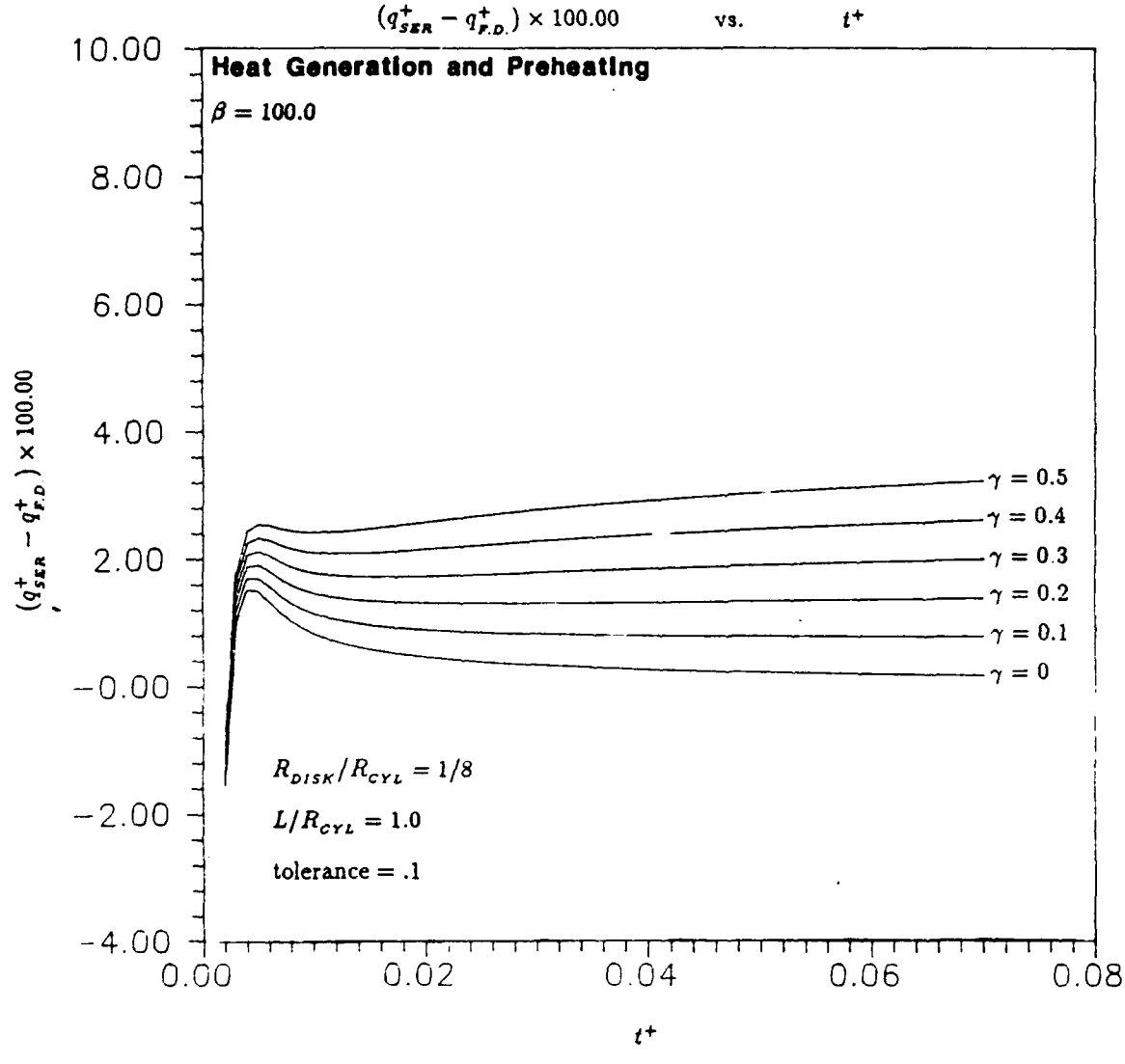

Figure 63. Results with Heat Generation and Preheating as γ Varies Using β = 100.0

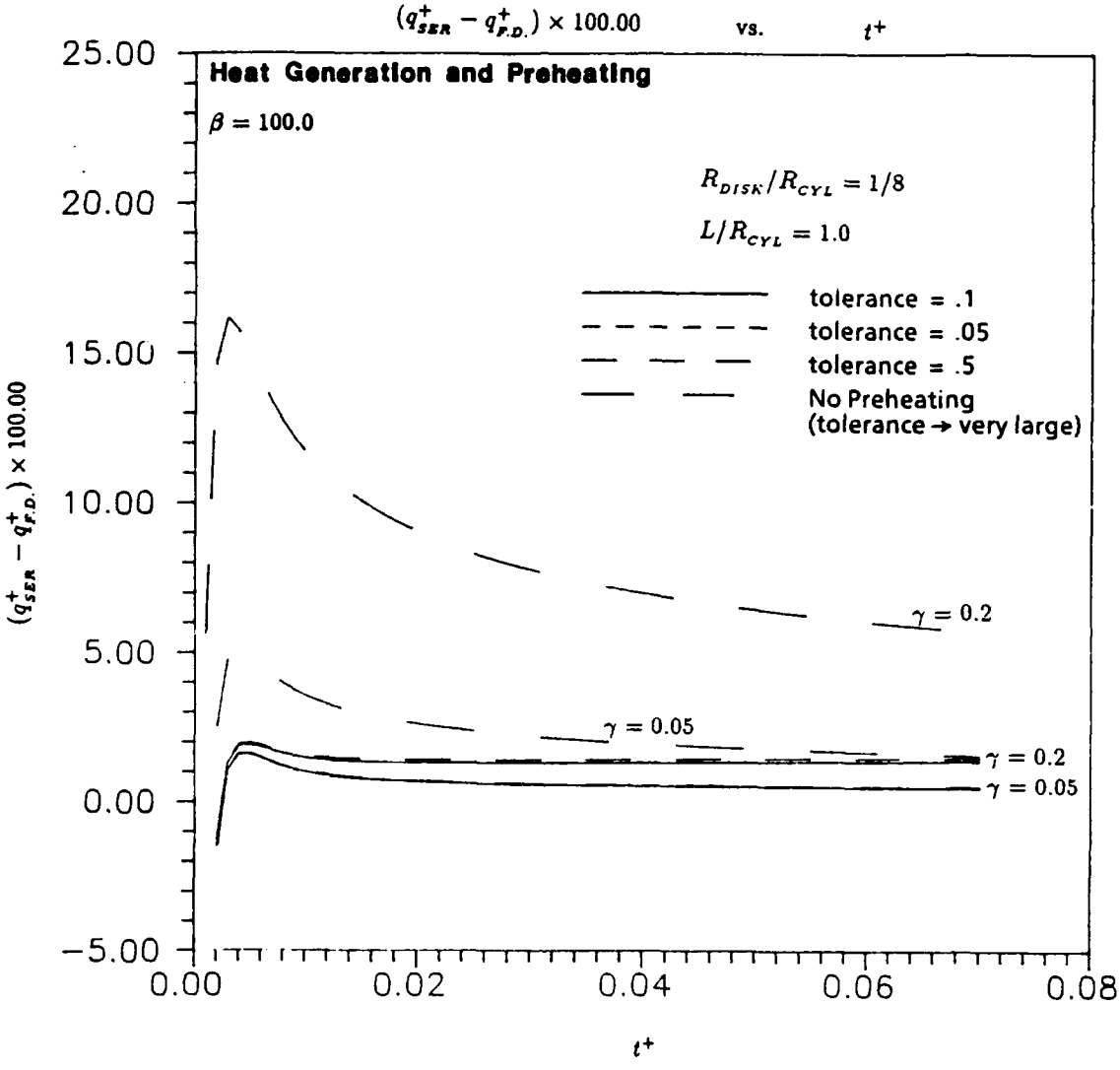

Figure 64. Results with Heat Generation and Preheating as the Tolerance Varies Using $\beta = 100.0$

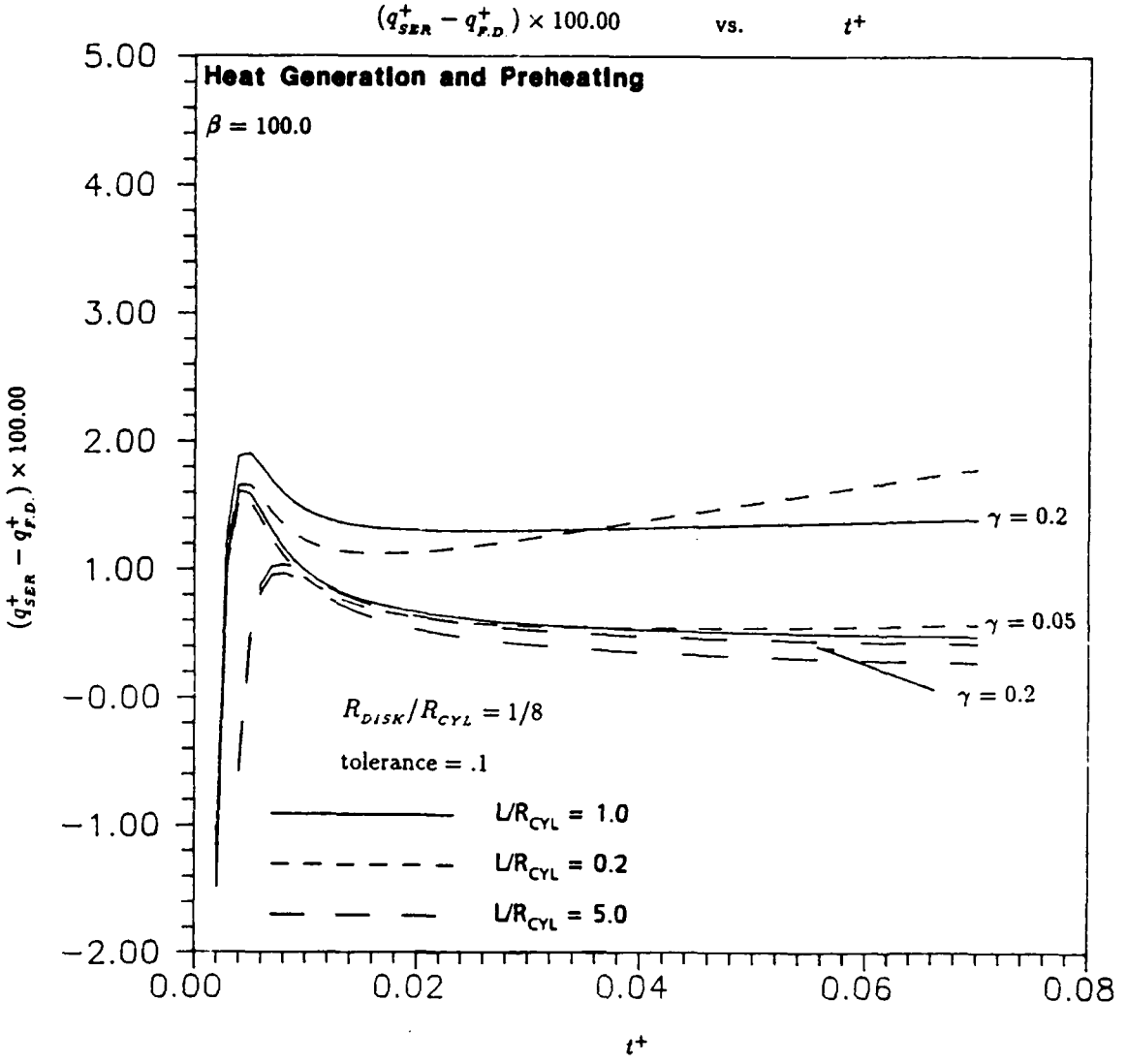

Figure 65. Results with Heat Generation and Preheating as L/R_{CYL} Varies Using $\beta = 100.0$

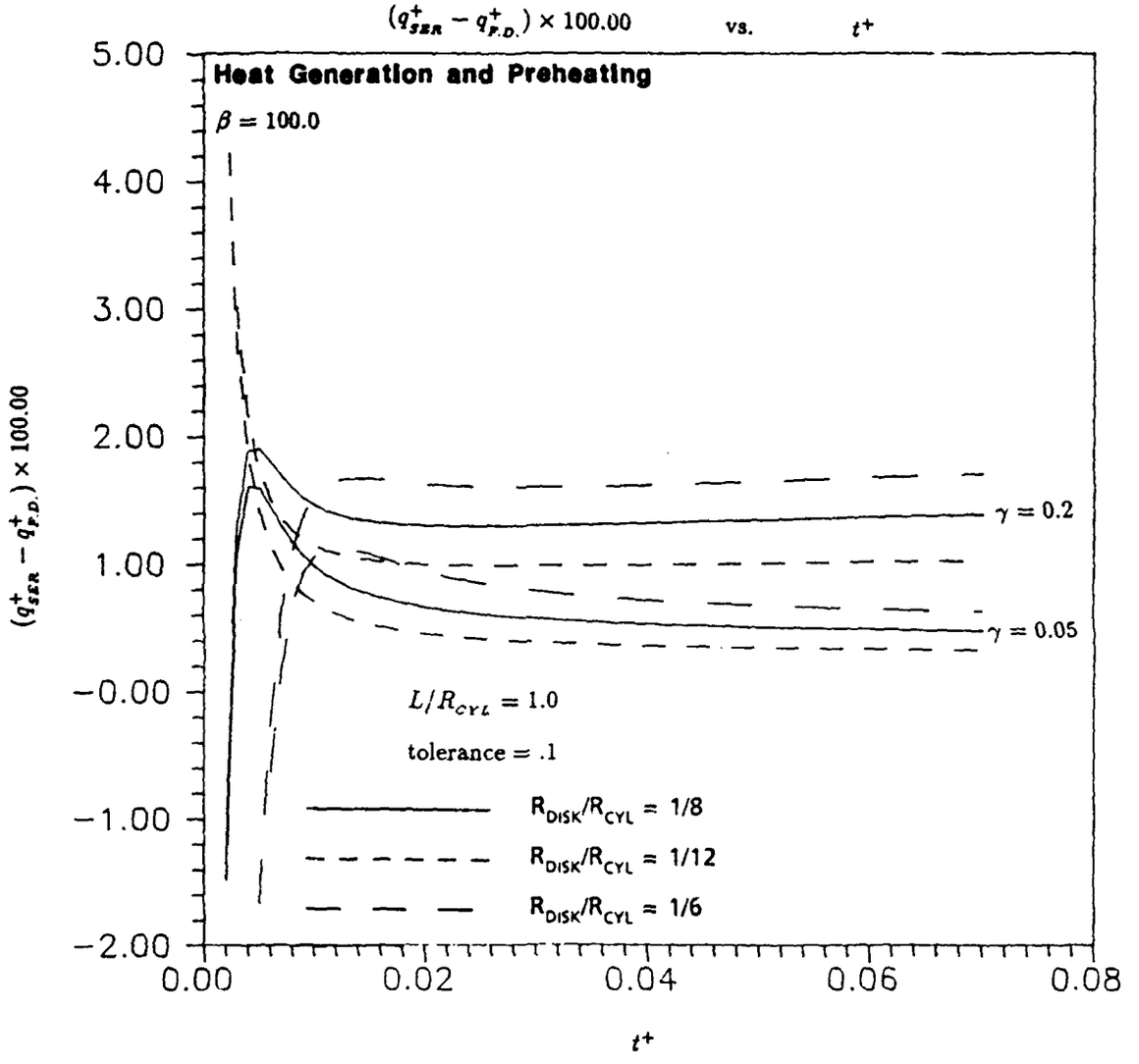

Figure 66. Results with Heat Generation and Preheating as R_{DISK}/R_{CYL} Varies Using $\beta = 100.0$

C.2 Results for the Non-Adiabatic Cases with No Heat Generation or Preheating Using ${}_dBi_{FRONT} = 1.0$

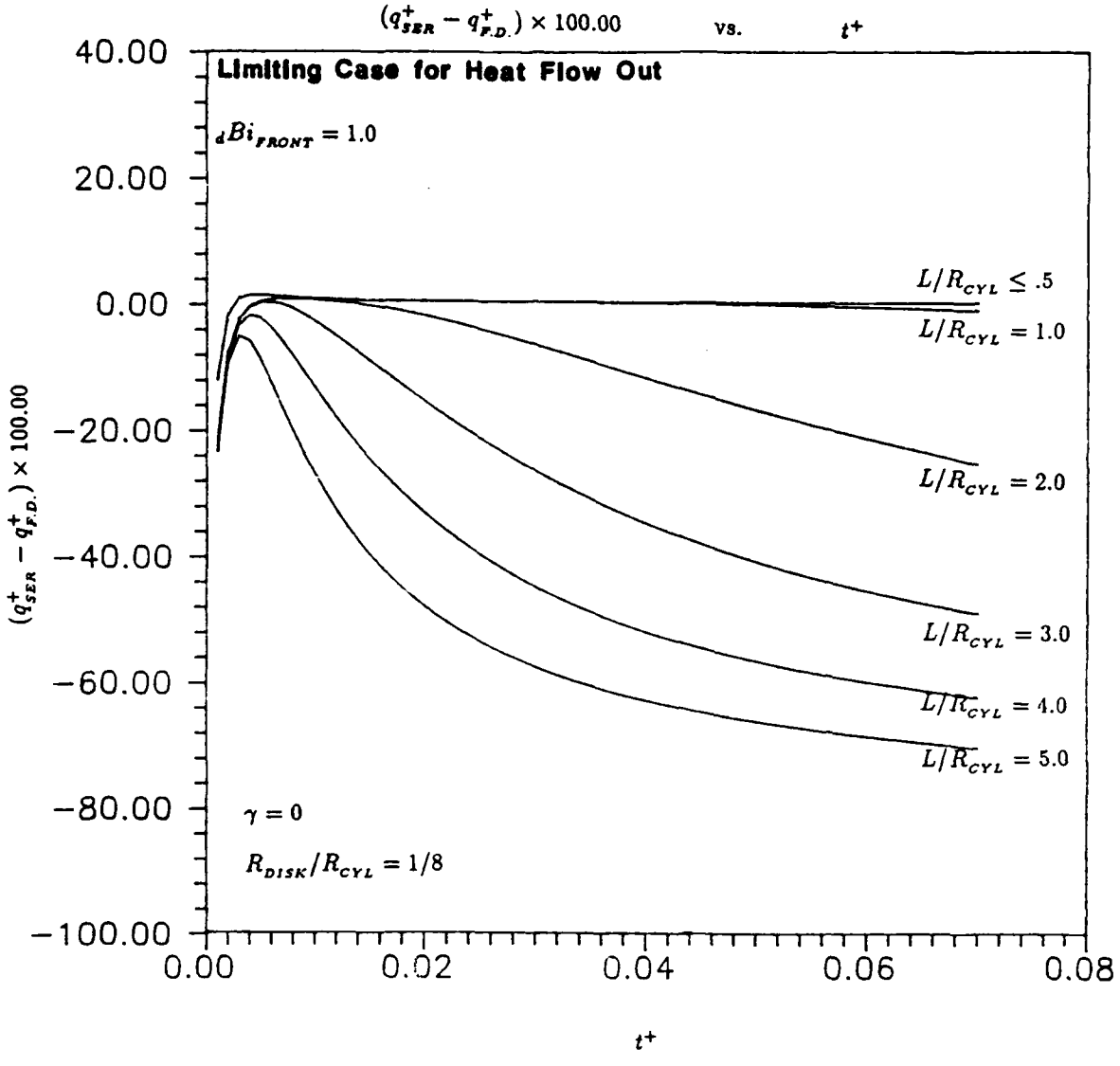

Figure 67. Results for the Limiting Case for Heat Flux Out Across the Outer-Radial Boundary with No Heat Generation as L/R_{CYL} Varies Using ${}_dBi_{FRONT} = 1.0$

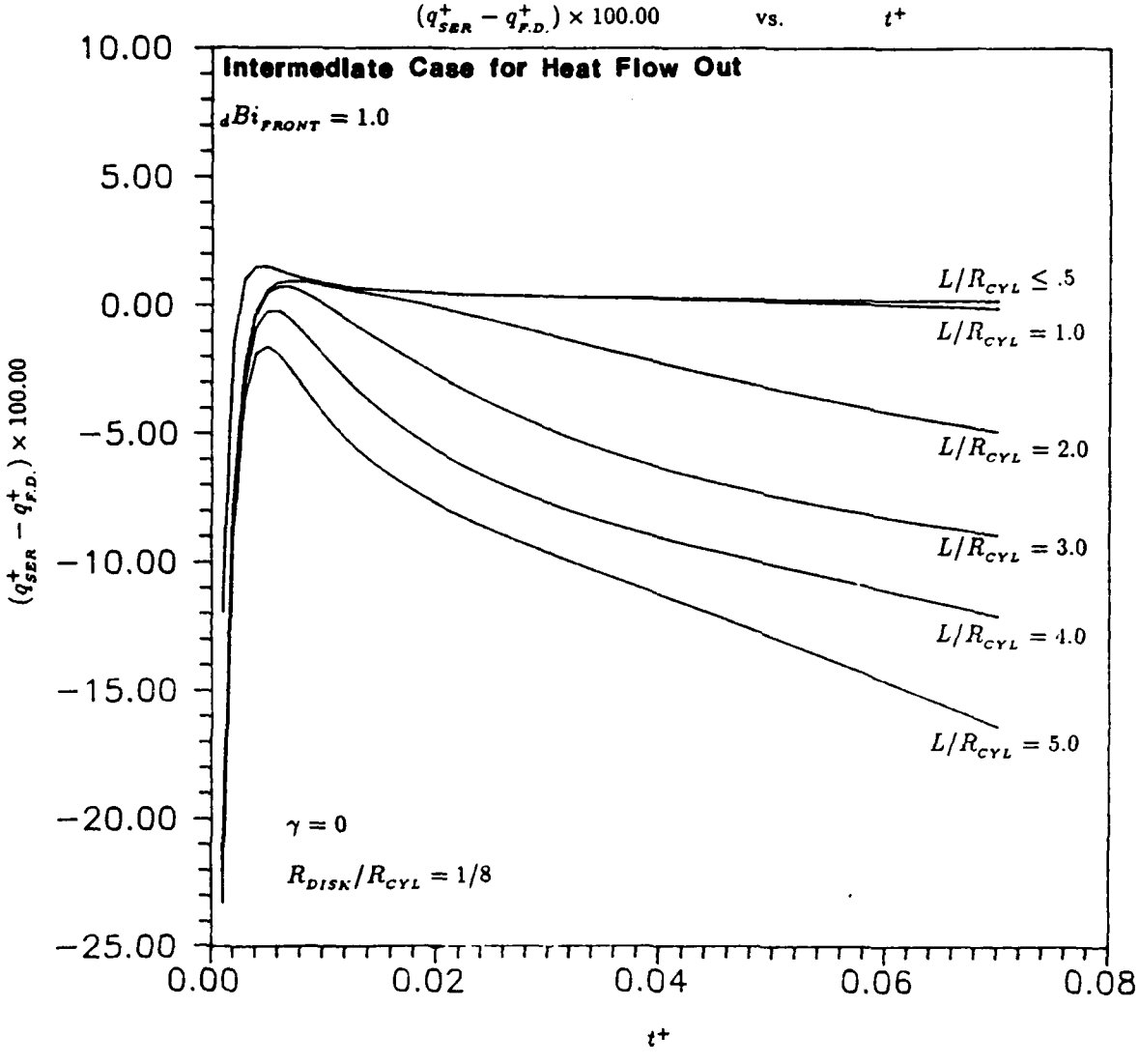

Figure 68. Results for the Intermediate Case for Heat Flux Out Across the Outer-Radial Boundary with No Heat Generation as L/R_{CYL} Varies Using ${}_dBi_{FRONT} = 1.0$

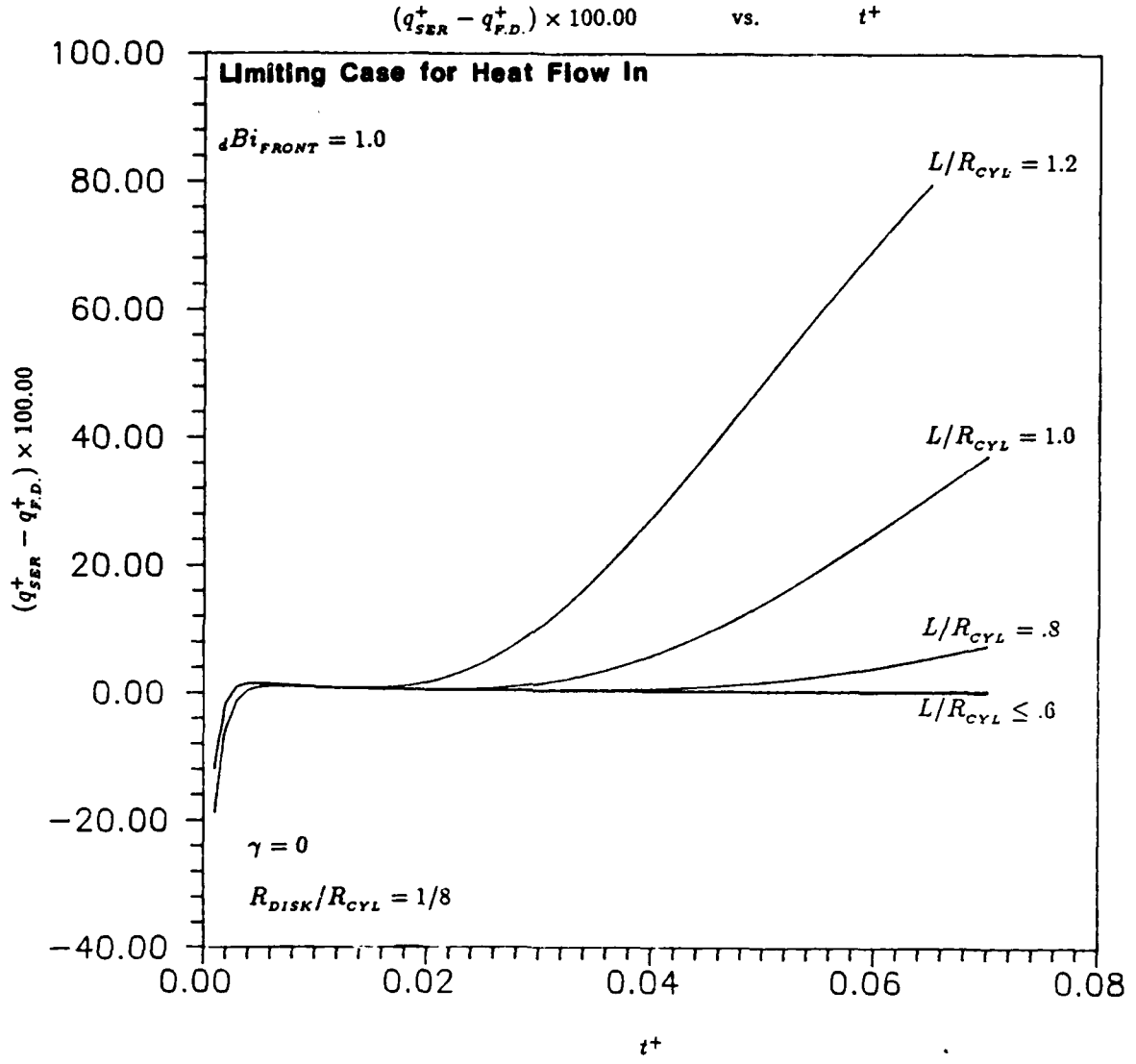

Figure 69. Results for the Limiting Case for Heat Flux In Across the Outer-Radial Boundary with No Heat Generation as L/R_{CYL} Varies Using ${}_dBi_{FRONT} = 1.0$

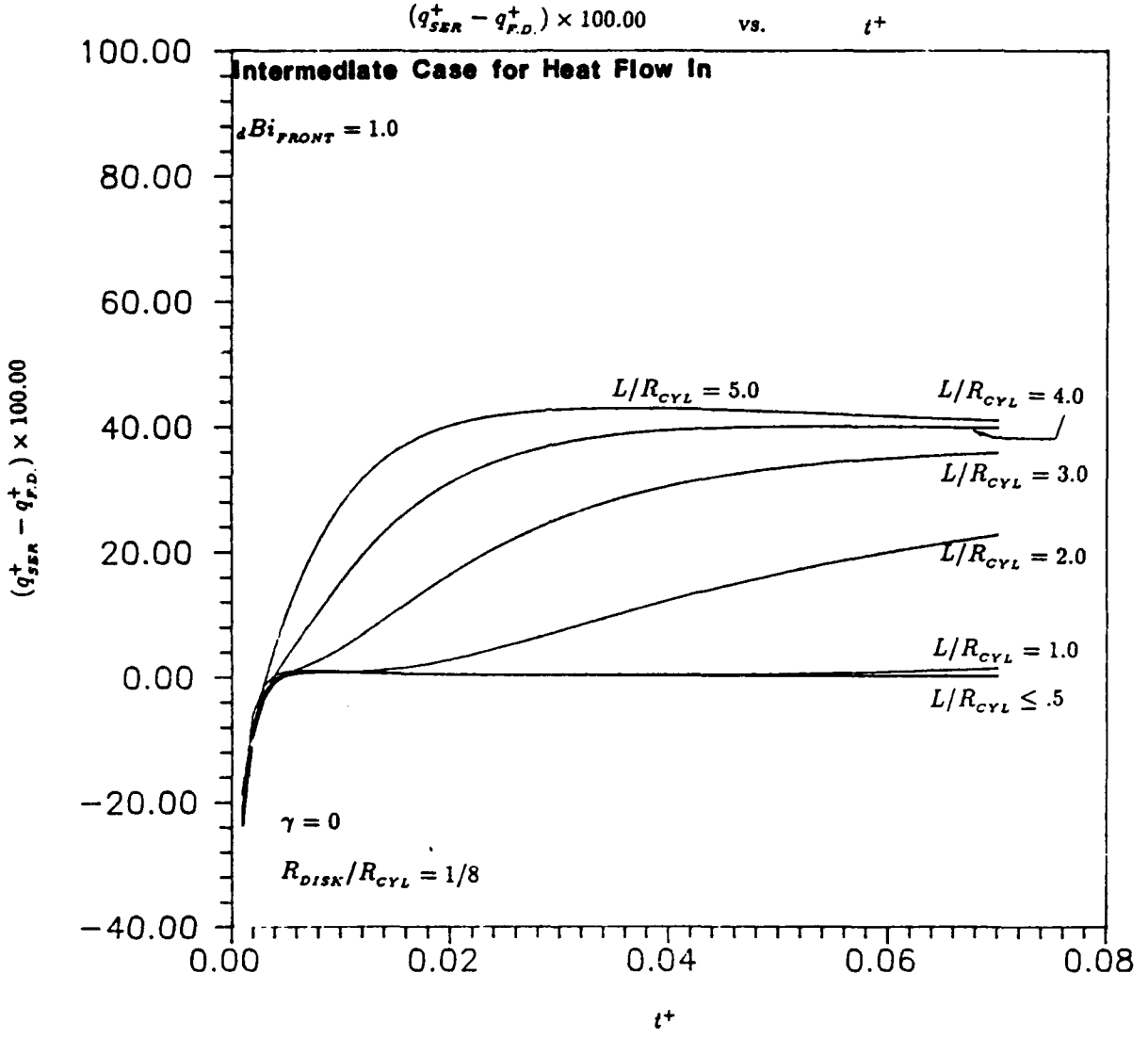

Figure 70. Results for the Intermediate Case for Heat Flux In Across the Outer-Radial Boundary with No Heat Generation as L/R_{CYL} Varies Using ${}_dBi_{FRONT} = 1.0$

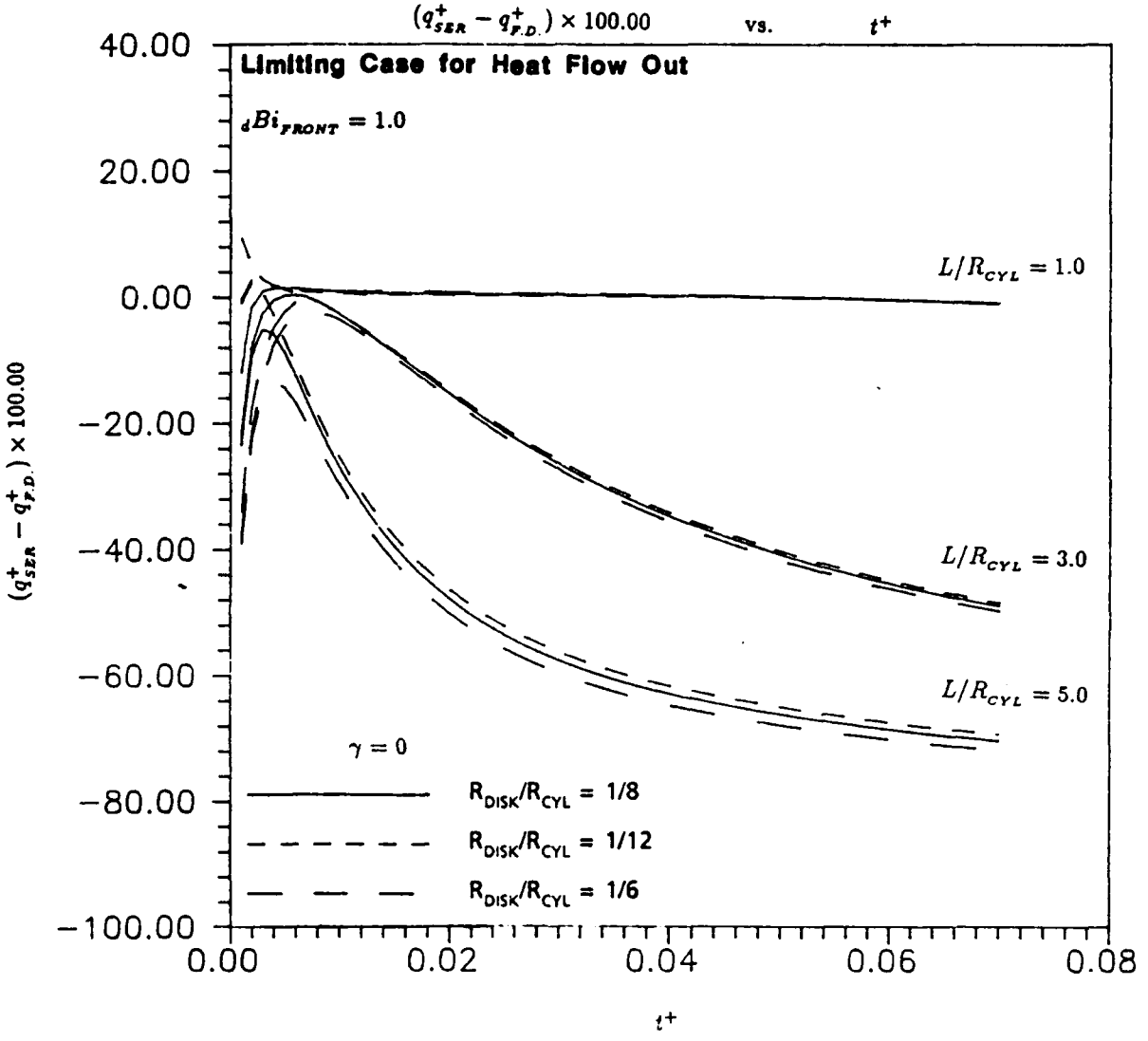

Figure 71. Results for the Limiting Case for Heat Flux Out Across the Outer-Radial Boundary with No Heat Generation as R_{DISK}/R_{CYL} Varies Using $_dBi_{FRONT} = 1.0$

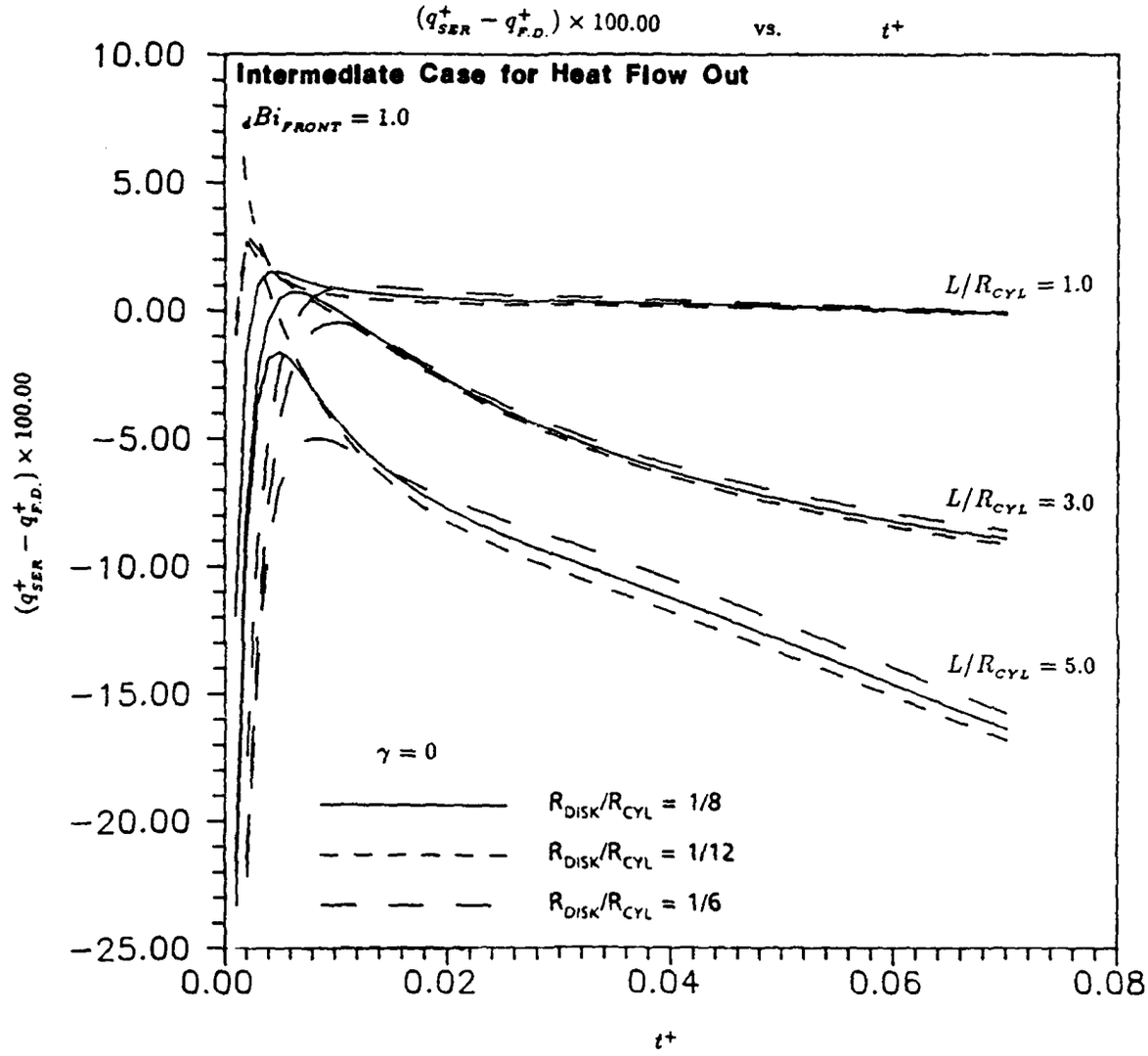

Figure 72. Results for the Intermediate Case for Heat Flux Out Across the Outer-Radial Boundary with No Heat Generation as R_{DISK}/R_{CYL} Varies Using $_dBi_{FRONT} = 1.0$

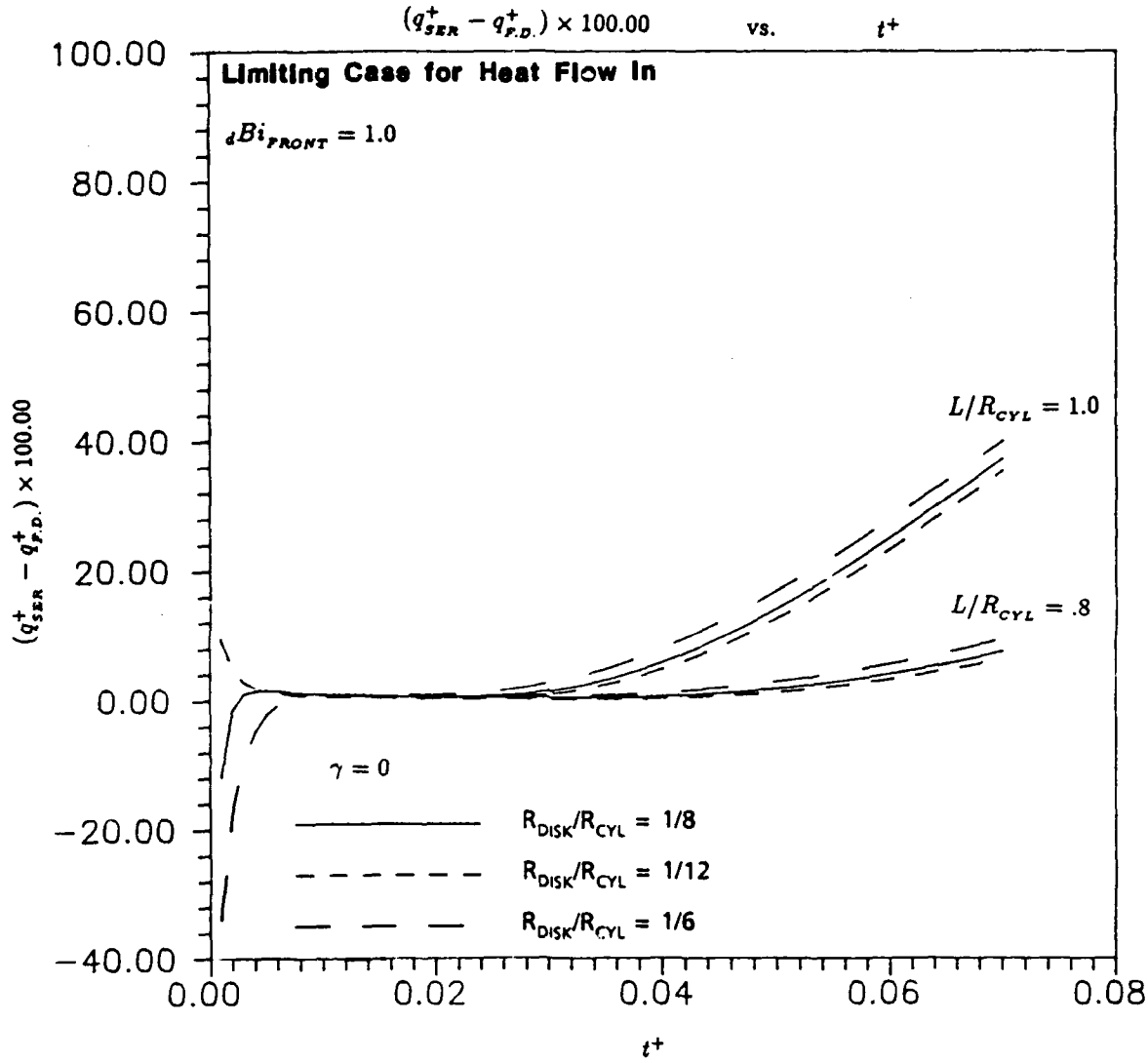

Figure 73. Results for the Limiting Case for Heat Flux In Across the Outer-Radial Boundary with No Heat Generation as R_{DISK}/R_{CYL} Varies Using $_dBi_{FRONT} = 1.0$

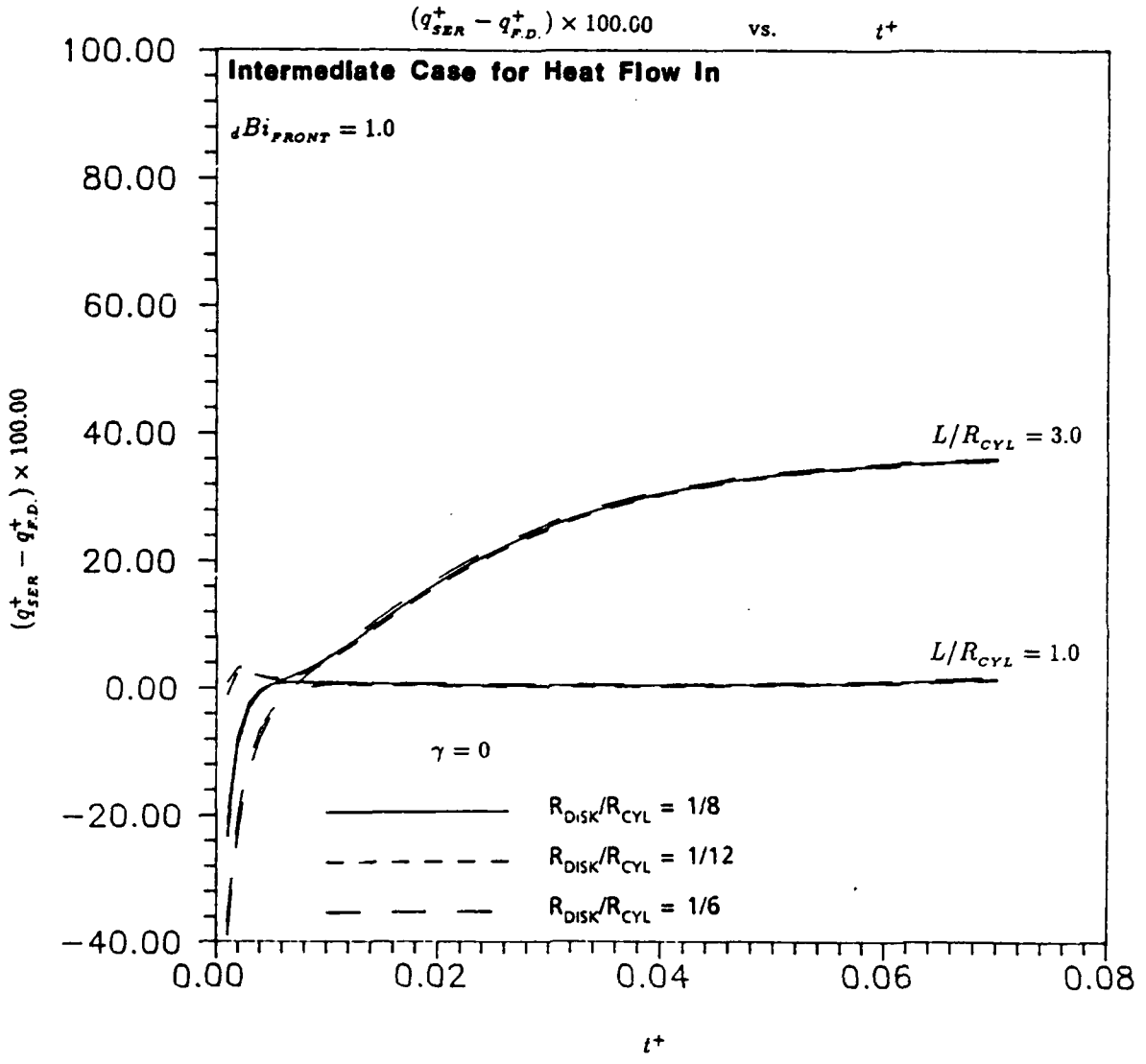

Figure 74. Results for the Intermediate Case for Heat Flux In Across the Outer-Radial Boundary with No Heat Generation as R_{DISK}/R_{CYL} Varies Using ${}_dBi_{FRONT} = 1.0$

C.3 Results for the Non-Adiabatic Cases with Heat Generation and Preheating Using $\beta = 100.0$

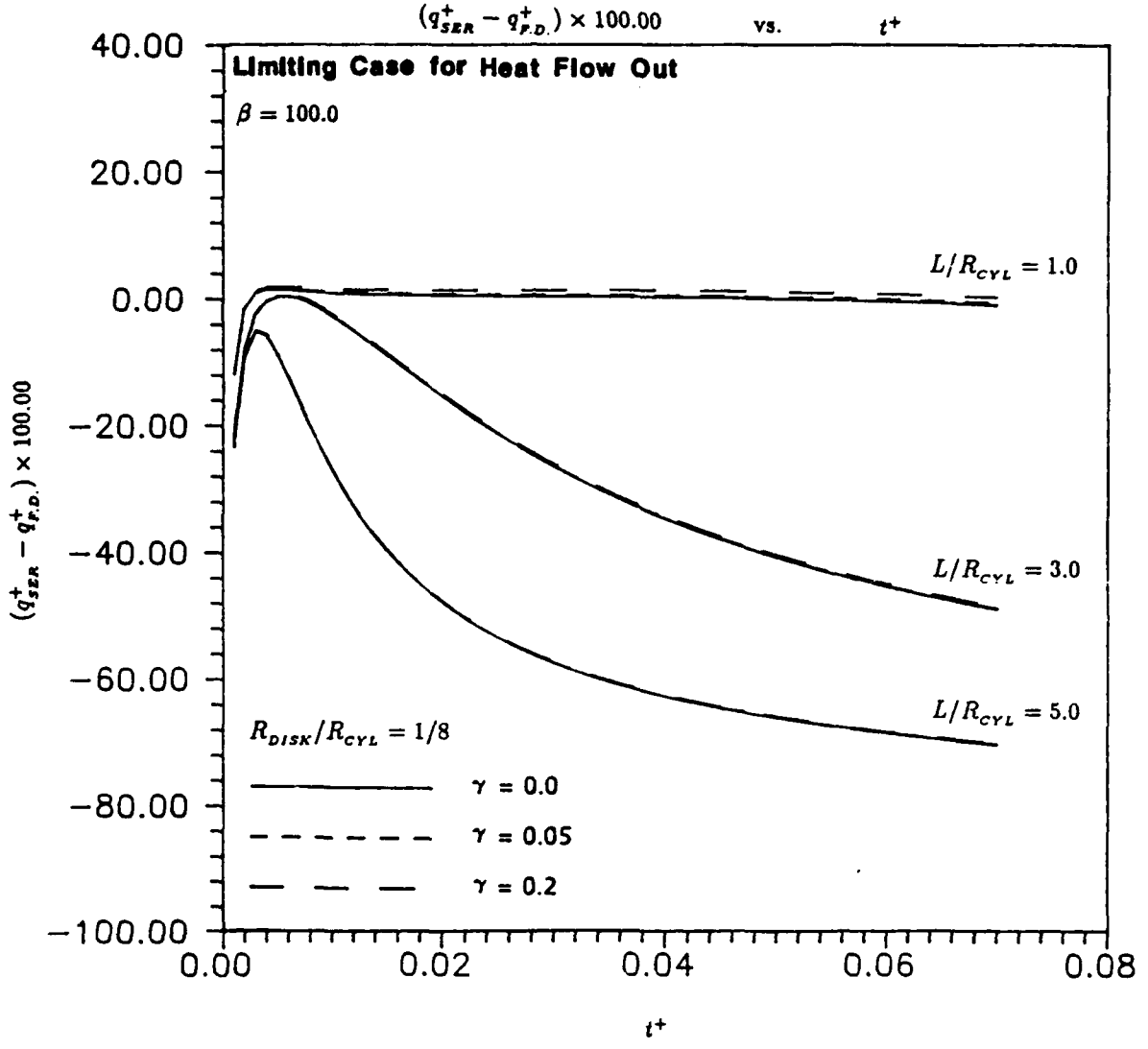

Figure 75. Results for the Limiting Case for Heat Flux Out Across the Outer-Radial Boundary with Heat Generation and Preheating Using $\beta = 100.0$

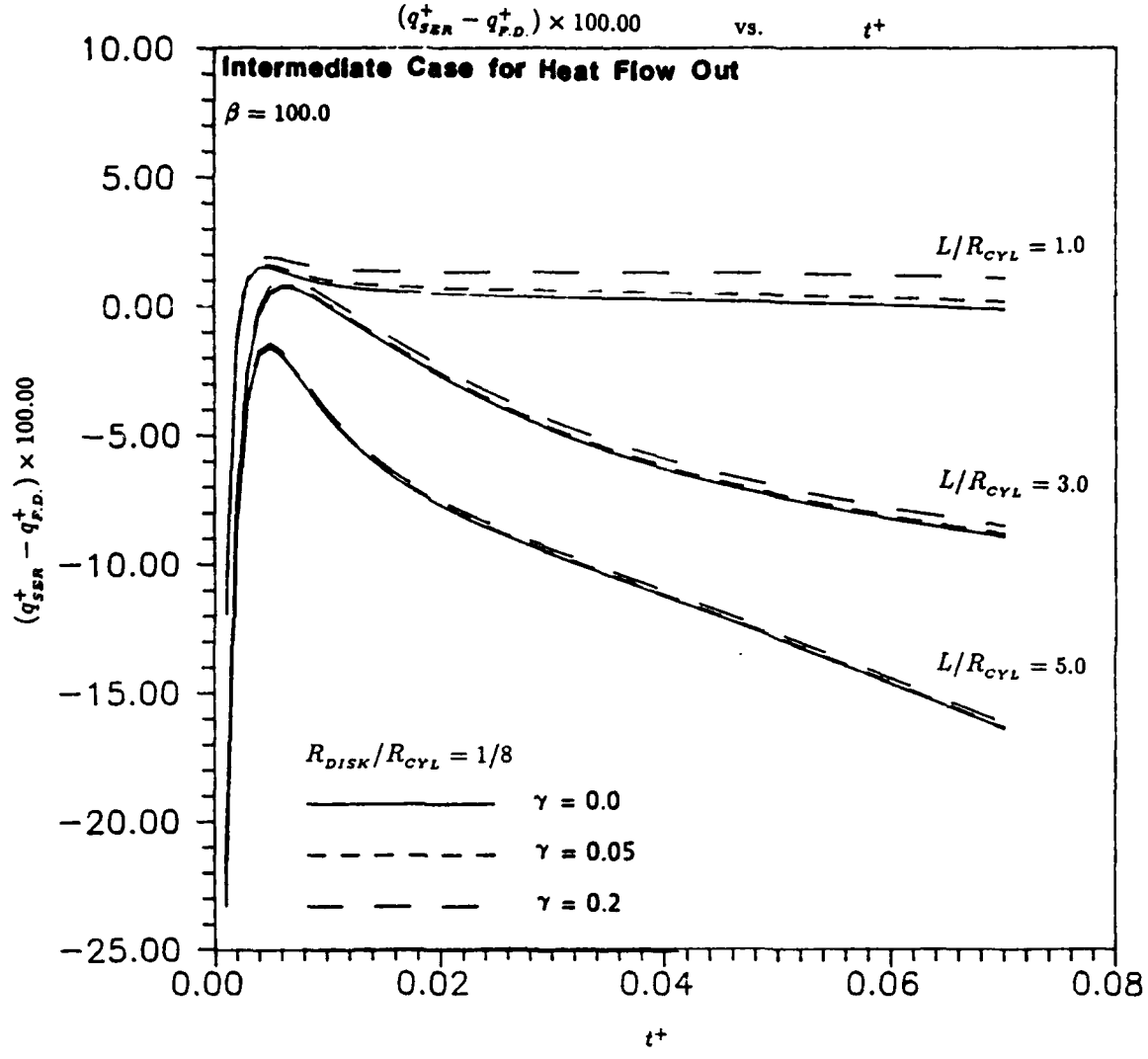

Figure 76. Results for the Intermediate Case for Heat Flux Out Across the Outer-Radial Boundary with Heat Generation and Preheating Using $\beta = 100.0$

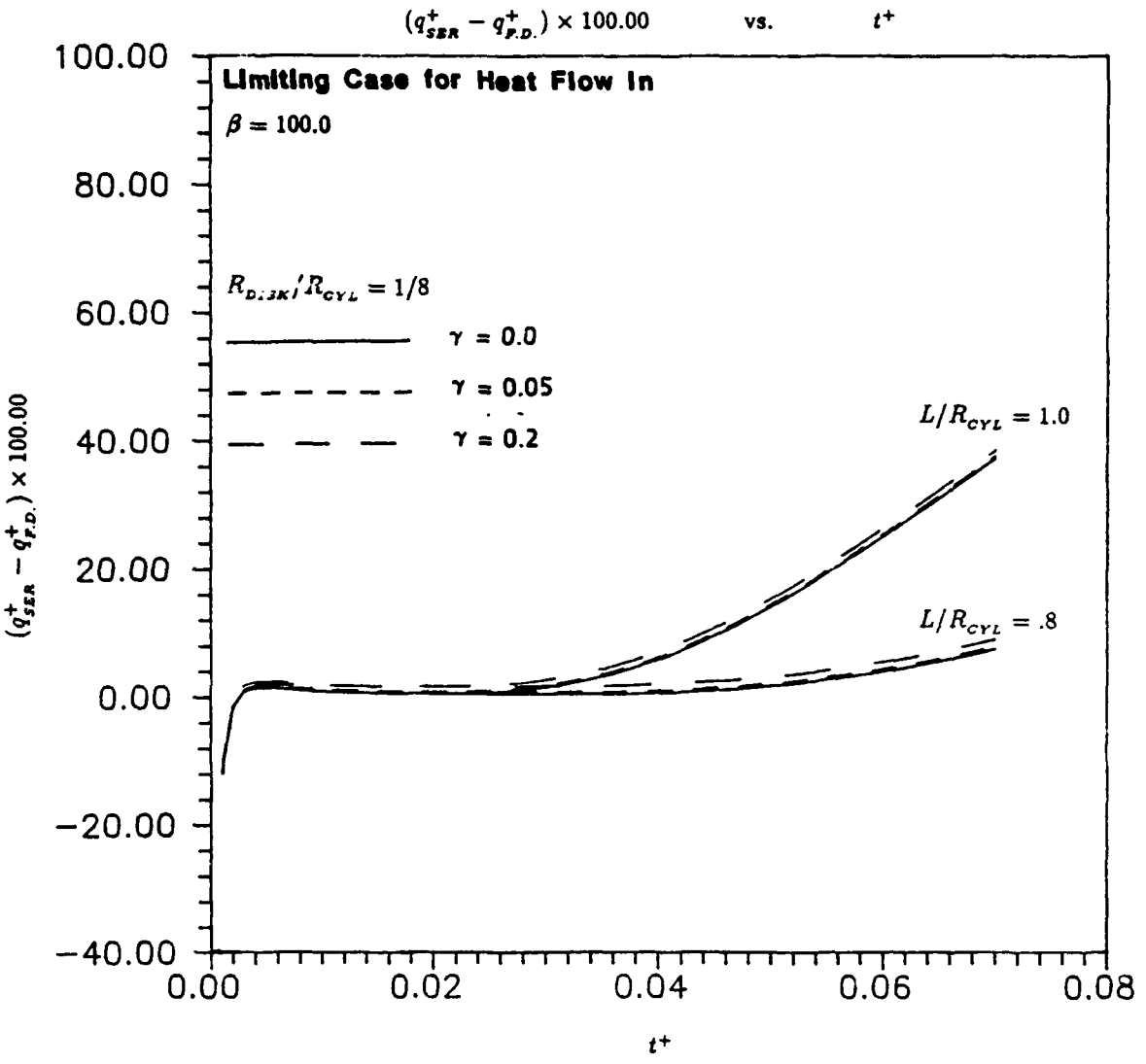

Figure 77. Results for the Limiting Case for Heat Flux In Across the Outer-Radial Boundary with Heat Generation and Preheating Using $\beta = 100.0$

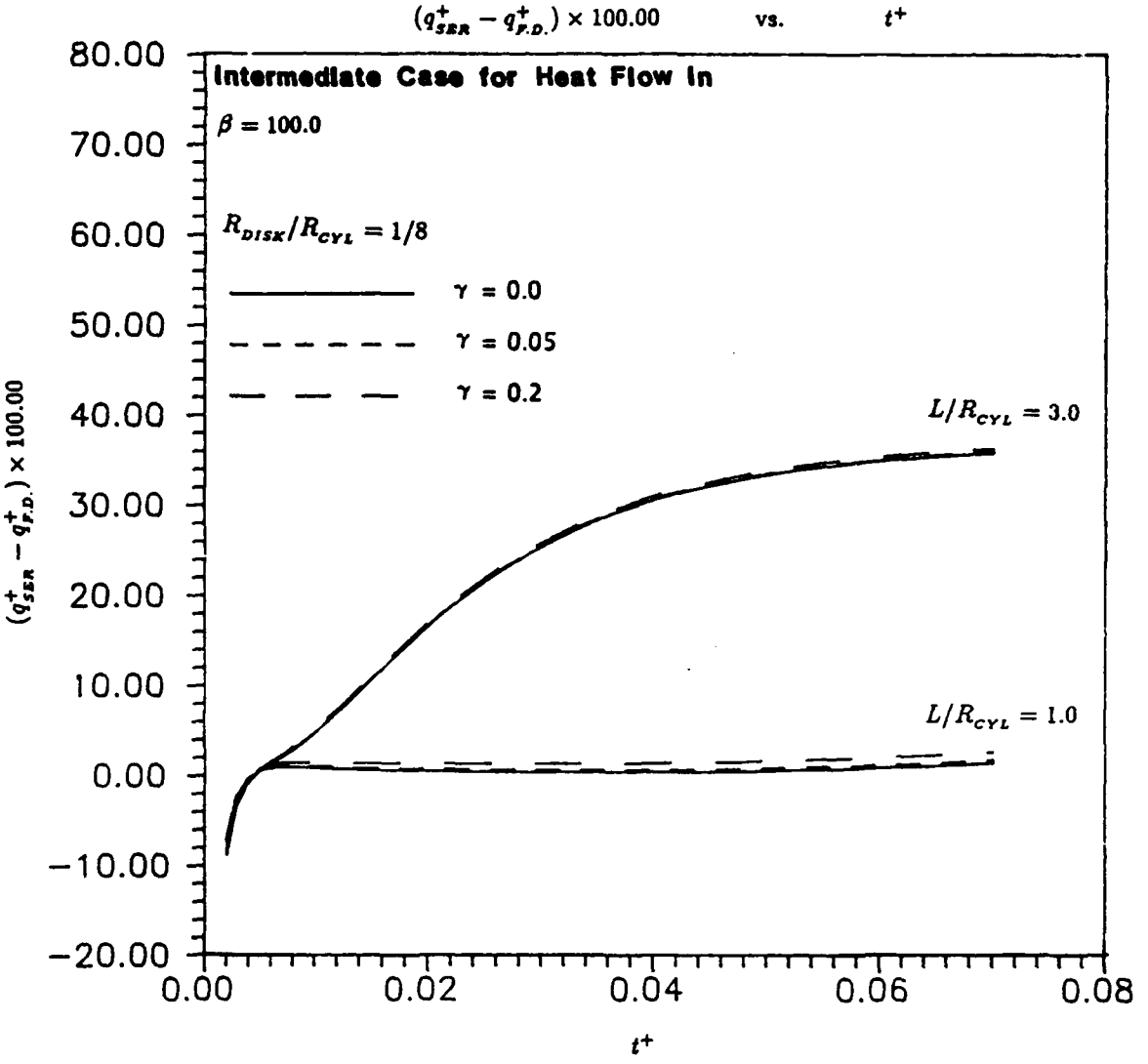

Figure 78. Results for the Intermediate Case for Heat Flux In Across the Outer-Radial Boundary with Heat Generation and Preheating Using $\beta = 100.0$

Appendix D. *Example Programs*

D.1 The Finite-Difference Model for the Single-Material Problem with Fully-Insulated, Outer-Radial Boundary Condition

```
      PROGRAM  GAGE2M
C  ************************************************
C  *  2LT JOSEPH A. BONAFEDE,  GA-88M              *
C  *  FALL 1987                                    *
C  *                                               *
C  *  ADVISOR:  DR. JAMES E. HITCHCOCK             *
C  ************************************************
C
C  GLOSSARY OF MAIN VARIABLES:
C  THAOLD - ARRAY STORING NON-DIMENSIONAL TEMPERATURE VALUES FOR
C           ALL GRID POINTS.  USE THAOLD TO STORE INITIAL VALUES
C           AND TO STORE VALUES DURING PREVIOS TIME STEP.
C           USED INTERNALLY
C  THANEW - ARRAY TO STORE NEW NON-DIMENSIONAL TEMPERATURE VALUES
C           CALCULATED DURING A NEW TIME STEP.
C           USED INTERNALLY
C  IMAX - DETERMINES NUMBER OF NODES IN THE RADIAL DIRECTION.  NUMBER
C         OF NODES IN THE RADIAL DIRECTION EQUALS (IMAX + 1).
C         INPUT PARAMETER
C  KMAX - DETERMINES THE NUMBER OF NODES IN THE Z DIRECTION (FRONT TO
C         BACK OF GAGE).  NUMBER OF NODES IN THE Z DIRECTION EQUALS
C         (KMAX + 1).
C         INPUT PARAMETER
C  IGEN - ARRAY WHICH STORES INFORMATION ABOUT TOP SURFACE NODES.
C         STORES VALUE OF 1.0 FOR A NODE IF THE NODE IS IN THE HEAT
C         GENERATING REGION AND A VALUE OF 0.0 FOR A NODE IF IT IS NOT.
C         USED INTERNALLY
C  IGENMX - LARGEST RADIAL NODE INCLUDED IN THE HEAT GENERATING REGION.
C           INPUT PARAMETER
C  DELT - TIME STEP (NON-DIMENSIONAL TIME).
C         INPUT PARAMETER
C  MAXT - MAXIMUM NUMBER OF TIME STEPS ALLOWED.
C         INPUT PARAMETER
C  TDIST - TIME STEP AT WHICH TO CHANGE TO THE EXTERNAL DISTURBANCE
C          PROBLEM (AS LONG AS TDIST .LE. MAXT).
C          INPUT PARAMETER
C  TIME1 - TIME STEP AT WHICH TO CHANGE TO THE EXTERNAL DISTURBANCE
C          PROBLEM IN THE PROGRAM.
```

```
C           TIME1=0 => EXTERNAL DISTURBANCE PROBLEM ALWAYS
C           2<=TIME1<=MAXT => SWITCH FROM NON-DISTURBANCE PROBLEM
C                             TO DISTURBANCE PROBLEM AT N=TIME1
C           TIME1=MAXT+1 => NON-DISTURBANCE PROBLEM ALWAYS
C         USED INTERNALLY
C  COUNT - NUMBER OF TIME STEPS INTO THE DISTURBANCE PROBLEM (I.E.
C         THE NUMBER OF TIME STEPS ALREADY RUN FOR THE DISTURBANCE
C         PROBLEM).
C         USED INTERNALLY
C  MAXTHA - LARGEST ABSOLUTE VALUE FOR NEW NON-DIMENSIONAL TEMPERATURE
C          IN THE TIME STEP (I.E. LARGEST VALUE STORED IT THANEW
C          ARRAY).

C          USED INTERNALLY
C  CHNG - ABSOLUTE CHANGE IN NON-DIMENSIONAL TEMPERATURE AT EACH
C        NODE DURING THE LAST TIME STEP.
C        USED INTERNALLY
C  VISCHNG - CHANGE IN NON-DIMENSIONAL TEMPERATURE AT EACH NODE DURING
C           THE LAST TIME STEP AS A FRACTION OF THE LARGEST VALUE FOR
C           NON-DIMENSIONAL TEMPERATURE IN THAT TIME STEP (I.E.
C           VISCHNG = CHNG/MAXTHA ).
C           USED INTERNALLY
C  MAXCH - MAXIMUM VALUE FOR VISCHNG DURING THE TIME STEP (AS LONG AS
C         THE VALUE FOR MAXTHA FOR THE TIME STEP IS NOT NEAR ZERO.  IF
C         THE VALUE FOR MAXTHA IS NEAR ZERO, USE ABSOLUTE CHANGE RATHER
C         THAN VISUAL CHANGE AS THE COVERGENCE CRITERIA.)
C         USED INTERNALLY
C  TOL - VALUE TO USE IN DETERMINING CONVERGENCE (STEADY STATE PROBLEMS
C       ONLY).  IF RATE OF VISUAL CHANGE IS LESS THAN TOL, THEN ASSUME
C       THAT THE PROGRAM HAS CONVERGED SUFFICIENTLY.
C       (I.E. MAXCH/DELT < TOL  => CONVERGENCE BECAUSE RATE OF CHANGE
C                                  IS SUFFICIENTLY SMALL              )
C       INPUT PARAMETER
C  LRRAT - THE GEOMETRY RATIO (LENGTH OF GAGE)/(RADIUS OF GAGE).
C         INPUT PARAMETER
C  GBIOT - THE TOP SURFACE BIOT NUMBER BEFORE THE DISTURBANCE.
C         INPUT PARAMETER
C  GBIOTB - THE BOTTOM SURFACE BIOT NUMBER BEFORE THE DISTRUBANCE.
C          INPUT PARAMETER
C  DBIOT - THE TOP SURFACE BIOT NUMBER AFTER THE DISTRUBANCE.
C         INPUT PARAMETER
C  DBIOTB - THE BOTTOM SURFACE BIOT NUMBER AFTER THE DISTURBANCE.
C          INPUT PARAMETER
C  BIOT - TOP SURFACE BIOT NUMBER AT THE PARTICULAR TIME STEP.
C        USED INTERNALLY
```

```
C  BIOTB - BOTTOM SURFACE BIOT NUMBER AT THE PARTICULAR TIME STEP.
C         USED INTERNALLY
C  GENRAT - THE "GENERATION RATIO" (QGEN/DBIOT)/(TFFINAL - TINIT).
C          INPUT PARAMETER
C  BFRAT - THE RATIO (TFBACK - TINIT)/(TFFRONT - TINIT) WHERE TFBACK
C         AND TFFRONT ARE THE FLUID TEMPERATURES DURING THE
C         DISTURBANCE PROBLEM.
C         INPUT PARAMETER
C  DGBIRAT - THE RATIO (DBIOT)/(GBIOT).
C           USED INTERNALLY
C  DELR - SPACIAL STEP IN THE NON-DIMENSIONAL RADIAL DIRECTION.
C        USED INTERNALLY
C  DELZ - SPACIAL STEP IN THE NON-DIMENSIONAL Z DIRECTION.
C        USED INTERNALLY
C  I - INDEX VARIABLE FOR NON-DIMENSIONAL RADIAL DIRECTION.
C     USED INTERNALLY
C  K - INDEX VARIABLE FOR NON-DIMENSIONAL Z DIRECTION.
C     USED INTERNALLY

C  N - INDEX VARIABLE FOR TIME STEPS.
C     USED INTERNALLY
C  RUNNUM - THE RUN NUMBER (USED FOR BOOK KEEPING PURPOSES).
C          INPUT VARIABLE
C  LAMR1,LAMZ1,LAMZ2,P1 - COMMON PRODUCT TERMS IN THE FINITE
C                              ELEMENT EQUATIONS.
C                              USED INTERNALLY

   DECLARE VARIABLES:
      IMPLICIT CHARACTER(A-Z)
      REAL  THAOLD(0:20,0:20),THANEW(0:20,0:20)
      REAL  IGEN(0:20)
      REAL  DELT
      INTEGER  MAXT,TDIST,TIME1,COUNT
      REAL  MAXTHA,CHNG,VISCHNG,MAXCH,TOL
      INTEGER  IMAX,KMAX,IGENMX
      REAL  LRRAT
      REAL  BIOT,BIOTB,GBIOT,GBIOTB,DBIOT,DBIOTB
      REAL  DGBIRAT,GENRAT,BFRAT
      REAL  DELR,DELZ,LAMR1,LAMZ1,LAMZ2,P1
      REAL  A1,A2,A3,A,B,C1,C,D
      INTEGER  RUNNUM
      INTEGER  I,K,N
      INTEGER  X,Y
C
C ---------------------------------------------------------------
```

```
C OPEN INPUT/OUTPUT FILES.
C
      OPEN(UNIT=1,FILE='G2INP',STATUS='OLD')
      OPEN(UNIT=2,FILE='G2OUT',STATUS='NEW')
      OPEN(UNIT=3,FILE='INIT',STATUS='OLD')
      OPEN(UNIT=10,FILE='DISKT',STATUS='NEW')
      REWIND(UNIT=1)
      REWIND(UNIT=3)
C
C -----------------------------------------------------------------
C  READ INPUT PARAMETERS.
C
      READ(1,*)
      READ(1,*) DELT
      READ(1,*) MAXT
      READ(1,*) TDIST
      READ(1,*) TOL
C
      READ(1,*) IMAX
      READ(1,*) KMAX
      READ(1,*) IGENMX
      READ(1,*) LRRAT


C
      READ(1,*) GBIOT
      READ(1,*) GBIOTB
      READ(1,*) DBIOT
      READ(1,*) DBIOTB
      READ(1,*) GENRAT
      READ(1,*) BFRAT
      READ(1,*) DGBIRAT
      READ(1,*) RUNNUM
C
C -----------------------------------------------------------------
C  INITIALIZE PARAMETER  NEEDED IN PRINTING OUT HEADER ( USING HEADER
C  INSTEAD OF JUST ECHOING THE INPUT ).
C
      IF (TDIST .LE. 1 ) THEN
         TIME1 = 0
      ELSEIF (TDIST .GT. MAXT) THEN
         TIME1 = MAXT + 1
      ELSE
         TIME1 = TDIST
      ENDIF
C
```

```
C ------------------------------------------------------------------
C  PRINT HEADER.
C
      WRITE(2,*)'RUN NUMBER ',RUNNUM
      WRITE(2,*)'INPUT VALUES:'
      WRITE(2,*)
      WRITE(2,*)'** GEOMETRY OF THE GAGE AND FINITE ELEMENT MESH **'
      WRITE(2,*)
      WRITE(2,*)'  GRID POINTS IN R-DIRECTION : 0 - ',IMAX
      WRITE(2,*)'  GRID POINTS IN Z-DIRECTION : 0 - ',KMAX
      IF (IGENMX .LT. 0) THEN
         WRITE(2,*)'  R-DIRECTION GRID POINTS INCLUDED'
         WRITE(2,*)'  IN THE HEAT GENERATING DISK     : NONE'
      ELSEIF (IGENMX .EQ. 0) THEN
         WRITE(2,*)'  R-DIRECTION GRID POINT INCLUDED'
         WRITE(2,*)'  IN THE HEAT GENERATING DISK     : 0'
      ELSE
         WRITE(2,*)'  R-DIRECTION GRID POINTS INCLUDED'
         WRITE(2,*)'  IN THE HEAT GENERATING DISK     : 0 - ',IGENMX
      ENDIF
      WRITE(2,*)
      WRITE(2,*)'  RATIO OF (LENGTH OF GAGE)/(RADIUS OF GAGE) = ',LRRAT
      WRITE(2,*)
      WRITE(2,*)
      WRITE(2,*)'**TIME STEP AND LIMITS INCLUDING EXTERNAL PARAMETERS**'
      WRITE(2,*)


      WRITE(2,*)'  DELTA T = ',DELT
      WRITE(2,*)
      WRITE(2,*)'  MAXIMUM NUMBER OF TIME STEPS = ',MAXT
      WRITE(2,*)'  TOLERANCE FOR CONVERGENCE = ',TOL
      WRITE(2,*)
      IF (TIME1 .EQ. 2) THEN
         WRITE(2,*)'  TIME STEP ASSIGNED TO THE "START UP"'
         WRITE(2,*)'  PROBLEM ( NO EXTERNAL DISTURBANCE )  : 1'
         WRITE(2,*)'       BIOT NUMBER AT THE TOP SURFACE = ',GBIOT
         WRITE(2,*)'       BIOT NUMBER AT THE BOTTOM SURFACE = ',GBIOTB
      ENDIF
      IF (TIME1 .GT. 2) THEN
         WRITE(2,*)'  TIME STEPS ASSIGNED TO THE "START UP"'
         WRITE(2,*)'  PROBLEM ( NO EXTERNAL DISTURBANCE )  : 1 - ',
     &             TIME1-1
         WRITE(2,*)'       BIOT NUMBER AT THE TOP SURFACE = ',GBIOT
         WRITE(2,*)'       BIOT NUMBER AT THE BOTTOM SURFACE = ',GBIOTB
      ENDIF
```

```
      IF ((TIME1 .EQ. 0).AND.(MAXT .GT. 1)) THEN
         WRITE(2,*)
         WRITE(2,*)'  TIME STEPS ASSIGNED TO THE PROBLEM'
         WRITE(2,*)'  WITH AN EXTERNAL DISTURBANCE      : 1 - ', MAXT
         WRITE(2,*)'       BIOT NUMBER AT THE TOP SURFACE = ',DBIOT
         WRITE(2,*)'       BIOT NUMBER AT THE BOTTOM SURFACE = ',DBIOTB
         WRITE(2,*)'       RATIO (QGEN/DBIOT)/(TFFINAL - TI) = ',GENRAT
         WRITE(2,*)'       RATIO (TFBACK - TI)/(TFFRONT - TI) = ',BFRAT
         WRITE(2,*)'       RATIO (DBIOT)/(GBIOT) = ',DGBIRAT
      ENDIF
      IF ((TIME1 .EQ. 0).AND.(MAXT .EQ. 1)) THEN
         WRITE(2,*)
         WRITE(2,*)'  TIME STEP ASSIGNED TO THE PROBLEM'
         WRITE(2,*)'  WITH AN EXTERNAL DISTURBANCE      : 1'
         WRITE(2,*)'       BIOT NUMBER AT THE TOP SURFACE = ',DBIOT
         WRITE(2,*)'       BIOT NUMBER AT THE BOTTOM SURFACE = ',DBIOTB
         WRITE(2,*)'       RATIO (QGEN/DBIOT)/(TFFINAL - TI) = ',GENRAT
         WRITE(2,*)'       RATIO (TFBACK - TI)/(TFFRONT - TI) = ',BFRAT
         WRITE(2,*)'       RATIO (DBIOT)/(GBIOT) = ',DGBIRAT
      ENDIF
      IF ((TIME1 .GT. 0).AND.(TIME1 .EQ. MAXT)) THEN
         WRITE(2,*)
         WRITE(2,*)'  TIME STEP ASSIGNED TO THE PROBLEM'
         WRITE(2,*)'  WITH AN EXTERNAL DISTURBANCE      : ',TIME1
         WRITE(2,*)'       BIOT NUMBER AT THE TOP SURFACE = ',DBIOT
         WRITE(2,*)'       BIOT NUMBER AT THE BOTTOM SURFACE = ',DBIOTB
         WRITE(2,*)'       RATIO (QGEN/DBIOT)/(TFFINAL - TI) = ',GENRAT
         WRITE(2,*)'       RATIO (TFBACK - TI)/(TFFRONT - TI) = ',BFRAT
         WRITE(2,*)'       RATIO (DBIOT)/(GBIOT) = ',DGBIRAT
      ENDIF
      IF ((TIME1 .GT. 0).AND.(TIME1 .LT. MAXT)) THEN
         WRITE(2,*)


         WRITE(2,*)'  TIME STEPS ASSIGNED TO THE PROBLEM'
         WRITE(2,*)'  WITH AN EXTERNAL DISTURBANCE      : ',
     &             TIME1,' - ',MAXT
         WRITE(2,*)'       BIOT NUMBER AT THE TOP SURFACE = ',DBIOT
         WRITE(2,*)'       BIOT NUMBER AT THE BOTTOM SURFACE = ',DBIOTB
         WRITE(2,*)'       RATIO (QGEN/DBIOT)/(TFFINAL - TI) = ',GENRAT
         WRITE(2,*)'       RATIO (TFBACK - TI)/(TFFRONT - TI) = ',BFRAT
         WRITE(2,*)'       RATIO (DBIOT)/(GBIOT) = ',DGBIRAT
      ENDIF
      WRITE(2,*)
      WRITE(2,*)
      WRITE(2,*)'RESULTS:'
```

```
      WRITE(2,*)
C
C -----------------------------------------------------------------
C  INITIALIZE ARRAYS AND OTHER PARAMETERS.
C
      READ(3,*)
      DO 100  K = 0,KMAX
         DO 110  I = 0,IMAX
            THANEW(I,K) = 0.
            READ(3,5) THAOLD(I,K)
            IF (TIME1 .EQ. 0) THAOLD(I,K) = THAOLD(I,K)*GENRAT*DGBIRAT
110      CONTINUE
100   CONTINUE
C
      DO 120  I = 0,IMAX
         IF (I .LE. IGENMX) THEN
            IGEN(I) = 1.
         ELSE
            IGEN(I) = 0.
         ENDIF
120   CONTINUE
C
      DELR = 1./FLOAT(IMAX)
      DELZ = 1./FLOAT(KMAX)
C
      LAMR1 = DELT/DELR**2
      LAMZ1 = DELT/DELZ**2
      LAMZ2 = DELT/DELZ
C
      P1 = (FLOAT(IMAX) - .5)/(FLOAT(IMAX) - .25)
C
C -----------------------------------------------------------------
C *****************************************************************
C -----------------------------------------------------------------
C  MAIN LOOP.
C


      IF (TIME1 .EQ. 0) THEN
         BIOT = DBIOT
         BIOTB = DBIOTB
      ELSE
         BIOT = GBIOT
         BIOTB = GBIOTB
      ENDIF
      COUNT = 0
```

```
      MAXCH = 99.99
C
C -------------------------------------------------------------
      DO 500  N = 1,MAXT
      IF ((MAXCH/DELT) .GT. TOL) THEN
C -------------------------------------------------------------
C
C
C        ------------------------------------------------
C        REDEFINE BIOT NUMBERS AND UPDATE THAOLD WHEN STARTING
C        THE DISTURBANCE PROBLEM.
C
         IF (N .EQ. TIME1) THEN
            BIOT = DBIOT
            BIOTB = DBIOTB
            DO 1000  I = 0,IMAX
                DO 1010  K = 0,KMAX
                  THAOLD(I,K) = THAOLD(I,K)*GENRAT*DGBIRAT
1010             CONTINUE
1000        CONTINUE
         ENDIF
C
C        ------------------------------------------------
C        SOLVE FOR NEXT TIME STEP.
C
C
C        FRONT OF GAGE
C
C
C
C        (A)
C
         A = 4.*(LRRAT**2)*LAMR1* THAOLD(1,0)
         B = 2.*LAMZ1* THAOLD(0,1)
         C1 = 1. - 4.*(LRRAT**2)*LAMR1 - 2.*LAMZ1 - 2.*LAMZ2*BIOT
         C = C1* THAOLD(0,0)
         IF (N .LT. TIME1) THEN
            D = 2.*LAMZ2*BIOT* IGEN(0)
         ELSE
            D = 2.*LAMZ2*BIOT*(1. + IGEN(0)*GENRAT)

         ENDIF
         THANEW(0,0) = A + B + C + D
C
C        (B)
```

```
C
      DO 600  I = 1,IMAX-1
         A1 = 1. - 1./(2.*FLOAT(I))
         A2 = 1. + 1./(2.*FLOAT(I))
         A3 = (LRRAT**2)*LAMR1
         A = A3*( A1* THAOLD(I-1,0) + A2* THAOLD(I+1,0) )
         B = 2.*LAMZ1* THAOLD(I,1)
         C1 = 1. - 2.*(LRRAT**2)*LAMR1 - 2.*LAMZ1 - 2.*LAMZ2*BIOT
         C = C1* THAOLD(I,0)
         IF (N .LT. TIME1) THEN
            D = 2.*LAMZ2*BIOT* IGEN(I)
         ELSE
            D = 2.*LAMZ2*BIOT*(1. + IGEN(I)*GENRAT)
         ENDIF
         THANEW(I,0) = A + B + C + D
600   CONTINUE
C
C     (C)
C
      A = 2.*(LRRAT**2)*LAMR1*P1* THAOLD(IMAX-1,0)
      B = 2.*LAMZ1* THAOLD(IMAX,1)
      C1 = 1. - 2.*(LRRAT**2)*LAMR1*P1 - 2.*LAMZ1 - 2.*LAMZ2*BIOT
      C = C1* THAOLD(IMAX,0)
      IF (N .LT. TIME1) THEN
         D = 2.*LAMZ2*BIOT* IGEN(IMAX)
      ELSE
         D = 2.*LAMZ2*BIOT*(1. + IGEN(IMAX)*GENRAT)
      ENDIF
      THANEW(IMAX,0) = A + B + C + D
C
C
C     INTERIOR OF GAGE
C
C
      DO 700  K = 1,KMAX-1
C
C        (D)
C
         A = 4.*(LRRAT**2)*LAMR1* THAOLD(1,K)
         B = LAMZ1*( THAOLD(0,K-1) + THAOLD(0,K+1) )
         C1 = 1. - 4.*(LRRAT**2)*LAMR1 - 2.*LAMZ1
         C = C1* THAOLD(0,K)
         THANEW(0,K) = A + B + C
C
C        (E)
```

```
C
            DO 750  I = 1,IMAX-1
               A1 = 1. - 1./(2.*FLOAT(I))
               A2 = 1. + 1./(2.*FLOAT(I))
               A3 = (LRRAT**2)*LAMR1
               A = A3*( A1* THAOLD(I-1,K) + A2* THAOLD(I+1,K) )
               B = LAMZ1*( THAOLD(I,K-1) + THAOLD(I,K+1) )
               C1 = 1. - 2.*(LRRAT**2)*LAMR1 - 2.*LAMZ1
               C = C1* THAOLD(I,K)
               THANEW(I,K) = A + B + C
750         CONTINUE
C
C           (F)
C
            A = 2.*(LRRAT**2)*LAMR1*P1* THAOLD(IMAX-1,K)
            B = LAMZ1*( THAOLD(IMAX,K-1) + THAOLD(IMAX,K+1) )
            C1 = 1. - 2.*(LRRAT**2)*LAMR1*P1 - 2.*LAMZ1
            C = C1* THAOLD(IMAX,K)
            THANEW(IMAX,K) = A + B + C
C
700      CONTINUE
C
C
C        BACK OF GAGE
C
C
C
C
C        (G)
C
         A = 4.*(LRRAT**2)*LAMR1* THAOLD(1,KMAX)
         B = 2.*LAMZ1* THAOLD(0,KMAX-1)
         C1 = 1. - 4.*(LRRAT**2)*LAMR1 - 2.*LAMZ1 - 2.*LAMZ2*BIOTB
         C = C1* THAOLD(0,KMAX)
         IF (N .LT. TIME1) THEN
            D = 0.
         ELSE
            D = 2.*LAMZ2*BIOTB* BFRAT
         ENDIF
         THANEW(0,KMAX) = A + B + C + D
C
C        (H)
C
         DO 800  I = 1,IMAX-1
            A1 = 1. - 1./(2.*FLOAT(I))
```

```
            A2 = 1. + 1./(2.*FLOAT(I))
            A3 = (LRRAT**2)*LAMR1
            A = A3*( A1* THAOLD(I-1,KMAX) + A2* THAOLD(I+1,KMAX) )
            B = 2.*LAMZ1* THAOLD(I,KMAX-1)
            C1 = 1. - 2.*(LRRAT**2)*LAMR1 - 2.*LAMZ1 - 2.*LAMZ2*BIOTB
            C = C1* THAOLD(I,KMAX)
            IF (N .LT. TIME1) THEN

               D = 0.
            ELSE
               D = 2.*LAMZ2*BIOTB* BFRAT
            ENDIF
            THANEW(I,KMAX) = A + B + C + D
800      CONTINUE
C
C        (I)
C
         A = 2.*(LRRAT**2)*LAMR1*P1* THAOLD(IMAX-1,KMAX)
         B = 2.*LAMZ1* THAOLD(IMAX,KMAX-1)
         C1 = 1. - 2.*(LRRAT**2)*LAMR1*P1 - 2.*LAMZ1 - 2.*LAMZ2*BIOTB
         C = C1* THAOLD(IMAX,KMAX)
         IF (N .LT. TIME1) THEN
            D = 0.
         ELSE
            D = 2.*LAMZ2*BIOTB* BFRAT
         ENDIF
         THANEW(IMAX,KMAX) = A + B + C + D
C
C        ------------------------------------------------------------
C        WRITE NON-DIMENSIONAL TEMPERATURE VALUES AT THE HEATED DISK
C        TO FILE "DISKT" (DURING DISTURBANCE PROBLEM ONLY).
C        ** MODIFIED TO WRITE TO "DISKT" ONLY AT INITIAL TIME STEP
C           OF DISTURBANCE PROBLEM AND AT TIME STEPS T+ = .001-.070
C           WITH DELT=.001 AFTER THE DISTURBANCE PROBLEM STARTS.
C           BE CAREFUL TO HAVE ENOUGH TIME STEPS TO HAVE ATLEAST
C           .070 IN NON-DIMENSIONAL TIME FOR THE DISTURBANCE (I.E.
C           NEED TO HAVE COUNT ATLEAST EQUAL TO 70 WHEN THE PROGRAM
C           FINISHES).
C
         IF (N .GE. TIME1) THEN
            IF ( (N.EQ.TIME1) .OR. ((TIME1.EQ.0).AND.(N.EQ.1)) ) THEN
               COUNT = 0
               WRITE(10,25) COUNT
               DO 1100  I = 0,IGENMX
                  WRITE(10,30) I,THAOLD(I,0)
```

```
1100          CONTINUE
            ENDIF
C
            X = N - MAX(TIME1,1) + 1
            Y = NINT(.001/DELT)
            IF ( MOD(X,Y) .EQ. 0 ) THEN
               COUNT = COUNT + 1
               WRITE(10,25) COUNT
               DO 1125  I = 0,IGENMX
                  WRITE(10,30) I,THANEW(I,0)
1125           CONTINUE
            ENDIF
          ENDIF


C
C         ------------------------------------------------
C         ROLL DOWN THAOLD(1:20,1:20) AND FIND MAXIMUM VISUAL
C         PERCENT CHANGE.  (BE CAREFUL NOT TO DIVIDE BY ZERO.)
C
          MAXTHA = 0.
          DO 900  I = 0,IMAX
             DO 910  K = 0,KMAX
                IF ( ABS(THANEW(I,K)) .GT. MAXTHA) THEN
                   MAXTHA = ABS(THANEW(I,K))
                ENDIF
910          CONTINUE
900       CONTINUE
C
          MAXCH = 0.
          DO 950  I = 0,IMAX
             DO 960  K = 0,KMAX
                CHNG = ABS( THANEW(I,K) - THAOLD(I,K) )
                IF ( MAXTHA .GT. 1.E-15) THEN
                   VISCHNG = CHNG/MAXTHA
                   IF (VISCHNG .GT. MAXCH) MAXCH = VISCHNG
                ELSE
                   IF (CHNG .GT. MAXCH) MAXCH = CHNG
                ENDIF
                THAOLD(I,K) = THANEW(I,K)
960          CONTINUE
950       CONTINUE
C
C ---------------------------------------------------------------
      ELSE
C ---------------------------------------------------------------
```

```
C
C        CONVERGES.  JUMP OUT OF LOOP.
C
         WRITE(2,*)
         WRITE(2,*)'CONVERGES AFTER ',N-1,' ITERATIONS.'
         WRITE(2,*)'MAXIMUM CHANGE ON THE LAST ITERATION WAS ',MAXCH,'.'
         GOTO 2000
C
C -----------------------------------------------------------------
      ENDIF
500   CONTINUE
C -----------------------------------------------------------------
C
C     IF YOU EXECUTE THESE STATEMENTS, THEN YOU COMPLETED THE
C     MAXIMUM NUMBER OF ITERATIONS FOR THE LOOP WITHOUT CONVERGING.
C     PRINT MESSAGE IF EXPECTING SOME CONVERGENCE (I.E. TOL > 0).
C
      IF (TOL .GT. 0.) THEN
         WRITE(2,*)

         WRITE(2,*)'QUITS WITHOUT CONVERGING AFTER ',N-1,' ITERATIONS.'
         WRITE(2,*)'MAXIMUM CHANGE ON THE LAST ITERATION WAS ',MAXCH,'.'
      ENDIF
C
C -----------------------------------------------------------------
C *****************************************************************
C -----------------------------------------------------------------
2000  CONTINUE
C
C -----------------------------------------------------------------
C  PRINT CHECK ON VALUE OF COUNT.
C
      IF (COUNT .LT. 70) THEN
         WRITE(2,*)
         WRITE(2,*)'WARNING: COUNT LESS THAN 70.  COUNT = ',COUNT
         WRITE(2,*)
      ELSE
         WRITE(2,*)
         WRITE(2,*)'VALUE OF COUNT IS ',COUNT
         WRITE(2,*)
         WRITE(2,*)
      ENDIF
C
C -----------------------------------------------------------------
C  FORMAT STATEMENTS.
```

```
C
5     FORMAT(20X,E17.10)
25    FORMAT(I5)
30    FORMAT(I5,5X,E17.10)
C
      END
```

D.2 The Finite-Difference Model for the Two-Material Problem with Fully-Insulated, Outer-Radial Boundary Condition

```
      PROGRAM  GAGE4M
C  ***************************************************
C  *  2LT JOSEPH A. BONAFEDE,  GA-88M                *
C  *  FALL 1987                                      *
C  *                                                 *
C  *  ADVISOR:  DR. JAMES E. HITCHCOCK               *
C  ***************************************************
C
C  GLOSSARY OF MAIN VARIABLES:
C  THAOLD - ARRAY STORING NON-DIMENSIONAL TEMPERATURE VALUES FOR
C           ALL GRID POINTS.  USE THAOLD TO STORE INITIAL VALUES
C           AND TO STORE VALUES DURING PREVIOUS TIME STEP.
C           USED INTERNALLY
C  THANEW - ARRAY TO STORE NEW NON-DIMENSIONAL TEMPERATURE VALUES
C           CALCULATED DURING A NEW TIME STEP.
C           USED INTERNALLY
C  IMAX - DETERMINES NUMBER OF NODES IN THE RADIAL DIRECTION.  NUMBER
C         OF NODES IN THE RADIAL DIRECTION EQUALS (IMAX + 1).
C         INPUT PARAMETER
C  KMAX - DETERMINES THE NUMBER OF NODES IN THE Z DIRECTION (FRONT TO
C         BACK OF GAGE).  NUMBER OF NODES IN THE Z DIRECTION EQUALS
C         (KMAX + 1).
C         INPUT PARAMETER
C  IGAGE - DETERMINES THE NUMBER OF NODES IN THE RADIAL DIRECTION
C          WHICH ARE INCLUDED IN THE GAGE.  THE RADIAL DIRECTION
C          NODES WHICH MAKE UP THE GAGE ARE NODES WITH I = 0 - IGAGE.
C          ALSO DETERMINES THE NON-DIMENSIONAL STEP SIZE IN THE
C          RADIAL DIRECTION.  THE NON-DIMENSIONAL STEP SIZE IN THE
C          RADIAL DIRECTION EQUALS 1./IGAGE (I.E. DELR = 1./IGAGE).
C          INPUT PARAMETER
C  IGEN - ARRAY WHICH STORES INFORMATION ABOUT TOP SURFACE NODES.
C         STORES VALUE OF 1.0 FOR A NODE IF THE NODE IS IN THE HEAT
C         GENERATING REGION AND A VALUE OF 0.0 FOR A NODE IF IT IS NOT.
C         USED INTERNALLY
C  IGENMX - LARGEST RADIAL NODE INCLUDED IN THE HEAT GENERATING REGION.
C           INPUT PARAMETER
C  DELT - TIME STEP (NON-DIMENSIONAL TIME).
C         INPUT PARAMETER
C  MAXT - MAXIMUM NUMBER OF TIME STEPS ALLOWED.
C         INPUT PARAMETER
C  TDIST - TIME STEP AT WHICH TO CHANGE TO THE EXTERNAL DISTURBANCE
C          PROBLEM (AS LONG AS TDIST .LE. MAXT).
```

```
C          INPUT PARAMETER
C  TIME1 - TIME STEP AT WHICH TO CHANGE TO THE EXTERNAL DISTURBANCE
C          PROBLEM IN THE PROGRAM.
C            TIME1=0 => EXTERNAL DISTURBANCE PROBLEM ALWAYS
C            2<=TIME1<=MAXT => SWITCH FROM NON-DISTURBANCE PROBLEM
C                              TO DISTURBANCE PROBLEM AT N=TIME1
C            TIME1=MAXT+1 => NON-DISTURBANCE PROBLEM ALWAYS
C          USED INTERNALLY

C  COUNT - NUMBER OF TIME STEPS INTO THE DISTURBANCE PROBLEM (I.E.
C          THE NUMBER OF TIME STEPS ALREADY RUN FOR THE DISTURBANCE
C          PROBLEM).
C          USED INTERNALLY
C  MAXTHA - LARGEST ABSOLUTE VALUE FOR NEW NON-DIMENSIONAL TEMPERATURE
C           IN THE TIME STEP (I.E. LARGEST VALUE STORED IN THANEW
C           ARRAY).
C           USED INTERNALLY
C  CHNG - ABSOLUTE CHANGE IN NON-DIMENSIONAL TEMPERATURE AT EACH
C         NODE DURING THE LAST TIME STEP.
C         USED INTERNALLY
C  VISCHNG - CHANGE IN NON-DIMENSIONAL TEMPERATURE AT EACH NODE DURING
C            THE LAST TIME STEP AS A FRACTION OF THE LARGEST VALUE FOR
C            NON-DIMENSIONAL TEMPERATURE IN THAT TIME STEP (I.E.
C            VISCHNG = CHNG/MAXTHA ).
C            USED INTERNALLY
C  MAXCH - MAXIMUM VALUE FOR VISCHNG DURING THE TIME STEP (AS LONG AS
C          THE VALUE FOR MAXTHA FOR THE TIME STEP IS NOT NEAR ZERO.  IF
C          THE VALUE FOR MAXTHA IS NEAR ZERO, USE ABSOLUTE CHANGE RATHER
C          THAN VISUAL CHANGE AS THE CONVERGENCE CRITERIA.)
C          USED INTERNALLY
C  TOL - VALUE TO USE IN DETERMINING CONVERGENCE (STEADY STATE PROBLEMS
C        ONLY).  IF RATE OF VISUAL CHANGE IS LESS THAN TOL, THEN ASSUME
C        THAT THE PROGRAM HAS CONVERGED SUFFICIENTLY.
C        (I.E. MAXCH/DELT < TOL  => CONVERGENCE BECAUSE RATE OF CHANGE
C                                   IS SUFFICIENTLY SMALL              )
C        INPUT PARAMETER
C  LRRAT - THE GEOMETRY RATIO (LENGTH OF GAGE)/(RADIUS OF GAGE).
C          INPUT PARAMETER
C  GBIOT - THE TOP SURFACE BIOT NUMBER BEFORE THE DISTURBANCE.
C          INPUT PARAMETER
C  GBIOTB - THE BOTTOM SURFACE BIOT NUMBER BEFORE THE DISTRUBANCE.
C           INPUT PARAMETER
C  DBIOT - THE TOP SURFACE BIOT NUMBER AFTER THE DISTRUBANCE.
C          INPUT PARAMETER
C  DBIOTB - THE BOTTOM SURFACE BIOT NUMBER AFTER THE DISTURBANCE.
```

```
C           INPUT PARAMETER
C  BIOT - TOP SURFACE BIOT NUMBER AT THE PARTICULAR TIME STEP.
C         USED INTERNALLY
C  BIOTB - BOTTOM SURFACE BIOT NUMBER AT THE PARTICULAR TIME STEP.
C          USED INTERNALLY
C  GENRAT - THE "GENERATION RATIO" (QGEN/DBIOT)/(TFFINAL - TINIT).
C           INPUT PARAMETER
C  BFRAT - THE RATIO (TFBACK - TINIT)/(TFFRONT - TINIT) WHERE TFBACK
C          AND TFFRONT ARE THE FLUID TEMPERATURES DURING THE
C          DISTURBANCE PROBLEM.
C          INPUT PARAMETER
C  DGBIRAT - THE RATIO (DBIOT)/(GBIOT).
C            USED INTERNALLY
C  RCGB - PROPERTY RATIO (RHO*CP)GAGE / (RHO*CP)MATERIAL B.

C          INPUT PARAMETER
C  KBG - PROPERTY RATIO (K)MATERIAL B / (K)GAGE.
C        INPUT PARAMETER
C  RCGGB - PROPERTY RATIO (RHO*CP)GAGE/(RHO*CP)WEIGHTED AVG GAGE AND B.
C          USED INTERNALLY
C  KGBG - PROPERTY RATIO (K)WEIGHTED AVG GAGE AND B / (K)GAGE.
C         USED INTERNALLY
C  DELR - SPACIAL STEP IN THE NON-DIMENSIONAL RADIAL DIRECTION.
C         USED INTERNALLY
C  DELZ - SPACIAL STEP IN THE NON-DIMENSIONAL Z DIRECTION.
C         USED INTERNALLY
C  DER - VALUE OF THE PARTIAL DERIVATIVE IN THE RADIAL DIRECTION
C        OF THE NON-DIMENSIONAL TEMPERATURE VARIABLE AT THE
C        OUTER BOUNDARY OF THE PROBLEM.  USE A ONE-SIDED,
C        BACKWARD FINITE DIFFERENCE.
C        USED INTERNALLY
C  MAXDER - THE LARGEST VALUE FOR DER (IN ABSOLUTE VALUE) DURING
C           THE WHOLE RUN.
C           USED INTERNALLY
C  I - INDEX VARIABLE FOR NON-DIMENSIONAL RADIAL DIRECTION.
C      USED INTERNALLY
C  K - INDEX VARIABLE FOR NON-DIMENSIONAL Z DIRECTION.
C      USED INTERNALLY
C  N - INDEX VARIABLE FOR TIME STEPS.
C      USED INTERNALLY
C  RUNNUM - THE RUN NUMBER (USED FOR BOOK KEEPING PURPOSES).
C           INPUT VARIABLE
C  LAMR1,LAMZ1,LAMZ2,P1,P2,P3 - COMMON PRODUCT TERMS IN THE FINITE
C                               ELEMENT EQUATIONS.
C                               USED INTERNALLY
```

```
C
C  DECLARE VARIABLES:
      IMPLICIT CHARACTER(A-Z)
      REAL  THAOLD(0:40,0:40),THANEW(0:40,0:40)
      REAL  IGEN(0:20)
      REAL  DELT
      INTEGER  MAXT,TDIST,TIME1,COUNT
      REAL  MAXTHA,CHNG,VISCHNG,MAXCH,TOL
      INTEGER  IMAX,KMAX,IGENMX,IGAGE
      REAL  LRRAT
      REAL  BIOT,BIOTB,GBIOT,GBIOTB,DBIOT,DBIOTB
      REAL  DGBIRAT,GENRAT,BFRAT
      REAL  RCGB,KBG,RCGGB,KGBG
      REAL  DELR,DELZ,LAMR1,LAMZ1,LAMZ2,P1,P2,P3
      REAL  DER,MAXDER
      REAL  A1,A2,A3,A,B1,B,C1,C2,C3,C,D
      REAL  NUMER,DENOM
      INTEGER  RUNNUM
      INTEGER  I,K,N
      INTEGER  X,Y


C
C -----------------------------------------------------------------
C OPEN INPUT/OUTPUT FILES.
C
      OPEN(UNIT=1,FILE='G4INP',STATUS='OLD')
      OPEN(UNIT=2,FILE='G4OUT',STATUS='NEW')
      OPEN(UNIT=3,FILE='INIT',STATUS='OLD')
      OPEN(UNIT=10,FILE='DISKT',STATUS='NEW')
      REWIND(UNIT=1)
      REWIND(UNIT=3)
C
C -----------------------------------------------------------------
C  READ INPUT PARAMETERS.
C
      READ(1,*)
      READ(1,*) DELT
      READ(1,*) MAXT
      READ(1,*) TDIST
      READ(1,*) TOL
C
      READ(1,*) IMAX
      READ(1,*) KMAX
      READ(1,*) IGAGE
      READ(1,*) IGENMX
```

```
      READ(1,*) LRRAT
C
      READ(1,*) GBIOT
      READ(1,*) GBIOTB
      READ(1,*) DBIOT
      READ(1,*) DBIOTB
      READ(1,*) GENRAT
      READ(1,*) BFRAT
      READ(1,*) DGBIRAT
C
      READ(1,*) RCGB
      READ(1,*) KBG
C
      READ(1,*) RUNNUM
C
C ---------------------------------------------------------------------
C  INITIALIZE PARAMETER  NEEDED IN PRINTING OUT HEADER ( USING HEADER
C  INSTEAD OF JUST ECHOING THE INPUT ).
C
      IF (TDIST .LE. 1 ) THEN
         TIME1 = 0
      ELSEIF (TDIST .GT. MAXT) THEN
         TIME1 = MAXT + 1
      ELSE
         TIME1 = TDIST
      ENDIF


C
C ---------------------------------------------------------------------
C  PRINT HEADER.
C
      WRITE(2,*)'RUN NUMBER = ',RUNNUM
      WRITE(2,*)'INPUT VALUES:'
      WRITE(2,*)
      WRITE(2,*)'** GEOMETRY OF THE GAGE AND FINITE ELEMENT MESH **'
      WRITE(2,*)
      WRITE(2,*)'  GRID POINTS IN R-DIRECTION : 0 - ',IMAX
      WRITE(2,*)'  GRID POINTS IN Z-DIRECTION : 0 - ',KMAX
      WRITE(2,*)'  R-DIRECTION GRID POINTS INCLUDED'
      WRITE(2,*)'  IN THE GAGE                    : 0 - ',IGAGE
      IF (IGENMX .LT. 0) THEN
         WRITE(2,*)'  R-DIRECTION GRID POINTS INCLUDED'
         WRITE(2,*)'  IN THE HEAT GENERATING DISK     : NONE'
      ELSEIF (IGENMX .EQ. 0) THEN
         WRITE(2,*)'  R-DIRECTION GRID POINT INCLUDED'
```

```
      WRITE(2,*)'  IN THE HEAT GENERATING DISK    : 0'
   ELSE
      WRITE(2,*)'  R-DIRECTION GRID POINTS INCLUDED'
      WRITE(2,*)'  IN THE HEAT GENERATING DISK     : 0 - ',IGENMX
   ENDIF
   WRITE(2,*)
   WRITE(2,*)'  RATIO OF (LENGTH OF GAGE)/(RADIUS OF GAGE) = ',LRRAT
   WRITE(2,*)
   WRITE(2,*)
   WRITE(2,*)'**TIME STEP AND LIMITS INCLUDING EXTERNAL PARAMETERS**'
   WRITE(2,*)
   WRITE(2,*)'  DELTA T = ',DELT
   WRITE(2,*)
   WRITE(2,*)'  MAXIMUM NUMBER OF TIME STEPS = ',MAXT
   WRITE(2,*)'  TOLERANCE FOR CONVERGENCE = ',TOL
   WRITE(2,*)
   IF (TIME1 .EQ. 2) THEN
      WRITE(2,*)'  TIME STEP ASSIGNED TO THE "START UP"'
      WRITE(2,*)'  PROBLEM ( NO EXTERNAL DISTURBANCE )  : 1'
      WRITE(2,*)'       BIOT NUMBER AT THE TOP SURFACE = ',GBIOT
      WRITE(2,*)'       BIOT NUMBER AT THE BOTTOM SURFACE = ',GBIOTB
      WRITE(2,*)
      WRITE(2,*)'       RATIO (RHO*CP)GAGE / (RHO*CP)MAT.B = ',RCGB
      WRITE(2,*)'       RATIO (K)MAT.B / (K)GAGE = ',KBG
   ENDIF
   IF (TIME1 .GT. 2) THEN
      WRITE(2,*)'  TIME STEPS ASSIGNED TO THE "START UP"'
      WRITE(2,*)'  PROBLEM ( NO EXTERNAL DISTURBANCE )  : 1 - ',
  &            TIME1-1
      WRITE(2,*)'       BIOT NUMBER AT THE TOP SURFACE = ',GBIOT
      WRITE(2,*)'       BIOT NUMBER AT THE BOTTOM SURFACE = ',GBIOTB
      WRITE(2,*)


      WRITE(2,*)'       RATIO (RHO*CP)GAGE / (RHO*CP)MAT.B = ',RCGB
      WRITE(2,*)'       RATIO (K)MAT.B / (K)GAGE = ',KBG
   ENDIF
   IF ((TIME1 .EQ. 0).AND.(MAXT .GT. 1)) THEN
      WRITE(2,*)
      WRITE(2,*)'  TIME STEPS ASSIGNED TO THE PROBLEM'
      WRITE(2,*)'  WITH AN EXTERNAL DISTURBANCE      : 1 - ', MAXT
      WRITE(2,*)'       BIOT NUMBER AT THE TOP SURFACE = ',DBIOT
      WRITE(2,*)'       BIOT NUMBER AT THE BOTTOM SURFACE = ',DBIOTB
      WRITE(2,*)'       RATIO (QGEN/DBIOT)/(TFFINAL - TI) = ',GENRAT
      WRITE(2,*)'       RATIO (TFBACK - TI)/(TFFRONT - TI) = ',BFRAT
      WRITE(2,*)'       RATIO (DBIOT)/(GBIOT) = ',DGBIRAT
```

```
      WRITE(2,*)
      WRITE(2,*)'       RATIO (RHO*CP)GAGE / (RHO*CP)MAT.B = ',RCGB
      WRITE(2,*)'       RATIO (K)MAT.B / (K)GAGE = ',KBG
   ENDIF
   IF ((TIME1 .EQ. 0).AND.(MAXT .EQ. 1)) THEN
      WRITE(2,*)
      WRITE(2,*)'  TIME STEP ASSIGNED TO THE PROBLEM'
      WRITE(2,*)'  WITH AN EXTERNAL DISTURBANCE      : 1'
      WRITE(2,*)'       BIOT NUMBER AT THE TOP SURFACE = ',DBIOT
      WRITE(2,*)'       BIOT NUMBER AT THE BOTTOM SURFACE = ',DBIOTB
      WRITE(2,*)'       RATIO (QGEN/DBIOT)/(TFFINAL - TI) = ',GENRAT
      WRITE(2,*)'       RATIO (TFBACK - TI)/(TFFRONT - TI) = ',BFRAT
      WRITE(2,*)'       RATIO (DBIOT)/(GBIOT) = ',DGBIRAT
      WRITE(2,*)
      WRITE(2,*)'       RATIO (RHO*CP)GAGE / (RHO*CP)MAT.B = ',RCGB
      WRITE(2,*)'       RATIO (K)MAT.B / (K)GAGE = ',KBG
   ENDIF
   IF ((TIME1 .GT. 0).AND.(TIME1 .EQ. MAXT)) THEN
      WRITE(2,*)
      WRITE(2,*)'  TIME STEP ASSIGNED TO THE PROBLEM'
      WRITE(2,*)'  WITH AN EXTERNAL DISTURBANCE      : ',TIME1
      WRITE(2,*)'       BIOT NUMBER AT THE TOP SURFACE = ',DBIOT
      WRITE(2,*)'       BIOT NUMBER AT THE BOTTOM SURFACE = ',DBIOTB
      WRITE(2,*)'       RATIO (QGEN/DBIOT)/(TFFINAL - TI) = ',GENRAT
      WRITE(2,*)'       RATIO (TFBACK - TI)/(TFFRONT - TI) = ',BFRAT
      WRITE(2,*)'       RATIO (DBIOT)/(GBIOT) = ',DGBIRAT
      WRITE(2,*)
      WRITE(2,*)'       RATIO (RHO*CP)GAGE / (RHO*CP)MAT.B = ',RCGB
      WRITE(2,*)'       RATIO (K)MAT.B / (K)GAGE = ',KBG
   ENDIF
   IF ((TIME1 .GT. 0).AND.(TIME1 .LT. MAXT)) THEN
      WRITE(2,*)
      WRITE(2,*)'  TIME STEPS ASSIGNED TO THE PROBLEM'
      WRITE(2,*)'  WITH AN EXTERNAL DISTURBANCE      : ',
     &            TIME1,' - ',MAXT
      WRITE(2,*)'       BIOT NUMBER AT THE TOP SURFACE = ',DBIOT
      WRITE(2,*)'       BIOT NUMBER AT THE BOTTOM SURFACE = ',DBIOTB
      WRITE(2,*)'       RATIO (QGEN/DBIOT)/(TFFINAL - TI) = ',GENRAT

      WRITE(2,*)'       RATIO (TFBACK - TI)/(TFFRONT - TI) = ',BFRAT
      WRITE(2,*)'       RATIO (DBIOT)/(GBIOT) = ',DGBIRAT
      WRITE(2,*)
      WRITE(2,*)'       RATIO (RHO*CP)GAGE / (RHO*CP)MAT.B = ',RCGB
      WRITE(2,*)'       RATIO (K)MAT.B / (K)GAGE = ',KBG
   ENDIF
```

```
      WRITE(2,*)
      WRITE(2,*)
      WRITE(2,*)'RESULTS:'
      WRITE(2,*)
C
C -----------------------------------------------------------------
C  INITIALIZE ARRAYS AND OTHER PARAMETERS.
C
      READ(3,*)
      DO 100  K = 0,KMAX
         DO 110  I = 0,IMAX
            THANEW(I,K) = 0.
            READ(3,5) THAOLD(I,K)
            IF (TIME1 .EQ. 0) THAOLD(I,K) = THAOLD(I,K)*GENRAT*DGBIRAT
110      CONTINUE
100   CONTINUE
C
      DO 120  I = 0,IGAGE
         IF (I .LE. IGENMX) THEN
            IGEN(I) = 1.
         ELSE
            IGEN(I) = 0.
         ENDIF
120   CONTINUE
C
      DELR = 1./FLOAT(IGAGE)
      DELZ = 1./FLOAT(KMAX)
C
      LAMR1 = DELT/DELR**2
      LAMZ1 = DELT/DELZ**2
      LAMZ2 = DELT/DELZ
C
      NUMER = 2.*RCGB*FLOAT(IGAGE)
      DENOM = RCGB*(FLOAT(IGAGE) - .25) + (FLOAT(IGAGE) + .25)
      RCGGB = NUMER/DENOM
C
      NUMER = (FLOAT(IGAGE) - .25) + KBG*(FLOAT(IGAGE) + .25)
      DENOM = 2.*FLOAT(IGAGE)
      KGBG = NUMER/DENOM
C
      P1 = (FLOAT(IMAX) - .5)/(FLOAT(IMAX) - .25)
      P2 = 1. - 1./(2.*FLOAT(IGAGE))
      P3 = 1. + 1./(2.*FLOAT(IGAGE))
C
C -----------------------------------------------------------
```

```
C ***************************************************************
C ---------------------------------------------------------------
C  MAIN LOOP.
C
      IF (TIME1 .EQ. 0) THEN
         BIOT = DBIOT
         BIOTB = DBIOTB
      ELSE
         BIOT = GBIOT
         BIOTB = GBIOTB
      ENDIF
      COUNT = 0
      MAXCH = 99.99
      MAXDER = 0.
C
C ---------------------------------------------------------------
      DO 500  N = 1,MAXT
      IF ((MAXCH/DELT) .GT. TOL) THEN
C ---------------------------------------------------------------
C
C
C        ------------------------------------------------------
C        REDEFINE BIOT NUMBERS AND UPDATE THAOLD WHEN STARTING
C        THE DISTURBANCE PROBLEM.
C
         IF (N .EQ. TIME1) THEN
            BIOT = DBIOT
            BIOTB = DBIOTB
            DO 1000  I = 0,IMAX
                DO 1010  K = 0,KMAX
                  THAOLD(I,K) = THAOLD(I,K)*GENRAT*DGBIRAT
1010            CONTINUE
1000        CONTINUE
         ENDIF
C
C        ------------------------------------------------
C        SOLVE FOR NEXT TIME STEP.
C
C
C        FRONT OF GAGE
C
C
C
C        (A)
C
```

```
      A = 4.*(LRRAT**2)*LAMR1* THAOLD(1,0)
      B = 2.*LAMZ1* THAOLD(0,1)
      C1 = 1. - 4.*(LRRAT**2)*LAMR1 - 2.*LAMZ1 - 2.*LAMZ2*BIOT
      C = C1* THAOLD(0,0)

      IF (N .LT. TIME1) THEN
         D = 2.*LAMZ2*BIOT* IGEN(0)
      ELSE
         D = 2.*LAMZ2*BIOT*(1. + IGEN(0)*GENRAT)
      ENDIF
      THANEW(0,0) = A + B + C + D
C
C     (B)
C
      DO 640  I = 1,IGAGE-1
         A1 = 1. - 1./(2.*FLOAT(I))
         A2 = 1. + 1./(2.*FLOAT(I))
         A3 = (LRRAT**2)*LAMR1
         A = A3*( A1* THAOLD(I-1,0) + A2* THAOLD(I+1,0) )
         B = 2.*LAMZ1* THAOLD(I,1)
         C1 = 1. - 2.*(LRRAT**2)*LAMR1 - 2.*LAMZ1 - 2.*LAMZ2*BIOT
         C = C1* THAOLD(I,0)
         IF (N .LT. TIME1) THEN
            D = 2.*LAMZ2*BIOT* IGEN(I)
         ELSE
            D = 2.*LAMZ2*BIOT*(1. + IGEN(I)*GENRAT)
         ENDIF
         THANEW(I,0) = A + B + C + D
640   CONTINUE
C
C     (C)
C
      A1 = RCGGB*(LRRAT**2)*LAMR1
      A = A1*( P2* THAOLD(IGAGE-1,0) + P3*KBG* THAOLD(IGAGE+1,0) )
      B = 2.*RCGGB*KGBG*LAMZ1* THAOLD(IGAGE,1)
      C1 = - RCGGB*(LRRAT**2)*P2*LAMR1
      C2 = - RCGGB*KBG*(LRRAT**2)*P3*LAMR1
      C3 = - 2.*RCGGB*KGBG*LAMZ1 - 2.*RCGGB*BIOT*LAMZ2
      C = (1. + C1 + C2 + C3)* THAOLD(IGAGE,0)
      IF (N .LT. TIME1) THEN
         D = 2.*RCGGB*BIOT*LAMZ2* IGEN(IGAGE)
      ELSE
         D = 2.*RCGGB*BIOT*LAMZ2*(1. + IGEN(IGAGE)*GENRAT)
      ENDIF
      THANEW(IGAGE,0) = A + B + C + D
```

```
C
C        (D)
C
         DO 660  I = IGAGE+1,IMAX-1
            A1 = 1. - 1./(2.*FLOAT(I))
            A2 = 1. + 1./(2.*FLOAT(I))
            A3 = RCGB*KBG*(LRRAT**2)*LAMR1
            A = A3*( A1* THAOLD(I-1,0) + A2* THAOLD(I+1,0) )
            B = 2.*RCGB*KBG*LAMZ1* THAOLD(I,1)
            C1 = - 2.*RCGB*KBG*(LRRAT**2)*LAMR1

            C2 = - 2.*RCGB*KBG*LAMZ1
            C3 = - 2.*RCGB*BIOT*LAMZ2
            C = (1. + C1 + C2 + C3)* THAOLD(I,0)
            IF (N .LT. TIME1) THEN
               D = 0.
            ELSE
               D = 2.*RCGB*BIOT*LAMZ2
            ENDIF
            THANEW(I,0) = A + B + C + D
660      CONTINUE
C
C        (E)
C
         A = 2.*RCGB*KBG*(LRRAT**2)*P1*LAMR1* THAOLD(IMAX-1,0)
         B = 2.*RCGB*KBG*LAMZ1* THAOLD(IMAX,1)
         C1 = - 2.*RCGB*KBG*(LRRAT**2)*P1*LAMR1
         C2 = - 2.*RCGB*KBG*LAMZ1
         C3 = - 2.*RCGB*BIOT*LAMZ2
         C = (1. + C1 + C2 + C3)* THAOLD(IMAX,0)
         IF (N .LT. TIME1) THEN
            D = 0.
         ELSE
            D = 2.*RCGB*BIOT*LAMZ2
         ENDIF
         THANEW(IMAX,0) = A + B + C + D
C
C
C        INTERIOR OF GAGE
C
C
         DO 700  K = 1,KMAX-1
C
C           (F)
C
```

```
            A = 4.*(LRRAT**2)*LAMR1* THAOLD(1,K)
            B = LAMZ1*( THAOLD(0,K-1) + THAOLD(0,K+1) )
            C1 = 1. - 4.*(LRRAT**2)*LAMR1 - 2.*LAMZ1
            C = C1* THAOLD(0,K)
            THANEW(0,K) = A + B + C
C
C           (G)
C
            DO 740  I = 1,IGAGE-1
               A1 = 1. - 1./(2.*FLOAT(I))
               A2 = 1. + 1./(2.*FLOAT(I))
               A3 = (LRRAT**2)*LAMR1
               A = A3*( A1* THAOLD(I-1,K) + A2* THAOLD(I+1,K) )
               B = LAMZ1*( THAOLD(I,K-1) + THAOLD(I,K+1) )
               C1 = 1. - 2.*(LRRAT**2)*LAMR1 - 2.*LAMZ1
               C = C1* THAOLD(I,K)

               THANEW(I,K) = A + B + C
740         CONTINUE
C
C           (H)
C
            A1 = RCGGB*(LRRAT**2)*LAMR1
            A = A1*( P2* THAOLD(IGAGE-1,K) + P3*KBG* THAOLD(IGAGE+1,K) )
            B1 = RCGGB*KGBG*LAMZ1
            B = B1*( THAOLD(IGAGE,K-1) + THAOLD(IGAGE,K+1) )
            C1 = - RCGGB*(LRRAT**2)*P2*LAMR1
            C2 = - RCGGB*KBG*(LRRAT**2)*P3*LAMR1
            C3 = - 2.*RCGGB*KGBG*LAMZ1
            C = (1. + C1 + C2 + C3)* THAOLD(IGAGE,K)
            THANEW(IGAGE,K) = A + B + C
C
C           (I)
C
            DO 760  I = IGAGE+1,IMAX-1
               A1 = 1. - 1./(2.*FLOAT(I))
               A2 = 1. + 1./(2.*FLOAT(I))
               A3 = RCGB*KBG*(LRRAT**2)*LAMR1
               A = A3*( A1* THAOLD(I-1,K) + A2* THAOLD(I+1,K) )
               B1 = RCGB*KBG*LAMZ1
               B = B1*( THAOLD(I,K-1) + THAOLD(I,K+1) )
               C1 = - 2.*RCGB*KBG*(LRRAT**2)*LAMR1
               C2 = - 2.*RCGB*KBG*LAMZ1
               C = (1. + C1 + C2)* THAOLD(I,K)
               THANEW(I,K) = A + B + C
```

```
760         CONTINUE
C
C           (J)
C
            A = 2.*RCGB*KBG*(LRRAT**2)*P1*LAMR1* THAOLD(IMAX-1,K)
            B1 = RCGB*KBG*LAMZ1
            B = B1*( THAOLD(IMAX,K-1) + THAOLD(IMAX,K+1) )
            C1 = - 2.*RCGB*KBG*(LRRAT**2)*P1*LAMR1
            C2 = - 2.*RCGB*KBG*LAMZ1
            C = (1. + C1 + C2)* THAOLD(IMAX,K)
            THANEW(IMAX,K) = A + B + C
C
700       CONTINUE
C
C
C         BACK OF GAGE
C
C
C
C         (K)
C
          A = 4.*(LRRAT**2)*LAMR1* THAOLD(1,KMAX)

          B = 2.*LAMZ1* THAOLD(0,KMAX-1)
          C1 = 1. - 4.*(LRRAT**2)*LAMR1 - 2.*LAMZ1 - 2.*LAMZ2*BIOTB
          C = C1* THAOLD(0,KMAX)
          IF (N .LT. TIME1) THEN
             D = 0.
          ELSE
             D = 2.*LAMZ2*BIOTB* BFRAT
          ENDIF
          THANEW(0,KMAX) = A + B + C + D
C
C         (L)
C
          DO 840  I = 1,IGAGE-1
             A1 = 1. - 1./(2.*FLOAT(I))
             A2 = 1. + 1./(2.*FLOAT(I))
             A3 = (LRRAT**2)*LAMR1
             A = A3*( A1* THAOLD(I-1,KMAX) + A2* THAOLD(I+1,KMAX) )
             B = 2.*LAMZ1* THAOLD(I,KMAX-1)
             C1 = 1. - 2.*(LRRAT**2)*LAMR1 - 2.*LAMZ1 - 2.*LAMZ2*BIOTB
             C = C1* THAOLD(I,KMAX)
             IF (N .LT. TIME1) THEN
                D = 0.
```

```
            ELSE
               D = 2.*LAMZ2*BIOTB* BFRAT
            ENDIF
            THANEW(I,KMAX) = A + B + C + D
840      CONTINUE
C
C        (M)
C
         A1 = RCGGB*(LRRAT**2)*P2*LAMR1
         A2 = RCGGB*KBG*(LRRAT**2)*P3*LAMR1
         A = A1* THAOLD(IGAGE-1,KMAX) + A2* THAOLD(IGAGE+1,KMAX)
         B = 2.*RCGGB*KGBG*LAMZ1* THAOLD(IGAGE,KMAX-1)
         C1 = - RCGGB*(LRRAT**2)*P2*LAMR1
         C2 = - RCGGB*KBG*(LRRAT**2)*P3*LAMR1
         C3 = - 2.*RCGGB*KGBG*LAMZ1 - 2.*RCGGB*BIOTB*LAMZ2
         C = (1. + C1 + C2 + C3)* THAOLD(IGAGE,KMAX)
         IF (N .LT. TIME1) THEN
            D = 0.
         ELSE
            D = 2.*RCGGB*BIOTB*LAMZ2* BFRAT
         ENDIF
         THANEW(IGAGE,KMAX) = A + B + C + D
C
C        (N)
C
         DO 860  I = IGAGE+1,IMAX-1
            A1 = 1. - 1./(2.*FLOAT(I))
            A2 = 1. + 1./(2.*FLOAT(I))


            A3 = RCGB*KBG*(LRRAT**2)*LAMR1
            A = A3*( A1* THAOLD(I-1,KMAX) + A2* THAOLD(I+1,KMAX) )
            B = 2.*RCGB*KBG*LAMZ1* THAOLD(I,KMAX-1)
            C1 = - 2.*RCGB*KBG*(LRRAT**2)*LAMR1
            C2 = - 2.*RCGB*KBG*LAMZ1
            C3 = - 2.*RCGB*BIOTB*LAMZ2
            C = (1. + C1 + C2 + C3)* THAOLD(I,KMAX)
            IF (N .LT. TIME1) THEN
               D = 0.
            ELSE
               D = 2.*RCGB*BIOTB*LAMZ2* BFRAT
            ENDIF
            THANEW(I,KMAX) = A + B + C + D
860      CONTINUE
C
C        (O)
```

```
C
      A = 2.*RCGB*KBG*(LRRAT**2)*P1*LAMR1* THAOLD(IMAX-1,KMAX)
      B = 2.*RCGB*KBG*LAMZ1* THAOLD(IMAX,KMAX-1)
      C1 = - 2.*RCGB*KBG*(LRRAT**2)*P1*LAMR1
      C2 = - 2.*RCGB*KBG*LAMZ1
      C3 = - 2.*RCGB*BIOTB*LAMZ2
      C = (1. + C1 + C2 + C3)* THAOLD(IMAX,KMAX)
      IF (N .LT. TIME1) THEN
         D = 0.
      ELSE
         D = 2.*RCGB*BIOTB*LAMZ2* BFRAT
      ENDIF
      THANEW(IMAX,KMAX) = A + B + C + D
C
C
C
C     ------------------------------------------------------------
C     WRITE NON-DIMENSIONAL TEMPERATURE VALUES AT THE HEATED DISK
C     TO FILE "DISKT" (DURING DISTURBANCE PROBLEM ONLY).
C     ** MODIFIED TO WRITE TO "DISKT" ONLY AT INITIAL TIME STEP
C        OF DISTURBANCE PROBLEM AND AT TIME STEPS T+ = .001-.070
C        WITH DELT=.001 AFTER THE DISTURBANCE PROBLEM STARTS.
C        BE CAREFUL TO HAVE ENOUGH TIME STEPS TO HAVE ATLEAST
C        .070 IN NON-DIMENSIONAL TIME FOR THE DISTURBANCE (I.E.
C        NEED TO HAVE COUNT ATLEAST EQUAL TO 70 WHEN THE PROGRAM
C        FINISHES).
C
      IF (N .GE. TIME1) THEN
         IF ( (N.EQ.TIME1) .OR. ((TIME1.EQ.0).AND.(N.EQ.1)) ) THEN
            COUNT = 0
            WRITE(10,25) COUNT
            DO 1100  I = 0,IGENMX
               WRITE(10,30) I,THAOLD(I,0)

1100        CONTINUE
         ENDIF
C
         X = N - MAX(TIME1,1) + 1
         Y = NINT(.001/DELT)
         IF ( MOD(X,Y) .EQ. 0 ) THEN
            COUNT = COUNT + 1
            WRITE(10,25) COUNT
            DO 1125  I = 0,IGENMX
               WRITE(10,30) I,THANEW(I,0)
```

```
1125           CONTINUE
            ENDIF
         ENDIF
C
C        ------------------------------------------------
C        ROLL DOWN THAOLD(1:20,1:20) AND FIND MAXIMUM VISUAL
C        PERCENT CHANGE.  (BE CAREFUL NOT TO DIVIDE BY ZERO.)
C
         MAXTHA = 0.
         DO 900  I = 0,IMAX
            DO 910  K = 0,KMAX
               IF ( ABS(THANEW(I,K)) .GT. MAXTHA) THEN
                  MAXTHA = ABS(THANEW(I,K))
               ENDIF
910         CONTINUE
900      CONTINUE
C
         MAXCH = 0.
         DO 950  I = 0,IMAX
            DO 960  K = 0,KMAX
               CHNG = ABS( THANEW(I,K) - THAOLD(I,K) )
               IF ( MAXTHA .GT. 1.E-15) THEN
                  VISCHNG = CHNG/MAXTHA
                  IF (VISCHNG .GT. MAXCH) MAXCH = VISCHNG
               ELSE
                  IF (CHNG .GT. MAXCH) MAXCH = CHNG
               ENDIF
               THAOLD(I,K) = THANEW(I,K)
960         CONTINUE
950      CONTINUE
C
C        ------------------------------------------------------
C        FIND MAXIMUM RADIAL DIRECTION DERIVATIVE AT OUTER
C        BOUNDARY OF THE PROBLEM.  SAVE THE MAXIMUM VALUE
C        FROM THE WHOLE RUN (ALL ITERATIONS INCLUDED) TO
C        PRINT OUT WHEN FINISHED WITH THE MAIN LOOP.
C
         DO 1200  K = 0,KMAX
            DER = (THANEW(IMAX,K) - THANEW(IMAX-1,K))/DELR
            IF (ABS(DER) .GT. ABS(MAXDER)) MAXDER = DER

1200     CONTINUE
C
C ---------------------------------------------------------------
      ELSE
```

```
C ---------------------------------------------------------------
C
C        CONVERGES.  JUMP OUT OF LOOP.
C
         WRITE(2,*)
         WRITE(2,*)'CONVERGES AFTER ',N-1,' ITERATIONS.'
         WRITE(2,*)'MAXIMUM CHANGE ON THE LAST ITERATION WAS ',MAXCH,'.'
         GOTO 2000
C
C ---------------------------------------------------------------
      ENDIF
500   CONTINUE
C ---------------------------------------------------------------
C
C     IF YOU EXECUTE THESE STATEMENTS, THEN YOU COMPLETED THE
C     MAXIMUM NUMBER OF ITERATIONS FOR THE LOOP WITHOUT CONVERGING.
C     PRINT MESSAGE IF EXPECTING SOME CONVERGENCE (I.E. TOL > 0).
C
      IF (TOL .GT. 0.) THEN
         WRITE(2,*)
         WRITE(2,*)'QUITS WITHOUT CONVERGING AFTER ',N-1,' ITERATIONS.'
         WRITE(2,*)'MAXIMUM CHANGE ON THE LAST ITERATION WAS ',MAXCH,'.'
      ENDIF
C
C ---------------------------------------------------------------
C ***************************************************************
C ---------------------------------------------------------------
2000  CONTINUE
C
C ---------------------------------------------------------------
C  PRINT VALUE OF RADIAL DIRECTION DERIVATIVE AT OUTER BOUNDARY THAT
C  WAS THE LARGEST (IN ABSOLUTE VALUE) DURING THE RUN.
C
      WRITE(2,*)
      WRITE(2,*)'MAXIMUM RADIAL DIRECTION DERIVATIVE AT OUTER BOUNDARY'
      WRITE(2,*)'DURING THE RUN WAS ',MAXDER,'.'
C
C ---------------------------------------------------------------
C  PRINT CHECK ON VALUE OF COUNT.
C
      IF (COUNT .LT. 70) THEN
         WRITE(2,*)
         WRITE(2,*)'WARNING: COUNT LESS THAN 70.  COUNT = ',COUNT
         WRITE(2,*)
      ELSE
```

```
            WRITE(2,*)

            WRITE(2,*)'VALUE OF COUNT IS ',COUNT
            WRITE(2,*)
            WRITE(2,*)
         ENDIF
C
C ---------------------------------------------------------------------
C  FORMAT STATEMENTS.
C
5        FORMAT(20X,E17.10)
25       FORMAT(I5)
30       FORMAT(I5,5X,E17.10)
C
         END
```

D.3 Code to Compare the Finite-Difference and the Series Solution Estimates for Surface Heat Flux

```
      PROGRAM  HTTR2M
C  ********************************************************************
C  *  2LT JOSEPH A. BONAFEDE,  GA-88M                                 *
C  *  FALL 1987                                                       *
C  *                                                                  *
C  *  ADVISOR:  DR. JAMES E. HITCHCOCK                                *
C  ********************************************************************
C
C  DRIVER FOR SUBROUTINE GETQ.
C  GETS INPUTS FOR CALL TO SUBROUTINE GETQ FROM THE INPUT FILE TO
C  GAGE2, I.E. "G2INP" .  OPENS THE OUTPUT FILE FOR GETQ WHICH IS
C  ALSO THE OUTPUT FILE FOR GAGE2, I.E. "G2OUT" (UNIT=2).
C  OPENS THE INPUT FILE FOR GETQ, I.E. "DISKT" (UNIT=10).
C  OPENS THE OUTPUT DATA FILES "PTVDF" (UNIT=11), "PTPDF" (UNIT=12),
C  "PTSER" (UNIT=13), AND "PTFD" (UNIT=14).
C
C  ** MODIFIED TO WORK WITH PROGRAMS GAGE2M OR GAGE2N AND
C  ** SENDS VALUE OF 70 FOR COUNT AND .001 FOR DELT ALWAYS.
C
C ---------------------------------------------------------------
C DECLARE VARIABLES.
C
      IMPLICIT CHARACTER(A-Z)
      INTEGER IGENMX,COUNT
      REAL DBIOT,DELT,GENRAT
      INTEGER MAXT,TDIST
C
C ---------------------------------------------------------------
C  OPEN INPUT AND OUTPUT FILES.
C
      OPEN(UNIT=1,FILE='G2INP',STATUS='OLD')
      OPEN(UNIT=2,FILE='G2OUT',STATUS='OLD')
      OPEN(UNIT=10,FILE='DISKT',STATUS='OLD')
      OPEN(UNIT=11,FILE='PTVDF',STATUS='NEW')
      OPEN(UNIT=12,FILE='PTPDF',STATUS='NEW')
      OPEN(UNIT=13,FILE='PTSER',STATUS='NEW')
      OPEN(UNIT=14,FILE='PTFD',STATUS='NEW')
      REWIND(UNIT=1)
C
C ---------------------------------------------------------------
C  GET INPUTS TO SUBROUTINE.
C
```

```
      READ(1,*)
      READ(1,*)
      READ(1,*) MAXT
      READ(1,*) TDIST
      READ(1,*)
      READ(1,*)
      READ(1,*)
      READ(1,*) IGENMX

      READ(1,*)
      READ(1,*)
      READ(1,*)
      READ(1,*) DBIOT
      READ(1,*)
      READ(1,*) GENRAT
C
      IF (TDIST .GT. MAXT) THEN
         WRITE(2,*)
         WRITE(2,*)'PROBLEM: TDIST GREATER THAN MAXT.  THIS WAS NOT'
         WRITE(2,*)'A DISTURBANCE PROBLEM.'
         STOP
      ENDIF
C
      DELT = .001
      COUNT = 70
C
C -------------------------------------------------------
C  CALL  SUBROUTINE.
C
      CALL  GETQ ( COUNT,IGENMX,DBIOT,DELT,GENRAT )
C
      END
C ***********************************************************************
C ***********************************************************************
      SUBROUTINE  GETQ ( NUMT,IMX,BIOT,DELT,GENRAT )
C
C  ********************************************************************
C  *  2LT JOSEPH A. BONAFEDE,  GA-88M                                 *
C  *  FALL 1987                                                       *
C  *                                                                  *
C  *  ADVISOR:  DR. JAMES E. HITCHCOCK                                *
C  ********************************************************************
C
C  THIS SUBROUTINE DETERMINES THE NON-DIMENSIONAL HEAT
C  TRANSFER RATE AT THE HEATED DISK FOR BOTH THE SERIES
```

```
C  SOLUTION AND THE FINITE DIFFERENCE SOLUTION.
C  THE SUBROUTINE COMPARES THE DIFFERENT VALUES AND PRINTS
C  THE RESULTS IN THE FILE "G2OUT" (UNIT=2).
C  DATA NEEDED TO DETERMINE THE NON-DIMENSIONAL HEAT TRANSFER
C  RATES IS STORED IN THE FILE "DISKT"  (UNIT=10).
C
C  GLOSSARY OF MAIN VARIABLES:
C  NUMT - THE NUMBER OF SURFACE HEAT TRANSFER VALUES TO CALCULATE.
C         INPUT
C  IMX - THE MAXIMUM VALUE FOR RADIAL NODE INCLUDED IN THE DISK,
C        I.E. IGENMX.  (NODES I=0,IMX ARE INCLUDED IN THE DISK.)
C        INPUT
C  BIOT - THE SURFACE BIOT NUMBER FOR THE DISTURBANCE PROBLEM.
C         INPUT

C  DELT - THE NON-DIMENSIONAL TIME STEP USED IN THE PROGRAM.
C         INPUT
C  GENRAT - THE NON-DIMENSIONAL RATIO (QG/DBIOT)/(TFFINAL - TI)
C           USED IN THE PROGRAM
C           INPUT
C  THANOW - MATRIX STORING THE VALUES FOR THATA(I) AT TIME = J
C           FOR I=0,IMX.
C           USED INTERNALLY
C  THAPRE - MATRIX STORING THE VALUES FOR THATA(I) AT TIME T = J-1
C           FOR I=0,IMX.
C           USED INTERNALLY
C  SUM - MATRIX WHICH STORES THE VALUES (THANOW(I)-THAPRE(I))/B
C        FOR I=0,IMX.  B IS A FUNTION OF TIME T (TIME OF THE SURFACE
C        HEAT TRANSFER VALUE) AND TIME J (TIME ASSOCIATED WITH THANOW).
C        USED INTERNALLY
C  B - THE DENOMINATOR TERM INSIDE THE SERIES FOR THE SERIES SOLUTION.
C      B IS A FUNCTION OF TIME T (TIME OF THE SURFACE HEAT TRANSFER
C      VALUE) AND TIME J (TIME ASSOCIATED WITH THANOW).
C      USED INTERNALLY
C  CONS - THE CONSTANT TERM IN THE SERIES SOLUTION.
C         USED INTERNALLY
C  CONFD - THE CONSTANT TERM IN THE FINITE DIFFERENCE SOLUTION.
C          USED INTERNALLY
C  XS - VARIABLE USED FOR AN INTERMEDIATE RESULT IN THE SERIES SOLUTION.
C       USED INTERNALLY
C  XFD - VARIABLE USED FOR AN INTERMEDIATE RESULT IN THE FINITE
C        DIFFERENCE SOLUTION.
C        USED INTERNALLY
C  QS - THE FINAL VALUE FOR AVERAGE SURFACE HEAT TRANSFER AT THE DISK
C       FOR THE SERIES SOLUTION.
```

```
C       USED INTERNALLY
C  QFD - THE FINAL VALUE FOR AVERAGE SURFACE HEAT TRANSFER AT THE DISK
C        FOR THE FINITE DIFFERENCE SOLUTION.
C        USED INTERNALLY
C  VISDIFF - THE PERCENT OF THE FULL SCALE VALUE (MAX THEORETICAL VALUE
C            FOR SURFACE HEAT TRANSFER) BY WHICH THE RESULTS FOR
C            AVERAGE SURFACE HEAT TRANSFER AT THE DISK DIFFER.
C            (FULL SCALE = 1. + GENRAT).
C            USED INTERNALLY
C  PERDIFF - THE PERCENT DIFFERENCE BETWEEN THE RESULTS FOR AVERAGE
C            SURFACE HEAT TRANSFER AT THE DISK (USING THE FINITE
C            DIFFERENCE VALUE IN THE DENOMINATOR).
C            USED INTERNALLY
C  T - INDEX DENOTING THE TIME STEP FOR WHICH WE ARE CURRENTLY
C      CALCULATING THE SURFACE HEAT TRANSFER.
C      USED INTERNALLY
C  J - INDEX DENOTING THE TIME STEP INSIDE THE SERIES (ASSOCIATED
C      WITH THANOW).
C      USED INTERNALLY
C  I - INDEX DENOTING THE RADIAL NODE (I=0,IMX).

C      USED INTERNALLY
C  PI - THE CONSTANT PI (3.141 ...)
C       USED INTERNALLY
C  DECLARE VARIABLES:
      IMPLICIT CHARACTER(A-Z)
      INTEGER  NUMT,IMX
      REAL  BIOT,DELT,GENRAT
      REAL  SUM(1:100),THAPRE(1:100),THANOW(1:100)
      REAL  PI,CONS,CONFD
      REAL  B,XS,XFD,QS,QFD
      REAL  VISDIFF,PERDIFF
      INTEGER  T,I,J
C
C ---------------------------------------------------------
C  GET PARAMETERS.
C
      PI = 4.*ATAN(1.)
      CONS = 2./(BIOT*SQRT(DELT*PI)*((FLOAT(IMX) + .5)**2))
      CONFD = 1./((FLOAT(IMX) + .5)**2)
C
C ---------------------------------------------------------
C  PRINT HEADER TO "G2OUT" (UNIT 2).
C
      WRITE(2,50)
```

```
C ------------------------------------------------
C  GET RESULTS FOR EACH TIME T.
C
      DO 500  T = 1,NUMT
C
         REWIND(UNIT=10)
C
C      /*READ VALUES AT TIME ZERO.*/
C
         READ(10,*)
         DO 600  I = 0,IMX
            READ(10,25) THAPRE(I)
600      CONTINUE
C
C      /*GET SUM(I) FROM J=1,T-1  FOR ALL I*/
C
         DO 700  I = 0,IMX
            SUM(I) = 0.
700      CONTINUE
         DO 800  J = 1,T-1
            B = SQRT(FLOAT(T-J)) + SQRT(FLOAT(T-J+1))
            READ(10,*)
            DO 850  I = 0,IMX
               READ(10,25) THANOW(I)
               SUM(I) = SUM(I) + (THANOW(I) - THAPRE(I))/B

               THAPRE(I) = THANOW(I)
850         CONTINUE
800      CONTINUE
C
C      /*GET FINAL VALUE OF SUM(I) FOR EACH I (INCLUDES TERM FOR*/
C      /* J=T).  ALSO, GET FINAL VALUES FOR QS AND QFD.        */
C
         QS = 0.
         QFD = 0.
         READ(10,*)
         DO 900  I = 0,IMX
            READ(10,25) THANOW(I)
            SUM(I) = SUM(I) + (THANOW(I) - THAPRE(I))
            IF (I .EQ. 0) THEN
               XS = .25*SUM(I)
               XFD = .25*(1. - THANOW(I))
            ELSE
               XS = 2.*FLOAT(I)*SUM(I)
               XFD = 2.*FLOAT(I)*(1. - THANOW(I))
```

```
            ENDIF
            QS = QS + XS
            QFD = QFD + XFD
900       CONTINUE
          QS = QS * CONS
          QFD = QFD * CONFD
C
C       /*COMPARE QS AND QFD AND PRINT RESULTS TO "G2OUT" (UNIT 2)*/
C       /*AND "PTDIFF" (UNIT 11)                                  */
C
          IF ( ABS(QFD) .GT. 1E-15 ) THEN
             VISDIFF = ((QS - QFD)*100.)/(1. + GENRAT)
             PERDIFF = ((QS - QFD)*100.)/ABS(QFD)
             WRITE(2,60) DELT*FLOAT(T),QS,QFD,VISDIFF,PERDIFF
             WRITE(11,80) DELT*FLOAT(T),VISDIFF
             WRITE(12,80) DELT*FLOAT(T),PERDIFF
             WRITE(13,80) DELT*FLOAT(T),QS
             WRITE(14,80) DELT*FLOAT(T),QFD
          ELSE
             VISDIFF = ((QS - QFD)*100.)/(1. + GENRAT)
             WRITE(2,70) DELT*FLOAT(T),QS,QFD,VISDIFF
             WRITE(11,80) DELT*FLOAT(T),VISDIFF
             WRITE(12,85) DELT*FLOAT(T)
             WRITE(13,80) DELT*FLOAT(T),QS
             WRITE(14,80) DELT*FLOAT(T),QFD
          ENDIF
C
500     CONTINUE
C
C -------------------------------------------------------------
C     FORMAT STATEMENTS.

25      FORMAT(10X,E17.10)
50      FORMAT('NON-DIM. TIME',T21,'HEAT TRANSFER',T41,'HEAT TRANSFER'/
     &         '(AFTER DISTURBANCE)',T21,'(SERIES SOLUTION)',T41,
     &         '(FINITE DIFF SOLU)',T61,'VISUAL DIFFERENCE',T81,
     &         'PERCENT DIFFERENCE')
60      FORMAT(F10.7,10X,4(E17.10,3X),'%')
70      FORMAT(F10.7,10X,3(E17.10,3X),'  NOT COMPARED')
80      FORMAT(F10.7,5X,E17.10)
85      FORMAT(F10.7,5X,'  NOT COMPARED')
C
        RETURN
        END
```

Bibliography

1. Carslaw, H. S. and J. C. Jaeger. *Conduction of Heat in Solids* (Second Edition). London: Oxford University Press, 1959.
2. Cook, W. J. and E. J. Felderman. "Reduction of Data from Thin-film Heat Transfer Gages: A Concise Numerical Technique," *AIAA Journal*, 4(3): 561–562 (March 1966).
3. *Hot Wire / Hot Film Anemometry Probes & Accessories.* Product Catalog HWACAT 184 15M 5M. TSI Incorporated, St. Paul, MN, 1983.
4. Incropera, Frank P. and David P. DeWitt. *Introduction to Heat Transfer.* New York: John Wiley & Sons, 1985.
5. Lileikis, Lieutenant Dennis E. *Unsteady Heat Transfer Resulting from the Rapid Charging of an Evacuated Tank with Conducting Walls.* MS Thesis, AFIT/GA/AA/86D-9, School of Engineering, Air Force Institute of Technology (AU), OH, December 1986.
6. Purdue University, Lafayette,Ind. Thermophysical Properties Research Center (Y.S. Touloukian, series editor). *Thermophysical Properties of Matter; The TPRC Data Series, Volume 10.* New York: IFI/Plenum, 1973.
7. Skinner, G.T. "Calibration of Thin Film Gage Backing Materials," *ARS Journal*, 31(5): 671–672 (May 1961).

Vita

Joseph A. Bonafede [redacted] He [redacted] was valedictorian. He then attended Cornell University under an AFROTC scholarship. He graduated with distinction from Cornell University in 1986 receiving a B.S. in Engineering from the School of Civil and Environmental Engineering. Upon graduation, he was commissioned into the United States Air Force and was assigned to the Air Force Institute of Technology.

[redacted]

UNCLASSIFIED
SECURITY CLASSIFICATION OF THIS PAGE

ADA206 134

REPORT DOCUMENTATION PAGE

Form Approved
OMB No. 0704-0188

1a. REPORT SECURITY CLASSIFICATION UNCLASSIFIED	1b. RESTRICTIVE MARKINGS
2a. SECURITY CLASSIFICATION AUTHORITY	3. DISTRIBUTION/AVAILABILITY OF REPORT Approved for public release; distribution unlimited
2b. DECLASSIFICATION/DOWNGRADING SCHEDULE	
4. PERFORMING ORGANIZATION REPORT NUMBER(S) AFIT/GA/AA/88M-1	5. MONITORING ORGANIZATION REPORT NUMBER(S)
6a. NAME OF PERFORMING ORGANIZATION School of Engineering 6b. OFFICE SYMBOL (If applicable) AFIT/ENY	7a. NAME OF MONITORING ORGANIZATION
6c. ADDRESS (City, State, and ZIP Code) Air Force Institute of Technology (AU) Wright-Patterson AFB, OH 45433-6583	7b. ADDRESS (City, State, and ZIP Code)
8a. NAME OF FUNDING/SPONSORING ORGANIZATION 8b. OFFICE SYMBOL (If applicable)	9. PROCUREMENT INSTRUMENT IDENTIFICATION NUMBER
8c. ADDRESS (City, State, and ZIP Code)	10. SOURCE OF FUNDING NUMBERS PROGRAM ELEMENT NO. / PROJECT NO. / TASK NO. / WORK UNIT ACCESSION NO.

11. TITLE (Include Security Classification)

A NUMERICAL INVESTIGATION OF THIN-FILM HEAT TRANSFER GAGES

12. PERSONAL AUTHOR(S)

Joseph A. Bonafede, B.S., 1Lt, USAF

13a. TYPE OF REPORT	13b. TIME COVERED	14. DATE OF REPORT (Year, Month, Day)	15. PAGE COUNT
MS Thesis	FROM _____ TO _____	1988 March	236

16. SUPPLEMENTARY NOTATION

17. COSATI CODES			18. SUBJECT TERMS (Continue on reverse if necessary and identify by block number)
FIELD	GROUP	SUB-GROUP	Surface Heat Flux, Heat Flux, Heat Transfer, Finite-Difference, Thin-Film Gages
20	13		
12	01		

19. ABSTRACT (Continue on reverse if necessary and identify by block number)

Thesis Advisor: Dr. James E. Hitchcock
Professor of Mechanical Engineering

20. DISTRIBUTION/AVAILABILITY OF ABSTRACT ☒ UNCLASSIFIED/UNLIMITED ☐ SAME AS RPT. ☐ DTIC USERS	21. ABSTRACT SECURITY CLASSIFICATION UNCLASSIFIED
22a. NAME OF RESPONSIBLE INDIVIDUAL Dr. James E. Hitchcock	22b. TELEPHONE (Include Area Code) (513) 255-2362 22c. OFFICE SYMBOL AFIT/ENY

DD Form 1473, JUN 86 *Previous editions are obsolete.*

SECURITY CLASSIFICATION OF THIS PAGE
UNCLASSIFIED

When using a thin-film gage to measure surface heat flux, one typically reduces the data for surface temperature to surface heat flux using a series solution for one-dimensional heat transfer in an initially isothermal, semi-infinite solid. However, the gage may not behave as an initially isothermal, semi-infinite solid due to multidimensional heat transfer and electrical preheating of the gage when the instrumentation is turned on.

To evaluate the accuracy of the series solution for use with thin-film gages, the heat transfer in a gage was numerically simulated using a two-dimensional, finite-difference model. The actual geometry of the probe was simplified to reduce the heat transfer to two dimensions. The simulation produced surface temperatures which were used in the series solution to find estimates of surface heat flux. The heat fluxes from the simulation and the series solution were then compared to evaluate the accuracy of the series solution.

The analysis provides good insight into the causes of inaccuracies when using the series solution. It also provides some quantitative results which may be helpful for estimating errors in actual laboratory use.